Imperial College London

Numerical General Relativity in Exotic Settings

Alexander Adam

December 19, 2013

Submitted in part fulfillment of the requirements for the degree of
Doctor of Philosophy in Theoretical Physics of Imperial College London
and the Diploma of Imperial College London

Abstract

In this thesis, we discuss applications of numerical relativity in a variety of complex settings. After introducing aspects of black hole physics, extra dimensions, holography, and Einstein-Aether theory we discuss how one can frame the problem of solving the static Einstein equations as an elliptic boundary value problem by inclusion of a DeTurck gauge fixing term. Having setup this background, we turn to our simplest application of numerical relativity, namely fractionalisation in holographic condensed matter. We explain how one may describe this phenomenon by studying particular classes of hairy black holes and analysing whether bulk flux is sourced by a horizon or charged matter. This problem is our simplest application of numerical relativity as the Einstein equations reduce to ODEs and the problem may be solved by shooting methods. We next turn to a discussion of stationary numerical relativity and explain how one can also view the problem of finding *stationary* black hole solutions as an elliptic problem, generalising the static results discussed earlier. Ergoregions and horizons are naively a threat to ellipticity, but by considering a class of spacetimes describing a fibration of the stationary and axial Killing directions over a Riemannian base space manifold, we show how the problem can nevertheless still be phrased in this manner. Finally we close with a discussion of black holes in Einstein-Aether theory. These unusual objects have multiple horizons as a consequence of broken Lorentz symmetry, and in order to construct such solutions we explain how to generalise the PDE methods of previous sections to construct solutions interior to a metric horizon where the Harmonic Einstein equations cease to be elliptic. Using this new machinery we rediscover the spherically symmetric static black holes that have been found in the literature and moreover present the first known rotating solutions of the theory.

In loving memory of my grandmother, Ida Ciancabilla Benocci.

Preface

Declaration of Originality

I declare that this thesis has been written by myself and constitutes a survey of my own research, except in cases where references are explicitly made to the work of others or to work that was done as part of a collaboration. In detail, the work discussed in chapters 2 and 3 of this thesis is based on material taken from the following publications:

- A. Adam, S. Kitchen, and T. Wiseman, *A numerical approach to finding general stationary vacuum black holes*, *Class.Quant.Grav.* **29** (2012) 165002, [`arXiv:1105.6347`]

- A. Adam, B. Crampton, J. Sonner, and B. Withers, *Bosonic Fractionalisation Transitions*, *JHEP* **1301** (2013) 127, [`arXiv:1208.3199`]

All calculations presented in chapter 3 are taken from the former and were performed by the present author. Chapter 2 is based on the second reference above and all analytic calculations, as well as the $T = 0$ numerics were carried out by the present author in collaboration with Crampton. Chapter 4 is based on work done in collaboration with Wiseman and Pau Figueras that is soon to be submitted for publication. The static calculations in this chapter (section 4.4) were also done in collaboration with Yosuke Misonoh.

All research discussed in this thesis was carried out during the time I was registered at Imperial College London, between October 2009 and October 2013. No part of this work has been submitted for any other degree at this or another institution.

Acknowledgments

I wold like to thank my supervisor, Dr Toby Wiseman for his advice during my time at Imperial College London and in particular for encouraging me to develop my numerical skills despite much initial opposition! I would also like to thank Professor Fay Dowker for many years of guidance and support throughout both my undergraduate and postgraduate years at Imperial. Thanks are also due to Benedict Crampton, Julian Sonner, Benjamin Withers, Sam Kitchen, Pau Figueras and Yosuke Misonoh for enjoyable collaborations.

More thanks than I can say here are owed to my colleagues in H606 for many enlightening and entertaining discussions over the years and for ensuring that no day was without excitement!

I'd also like to thank particularly my parents and close friends who have provided me with invaluable moral support whilst I've been carrying out my research without which none of this would have been possible. The author is also grateful for the financial support that has been provided under a doctoral training grant by the Science and Technologies Facilities Council (STFC).

Copyright Declaration

Contents

List of Figures

1. Gravitational Theory in Exotic Settings

1.1. Introduction

Einstein's theory of General Relativity has revolutionised our understanding of the universe, and stands as one of the greatest achievements of modern physics. The mathematical structure of the theory is however rather complex and nearly a century after its inception, only a handful of exact solutions to the Einstein field equations have been discovered, rendering numerical techniques invaluable. Numerical relativity has since become an extremely diverse field, its usefulness continuing to increase with the dramatic rise in modern computing power. Today the subject has a plethora of remarkable applications ranging from simulations of neutron star structure and the relativistic fluid dynamics of supernova explosions though to the study of gravitational radiation from phase transitions in the early universe [3, 4, 5, 6]. In addition to these astrophysical and cosmological applications, numerical general relativity has become invaluable in fundamental theoretical physics, notably quantum gravity. In this arena, studies of black holes have shed light on various unusual aspects of strongly coupled gauge theories and matrix theories, many of which are of direct relevance to condensed matter physics [7, 8, 9, 10, 11]. In turn, studies of the latter have began to yield insights into open questions relating to the thermodynamics of horizons and unitarity in black hole evaporation [12, 13, 14, 15, 16]. The study of exotic black holes serves as the unifying theme of this thesis, whether in the context of dual descriptions of quantum field theories, cosmologically interesting models of gravitational Lorentz symmetry breaking or simply to elucidate the rather striking phase structure of gravity in higher dimensions.

In the remainder of this chapter, we will turn to a survey of some of the topics outlined above. In section 1.2, we shall provide an overview of aspects of black holes in higher dimensions and how they differ from their four dimensional counterparts. We will also introduce holography and the famous AdS/CFT correspondence. Originating in the work of 't Hooft, [17] and finding its first explicit realisation in string theory, [18] this striking result relates gravitational physics in a given dimension to a quantum field theory in (at least) one dimension lower. We take a relativist's perspective where the emphasis is on gravitational aspects of the correspondence and the key role played by black holes. Given the difficulty in finding analytic solutions in gravitational theories (particularly in higher dimensions or when coupled to exotic matter), we move in section 1.3 to a discussion of elliptic methods for numerical relativity. Although the full Einstein equations constitute a complicated hyperbolic system, in many static and stationary scenarios, if only the solution exterior to a horizon is required, one can recast the problem in a rather different way. In fact, by inclusion of a DeTurck gauge fixing term [19], the system becomes an elliptic boundary value problem that can be solved by standard numerical algorithms such as the Newton method, using only desktop computing resources [20, 21]. Much of the remainder of the thesis will constitute an application of a generalisation of these techniques to exotic stationary black holes. Finally in section 1.4 we change direction somewhat to introduce an unusual modification of gravity, known as Einstein-Aether theory. This theory is consistent with all current observational constraints and differs from general relativity in that it spontaneously breaks Lorentz symmetry by the inclusion of a dynamical timelike vector field, introducing a preferred frame in the universe [22, 23, 24]. The consequences of this for black hole theory will be discussed in detail in the final chapter of this thesis.

The main body of this thesis is divided into three chapters. Chapter 2, contains our simplest application of numerical relativity - this is in the area of AdS/CFT where we show how to construct gravitational duals to 'fractionalisation transitions' in condensed matter. As we shall discuss, the problem amounts to constructing a family of static neutral and charged black holes with and without scalar hair. Since these black holes are static, the Einstein equations become ordinary differential equations (ODEs) and the full machinery of elliptic numerical relativity is not required. We proceed by more conventional shooting methods to construct the solutions and discuss their physical implications. We briefly comment on extensions of this work however involving 'striped' phases where the equations become partial differential equations (PDEs) and the full technology of elliptic numerical relativity could prove extremely useful. In chapter 3 we discuss how to generalise the techniques of section 1.3 to the case of stationary (rather than static) situations. We will discuss this construction in detail, paying attention in particular to the boundary conditions required for the PDE system to be regular at any horizons and axes of symmetry. In the final part of this thesis, chapter 4 we discuss the rather peculiar black holes that exist in Einstein-Aether theory. As a consequence of the broken

Lorentz symmetry in the theory, these solutions have several horizons corresponding to trapping gravitational and aether perturbations of different spin. We discuss an extension of the stationary techniques of chapter 3 that uses ingoing Eddington-Finkelstein coordinates to construct the interior black hole solution by solving a mixed hyperbolic-elliptic system. This is an important ingredient, as we will need to be able to construct the solution interior to the metric horizon in order to fully display the exotic structure of these black holes. We discuss in detail how to construct the static solutions in the literature by completely different techniques and then proceed to present the first known (general) rotating solutions of the theory.

1.2. Higher Dimensional Black Holes, AdS/CFT and Holography

Originally thought to be mere mathematical curiosities, it is now almost certain that black holes exist in our universe (see e.g. [25]). With the advent of string/M theory, it has become natural to extend one's study of physics to higher dimensions and hence to investigate also black holes in dimensions $D > 4$. The study of these solutions is given even greater weight by certain models with TeV scale gravity where such black holes may turn out to be observable at the LHC and the next generation of supercolliders, potentially providing a window into Planck scale physics [26, 27, 28]. Even more remarkable is that by virtue of the AdS/CFT correspondence, some of these higher dimensional solutions may be of relevance to the quark-gluon plasma in particle physics, [29, 30, 31, 32] and strikingly as mentioned previously, even to low energy condensed matter physics.

In this section, we provide an overview of black hole physics in four and higher dimensions, discussing the concepts of Killing vectors, isometries, no-hair and uniqueness theorems as well as some of the famous analytic vacuum solutions that have been obtained. We shall also introduce aspects of Euclidean quantum gravity and its relationship to black hole radiation and thermodynamics. Holography and the AdS/CFT correspondence are then introduced and a survey of the 'holographic dictionary' is given, where the central role played by black holes in the construction of holographic duals becomes apparent.

Black holes are a particular class of solutions to the Einstein equations, which are most elegantly obtained by way of a variational principle. In the second order formalism that we employ throughout this thesis, the metric is the (gravitational) dynamical variable and the relevant action coupled to matter contains (in its most general form) an Einstein-Hilbert term $S_{EH}[g]$, a Gibbons-Hawking boundary term

$S_B[g]$, a non-dynamical term S_0 and finally (in non-vacuum settings) a contribution from the matter action $S_M[g, \psi]$ [33]. Working in $(-, +, +, +)$ signature and in units where the speed of light $c = 1$ we have

$$\begin{aligned} S[g, \psi] &= S_{EH}[g] + S_B[g] - S_0 + S_M[g, \psi]\,, \\ S_{EH}[g] &= \frac{1}{16\pi G}\int_{\mathcal{V}} \sqrt{-g}\, R\,, \\ S_B[g] &= \frac{1}{8\pi G}\int_{\partial\mathcal{V}} \sqrt{|h|}\, \epsilon\, K\,, \\ S_0 &= \frac{1}{8\pi G}\int_{\partial\mathcal{V}} \sqrt{|h|}\, \epsilon\, K_0\,, \\ S_M[g, \psi] &= \int_{\mathcal{V}} \sqrt{-g}\, \mathcal{L}_M(\psi)\,, \end{aligned} \tag{1.2.1}$$

where $\mathcal{V}$ denotes some submanifold of the spacetime manifold $\mathcal{M}$. R is the Ricci scalar, h is the determinant of the induced metric on $\partial\mathcal{V}$ (the boundary of $\mathcal{V}$) and K is the trace of the extrinsic curvature of $\partial\mathcal{V}$. The quantity K_0 is the extrinsic curvature of $\partial\mathcal{V}$ embedded in flat space as we shall discuss below. With our conventions (defined above (1.2.1)), the numerical factor ϵ is $+1$ when $\partial\mathcal{V}$ is timelike and -1 when $\partial\mathcal{V}$ is spacelike.

The Gibbons-Hawking term must a-priori be included when $\mathcal{M}$ is a manifold with boundary, to ensure well-posedness of the associated Dirichlet variational problem, where the induced metric on this boundary is held fixed. It turns out to have physical relevance as well, contributing to the on shell action and hence the thermodynamics of gravitational solutions. The term S_0 affects only the numerical value of the action and does not contribute to local dynamics. It should nevertheless be included formally when $\mathcal{M}$ is non-compact to regularise the total gravitational action, which is otherwise divergent. (When $\mathcal{M}$ is compact, this term is unnecessary). As a simple example of such a contribution, an appropriate choice for asymptotically flat spacetimes (which results in zero action for flat space) is obtained as mentioned above, by taking K_0 to be the extrinsic curvature of $\partial\mathcal{V}$ embedded in flat space[1]. Finally, the action $S_M[g, \psi]$ may be used to couple any desired matter fields ψ to the system. Examples could include standard model fields or more exotic matter contributions motivated by string theory reductions, the latter in particular playing a role in holography as we shall see in chapter 2.

[1] The choice of K_0 is tantamount to a choice of regularisation scheme for the gravitational action and the choice we have just mentioned, useful for asymptotically flat spacetimes, is of course not the only possibility. In particular, for asymptotically AdS spacetimes that we discuss later in the context of holography in section 1.2.5 and chapter 2, the terms that one must add to renormalise the on shell action are more complex. See for instance [34].

The Einstein field equations are obtained on varying the total action (1.2.1) with respect to the metric, subject to the condition that $\delta g_{\mu\nu}|_{\partial\mathcal{V}} = 0$. In our conventions they take the form

$$R_{\mu\nu} - \frac{1}{2} g_{\mu\nu} R = 8\pi G T_{\mu\nu}\,, \tag{1.2.2}$$

where $T_{\mu\nu} = -\frac{2}{\sqrt{-g}}\frac{\delta(\sqrt{-g}\mathcal{L}_M)}{\delta g^{\mu\nu}}$ is the stress energy tensor. For the remainder of this section we discuss the general characteristics of black hole solutions of these equations.

Heuristically, a spacetime $(\mathcal{M}, g)$ is said to contain a black hole if there exist outgoing null geodesics within it that never reach future null infinity $\mathscr{I}^+$. This motivates the formal definition of the black hole region $\mathcal{B}$ of some spacetime manifold $\mathcal{M}$ as the set of points that do not belong to the causal past of future null infinity

$$\mathcal{B} = \mathcal{M} - J^-(\mathscr{I}^+)\,. \tag{1.2.3}$$

This definition mathematically captures the famous statement that a black hole is a region of spacetime from which light and timelike observers cannot escape. The boundary ∂ between the black hole region and the rest of the manifold serves as a 'surface of no return' and defines the black hole event horizon $\mathcal{H}$,

$$\mathcal{H} = \partial\mathcal{B} = \partial(J^-(\mathscr{I}^+))\,, \tag{1.2.4}$$

(where we have assumed that $\mathcal{M}$ itself has no boundary).

The equations (1.2.3), (1.2.4) above define precisely what is meant by a black hole and its horizon in term of global causal structure. In this thesis, we will be concerned for the most part only with the local properties of solutions to the Einstein equations and further global definitions of singularities, and horizons will therefore not be required in what follows. The above definitions are nevertheless included for completeness and further such details may be found in [35, 36].

1.2.1. Killing Fields, Static and Stationary Spacetimes

The Einstein equations are a complicated system of nonlinear partial differential equations and non-trivial exact solutions are in general very difficult to find. It will be convenient in discussing black hole solutions to use symmetries to classify different spacetimes and this motivates the introduction of Killing vectors. In this section we follow [33].

A tensor $T^{\alpha\cdots}_{\beta\cdots}$ is said to be Lie transported along a curve $\mathcal{C}$ (parameterised by λ)

if its Lie derivative along $\mathcal{C}$ is zero: $\mathcal{L}_u T^{\alpha\cdots}_{\beta\ldots} = 0$ where $u^\alpha = dx^\alpha/d\lambda$ is the curve's tangent vector. If adapted co-ordinates are now chosen such that only $x^0 \equiv \lambda$ varies on $\mathcal{C}$, it follows that $u^\alpha \doteq \delta^\alpha_0$ and hence that $\partial_\beta u^\alpha \doteq 0$. (The symbol $\doteq$ denotes equality in the specified coordinate system). One then has that $\mathcal{L}_u T^{\alpha\cdots}_{\beta\ldots} \doteq T^{\alpha\cdots}_{\beta\ldots,\mu} u^\mu \doteq \frac{\partial}{\partial x^0} T^{\alpha\ldots}_{\beta\ldots} = 0$ and consequently the tensor's components are all independent of x^0 in the chosen coordinate system. Conversely, it can be shown that if in some coordinate system the components of a tensor do not depend on some coordinate y, the Lie derivative of the tensor in the direction $\partial/\partial y$ will vanish.

As a consequence of the discussion above, if there exists a coordinate system in which the components of the metric do not depend on one of the coordinates, it follows that $\mathcal{L}_\xi g_{\alpha\beta} = 0$. The associated vector field ξ^α is called a *Killing* vector field and is a generator of *isometries* (diffeomorphisms of the metric). The condition that a vector field be Killing is known as Killing's equation and is most conveniently written as

$$\mathcal{L}_\xi g_{\alpha\beta} = \nabla_\alpha \xi_\beta + \nabla_\beta \xi_\alpha = 0\,, \tag{1.2.5}$$

where the definition of the Lie derivative in terms of the covariant derivative as well as metric compatibility $\nabla_\gamma g_{\alpha\beta} = 0$ have been used.

Having defined Killing vectors, it is useful to introduce the notion of a *Killing horizon*. A Killing horizon is a hypersurface in a spacetime $(\mathcal{M}, g)$ on which the norm of a Killing vector goes to zero. Equivalently, a null hypersurface Σ, (that is to say a hypersurface with a null normal vector), is a Killing horizon of a Killing vector field ξ^α if the latter is normal to Σ. It is in general *not* the same region as the event horizon although for certain classes of spacetime (notably the stationary spacetimes we introduce below) these regions can coincide. Notice the marked difference in the definitions of these two different horizons - an event horizon is introduced in terms of global causal structure, whilst a Killing horizon can be understood in terms of local coordinates. We may now proceed to classify different spacetimes according to their isometries.

An asymptotically flat spacetime is said to be *stationary* if it admits a Killing vector field k which is timelike in a neighbourhood of $\mathcal{J}^\pm$. By the considerations above, this implies that there exists a coordinate system in which the metric coefficients are independent of the time coordinate t, $g_{\alpha\beta,t} \doteq 0$ with $k = \partial/\partial t$.

A stationary spacetime is also *static* if the timelike Killing field k is hypersurface orthogonal. That is to say, if the spacetime admits a foliation (heuristically a 'slicing') into hypersurfaces such that the Killing field k is everywhere orthogonal to these surfaces. Frobenius's theorem gives the necessary and sufficient condition for hypersurface orthogonality, namely that a given vector field u^α is hypersurface orthogonal if and only if $u_{[\alpha;\beta}u_{\gamma]} = 0$ [35]. It can be shown that this is equivalent to the statement that the vector field is irrotational and one may further rephrase this as the requirement that the metric (written in coordinates adapted to the static symmetry) is invariant under time reversal symmetry $t \to -t$ and hence contains no off diagonal time pieces. We finally reiterate that for static spacetimes, the event and Killing horizons coincide, a fact that can be used to obtain global information about the spacetime (the event horizon) from local information (the Killing horizon) and is very useful in practice to locate the event horizon.

A spacetime is said to be *axisymmetric* if,

1. It admits a Killing vector field m that is spacelike in a neighbourhood of $\mathscr{J}^\pm$.
2. The Killing field m generates a one-parameter group of isometries isomorphic to $U(1)$.

A spacetime is *both* stationary and axisymmetric if it simultaneously satisfies the definitions of stationarity and axisymmetry *and* in addition satisfies $[k, m] = 0$. One conventionally chooses adapted coordinates for such spacetimes with $m = \frac{\partial}{\partial t}$ and $k = \frac{\partial}{\partial \phi}$ where ϕ is identified with period 2π. Such stationary solutions are of great importance in physics as they approximate the exterior gravitational field of rotating bodies and are consequently of relevance in astrophysics. We will shortly return to these classes of spacetimes in the context of uniqueness theorems for black holes where we introduce the Rigidity Theorem, a result that plays an important role in our work in chapter 3.

1.2.2. No Hair Theorems and Black Hole Uniqueness

Before presenting particular black hole solutions in four and higher dimensions, we discuss further some general results in black hole theory. In this section we introduce the notions of black hole uniqueness and the related 'no hair' theorems. Further details may be found in the reviews [37, 38, 39, 40]. 'No hair' refers to the property that the space of all black hole solutions in a given dimension is parameterised by a (small) number of asymptotically measured quantities. In this sense, a black hole is very different from a star or for that matter from a speculative ultra compact remnant of gravitational collapse. Such objects would require an arbitrarily large number of multipole moments to specify their states and the remarkable physical content of the no hair theorems is that almost all of this additional information is 'lost'[2] during gravitational collapse to form a black hole. In $D = 4$, it has been

[2]Some of the information is likely radiated away to infinity during collapse in the form of gravitational waves, but a portion inevitably also falls within the horizon when it forms and remains trapped inside the black hole forever (at least at the classical level).

shown, (see for example [41, 42]), that only four parameters are required to completely specify a black hole state: the mass M, angular momentum J, electric charge Q and magnetic charge P[3]. These are further known to correspond to conserved quantities. In higher dimensions, it is still believed to be true that a black hole can be completely specified by a small number of parameters [39], but the existence of non conserved dipole charges in the $D = 5$ rotating black ring solution of [44, 45], (discussed briefly in section 1.2.4) explicitly demonstrates that these parameters need no longer correspond to *conserved* charges when $D > 4$.

Black hole uniqueness refers to a property of the space of black hole solutions whereby specification of a given set of asymptotic parameters (as defined above with regards to the no hair theorem) selects a *unique* black hole as opposed to some collection of black holes. In $D = 4$, uniqueness has been proven, although the proof relies heavily on results that are very specific to $D \leq 4$. In particular, the Hawking black hole topology theorem which guarantees that spatial cross sections of the event horizon in $D = 4$ are topologically S^2 is crucial in the proof. This result makes use of the Gauss-Bonnet theorem (valid in two dimensions) to prove that the two dimensional spatial cross sections of the horizon are spherical/toroidal, followed then by a topological argument to eliminate the toroidal possibility [36]. These results have been strengthened by Chrusciel and Wald using topological censorship [46] which states that in an asymptotically flat and globally hyperbolic spacetime obeying the null energy condition, any causal curve that starts and ends at infinity can be continuously deformed to infinity. Although this result holds for all D, the topological restrictions it implies are only strong for $D < 4$, and little extra is gained in $D > 4$ [39].

In higher dimensions, it is known from the above discussion that the topological restrictions on the horizon are relaxed and there are several examples of black hole solutions (see sections 1.2.4, 1.2.4) that explicitly demonstrate that non spherical event horizons are possible. Moreover one finds that black hole uniqueness does not in general hold in higher dimensions. (There are some specific uniqueness results for $D > 4$, static, asymptotically flat spacetimes which are discussed briefly below, but general uniqueness no longer holds). The breakdown of the uniqueness theorems implies the existence of a nontrivial phase diagram where a variety of black hole phases can coexist with the *same* asymptotic charges. In principle, there could be

[3]In making this statement, we have implicitly assumed that we are considering Einstein-Maxwell theory in asymptotically flat spacetimes. Even in flat space in $D = 4$, the situation is different if one allows Yang-Mills fields (see e.g. [43]) and black holes with non-Abelian hair become possible. Note also that even though we restrict our discussion here to asymptotically flat spacetimes, in section 1.2.5 we briefly mention how black hole uniqueness fails in asymptotically AdS space, allowing for black holes with scalar hair there.

phase transitions between the different regions of the diagram, and it is therefore of interest to know which phases are entropically favoured in a given dimension and in a given range of parameter space, a topic of considerable importance in applications of holography.

The breakdown of black hole uniqueness in $D > 4$ leaves a plethora of exotic higher dimensional solutions. Classification and solution generating techniques (e.g. the Petrov classification and Newman-Penrose formalism [47]) valid in $D = 4$ do not readily generalise to $D > 4$ and hence a full higher dimensional, analytic classification of solutions may be impossible, highlighting the importance of numerical relativity in these settings. We now discuss in more detail some specific uniqueness and no hair results and introduce some of the analytic black hole solutions in D dimensions.

In $D = 4$, spherically symmetric vacuum solutions of the Einstein's equations are static and asymptotically flat. This result is known as Birkhoff's theorem [36, 48]. There is further a theorem due to Israel, Bunting and Masood that states that if (M, g) is a static, asymptotically flat vacuum spacetime, non-singular on and outside an event horizon, then (M, g) is the Schwarzchild metric [49, 50]. This proves that static, vacuum, multi black hole solutions do not exist and that Schwarzchild is the unique spherically symmetric, asymptotically flat, vacuum black hole. Physically, Birkhoff's theorem implies that the gravitational field outside a pulsating sphere remains Schwarzchild at all times and hence there is no monopole gravitational radiation. These results extend to higher dimensions $D > 4$, and the associated generalisation of the Schwarzchild solution is called a Schwarzchild-Tangherlini black hole and has analogous uniqueness properties [39, 51].

In the case of Einstein-Maxwell theory, there exists a generalisation of the Birkhoff result which proves that spherically symmetric, asymptotically flat, electrovacuum black holes must be Reissner-Nordstrom (RN), if one restricts to non-degenerate event horizons or either RN or one of the Majumdar-Papapetrou multi RN solutions if one allows degenerate horizons [52]. In principle, the above theorems allow a *complete* classification of static electrovacuum black holes in any dimension.

For stationary spacetimes in $D = 4$, there is a theorem due to Hawking and Wald that states that if (M, g) is a stationary, non-static, asymptotically flat solution of the Einstein-Maxwell equations that is non-singular on, and outside, a connected event horizon then,

1. (M, g) is axisymmetric

2. The event horizon is a Killing horizon of $\xi = k + \Omega_H m$ for some $\Omega_H \neq 0$.

where as before in adapted coordinates, the Killing vectors $k = \partial/\partial t$ and $m = \partial/\partial\phi$.

This important result known as the *(Strong) Rigidity Theorem* proves that for black holes, stationary $\implies$ axisymmetric [36, 40]. (Notice that in the static case, it also proves our previous claim that the Killing and event horizons coincide). The physical interpretation of the rigidity theorem is that the horizon of a rotating *stationary* black hole is generated by an isometry of the spacetime itself. One could envision a situation where there was rotation in a direction that is not an isometry, but then physically we would expect such a solution to emit gravitational radiation, and thus cease to be stationary. There is also a further theorem relevant in the stationary case due to Carter, Mazur and Robinson [41, 42, 53] that states that if (M, g) is an asymptotically flat, stationary, electrovacuum spacetime, non-singular on and outside a connected event horizon, then (M, g) is a member of the four-parameter (M, J, Q, P) Kerr-Newman family.

The rigidity theorem has been extended to higher dimensions and guarantees the existence of at least one rotational isometry [54, 55]. Curiously all the known analytic higher dimensional stationary solutions such as the Myers-Perry black holes and the Emparan-Reall black rings however have more than just a single such rotational isometry. For a long time, it was unclear whether this result was always true in higher dimensions or whether it was merely a reflection of our inability to find solutions with little symmetry due to the extreme complexity of the equations [39]. Recently, however there has been work on constructing perturbations to the near horizon geometries of Myers-Perry black holes, that preserve only a single rotational isometry and nothing more [56, 57, 58]. One can use these perturbations to generate new branches of (numerical) black hole solutions that demonstrate that there are indeed higher dimensional black holes with less symmetry. In any event, it is clear that the stationary case is much less constrained than the static case and a full theoretical classification of higher dimensional stationary black holes remains elusive.

1.2.3. Black Hole Mechanics and Thermodynamics

Quite remarkably, it was shown in the 1970s, that classical black holes obey a set of equations analogous to the four laws of thermodynamics [59]. These laws of black hole mechanics are rigorous mathematical results that follow only from the Einstein equations, and the energy conditions on the spacetime matter content [35, 36]. In this section we briefly outline these laws and their striking implications.

The *zeroth law* of black hole mechanics states that for a stationary black hole, a quantity known as the surface gravity κ is constant across the event horizon (where the latter is a Killing horizon of the vector $\xi = \kappa + \Omega_H m$ that was defined previously)

$$\kappa = const\,. \tag{1.2.6}$$

The surface gravity κ may be interpreted as the force required of an observer at ∞ to keep a particle of unit mass stationary at the event horizon. Physically the local acceleration of a test body at the event horizon diverges, but the gravitational redshift factor goes to zero. The surface gravity is heuristically a product of the two where the limit is well defined and it can be elegantly written in the form

$$\kappa^2 = -\frac{1}{2} t^{\alpha;\beta} t_{\alpha;\beta}|_{\mathcal{H}}\,, \tag{1.2.7}$$

where t^α is the normalised tangent to the null geodesic generators of the horizon [33]. It is important to emphasise that surface gravity is only a well defined concept for stationary black holes as they have Killing horizons, a matter we shall return to shortly.

The *first law* of black hole mechanics relates changes in the mass δM of a black hole to changes in the area δA of its event horizon, angular momentum δJ, and charges δQ^a, where the latter arise from the matter theory to which gravity is coupled, (an example being the electric charge of Einstein-Maxwell theory)

$$\delta M = \frac{\kappa}{8\pi}\delta A + \Omega_H \delta J + \phi^a \delta Q^a\,. \tag{1.2.8}$$

In the equation above, κ and Ω_H are the surface gravity and angular velocity of the horizon respectively, and the ϕ^a are the potentials associated to the conserved charges Q^a. (In the Einstein-Maxwell theory example, $a = 1$ and there is a single ϕ 'conjugate' to the conserved $U(1)$ electric charge that physically measures the electric potential difference between the event horizon and spacelike infinity i^0). The first law holds for stationary black holes, that is to say, processes where the initial state of the system is a stationary black hole, and the final state is a stationary black hole. (The analogy in thermodynamics is that of a quasistatic process, where the initial and final states are both in equilibrium).

It is important to stress at this point that both the zeroth and first laws of black hole mechanics are non-dynamical statements that hold (as stated) only for stationary solutions. As alluded to above, the technical reason behind this restriction is that the classical proofs of the theorems use the properties of Killing horizons and whilst the event horizons of stationary black holes are guaranteed to be Killing by the rigidity theorem, this is not true for dynamical spacetimes. There is however a body of work on attempts to generalise the zeroth and first laws to dynamical, non-equilibrium situations. This is of considerable physical interest as essentially all realistic (astrophysical or collider) scenarios involving black holes will inevitably be fully dynamical. One is led to introduce the concepts of isolated and dynamical horizons, which allows progress to be made in this regard, but much still remains unanswered - there is as of yet no conclusive notion of surface gravity in such situations for example (see for instance [60, 61]).

In contrast to the zeroth and first laws, the *second law* of black hole mechanics constrains the possible *dynamical* evolution of black holes (e.g. black hole mergers) and states that the total area of event horizons is non-decreasing

$$\delta A \geq 0 \,. \tag{1.2.9}$$

This law is also known as *Hawking's area theorem* and can be proved by application of the Raychaudhuri equation to the null geodesic congruence that generates the horizon. It assumes only that matter obeys the weak energy condition, and in particular is a fully dynamical statement, that does not require a notion of Killing horizon. (That the event horizon is a null surface, can be seen from considerations of causal structure alone).

Finally, the *third law* of black hole mechanics states that the so called *extremal* limit of black holes, corresponding to vanishing surface gravity $\kappa = 0$ cannot be reached in finite time by any physical process [62]. (Again, extremality is defined with respect to stationary equilibrium black holes such that κ is defined).

It was later shown by Hawking in the framework of quantum field theory in curved spacetime that this similarity between black hole mechanics and thermodynamics is more than an analogy and that quantum black holes radiate as thermodynamic objects with an associated temperature. In the case of a static black hole, this takes the form

$$T_H = \frac{\kappa}{2\pi} \,, \tag{1.2.10}$$

(where the Planck and Boltzmann constants have been set to unity) [63]. Motivated by the suggestive appearance of the Hawking area theorem, Bekenstein had previously conjectured that the entropy of a black hole is proportional to its horizon area [64]. With this identification, together with Hawking's derivation of a temperature, the laws of black hole mechanics *are* in effect the laws of thermodynamics[4]. One

[4]Hawking's identification of black hole mechanics with black hole thermodynamics also fixes the constant of proportionality relating the black hole entropy to the horizon area as $S = \frac{A}{4}$.

of the major outstanding problems in quantum gravity research is to shed light on the underlying microstates that account for this black hole entropy, a question that has at least partially been answered for supersymmetric black holes in string theory [65], and constitutes one of the great triumphs of that theory.

Hawking's original derivation uses canonical techniques and is fully Lorentzian in character. In the remainder of this section, however we shall outline an equilibrium derivation that uses the Euclidean path integral formulation and corresponds to considering the canonical ensemble for gravity [66, 67]. We will show through the example of a static black hole how the temperature may be computed directly from the metric.

Euclidean Quantum Gravity is defined by the Feynman path integral

$$\mathcal{Z} = \int \mathcal{D}g\mathcal{D}\phi \, e^{-\hat{I}[g,\phi]} \,, \tag{1.2.11}$$

where the Euclidean action $\hat{I}$ is related to the Lorentzian action I by $\hat{I} = -iI$. Equation (1.2.3) is in fact rather difficult to define technically as the measure on the space of metrics $\mathcal{D}g$ is generically ill defined. Moreover, the integral is divergent as is commonplace in quantum field theory and a regularisation and renormalisation procedure is required to make sense of this fact [67]. It is expected that the dominant contribution to the integral will come from a saddle point of the action, corresponding to a solution of the classical field equations if one exists. (It can be argued that this must be the case in order to recover classical general relativity in an appropriate limit). In such a saddle point approximation, the action is expanded as a Taylor series about background fields g_0 and ϕ_0

$$\hat{I}[g,\phi] = \hat{I}[g_0,\phi_0] + I_2[\bar{g},\bar{\phi}] + ... \,, \tag{1.2.12}$$

where $g_{ab} = g_{0ab} + \bar{g}_{ab}$, $\phi = \phi_0 + \bar{\phi}$ and $I_2[\bar{g},\bar{\phi}]$ is quadratic in the fluctuations $\bar{g}$ and $\bar{\phi}$. The path integral then takes the form

$$log\mathcal{Z} = -\hat{I}[g_0,\phi_0] + log\int \mathcal{D}\bar{g}\mathcal{D}\bar{\phi}\, e^{I_2[\bar{g},\bar{\phi}]} + \dots \,, \tag{1.2.13}$$

where the first term is physically the contribution from the background fields, and the second term encodes one-loop quantum corrections around this background. Since $I_2[\bar{g},\bar{\phi}]$ is quadratic in fluctuations, the one loop term is a Gaussian integral and may be evaluated exactly to arrive at a one-loop determinant. The latter technically requires a regularisation procedure to be well defined (generally dimensional regularisation or zeta function regularisation) but this will not be needed in the discussion that follows (see [67] for the full calculation of this term). The reason for this is that (1.2.13) is in fact a derivative expansion in '$l_p^2\partial^2$' where l_p

is the Planck length and ∂^2 denotes terms with two derivatives of the metric[5]. In a 'semi-classical' limit, where 'higher derivatives' are small (being irrelevant), all one loop (and higher) quantum corrections are hence suppressed compared to the leading term. All that remains therefore is to evaluate the dominant contribution to $log\mathcal{Z}$, namely the Euclidean action evaluated on a classical solution to the Einstein equations. The simplest non-trivial example would be to compute the action for the Euclidean, static, vacuum ($\phi_0 = 0$) Schwarzchild metric, but it is instructive to instead consider the (slightly) more general spherically symmetric vacuum solution

$$ds^2 = f(r)d\tau^2 + f^{-1}(r)dr^2 + r^2 d\Omega^2\,, \tag{1.2.14}$$

where we have analytically continued to Euclidean signature through $\tau = it$, and it is assumed that there exists an r_0 such that $f(r_0) = 0$ (where f is at least $\mathbb{C}^2$, and $f'(r_0) \neq 0$). Although in these coordinates it appears that there is a singularity at $r = r_0$, on changing variables to $R = f^{1/2}$, expanding in the vicinity of $r = r_0$ and subsequently redefining $R' = 2/(f'(r_0))$ the metric becomes

$$ds^2 = dR'^2 + \frac{f'(r_0)^2 R'^2}{4} d\tau^2 + r_0^2 d\Omega^2\,, \tag{1.2.15}$$

where it is manifest now that the apparent singularity at $r = r_0$ is analogous to the 'singularity' at the origin of plane polar coordinates. This Euclidean metric will consequently be regular at $r = r_0$, ($R = 0$) if τ is regarded as an angular variable with period $4\pi/f'(r_0)$. (If this identification is not made, the metric has a conical deficit angle, and hence a conical singularity at the origin and such configurations are expected to be exponentially suppressed in the path integral).

This periodicity in imaginary time (demanded by regularity) is equivalent to putting the theory at finite temperature. This can be seen in the context of quantum field theory as follows. The amplitude to transition between the states $\mid q, t\rangle$ and $\mid q', t'\rangle$ is given by the functional integral

$$\langle q', t' \mid q, t\rangle = \int \mathcal{D}q(t) e^{iS[q(t)]}\,. \tag{1.2.16}$$

If one Euclideanises $t \to -it_E, t' - t \to -i\beta, iS \to -S_E$, and considers closed time

[5]Schematically, the leading term in 1.2.13 comes with a power of ∂^2/l_p^2, where by ∂^2 we schematically mean terms involving two derivatives of the metric such as the Ricci and Riemann tensors and their contractions. The subleading terms then go as ∂^4, $l_p^2\partial^6$ etc. To develop this expansion explicitly requires considerably more Euclidean quantum gravity machinery than we have discussed here (see for instance [67])

paths $q' = q(t_E + \beta) = q = q(t_E)$, one finds further that

$$
\begin{aligned}
\langle q, t' \mid q, t\rangle &= \sum_q \langle q, t \mid e^{-\beta\hat{H}} \mid q, t\rangle = Tr(e^{-\beta\hat{H}}) \\
&= \int_{q(t_E)+\beta=q(t_E)} \mathcal{D}q(t_E) e^{-S[q(t_E)]}\,, \qquad (1.2.17)
\end{aligned}
$$

where $\hat{H}$ is the Hamiltonian and a complete set of states was inserted in the matrix element $\langle q, t' \mid q, t\rangle$ to obtain the trace part of (1.2.17). It is then apparent that the Euclidean path integral on a closed time path is equivalent to the statistical mechanics partition function at temperature $T = 1/\beta$. Consequently the equilibrium temperature of the above black hole in the canonical ensemble is $T = 1/\beta = f'(r_0)/4\pi$. This result agrees with the Hawking temperature that one finds from Lorentzian canonical quantisation. We close this section by noting that there are many subtleties in the Euclidean formulation of black hole thermodynamics. In particular, equilibrium at the Hawking temperature can be unstable. As an example, if a Schwarzchild black hole absorbs radiation, its mass increases and its temperature hence decreases. Said in another way, in this ensemble, the black hole has negative specific heat. This instability can also be seen by studying the phase structure of Euclidean quantum gravity in a finite cavity, held in contact with a heat bath at fixed temperature [68, 69]. In this setting, one finds that there are in general three saddle points of the action, corresponding to a large black hole, small black hole and hot flat space respectively. The latter dominates at low temperatures, whilst above a certain threshold there is a transition (analogous to the Hawking-Page transition in AdS [70]) above which the large black hole dominates. One can show that whilst 'hot flat space' and the large black hole are stable, the small black hole has a Euclidean negative mode and is unstable, serving as a metastable vacuum that allows the system to pass from one minimum to the other by way of thermal fluctuations. This negative mode is believed to arise as a direct consequence of its negative specific heat. It is unclear in such cases whether the derivation of the black hole temperature we have discussed is strictly valid as such metastable configurations do not dominate the Euclidean action.

1.2.4. Examples of Asymptotically Flat Black Holes

We now proceed to discuss some of the asymptotically flat[6] analytic solutions to the Einstein equations that have been discovered in four and higher dimensions. Several of these solutions will feature explicitly in the chapters that follow in this thesis, but in particular they also act as a useful starting point for numerics, serving as initial data for calculation that construct some of the more exotic black hole solutions that can only be found numerically. We begin our review with static solutions:

Asymptotically Flat Static Black Holes

The unique family of static, vacuum black holes in D spacetime dimensions are the spherically symmetric Schwarzchild-Tangherlini solutions [51], with metric

$$ds^2 = -\left(1 - \frac{\mu}{r^{D-3}}\right) dt^2 + \frac{dr^2}{1 - \frac{\mu}{r^{D-3}}} + r^2 d\Omega_{D-2}^2 \,, \tag{1.2.18}$$

where the 'mass parameter'

$$\mu = \frac{16\pi GM}{(D-2)\Omega_{D-2}} \,. \tag{1.2.19}$$

(In the above, $\Omega_{D-2} = 2\pi^{\frac{d-1}{2}}/\Gamma(\frac{d-1}{2})$ is the volume of S^{D-2}). These black holes are asymptotically flat and the familiar four dimensional Schwarzchild solution is obtaining on setting $D = 4$. There is a true curvature singularity at $r = 0$ and a Killing horizon (and hence event horizon as the solution is static) at the Schwarzchild horizon radius $r_0 = \mu^{\frac{1}{(D-3)}}$.

These solutions may be used as the starting point to construct more complex higher dimensional solutions by using the result that the direct product of two Ricci-flat manifolds is itself Ricci-flat and hence a solution of the vacuum Einstein equations [39]. Given a vacuum solution $\mathcal{S}$ in D dimensions, one may construct a new solution with metric

$$ds_{D+p}^2 = ds_D^2(\mathcal{S}) + \sum_{i=1}^{p} dx^i dx^i \,, \tag{1.2.20}$$

describing a *black p-brane*, or *black string* in the special case ($p = 1$). In contrast to the Schwarzchild-Tangherlini black holes, these black brane solutions have extended

[6]We will also have cause to mention here certain solutions which are not asymptotically flat and in section 1.2.5, we will introduce some of the salient features of black hole solutions in asymptotically AdS spacetime, as this is an important ingredient in applications of holographic duality.

horizons with topology $\mathcal{H} \times \mathbb{R}^p$, (where $\mathcal{H} \subset \mathcal{S}$ is the horizon of $\mathcal{S}$) and are not asymptotically flat. Furthermore, as a consequence of the Hawking horizon topology theorem introduced in the previous section, they can only arise in $D \geq 5$. One can also understand this here by way of the observation that there are no asymptotically flat vacuum black holes in $D = 3$ to form the necessary direct product structure with in 1.2.20. Heuristically, this is a consequence of the quantity GM being dimensionless in $D = 3$, so that there is no length scale to set the location of a putative black hole horizon in this case [39].

It is well-known that these black brane solutions exhibit a classical instability called the Gregory-Laflamme instability [71, 72]. This is best illustrated by way of a black string constructed by taking the direct product of the $D = 4$ Schwarzchild solution with a flat direction z. The behaviour of the system under linearised gravitational perturbations is analysed by decomposing such perturbations into scalar, vector and tensor modes with respect to the Lorentz symmetry of the background spacetime $ds^2_D(\mathcal{S})$. It is found that whilst the string is stable to scalar and vector perturbations as well as tensor perturbations homogeneous in the z direction, there is an instability for long wavelength tensor perturbations with a z dependence. More precisely, the frequency ω of these tensor perturbations, which appears in the combination $\sim e^{-i(\omega t - kz)}$, acquires a positive imaginary part when $k < k_{GL} \sim 1/r_0$[7] where r_0 is the Schwarzchild horizon radius. In a manner somewhat analogous to the Rayleigh-Taylor instability of fluid dynamics, the Gregory-Laflamme instability will tend to cause the black string to fragment into an array of localised black holes. This behaviour can in fact be understood on physical grounds by appealing to the laws of black hole mechanics. As a consequence of the second law, dynamical processes occur in the direction of non-decreasing horizon area, and indeed a fragmentation of the string into localised black holes will increase the horizon area of the final state. Rephrasing the above in the language of black hole thermodynamics, the array of localised black holes becomes thermodynamically favoured compared to the non-uniform perturbed black string as it has higher entropy and hence the instability occurs spontaneously [39, 75].

The precise dynamical details of the Gregory-Laflamme instability and notably the end state however remain a matter of some controversy. Numerical relativity has been key here in establishing evidence that this end state is indeed likely a localised black hole as described above [74, 76, 77]. The very fact that this happens however, namely that the inhomogeneities grow large enough to cause the string to fragment into a collection of black holes is quite remarkable as it indicates the possibility of

[7] The phases of black holes/strings in Kaluza-Klein theory are conventionally defined in (n, μ) parameter space where n is the relative binding energy and μ is a dimensionless mass parameter. It has been shown numerically that in $D = 5$ the Gregory Laflamme point is at $\mu_{GL} = 3.52$ [73] and in $D = 6$ at $\mu_{GL} = 2.31$ [74].

some novel topology changing phase transition within semiclassical general relativity [78]. Furthermore the order of this transition is of interest as in the event of a first order transition[8], one would expect it to be accompanied by a tremendous burst of energy that has been dubbed a 'thunderbolt' (since the total mass of the final state must be lower than or equal to the initial state and the excess must be lost as radiation). Since the topology change in principle exposes a naked singularity during the transition, this burst of radiation would likely be classically singular [79]. We close our discussion of Gregory-Laflamme by noting that the analysis above for the black string carries over to the case of black branes, which are also classically unstable to perturbations $\sim e^{(-i\omega t+i\boldsymbol{k}\cdot\boldsymbol{x})}$ with $|\boldsymbol{k}| \leq k_{GL}$ (where the wavevector $\boldsymbol{k}$ is along the p directions tangential to the brane) [75]. By similar calculations, it can be shown that in contrast, the Schwarzchild-Tangherlini black holes are classically, perturbatively stable.

Asymptotically Flat Stationary Black Holes

The generalisation of the static, vacuum, spacetimes described above to the stationary case is extremely non-trivial [80]. It is convenient to start in $D = 4$ where one has the Kerr spacetime. In the conventional Boyer-Lindquist coordinates (t, r, θ, ϕ) with $t^\alpha = \frac{\partial x^\alpha}{\partial t}, \phi^\alpha = \frac{\partial x^\alpha}{\partial \phi}$ Killing, it takes the form

$$\begin{aligned} ds^2 &= -\left(1 - \frac{2Mr}{\rho^2}\right) dt^2 - \frac{4Mar\sin^2\theta}{\rho^2} dt d\phi + \frac{\Sigma}{\rho^2}\sin^2\theta d\phi^2 \\ &\quad + \frac{\rho^2}{\Delta} dr^2 + \rho^2 d\theta^2 \\ &= -\frac{\rho^2\Delta}{\Sigma} dt^2 + \frac{\Sigma}{\rho^2}\sin^2\theta(d\phi - \omega dt)^2 + \frac{\rho^2}{\Delta} dr^2 + \rho^2 d\theta^2 \,, \end{aligned} \tag{1.2.21}$$

where $\rho^2 \equiv r^2 + a^2\cos^2\theta$, $\Delta \equiv r^2 - 2Mr + a^2$, $\Sigma \equiv (r^2 + a^2)^2 - a^2\Delta\sin^2\theta$ and $\omega \equiv -\frac{g_{t\phi}}{g_{\phi\phi}}$ where the quantities M and a are constants that parameterise the space of solutions. The metric (1.2.21) has a Killing horizon at $r = M + \sqrt{M^2 - a^2}$ (as we show shortly), and by the rigidity theorem this is also the event horizon.

It is apparent from the form of 1.2.21 that the Kerr metric takes the form of a co-rotating frame of reference with 'angular velocity' ω. When evaluated at the horizon, ω gives the angular velocity of the black hole. Furthermore it can be shown (through Komar integrals) that M is the mass of the spacetime and $a = J/M$ is its angular momentum per unit mass. In what follows, we follow closely [33].

[8]The transition from black string to black hole seeded by the Gregory Laflamme instability has indeed been demonstrated to be first order for $D \leq 13$ and second order for $D \geq 14$ [79].

The Kerr metric has singularities at $\Delta = 0$ and $\rho = 0$ and an examination of the squared Riemann tensor for this spacetime

$$R^{\alpha\beta\gamma\delta}R_{\alpha\beta\gamma\delta} = \frac{48M^2(r^2 - a^2\cos^2\theta)(\rho^4 - 16a^2r^2\cos^2\theta)}{\rho^{12}}\,, \tag{1.2.22}$$

shows that $\rho^2 = 0$ is a true curvature singularity, whilst nothing pathological occurs at $\Delta = 0$ indicating that the latter is likely a coordinate singularity.

To explore its physical properties further, it is instructive to consider the behaviour of various different types of observer in the Kerr spacetime. Observers with zero angular momentum $\tilde{L}$ satisfy $\tilde{L} \equiv u_\alpha\phi^\alpha = g_{\phi t}\dot{t} + g_{\phi\phi}\dot{\phi} = 0$ where overdots denote differentiation with respect to proper time τ. From 1.2.21, it is apparent that this implies that

$$\Omega \equiv \frac{d\phi}{dt} = \omega\,, \tag{1.2.23}$$

and hence such zero angular momentum observers rotate with the black hole. This is an example of the phenomenon of *frame dragging* (also called the Lense-Thirring effect) and is exhibited by all rotating bodies in general relativity.

Static observers have by definition a four velocity proportional to the Killing vector t^α, $u^\alpha = \gamma t^\alpha$, where $\gamma \equiv (-g_{\alpha\beta}t^\alpha t^\beta)^{-1/2}$ is a normalisation factor. The vector t^α is not timelike everywhere but becomes null when $\gamma^{-2} = -g_{tt} = 0$ or equivalently $r^2 - 2Mr + a^2\cos^2\theta = 0$. The solution to this equation $r = r_{sl}$ defines the radial position of the 'static limit'. That is to say static observers cannot exist everywhere in the Kerr spacetime but only up to this static limit r_{sl} corresponding to $g_{tt} = 0$. In the region $r < r_{sl} = M + \sqrt{M^2 - a^2\cos^2\theta}$, it is not possible to remain static even if an arbitrarily large force is applied, and all timelike observers are forced to rotate with the black hole.

Finally, it is instructive to consider stationary observers with constant angular velocity $d\phi/dt = \Omega$ moving in the ϕ direction. These have four velocity $u^\alpha = \gamma(t^\alpha + \Omega\phi^\alpha)$, where the combination $t^\alpha + \Omega\phi^\alpha$ is a Killing vector of the Kerr spacetime and $\gamma = [-g_{\alpha\beta}(t^\alpha + \Omega\phi^\alpha)(t^\beta + \Omega\phi^\beta)]^{-1/2}$ is again a normalisation factor. As with static observers, these observers also cannot exist everywhere as for this to be possible, the combination $t^\alpha + \Omega\phi^\alpha$ must remain timelike throughout the spacetime and this fails to hold when $\gamma^{-2} = -g_{\phi\phi}(\Omega^2 - 2\omega\Omega + g_{tt}/g_{\phi\phi}) < 0$ (with $\omega = -g_{t\phi}/g_{tt}$).

The requirement that $\gamma^{-2} > 0$ translates into an inequality for the angular velocity $\Omega_- < \Omega < \Omega_+$ where $\Omega_\pm = w \pm \sqrt{\omega^2 - g_{tt}/g_{\phi\phi}} = \omega \pm (\Delta^{-1/2}\rho^2)/\Sigma\sin\theta$. If one notes now that a stationary observer with $\Omega = 0$ is by definition a static observer, and that as discussed previously such observers exist only outside the static limit r_{sl} defined previously, it becomes clear that Ω_- changes sign at r_{sl}. As r decreases from r_{sl}, Ω_- increases, whilst Ω_+ decreases until the two become equal $\Omega_- = \Omega_+$ at which point, $\Omega = \omega$ and the stationary observer is compelled to rotate around the black hole with angular velocity ω. This happens when $\Delta = 0$, or equivalently $r^2 - 2Mr + a^2 = 0$, the largest root of which, $r = r_+ = M + \sqrt{M^2 - a^2}$ defines the outer event horizon of the Kerr black hole.

That this is an event horizon can be seen on noting that the Killing vector $t^\alpha + \Omega\phi^\alpha$ becomes null at $r = r_+$ and hence the surface is a Killing horizon of $t^\alpha + \Omega\phi^\alpha$. (This is to be contrasted with Schwarzchild where it is t^α that becomes null at the horizon). The strong rigidity theorem then implies that this region is an event horizon. The angular velocity of the black hole is defined with respect to this outer horizon as $\Omega_H \equiv \omega(r_+) = a/(r_+^2 + a^2)$. (Note the equation defining the location of the horizon r_+ also admits a second 'inner horizon' solution at $r = r_-$ which we will not have cause to discuss here).

Physically, there is an upper bound on the angular momentum $a \leq M$ of a Kerr black hole beyond which there are no horizons (the relevant quadratic equation has no real roots) and the metric describes a naked singularity - a singularity that is not shielded by a horizon. A Kerr black hole with $a = M$ is said to be extremal as it can be shown to have vanishing surface gravity ($\kappa = 0$).

We end our discussion of Kerr by noting one further, unusual property of the spacetime. In the region between the outer horizon and the static limit $r_+ < r < r_{sl}$ known as the *ergoregion*, the killing vector t^α is spacelike. The conserved energy of a particle in that region can therefore be negative and it turns out that this may in principle allow an external agent to extract the rotational energy of the black hole via a mechanism known as the *Penrose process*. This phenomenon may be of importance in the formation of astrophysical jets [81].

There exists a generalisation of the Kerr solution to dimensions $D > 4$ known as the Myers-Perry solution [82, 83]. Naively, one might expect these spacetimes to be very similar to the $D = 4$ Kerr black holes, in the same sense that the $D > 4$ Schwarzchild-Tangherlini black holes offer little new physics when compared with their four dimensional cousins. It turns out however, that they exhibit some rather different behaviour, an observation that can be attributed to the fact that the properties of rotation change significantly when the spacetime dimension is greater than four.

Primarily, when $D > 4$ there is the possibility of rotation in more than one independent plane. Formally, this is because the rotation group $SO(D-1)$ has as its maximal commuting subgroup $U(1)^N$ with $N \equiv \mathrm{Int}[(D-1)/2]$ and hence there can be N such independent rotation planes and angular momenta.

In addition, the relative competition between the gravitational and centrifugal potentials changes as D is varied. The Newtonian potential depends explicitly on the spacetime dimension as $\sim -\frac{GM}{r^{D-3}}$, whilst the centrifugal term $\sim \frac{J^2}{M^2 r^2}$ has no such dependence (since rotation is confined to a plane). The competition between these two potentials therefore changes as the spacetime dimension changes and can lead to qualitatively different physics [39]. The Myers-Perry metric with rotation in a single plane[9] takes a form similar to Kerr,

$$\begin{aligned} ds^2 &= -dt^2 + \frac{\mu}{r^{D-5}\Sigma}(dt - a\sin^2\theta d\phi)^2 + \frac{\Sigma}{\Delta}dr^2 + \Sigma d\theta^2 + (r^2+a^2)\sin^2\theta d\phi^2 \\ &\quad + r^2\cos^2\theta d\Omega^2_{(D-4)}\,, \end{aligned} \tag{1.2.24}$$

where $\Sigma = r^2 + a^2\cos^2\theta$ and $\Delta = r^2 + a^2 - \mu/r^{D-5}$. (Note that we have used a different definition of Σ compared with the discussion of the Kerr metric, which is recovered on setting $D = 4$). μ is proportional to the mass of the spacetime, and a to the angular momentum per unit mass. In $D = 5$, it turns out that the behaviour of these solutions is qualitatively similar to $D = 4$ Kerr, in that they have an upper bound on their angular momentum, but in $D > 5$, an ultra-spinning regime becomes possible where these black holes can exist with arbitrarily large angular momentum. Ultimately in this limit, the Myers-Perry solutions resemble black membranes with horizon topology $\mathbb{R}^2 \times S^{D-4}$ and become qualitatively different from localised Kerr-like objects [39].

We have already seen through the examples of black branes that non spherical horizon topologies are permitted in higher dimensions, but perhaps the most spectacular demonstration that the Hawking topology theorem no longer holds in $D > 4$ is the existence of the rotating black ring solution in $D = 5$ [44]. The existence of such solutions may be understood through the following heuristic construction: One may imagine taking one of the black string solutions described above with horizon topology $S^q \times \mathbb{R}$ and bending it to form an object with the horizon topology of a ring, $S^q \times S^1$. Such an object would tend to collapse as the S^1 is contractible, but the system can be stabilised by allowing it to rotate, whereupon the centrifugal force can counterbalance this tendency to collapse. There exist also further generalisations of these black ring metrics that describe a central black hole surrounded by one or more black rings which go by the name of black Saturns, further demonstrating the exoticness of solutions in $D > 4$ [84]. Given this violation of the Hawking topology theorem, one might also expect from the discussion in section 1.2.2, a violation of black hole uniqueness. This is indeed explicitly manifested through the coexistence

[9]Solutions with arbitrary rotation in any of the N rotation planes may also be constructed (see for instance [39]).

of Myers-Perry black holes and neutral black rings in certain regions of parameter space. This non-uniqueness can in fact be made continuous if black rings carrying 'dipole charges' are considered [45], although a 'no-dipole-hair' theorem has recently been proven for static, asymptotically flat higher dimensional black holes and so this non-uniqueness is confined to stationary solutions [85].

It is useful to review the above analytic solutions as they serve as explicit realisations of the exotic nature of the phase space of black holes in $D > 4$. Moreover, it is important to emphasise that the solutions we have presented essentially constitute the entirety of the known analytic solutions in higher dimensions, highlighting the importance of numerical relativity in this field and ultimately motivating our introduction to the subject later in this chapter. Whilst in the asymptotically flat static case, all solutions are known analytically (as Schwarzchild is unique), in the stationary case, as mentioned previously in section 1.2.2, there exist deformations of the Myers-Perry class of solutions which can only be constructed numerically. In AdS space (as well as dS space) in $D \geq 5$, even less is known analytically and it has not been possible to find an explicit metric describing a black ring solution, although approximation techniques, notably matched asymptotic expansions have been used to make progress [86]. Furthermore, numerical methods have been instrumental in conjecturing the structure of the phase diagram of ring and multi ring solutions in $D \geq 5$ [87, 88]. Interestingly, in the case of compact extra dimensions, in contrast to the asymptotically flat case, numerical methods are needed to construct even *static* vacuum black hole solutions, as discussed extensively in the literature in the context of $D = 5$ Kaluza-Klein theory [89].

1.2.5. Holography and the AdS/CFT Correspondence

We now turn to a discussion of the remarkable AdS/CFT correspondence. This is a duality that has been conjectured to exist between a string theory defined on some spacetime and a quantum (often conformal) field theory defined on the conformal boundary of that spacetime. The canonical (and original example) conjectures the equivalence between the following theories:

- Type IIB superstring theory (with string coupling g_s) on $AdS_5 \times S^5$ where both the AdS_5 and S^5 have the same radius L.

- $\mathcal{N} = 4$ super-Yang Mills theory in four dimensions, with gauge group $SU(N)$ and Yang-Mills coupling g_{YM}.

The equivalence relates the parameters in the two theories as follows:

$$g_s = g_{YM}^2\,, \qquad\qquad L^4 = 4\pi g_s N(\alpha')^2\,, \tag{1.2.25}$$

where $\alpha' = l_s^2$, is the square of the string length scale. Such an equivalence is heuristically motivated by the observation that the isometry group of AdS_5, namely $SO(2,3)$ is the same as the conformal group of $\mathcal{N}=4$ super Yang-Mills in four dimensions, but this correspondence implies something far stronger, namely that the partition functions defining the two theories are in fact equal [18, 90, 91, 92]. Due to the complexity of studying string theory on curved backgrounds, whilst this conjecture as stated is striking, it is difficult to use in practice. It turns out therefore to be useful to consider two limits of the above duality. If we keep the 't Hooft coupling $\lambda \equiv g_{YM}^2 N = g_s N$ fixed but let $N \to \infty$, the perturbation theory on the field theory side can be organised as a topological expansion in planar Feynman diagrams with subleading non-planar corrections that all vanish in this limit [17]. Since $g_s = \lambda/N$ (with λ fixed), this limit corresponds to weakly coupled string perturbation theory. Having taken this limit, the only remaining parameter is λ. Perturbation theory in QFT corresponds to $\lambda \ll 1$, but it is instructive to instead consider what happens when $\lambda \gg 1$. It can be shown by consideration of the low energy effective action of string theory that in the large λ limit, higher curvature corrections are suppressed and the theory reduces to *semi-classical* type IIB supergravity [93]. Practically speaking, if one omits fermions (as is standard practice in the study of classical solutions to supergravity), we then have a correspondence between semi-classical general relativity coupled to matter on some spacetime and quantum field theory on the conformal boundary of the spacetime. Note also that whilst the gravity theory is weakly coupled, the gauge theory is strongly interacting (and not in its perturbative regime) in this limit.

Various generalisations of the original duality now exist [94], but the essential elements of the construction remain the same. A gravitational theory defined on a background that asymptotes to a product of some manifold with well defined asymptotics (often asymptotically AdS or a deformation thereof) with a compact space is dual to a quantum field theory in (usually) one dimension less than the non-compact space, defined on the boundary of the latter. This equivalence has become known as *gauge-string duality* (also *gauge-gravity duality*) or *holography*[10], and it is this form of the duality that will be discussed in this thesis. In order to

[10]This is in reference to the *holographic principle* [95, 96] which states that the physical description of a volume of space can be thought of as encoded on the surface of that region. AdS/CFT is hence an explicit realisation of this principle.

proceed to use this though, we need to discuss the mapping of observables from one side of the duality to the other - the 'Holographic Dictionary'.

Setup and Holographic Dictionary

In order to use holography in practical scenarios, it is useful to push the correspondence somewhat further than what we have discussed thus far. In the Wilsonian approach, QFTs are most elegantly defined via an ultraviolet cutoff or ultraviolet fixed point, the latter rendering the theory valid at all scales. Such a fixed point is a useful conceptual place to begin a holographic construction. By definition at this point, the theory is scale invariant and in general we have the symmetry

$$t \to \lambda^z t\,, \quad \mathbf{x} \to \lambda \mathbf{x}\,, \tag{1.2.26}$$

where we note that we have assumed spatial isotropy and emphasise that the scaling symmetry need not act the same way on space and time - hence the inclusion of the dynamical critical or *Lifshitz* exponent z. The holographic prescription then suggests that we consider a spacetime metric in one dimension higher in which these symmetries are realised geometrically. One is led to consider [97],

$$ds^2 = L^2 \left(-\frac{dt^2}{r^{2z}} + \frac{dx_i dx^i}{r^2} + \frac{dr^2}{r^2} \right)\,, \tag{1.2.27}$$

where $i = 1, \ldots, d-1$, (d being the number of spacetime dimensions of the dual QFT). The claim of gauge-gravity duality is then that the physics of some strongly coupled, dual field theory is encapsulated in the gravitational background (1.2.27). The $z > 1$ case is a candidate dual to some non-relativistic QFT, whilst the $z = 1$ case corresponds to AdS space, and for this particular value, the symmetries at the fixed point are relativistic[11]. We restrict attention to the $z = 1$ case in this introduction for simplicity, although aspects of the Lifshitz case (and generalisations) will appear in chapter 2. The extra dimension r is to be interpreted as a geometrisation of the field theory energy scale, with the scale invariant theory (1.2.27) describing the high energy (small r) physics. One may then deform this theory by relevant operators or by introducing finite temperature/chemical potential to describe interesting IR physics. To do this, one considers a general metric ansatz (without the symmetry (1.2.26)) and solves the Einstein equations (coupled to whatever matter content exists in the bulk). In the case of vacuum gravity with negative cosmological

[11]In the $z = 1$ case, in addition to rotations, spacetime translations and dilatations, the theory also has Lorentz boost symmetries as well as special conformal symmetries.

constant, one finds an AdS Schwarzchild black hole[12]

$$ds^2 = \frac{L^2}{r^2}\left(-f(r)dt^2 + \frac{dr^2}{f(r)} + dx^i dx_i\right) \text{ with } f(r) = 1 - \left(\frac{r}{r_+}\right)^d . \tag{1.2.28}$$

This solution is asymptotically AdS, but differs from this in the IR (large r) region, having a horizon at $r = r_+$. By the arguments of section 1.2.3, this horizon has a temperature and this immediately suggests that this IR physics is the dual description to placing our QFT at finite temperature. To describe finite charge density or chemical potential μ due to for example a global $U(1)$ symmetry in the QFT, we need only include a $U(1)$ gauge field in the bulk action. This can source charge density directly, and also allows the distinct possibility of charge density being sourced by a Reissner-Nordstrom AdS black hole in the bulk [7],

$$\begin{aligned} ds^2 &= \frac{L^2}{r^2}\left(-f(r)dt^2 + \frac{dr^2}{f(r)} + dx^i dx_i\right), \qquad A_t = \mu\left(1 - \left(\frac{r}{r_+}\right)^{(d-2)}\right) \\ \text{with} \quad f(r) &= 1 - \left(1 + \frac{r_+^2\mu^2}{\gamma^2}\right)\left(\frac{r}{r_+}\right)^d + \frac{r_+^2\mu^2}{\gamma^2}\left(\frac{r}{r_+}\right)^{2(d-1)} \end{aligned} \tag{1.2.29}$$

and $\gamma^2 = \frac{(d-1)e^2L^2}{(d-2)\kappa^2}$ (e and κ are the electromagnetic and gravitational coupling constants that appear in the bulk action respectively). To describe non-trivial low energy physics then, we see that our bulk gravitational action in principle has several fields in addition to the metric $g_{\mu\nu}$, such as gauge fields A_μ as well as scalars (that will be discussed shortly). All these fields tend to particular values on the boundary and this plays a crucial role in what follows. We have

$$\begin{aligned} g_{\mu\nu}(r) &= \frac{L^2}{r^2} g_{(0)\mu\nu} + \dots , \\ A_\mu(r) &= A_{(0)\mu} + \dots \qquad \text{as} \quad r \to 0 , \end{aligned} \tag{1.2.30}$$

where we work in Graham-Fefferman coordinates (the AdS analogue of Gaussian normal coordinates) with $g_{rr} = \frac{L^2}{r^2}$ and $g_{ra} = 0$ where $a = \{t, i\}$. It turns out that we may then interpret $g_{(0)\mu\nu}$ and $A_{(0)\mu}$ as the background metric and source of the dual field theory respectively as we now review.

In addition to perturbing the scale invariant QFT by finite temperature/chemical potential, one may also consider directly perturbing by relevant operators. It is first

[12]In cases, where $z \neq 1$, one would again generically find a black hole with a horizon in the IR of the spacetime, but the asymptotics would correspond to Lifshitz and not AdS. Such solutions may be found numerically, but are likely impossible to write down in closed analytic form.

instructive to rewrite the introduction of finite temperature and chemical potential in this language. Recall that the (QFT) stress tensor is defined as $T^{\mu\nu} = \delta S/\delta g_{(0)\mu\nu}$[13] and consider perturbing the bulk metric such that its boundary value becomes $g_{(0)} + \delta g_{(0)}$. The field theory action changes according to $\delta S = \int d^d x \sqrt{-g_{(0)}}\, \delta g_{(0)\mu\nu} T^{\mu\nu}$ and equality of the bulk and boundary path integrals then requires

$$Z_{\text{bulk}}[g \to g_{(0)} + \delta g_{(0)}] = \langle e^{i\int d^d x \sqrt{-g_{(0)}}\, \delta g_{(0)\mu\nu} T^{\mu\nu}} \rangle_{QFT}\,, \tag{1.2.31}$$

from which we see explicitly the claim above, that the boundary value of the bulk metric gives the background field theory metric. Similarly, the field theory current associated to the global $U(1)$ symmetry is $J^\mu = \delta S/\delta A_{(0)\mu}$, and we may write an analogous relation on perturbing the boundary value of $A_{(0)\mu}$, which shows that the boundary value of the bulk gauge field gives the source of the dual theory. More generally the *holographic dictionary* states that there is a map between QFT operators $\mathcal{O}$ and bulk dynamical fields ϕ defined by

$$Z_{\text{bulk}}[\phi \to \phi_{(0)} + \delta\phi_{(0)}] = \langle e^{i\int d^d x \sqrt{-g_{(0)}}\, \delta\phi_{(0)} \mathcal{O}} \rangle_{QFT}\,. \tag{1.2.32}$$

We see that that this describes the perturbation of the field theory Lagrangian by $\delta\phi_{(0)}\mathcal{O}$ and if the operator $\mathcal{O}$ is relevant, this perturbation generates a renormalisation group flow into the IR. The quantity $\phi_{(0)}$ is defined by including the bulk field $\phi(r)$ in the gravitational action and examining the boundary behaviours admitted by its equation of motion. As an example, for a real scalar one finds

$$\phi(r) = \left(\frac{r}{L}\right)^{d-\Delta} \left(\phi_{(0)} + \ldots\right) + \left(\frac{r}{L}\right)^{\Delta} \left(\phi_{(1)} + \ldots\right) \qquad \text{as} \quad r \to 0\,, \tag{1.2.33}$$

where the quantity Δ is one of the solutions of the quadratic $(Lm)^2 = \Delta(\Delta - d)$ [34]. (There are two solutions: Δ and $d - \Delta$) and the ellipses in this expansion consist of terms involving higher powers of (r/L), the coefficients of which are determined uniquely in terms of $\phi_{(0)}$ and $\phi_{(1)}$. (Since the field equations are second order, there are only two undetermined constants). Moreover, one can show that the scaling dimension of the dual operator $\mathcal{O}$ is equal to Δ and from this we see that the operator is relevant or marginal when $\Delta \leq d$ [90]. Finally, to complete our survey of the holographic dictionary we note that it turns out that the expectation value of the dual operator $\mathcal{O}$ (which will generically be induced by the deformations described above) is given by $\langle\mathcal{O}\rangle = \frac{(2\Delta-d)}{L}\phi_1$[14].

[13]There is usually a -2 in the definition of the stress tensor, so that $T^{\mu\nu} = -2\delta S/\delta g_{(0)\mu\nu}$ but we have chosen to absorb this into the normalisation of S here, to avoid factors of two later.

[14]To derive the expression for $\langle\mathcal{O}\rangle$, one must add counterterms to the on shell action, according

We close our overview of applied holography by noting one final ingredient that will be relevant to the discussion in chapter 2. We have thus far discussed the inclusion of vector and real scalar fields in the bulk gravitational action, but it is also of interest to consider a charged, complex scalar (with an associated gauge covariant derivative). Much of the richness in condensed matter arises due to the onset of ordered phases at low temperatures that arise as instabilities of the (naive) vacuum to the formation of a symmetry breaking condensate. A striking example of such a phenomenon is superconductivity and the inclusion of a bulk charged scalar, allows for a holographic description of this phenomenon. The normal phase is described by the Reissner-Nordstrom black hole which becomes unstable below a critical temperature [99], leading to a new branch of black holes that support charged scalar 'hair' and describe the broken superconducting phase[15].

1.3. Static Elliptic Numerical Relativity

The classic approach to find static and stationary gravitational solutions is to simulate a dynamical collapse of matter that is likely to form the solution of interest. Such techniques are well understood and extremely powerful, but unfortunately also typically highly complicated, requiring large computing resources. Moreover, in order to find the correct (late-time) solution by these methods, one would have to run a given dynamical evolution for a long time to ensure that the solution in question has 'rung-down' to a stationary state, losing all its excitations as gravitational radiation. This can in fact be a serious challenge and if one is only interested in the final state, it is natural to ask if we are doing a great deal more work than necessary by using such methods. A second motivation for developing alternative techniques for constructing stationary solutions is that some are likely to be unstable (at least in certain regions of parameter space). This is of particular relevance for example in holographic condensed matter where these unstable geometries can play a crucial physical role (see chapter 2). Another example is in Kaluza-Klein theory where to shed light on the global phase structure of the space of solutions, it is important to construct the inhomogeneous black string solutions which suffer a Gregory-Laflamme instability. Whilst one could envision tuning initial data in some dynamical collapse process to find such unstable solutions, it is likely that in practice this would be very

to the prescription of holographic renormalisation [34, 98]. The counterterms differ according to which solution for Δ is chosen. An example can be found in chapter 2, but we will not need the full formalism here.

[15]Violation of the black hole 'no hair' theorems is possible even in $D = 4$ in this setting as we are in asymptotically AdS, as opposed to asymptotically flat spacetime.

hard. In this section we shall review the elliptic approach[16] to numerical relativity, that has proven extremely useful in building both static and stationary solutions.

1.3.1. Ansatz for Static Black Holes

We shall develop the approach to the static vacuum case following the methods of Headrick, Kitchen and Wiseman [21]. Consider a general, non-extremal static black hole solution with a single component horizon so that we may write the metric as

$$ds^2 = -N(x)^2 dt^2 + h_{ij}(x) dx^i dx^j \,, \tag{1.3.34}$$

where $\partial/\partial t$ is the Killing vector that generates the static $U(1)$ isometry and the norm of this vector vanishes at the black hole horizon. (Note also that N is normalised such that $N \to 1$ at infinity). One can calculate the surface gravity for this form of the solution and one finds that it is given by the function $\kappa = \partial_n N|_{N=0}$, where n is the unit vector that is normal to the horizon in a constant t slice. By the zeroth law of black hole mechanics, this quantity is a constant across the horizon. We may now follow Euclidean quantum gravity, and analytically continue this metric to Riemannian signature by passing to an imaginary time coordinate $\tau = it$,

$$ds^2 = N(x)^2 d\tau^2 + h_{ij}(x) dx^i dx^j \tag{1.3.35}$$

where to satisfy the requirement that the metric be smooth at the horizon (and in particular to ensure the absence of conical singularities there) we make τ an angular coordinate with period $\tau \sim \tau + 2\pi/\kappa$. To make this discussion more explicit, we can choose Gaussian normal coordinates to the horizon where we have $x^i = \{r, x^a\}$ and without loss of generality we may choose the horizon to be at $r = 0$. Near the horizon, the metric then looks like

$$ds^2 \sim (\kappa^2 r^2 d\tau^2 + dr^2) + \tilde{h}_{ab}(r, x) dx^a dx^b \,, \tag{1.3.36}$$

[16] Some comments on the history of this approach are in order: It is only with the recent observation that black hole uniqueness is violated in $D > 4$ that numerical gravity in higher dimensions took centre stage. Interestingly, a key ingredient in the classic proofs of $4D$ black hole uniqueness was to formulate the associated stationary problem as an elliptic system [53], in a similar manner to what we shall do. This same elliptic problem has also featured prominently in the context of relativistic stars [100, 101, 102, 103] and to find exotic charged solutions [104, 105]. In these cases, the Weyl form of the metric, together with the isometries can be used to reduce the problem to an elliptic one. In higher dimensions, things are much less constrained, but there are some uniqueness theorems for *vacuum* solutions that phrase the problem as an elliptic system, again exploiting the Weyl form of the metric [74, 106, 107, 108, 109].

where we can now see explicitly that the shrinking Euclidean time circle forms the angle of polar coordinates in $\mathbb{R}^2$ where r is the usual radial variable. We now stress an important point, namely that although this polar coordinate chart breaks down at $r = 0$, there is nothing pathological about this location, as can be seen simply by shifting to coordinates of the form $X = r\cos(\kappa\tau)$ and $Y = r\sin(\kappa\tau)$. In this way, one can write the metric in a chart that covers the horizon. (Whilst it is almost always sensible, particularly for numerical implementations, to choose coordinates adapted to the isometries of the problem, one should always bear in mind that one can always go to these 'Cartesian' coordinates where there is then no horizon boundary).

In summary, a static black hole may be written as a smooth Euclidean geometry where Euclidean time is periodic and the Killing vector $\partial/\partial\tau$ generates a $U(1)$ isometry. There is no boundary at the horizon (the fixed point set of the isometry) and the geometry is regular there[17]. A useful feature of this line of reasoning is that analytic continuation in time is precisely what is done in semi-classical quantum gravity to consider finite temperature. If one imposes boundary data that fixes the proper size of this Euclidean time circle asymptotically, we then have the rather physical interpretation of working in the canonical ensemble at fixed temperature. We note also that since vacuum solutions of the Einstein equations are Ricci flat, the procedure of finding static vacuum black holes may now be regarded as part of the more general problem of finding Ricci flat Riemannian geometries. This has a variety of applications beyond black hole theory, and notably might provide new ways to construct the complex, Kähler and Calabi-Yau metrics that underpin our current understanding of string compactifications [110, 111].

We now discuss how to view the problem of finding Ricci flat Riemannian geometries as an elliptic boundary value problem.

1.3.2. Hyperbolicity, Ellipticity and the Harmonic Einstein Equation

The mathematical structure of the vacuum Einstein equations $R_{\mu\nu} = 0$ is important to develop in some detail. In order to do so, we first introduce some formal aspects of the theory of partial differential equations (we follow [112, 113, 114, 115]). We

[17] The situation is in fact slightly more subtle as we will discuss in chapter 3. If one uses coordinates that manifest the static isometry, there will be a 'fictitious boundary' at the horizon, where the coordinate chart breaks down. Regularity conditions should be imposed there and are derived by examining the coordinate transformation to a chart which does cover the horizon. In the stationary case a similar situation also arises at axes of rotational symmetry.

begin by considering the system of equations

$$u_t = P(D)u \,, \qquad P(D) := \sum_{|\nu|\leq m} A^\nu D_\nu = \sum_{|\nu|\leq m} A^\nu \frac{\partial^{|\nu|}}{\partial x_1^{\nu_1}\dots\partial x_n^{\nu_n}} \,, \tag{1.3.37}$$

where $u(x,t) = (u_1(x,t), u_2(x,t), \dots)$, $u_t = \frac{\partial u}{\partial t}$, $\nu = (\nu_1, \dots, \nu_n)$ (with the v_i non-negative integers) and $|\nu| = \nu_1 + \dots + \nu_n$. We are interested in the so called *Cauchy problem* for the above PDE system, defined as follows: Given initial data at some time $t = 0$, $u(x,0) = f(x)$, under what conditions can one guarantee the existence of a unique solution $u(x,t)$ for all $t > 0$.

The system (1.3.37) can be solved formally by appealing to Fourier analysis. If we write the initial data for the Cauchy problem as

$$f(x) = \frac{1}{(2\pi)^{n/2}} \int_{-\infty}^{\infty} e^{ik.x} \phi(k) dk \,,$$

then one may check explicitly that the solution is given by

$$u(x,t) = \frac{1}{(2\pi)^{n/2}} \int_{-\infty}^{\infty} e^{ik.x} e^{P(ik)t} \phi(k) dk \,, \tag{1.3.38}$$

where $P(ik)$ is the *symbol* of the associated differential operator $P(D)$. (The symbol is defined by $P(D)e^{ik.x} = P(ik)e^{ik.x}$ and is formally obtained by substitution of ik_j for $\partial/\partial x_j$ in the expression for $P(D)$). It is clear already at this level, that whilst (1.3.38) represents a formal solution of the system (1.3.37), the integral itself may have serious convergence problems if $|e^{P(ik)t}|$ is unbounded for large k (where the norm here is to be interpreted as a matrix norm). It is this observation that leads to the notion of *well-posedness*, namely that we require sensible *physical* solutions of a PDE system to depend continuously on the initial data f (in some norm). Moreover for given initial data, that solution should be *unique*. More precisely, the Cauchy problem defined above is said to be well-posed if there exist constants α, K such that

$$|e^{P(ik)t}| \leq K e^{\alpha t} \qquad \forall t > 0 \,, k \,. \tag{1.3.39}$$

One may then demonstrate, using the equivalence of norms, that the above condition is equivalent to the existence of a bound on the solution itself in terms of the initial data,

$$||u(\cdot,t)|| \leq K e^{\alpha t} ||f|| \qquad \forall t > 0 \,, \tag{1.3.40}$$

where $||\cdot||$ is usually taken to be a Sobolev norm.

As an elementary example, we note that the wave equation $y_{tt} = y_{xx}$ is well-posed according to the definition above as it may be written as

$$u_t = Au_x \ , \qquad A = \begin{pmatrix} 0 & 1 \\ 1 & 0 \end{pmatrix} ,$$

where we have defined $u_1 = y_t, u_2 = y_x$. Since the matrix A may then be diagonalised by a unitary transformation U, the symbol takes the form,

$$P(ik) = ikA = U^\dagger \begin{pmatrix} ik & 0 \\ 0 & -ik \end{pmatrix} U \, ,$$

and hence $|e^{P(ik)t}| = 1$ thus proving well-posedness.

In many cases, as with the preceding examples, it is possible to reduce the task of checking for well-posedness to an algebraic calculation. In particular, one may show in general that the Cauchy-problem for first order systems (i.e. those of the form (1.3.37) but restricted to at most single spatial derivates) is well-posed if and only if the symbol (i.e. $A^\nu k_\nu$) has pure imaginary eigenvalues and is diagonalisable [113]. We call such a system for which the Cauchy problem is well-posed *strongly hyperbolic*, and thus the latter conditions on the symbol define strong hyperbolicity. If the eigenvalues of the symbol are pure imaginary, but it does not possess a complete set of eigenvectors (i.e. it is not diagonalisable), the PDE system is *weakly hyperbolic*. Weak hyperbolicity is insufficient to guarantee well-posedness as we have defined it in (1.3.40). We note also the case where the A^ν matrices are symmetric, in which case the system is *symmetric hyperbolic*. Symmetric hyperbolicity implies strong hyperbolicity (as the symbol is then diagonalisable by a unitary transformation) and thus such systems are well-posed.

Higher order linear PDEs can generically be rewritten as systems of first order equations, and thus the definitions of hyperbolicity given above may then also be applied to such systems. It is important nevertheless to give a separate definition of hyperbolicity for second order equations (that also extends to higher orders and to the nonlinear case [114]). Note that following [112], we previously defined the symbol of the differential operator in equation (1.3.37) for systems that are first order in time. This definition necessarily picks a preferred 'time' coordinate. One can in fact give a more covariant definition of the symbol that also extends to systems that are higher order in time (e.g. the second order systems we would like to discuss). We consider

$$\mathcal{D}[u(x^\alpha)] = F(x^\alpha) \ , \qquad \mathcal{D} := \sum_{|\nu|\leq m} A^\nu D_\nu = \sum_{|\nu|\leq m} A^\nu \frac{\partial^{|\nu|}}{\partial t^{\nu_1}\dots\partial x_n^{\nu_n}} \ , \tag{1.3.41}$$

where the time coordinate $t = x_1$ is now part of $\mathcal{D}$ and has no preferred significance. The symbol of the operator $\mathcal{D}$ is then defined as before by making the transformation $\partial \to ik$. To be explicit, in the case of a second order equation, equation (1.3.41) may be rewritten as $(Q^{jk}\partial_j\partial_k + R^j\partial_j + S)\phi = 0$ with $\partial_j = \frac{\partial}{\partial x^j}$, and the principal symbol is then $-Q^{jk}k_jk_k$. (The qualifier *principal* here indicates that only the highest order terms in the symbol are retained. The reader may take this as the defining equation of the principal symbol for second order PDEs). A second order PDE is hyperbolic if its *principal symbol* has real, non-zero eigenvalues, with a single eigenvalue of opposite sign to the rest and hence hyperbolicity is governed by the matrix Q^{jk}. Strong hyperbolicity requires in addition that the principal symbol be diagonalisable and weak hyperbolicity refers to those hyperbolic equations with a non-diagonalisable principal symbol. Strong hyperbolicity defined in this way again guarantees well-posedness.

In order to discuss general relativity, the preceding discussions of well-posedness must be extended to encompass also nonlinear systems of PDEs with non-constant coefficients. There are various approaches to this problem and we only outline aspects here (see [113] in particular for a very clear exposition.). In the general case, the A^ν matrices that enter equation (1.3.37) are functions of the spacetime coordinates as well as the unknown vector function u, i.e. $A^\nu = A^\nu(t, x, u)$. (Here we are assuming *quaslinearity* so that there is no dependence on ∇u). One can show that for some systems a *linearisation principle* holds, namely that a nonlinear PDE problem is well-posed at $u = u_0$ if the linear problem obtained by linearising about u_0 is well-posed [113]. For technical reasons however, in the nonlinear case, most solutions ultimately develop singularities in finite time and hence well-posedness is only meaningful for short times [112]. Moreover, it is also important to note that there exist systems where this principle fails - the linearisation is well-posed and yet the full nonlinear problem is not [113]. In addition to linearisation, there is also the powerful *localisation principle*. This relates well-posedness of the general problem with variable coefficients to a constant coefficient problem. That is to say, if well-posedness is proven for the *frozen* coefficient problem that has $A^\nu = A^\nu(x_0, t_0, u_0)$, then the corresponding variable coefficient problem is also well-posed [113]. Such a localisation principle unfortunately emphatically does not hold for general PDEs, but it may be shown to hold in the strongly hyperbolic case[18]. Well-posedness of the full non-linear problem may then reliably be studied by linearising the equations and freezing coefficients.

Being able to cast systems of PDEs in strongly hyperbolic form is extremely useful for numerical implementation. The principal reason for this being that such systems are guaranteed to be well-posed (at least for short times) and hence one has bounds on the growth of the solution and its derivatives. Provided one then uses stable algorithms, any errors that accrue over the course of a simulation may themselves be bounded. (In particular the error goes to zero as some power of the step size with the coefficient of proportionality known).

Physically, hyperbolic equations admit wave-like solutions which travel along the *characteristic* directions of the equation given by the zeros of the principal symbol. The speeds of these disturbances are moreover given by the magnitudes of the eigenvalues of the princpal symbol. In addition to hyperbolic equations, we will also in what follows be interested in aspects of the theory of elliptic equations which we now discuss.

The differential operator $\mathcal{D}$ in (1.3.41) is said to be *elliptic* if its principal symbol is invertible,

$$\sum_{|\nu|=m} A_\nu (ik_1)^{\nu_1} \dots (ik_n)^{\nu_n} \neq 0 \qquad \forall k_i \neq 0\,, \tag{1.3.42}$$

and has real eigenvalues of the same sign (either all positive or all negative) [115]. The operator is further *strongly elliptic* if the principal symbol is diagonalisable and *weakly elliptic* if it is not, in which case it does not possess a complete set of eigenvectors. The fact that the principal symbol is invertible indicates the absence of real characteristic directions and thus elliptic equations do not describe the propagation of information. (Indeed they often arise as the description of the *steady state* of hyperbolic systems). It is important to stress that the Cauchy problem defined previously is ill-posed for elliptic equations. The correct way to specify data for such systems is as a Dirichlet/Neumann or mixed boundary value problem where data is supplied on all spatial boundaries of the problem and the equations are then

[18] Well-posedness of PDEs can be shown to be equivalent to the existence of an ‘energy norm’, a positive definite Hermitian form $H(k)$ satisfying $H(k)P(ik) + P^\dagger(ik)H(k) \leq 2\alpha H(k)$ (where the inequality is saturated with $\alpha = 0$ for first order systems). In the non-constant coefficient case $H = H(k,t,x,u)$. Hyperbolicity for full nonlinear systems may then be defined directly in this context: If the Hermitian form depends explicitly on k the system is strongly hyperbolic. If it does not, it is symmetric hyperbolic. (Weak hyperbolicity again refers to the absence of a complete basis). With these definitions for the nonlinear problem, one can prove well-posedness in the sense of (1.3.40) which can then be related to well-posedness of the linearised and localised problems schematically leading to the principles sketched in the main text [112].

solved within the domain of interest. Having summarised the relevant aspects of the theory of PDEs, we may now proceed to apply this formalism to the general theory of relativity.

The Einstein equations are second order quasilinear PDEs in the metric components. To proceed, we begin by linearising these equations in perturbations $h_{\mu\nu}$ about some background spacetime $g_{\mu\nu}$. The equations then become

$$\delta R_{\mu\nu} \equiv \Delta_R h_{\mu\nu} = \Delta_L h_{\mu\nu} + \nabla_{(\mu}\nu_{\nu)} \,, \tag{1.3.43}$$

with

$$\Delta_L h_{\mu\nu} \equiv -\frac{1}{2}\nabla^2 h_{\mu\nu} - R_{\mu}{}^{\kappa}{}_{\nu}{}^{\lambda} h_{\kappa\lambda} + R_{(\mu}{}^{\kappa} h_{\nu)\kappa} \,, \qquad \nu_\mu \equiv \nabla_\nu h^{\nu}{}_{\mu} - \frac{1}{2}\partial_\mu h \,, \tag{1.3.44}$$

where the operator Δ_L is known as the Lichnerowicz operator. As discussed above, the qualitative character of a PDE is determined by studying its principal symbol. This corresponds (in real-space) to retaining only the largest derivative contributions to the full equation - here the two derivative terms. Denoting such contributions to Δ_R as P_g, we have that

$$P_g h_{\mu\nu} = \frac{1}{2}\left(g^{\alpha\beta}\partial_\mu\partial_\alpha h_{\beta\nu} + g^{\alpha\beta}\partial_\nu\partial_\alpha h_{\beta\mu} - g^{\alpha\beta}\partial_\alpha\partial_\beta h_{\mu\nu} - g^{\alpha\beta}\partial_\mu\partial_\nu h_{\alpha\beta}\right) \,. \tag{1.3.45}$$

(Note that the principal symbol can be obtained from the above equation by pulling out the metric perturbation and exchanging derivatives for wavenumbers $\partial_\alpha \to k_\alpha$, but we can equivalently work in real space with P_g). This linear operator governs the short wavelength behaviour of perturbations about the background and hence determines the character of the equations. As discussed above, the condition that $R_{\mu\nu} = 0$ be elliptic about some background g is that the principal symbol be non-vanishing for all wavenumbers. Physically, this corresponds to the requirement that nowhere can we find a point where short wavelength perturbations propagate as a wave. That is to say, writing $h_{\mu\nu} = a_{\mu\nu}e^{ik_\alpha x^\alpha}$ for some constants $a_{\mu\nu}$ and any real non-zero k_μ, ellipticity requires that $P_g h_{\mu\nu} \neq 0$ everywhere.

The Euclidean Einstein equations as we have defined them however are not elliptic. In fact, they are elliptic only on the 'physical' degrees of freedom with the principal symbol annihilating pure gauge modes[19]. To see this more explicitly, observe that for perturbations of the form $h_{\mu\nu} = \partial_{(\mu}u_{\nu)}$ where u is some arbitrary vector field, the aforementioned ellipticity condition is violated as $P_g h_{\mu\nu} = 0$. Since we may

[19]By 'physical' we refer to transverse metric perturbations. These are only true physical modes in certain gauges (e.g Lorenz gauge) but we shall use this terminology for convenience of expression nonetheless

think of a diffeomorphism generated by some vector field u as a perturbation of the form $h_{\mu\nu} = \nabla_{(\mu}u_{\nu)}$, which on small scales reduces to $h_{\mu\nu} = \partial_{(\mu}u_{\nu)}$, we may regard the lack of ellipticity of $R_{\mu\nu} = 0$ as a consequence of gauge invariance. Moreover, note also that we may write any metric perturbation as $h_{\mu\nu} = \hat{h}_{\mu\nu} + \nabla_{(\mu}u_{\nu)}$, where the former part is the 'physical' transverse mode satisfying $\partial_\nu \hat{h}^\nu{}_\mu - \frac{1}{2}\partial_\mu \hat{h} = 0$ and the latter is the longitudinal, pure gauge part. We have shown above that the principal symbol annihilates the gauge mode and one may also show that it acts on the transverse mode as a Laplacian $-\frac{1}{2}\nabla^2$. We conclude therefore that the Einstein equations are *weakly* elliptic in Euclidean signature (and *weakly* hyperbolic in Lorentzian signature)[20]. More heuristically, one could preempt this behaviour by observing that whilst the Einstein equations in D dimensions appear at first sight to be $\frac{1}{2}D(D+1)$ equations for $\frac{1}{2}D(D+1)$ metric variables, the D conditions coming from gauge invariance (or the Bianchi identity), together with the D initial value constraints reduce the number of 'physical' equations to $\frac{1}{2}D(D-3)$ making the PDE system underdetermined.

Without an elliptic system of PDEs, we cannot regard the system as a boundary value problem as we wish to do and hence to proceed further, we will have to remedy this. Aside from the fact that we would like the frame the problem in this manner, it is also instructive to discuss other reasons why the the weak ellipticity can cause difficulties and an alternative formulation is desirable. This is particularly true for numerical implementations. Consider for concreteness, a scenario where we represent the metric by the values of its components on some set of lattice points. To be faithfully representable in this manner, the metric components should be smooth on the (real space) scale of the lattice spacing. There is no reason however that this smoothness condition should be preserved by diffeomorphisms and therein lies the problem. Even if our lattice is fine enough to represent a given metric satisfying $R_{\mu\nu} = 0$, other metrics in the same (diffeomorphism) class will not in general be representable and we will need to control which representative of the class we aim for to get a good solution. More practically, since short-wavelength pure gauge modes are not damped out, small errors will accumulate and could eventually cause instabilities.

[20]We note in both signatures that this a slight abuse of terminology as according to the definitions above, weak hyperbolicity and ellipticity do not permit zero eigenvalues of the principal symbol. Following the literature [20, 21], we relax the previous textbook definitions slightly here to allow for zero eigenvalues. The key point is that in both signatures the equations are of 'weak' character (in the sense defined earlier) as the principal symbol does not posses a complete set of eigenvectors. To see this formally one must observe that the multiplicity of the zero eigenvalues of the principal symbol is greater than the dimension of its kernel (which guarantees it cannot be diagonalised).

To proceed, instead of considering the vacuum equations $R_{\mu\nu} = 0$ we will instead consider what we term the *Harmonic* Einstein equation, sometimes also called the Einstein-DeTurck equation[19], $R^H_{\mu\nu} = 0$ where

$$R^H_{\mu\nu} \equiv R_{\mu\nu} - \nabla_{(\mu}\xi_{\nu)} \,, \qquad \xi^\alpha \equiv g^{\mu\nu}(\Gamma^\alpha{}_{\mu\nu} - \bar{\Gamma}^\alpha{}_{\mu\nu}) \,. \tag{1.3.46}$$

Here Γ is the usual Levi-Civita connection of g, but $\bar{\Gamma}$ is another connection, the reference connection that we are free to choose. The quantity ξ is constructed from the difference of two connections and is hence a *globally* defined vector field. (This is worth emphasising as although in this 'a posteriori' gauge fixing prescription, the gauge invariance is lifted on fixing ξ, the method nevertheless remains fully covariant. The principal part of the linearisation of the Harmonic Einstein equations about the background g simplifies substantially and is given by

$$P^H_g h_{\mu\nu} = -\frac{1}{2} g^{\alpha\beta}\partial_\alpha\partial_\beta h_{\mu\nu} \,. \tag{1.3.47}$$

For static black holes, as discussed in the previous subsection we may analytically continue the geometry to a Riemannian manifold and the equations are then strongly elliptic by our previous definitions as desired. (To show this physically, one takes $h_{\mu\nu} = a_{\mu\nu}e^{ik_\alpha x^\alpha}$ as before, and then $P^H_g h_{\mu\nu} = \frac{1}{2}k^\alpha k_\alpha h_{\mu\nu}$ which only vanishes when $h_{\mu\nu} = 0$ or $k_\mu = 0$). If we work instead in Lorentzian signature, the equations are not elliptic (one can clearly violate the ellipticity condition by choosing k to be a null vector), but are strongly hyperbolic. The Harmonic Einstein equations were in fact used historically in this latter context to prove well posedness of the (dynamical) hyperbolic initial value problem for general relativity [116].

In order to completely specify the Harmonic Einstein equations, we must now make some choice for the reference connection $\bar{\Gamma}$. In what follows, we will reduce the freedom in the definition above somewhat by taking $\bar{\Gamma}$ to be the Levi-Civita connection of a reference metric that we are free to choose and that we will then consider fixed. In this specific case, one may then write the DeTurck vector as

$$\xi_\mu = g^{\alpha\beta}\left(\bar{\nabla}_{(\alpha}g_{\beta)\mu} - \frac{1}{2}\bar{\nabla}_\mu g_{\alpha\beta}\right) \,, \tag{1.3.48}$$

where $\bar{\nabla}$ is the covariant derivative of the metric $\bar{g}$.

In order to check that the gauge symmetry has been completely fixed, it is useful to perform a simple parameter count at this point. In D dimensions there are D local coordinate degrees of freedom (associated with diffeomorphisms) to fix in order to remove the gauge invariance associated with the Ricci flatness condition. The vanishing of the DeTurck vector ξ may be thought of as providing these additional D (local) conditions. It is instructive to note that the DeTurck scheme of gauge fixing may be viewed as analogous to the generalised harmonic coordinates of Friederich and Garfinkle [117, 118]. In generalised harmonic coordinates, one would write (in some local chart) $\xi^\alpha = g^{\mu\nu}\Gamma^\alpha_{\mu\nu} + H^\alpha$ for some H^α. Note however that H^α need not be a globally defined vector field and hence our method should really be thought of as a global version of these coordinates. Locally, to make contact with our method, one would choose $H^\alpha = -g^{\mu\nu}\bar{\Gamma}^\alpha_{\mu\nu}$ and then the vanishing of ξ becomes a generalised harmonic gauge condition. In more detail, if one chooses $\bar{\Gamma}^\alpha_{\mu\nu} = 0$ in some chart with coordinate functions x^α, then the vanishing of the DeTurck vector ξ implies that $\nabla^2_S x^\alpha = 0$, where ∇_S is the scalar Laplacian and thus the coordinate functions are harmonic. (This relation is why they have become known as harmonic coordinates and more generally, for an arbitrary choice of reference connection, one has the 'sourced' equation $\nabla^2_S x^\alpha = H^\alpha$ corresponding to *generalised* harmonic coordinates).

We must now turn to an important issue; Whilst a Ricci flat solution with $\xi = 0$ does indeed solve the Harmonic Einstein equations $R^H_{\mu\nu} = 0$, there is no reason a priori to expect that the reverse is true, namely that a *general* solution to the latter equation will also solve the Ricci flatness condition. It is important to now elaborate on why solving $R^H_{\mu\nu} = 0$ may lead to a Ricci flat solution in a gauge where $\xi = 0$. Furthermore, a related subtlety concerns the issue of under what circumstances such coordinates with $\xi = 0$ actually exist. Demonstrating local existence is relatively straightforward. One considers the effect of a small diffeomorphism on the DeTurck vector, under which we have that $\delta\xi^\mu = -\Delta_V w^\mu$ (where w^μ is the vector that generates the diffeomorphism and Δ_V is an operator we do not write out explicitly). Since it can be shown that Δ_V is a purely elliptic operator, then by the existence theorems for ellliptic PDEs, we may argue that there exist local coordinates such that $\xi'^\mu = \xi^\mu + \delta\xi^\mu = 0$. The question of global existence however is considerably more difficult and only partial results are known. These are conventionally phrased in the language of harmonic maps between manifolds, the condition $\xi = 0$ in this language being equivalent to the statement that the identity map be harmonic. An example of one such partial result is that Eells and Sampson have proven existence of a harmonic identity map with the assumption that the sectional curvature of the target space metric be non-positive [119].

1.3.3. Ricci Flatness, Solitons, and Maximum Principles

A solution to the Harmonic Einstein equations $R_{\mu\nu} = \nabla_{(\mu}\xi_{\nu)}$ with non-vanishing DeTurck vector ξ is termed a Ricci soliton. As explained above, we are interested in true Ricci flat solutions as opposed to solitons and would like to determine under what conditions we will find such solutions. Insight can be gleaned from studying the contracted Bianchi identity applied to the Harmonic Einstein equations (1.3.46), which yields the following PDE for the DeTurck vector

$$\nabla^2 \xi_\mu + R_\mu{}^\nu \xi_\nu = 0 \,. \tag{1.3.49}$$

In the Lorentzian context, if one ensures that ξ and its normal derivative $\partial_n \xi$ vanish on some Cauchy surface, then since equation (1.3.49) is a hyperbolic equation, ξ will remain zero under evolution of the metric in time and we are guaranteed a Ricci flat solution[21].

In the Riemannian elliptic case, whilst the situation is more complex, one has *local uniqueness* of solutions. That is to say, a given solution with well-posed boundary conditions cannot be continuously deformed into another without a suitable adjustment of the boundary data. An immediate consequence of this is that if a Ricci flat solution can be found, then solitons cannot be 'perturbatively' near to it. In practice therefore, solitons are not generally a problem and it is straightforward to determine whether one is converging to a true solution or not - one need only explicitly check the DeTurck vector on the solution in question. (We choose to compute $\phi = \xi^\mu \xi_\mu$ and if it is non-zero anywhere, one can restart the numerics with different data). That said, there are theorems that constrain the existence of solitons in the static case. If we rewrite equation (1.3.49) as $\mathcal{D}.\,\xi = 0$, where $\mathcal{D}_\mu{}^\nu \equiv \nabla^2 \delta_\mu{}^\nu + R_\mu{}^\nu$, we see that a necessary condition for a soliton to exist is that $\mathcal{D}.\,\xi$ must admit non-trivial solutions, i.e. $\mathcal{D}$ must have non-trivial kernel. It has been proven by Bourguignon that this condition is highly restrictive and there are in fact no Ricci solitons on a compact manifold without boundary for *any* choice of ξ [120]. Moreover, as we now review, in non-compact static settings, if the asymptotic boundary conditions are compatible with $\xi = 0$ it can be shown by way of a maximum principle that the kernel is also trivial and one is again guaranteed Ricci flat solutions.

Asymptotics and Maximum Principles

In treating the construction of static black holes as a Riemannian elliptic problem, we must impose data on any boundaries for the PDE system to be well-posed.

[21] To make contact with the formalism used in these dynamical settings, we note that the conditions $\xi^\mu = 0$ and $\partial_n \xi^\mu = 0$ are imposed on a spacelike initial data hypersurface Σ_{t_0} in the ADM splitting. The condition $\xi^\mu = 0$ is not a constraint on the initial data, but on the choice of reference metric. On the other hand, $\partial_n \xi^\mu = 0$ is a non-trivial constraint on the initial data that is equivalent to imposing the $(D-1)$ components of the momentum constraint together with the Hamiltonian constraint.

Whilst there is no horizon boundary, one must impose data asymptotically, (or at some finite value if the spacetime is cut-off there, for example to consider a black hole in a box). Explicitly, in the asymptotically flat case, the metric behaves for large r as

$$ds^2 = g_{\mu\nu}dx^\mu dx^\nu = d\tau^2 + \delta_{ij}dx^i dx^j + \mathcal{O}(r^{-p})\,, \qquad (1.3.50)$$
$$\partial_i g_{\mu\nu} = \mathcal{O}(r^{-p-1})\,, \quad \partial_i\partial_j g_{\mu\nu} = \mathcal{O}(r^{-p-2})\,,$$

where $p > 0$, $r = \sqrt{\delta_{ij}x^i x^j}$ and for a Ricci flat solution, we expect that $p = D-3$. (More complex asymptotics are considered in [121]). We also require that the reference metric is asymptotically flat, and hence is governed by the same structure as above. From this one may compute the behaviour of the DeTurck vector ξ to find

$$\xi^\tau = \mathcal{O}(r^{-p-1})\,, \quad \xi^i = \mathcal{O}(r^{-p-1})\,, \qquad (1.3.51)$$

from which we see that ξ goes to zero asymptotically and hence these asymptotic boundary conditions are consistent with the operator equation $\mathcal{D}.\,\xi = 0$ having trivial solution.

Let us now contract equation (1.3.49) with ξ and use the result $R_{\mu\nu} = \nabla_{(\mu}\xi_{\nu)}$ to obtain

$$\nabla^2\phi + \xi^\mu\partial_\mu\phi = 2(\nabla_\mu\xi_\nu)(\nabla^\mu\xi^\nu) \geq 0\,, \qquad (1.3.52)$$

where as before $\phi = \xi^\mu\xi_\mu$ and the right hand side is of course strictly positive or zero for a Riemannian manifold. One can show that the solutions of (1.3.52) are constrained by a *maximum principle* that states that if ϕ is non-constant then it must attain a maximum on the boundary of the manifold (and moreover ϕ has positive gradient at this maximum). It follows that a necessary condition for a solution to be a Ricci soliton is that either ϕ is a non-zero constant, or alternatively it must have a boundary maximum. In the first case, where ϕ is a non-zero constant, we must have that $\nabla_\mu\xi_\nu = 0$ and hence the solution is in fact Ricci-flat (albeit still a soliton). In the second case where ϕ attains a maximum at the boundary of the manifold or in some asymptotic region, the existence of solitons is constrained by the data prescribed there. In our asymptotically flat example, we have that $\phi \to 0$ in the asymptotic region, but since it must reach a maximum there, and is strictly positive in the interior of the domain, we conclude that $\phi = 0$ throughout the domain and have thus ruled out the existence of Ricci solitons with these boundary conditions.

1.3.4. Numerical Implementations

We close this section by outlining some of the methods to numerically solve the Harmonic Einstein equations. We begin with a treatment of the canonical method used to solve elliptic systems, namely local relaxation which we will shortly show is equivalent in our setting to the famous Ricci flow. We then proceed to review the multidimensional Newton method.

Ricci Flow and Local Relaxation

From the analysis of section (1.3.2), the Harmonic Einstein equations have derivative structure $R^H_{\mu\nu} = -\frac{1}{2}g^{\alpha\beta}\partial_\alpha\partial_\beta g_{\mu\nu} + L_{\mu\nu}$, where $L_{\mu\nu}$ represent terms with less than two derivatives. In local relaxation, instead of proceeding to solve the elliptic equations $R^H_{\mu\nu} = 0$ directly, one searches instead for fixed points of the parabolic diffusion equation

$$\frac{\partial g_{\mu\nu}(\lambda)}{\partial\lambda} = -2R^H_{\mu\nu}\,. \tag{1.3.53}$$

These equations are then discretised on a lattice of points, and local relaxation is implemented for example by the standard algorithm due to Jacobi, whereby given some initial guess for $g_{\mu\nu}$ throughout the domain, one iteratively improves the solution at each point using an update computed from (1.3.53) that depends on nearby points. (Depending on the order of the differencing, the update can depend on neighbouring points, next to nearest neighbours etc.).

Regardless of the details of how local relaxation is implemented (Jacobi, Gauss-Siedel, etc), the continuum diffusion equation that is to be solved is of the form

$$\frac{\partial g_{\mu\nu}(\lambda)}{\partial\lambda} = -2R_{\mu\nu} + 2\nabla_{(\mu}\xi_{\nu)}\,, \tag{1.3.54}$$

which is precisely the Ricci-DeTurck flow, where the second term as discussed previously corresponds to an infinitesimal diffeomorphism, so that the flow is diffeomorphic to the Ricci flow of Hamilton

$$\frac{\partial g_{\mu\nu}(\lambda)}{\partial\lambda} = -2R_{\mu\nu}\,, \tag{1.3.55}$$

which has garnered recent fame in pure mathematics for its pivotal role in the proof of the Poincaré conjecture. (An overview of several aspects of Ricci flow can be found in [122]). We give some initial guess for the parabolic flow and then run the flow for sufficient time so that we approach the fixed point as closely as desired. Such a point will then satisfy $R_{\mu\nu} = 0$ as required. An elegant feature of the Ricci flow picture is that whilst some choice of reference metric is required to construct the vector ξ that we need to include to make the Einstein DeTurck equation elliptic (and hence the resulting diffusion equation parabolic), the Ricci-DeTurck flow is in fact diffeomorphic to pure Ricci flow which makes no mention of ξ and therefore the reference metric. What this means is that given some initial guess metric, whilst different choices of reference will change the path taken by the flow in the space of metrics, it will *not* change the path in the space of physical geometries (i.e. metrics modulo diffeomorphisms) - this path is always the same. Moreover, provided one chooses a reference metric that shares the same isometries as the 'physical' spacetime metric, then the Harmonic Einstein tensor will also be symmetric under these isometries and furthermore these isometries will be preserved under the flow.

It is instructive to study Ricci flow itself a little further. Physically it can be thought of as a diffusion equation for geometry that locally tries to smooth out curvature. Suppose we have some Ricci flat solution $g_{\mu\nu}$ and wish to consider the Ricci flow of a perturbation $h_{\mu\nu}$ to this. From (1.3.43) we have

$$\frac{\partial h_{\mu\nu}}{\partial \lambda} = -2\Delta_L h_{\mu\nu} - 2\nabla_{(\mu}\nu_{\nu)}\,, \tag{1.3.56}$$

where the last term is an infinitesimal diffeomorphism generated by v. For Euclidean space, this flow is then diffeomorphic to a flow where each component of the metric diffuses as, $\frac{\partial h_{\mu\nu}}{\partial \lambda} = \delta^{\alpha\beta}\partial_\alpha\partial_\beta h_{\mu\nu}$ and hence we conclude that Euclidean space is stable to linear perturbations. The flow however has many additional striking non-linear features that cannot easily be seen at this perturbative level. For example, it collapses regions of positive curvature, a fact that can seen by studying the Ricci flow of the round sphere whose radius shrinks with time, eventually collapsing to zero radius in finite time. A further important property of Ricci flow is that it can be shown to preserve asymptotic flatness for short times [123].

It is important to note that a Ricci flat solution will only be stable to perturbations if the Lichnerowicz operator is positive (has positive eigenvalue spectrum). Whilst one is justified in assuming the absence of zero modes, as these can be removed by specification of appropriate boundary data, it is unclear that Δ_L must have a positive spectrum and indeed in a variety of scenarios it does not, so that there exist eigenfunctions with negative eigenvalue. When perturbed by these, such eigenmodes grow exponentially so that at late times the perturbation will flow away from the fixed point in these directions, perhaps ending at some other fixed point. Indeed a fundamental property of static black holes is that the positivity of Δ_L on these backgrounds is tied to their thermodynamics[22] (since the Euclidean action is simply related to the free energy [56]) and many simple examples of interest possess negative modes. A classic example is the Euclidean Schwarzchild black hole which has a single negative mode discovered by Gross, Perry and Yaffe [128]. Negative modes can present a problem for numerics as one has to fine tune initial data in order to hit a solution. We will not review this procedure here, but refer the reader to the literature [21]. Due to the difficulties associated with negative modes, all subsequent elliptic numerics in this thesis will make use of a different numerical algorithm to solve such systems namely Newton's method, a subject to which we now turn. It is worth emphasising beforehand though that despite its difficulties, local relaxation remains in many ways simpler and more elegant than Newton's method and moreover, there are physically relevant situations that are stable under Ricci flow where these techniques are directly useful, a prime example being to find solutions in AdS/CFT where the boundary metric is a black hole [121].

Newton's Method

As we have just seen, whilst local relaxation is elegant and simple to implement it suffers the problem of sensitivity to negative modes and becomes ill suited to use in many practical situations. Fortunately, there is another standard technique to solve elliptic systems known as Newton's method that is insensitive to the stability of the fixed points. Unfortunately it is somewhat more technical to implement than local relaxation and is arguable less elegant (in that it doesn't share the beautiful global geometric features of Ricci flow, such as independence of the background metric). In addition, the basin of attraction for the Newton method is generically rather small (and background dependent), so choosing an initial guess can be something of a challenge. The optimal approach is in fact probably to start with some initial guess, and then use Ricci flow (which doesn't need to start within a basin of attraction) to relax close enough to a solution and then switch to the Newton method (before the negative mode becomes an issue) when one is within the basin of attraction of the fixed point. We should then converge very rapidly to a solution.

[22] Gubser and Mitra conjectured a link between classical and thermodynamic instabilities of horizons [124, 125]. They argued that there is a gravitational instability of a black brane precisely if the horizon has a thermodynamic instability (i.e. negative specific heat). The argument proceeds by using Euclidean quantum gravity to calculate the free energy from the gravitational action and then proves that solutions have Euclidean negative modes if they have negative specific heat (see [126] for a clear account of this and moreover a discussion of when the converse also holds). Many assumptions are made in these analyses and it has now been demonstrated that there are counterexamples to the general conjecture [127].

To implement the Newton method, we again imagine discretising our system on a lattice. If we perturb the metric g as $g + \epsilon\delta g$, the Harmonic Einstein tensor changes as

$$R^H_M(g + \epsilon\delta g) = R^H_M(g) + \epsilon\, \mathcal{O}(g)_M{}^N \delta g_N + O(\epsilon^2)\,, \tag{1.3.57}$$

where the matrix $\mathcal{O}(g)^N_M$ is the linearisation of the Harmonic Einstein tensor R^H_M. If we begin with some initial guess metric $g^{(A)}_M$, then Newton's method iteratively improves this guess as

$$g^{(A+1)}_M = g^{(A)}_M - (\mathcal{O}(g^{(A)})^{-1})_M{}^N R^H_N(g^{(A)})\,. \tag{1.3.58}$$

As with the well-known one dimensional version, this method moves along the tangent to the equations to find a solution and will converge very quickly when it is near a fixed point. As with Ricci flow, provided the reference metric is chosen to share the same isometries as the physical metric, then the Harmonic Einstein tensor will be symmetric under these and the Newton method will preserve this structure.

In summary, the Newton method has the very important advantage over the Ricci-DeTurck flow that it is not sensitive to negative modes and this makes it much more practically useful than local relaxation, provided one can construct a suitable initial guess. The payoff is that its numerical implementation is somewhat non-trivial and in particular it assumes that the linear problem $\mathcal{O}.V = R^H$ can be solved for the vector V. In settings where a 'good' initial guess can be physically motivated, the Newton method is very powerful - we shall see this in detail when we use it to construct static and stationary black holes in a modified theory of gravity known as Einstein Aether theory in chapter (4). There we will see that we have analytic forms for the initial guess that are expected to be close to the new solutions and the Newton method then rapidly converges to the desired fixed points.

1.4. Einstein-Aether Gravity

In recent years there has been considerable interest in the possibility that Lorentz invariance is violated by quantum gravity effects. Indeed, such Lorentz violating processes underpin much of the current phenomenology of theories such as loop quantum gravity as well as certain aspects of string theory (see for example [129, 130, 131, 132]). Whilst in the context of particle physics, Lorentz violation in the matter sector, captured within the framework of the Standard Model Extension (SME) [133] is highly constrained, in gravitational settings the situation is far less restricted

[134, 135]. One can break Lorentz symmetry by the inclusion of fixed background fields but this is not an option in the presence of gravity as if we are to preserve the precise experimental successes of pure general relativity, we had better maintain general covariance. One option is to promote the Lorentz violating background fields to dynamical fields that are governed by a generally covariant action and in this chapter we will discuss a model example of Lorentz violation in the gravitational sector known as Einstein-Aether theory which does just this. In particular, this theory spontaneously breaks Lorentz symmetry and has the property that every field configuration one might imagine breaks Lorentz symmetry everywhere, even in the 'vacuum'. (Of course, almost any gravitational solution in general relativity breaks Lorentz symmetry but what one has in mind with Einstein-Aether theory is something stronger than that. In detail, whilst a solution in general relativity might break Lorentz symmetry, it must ultimately be restored on small scales, as the geometry locally looks like Minkowski space. In Einstein-Aether theory however, this is no longer true as Lorentz symmetry is broken even on small scales by the aether field that we introduce shortly).

If Lorentz violation is to preserve isotropy at every point (three dimensional rotations), then the associated background field (that breaks Lorentz symmetry) must be described by a timelike vector at each point in spacetime. In Einstein-Aether theory this is described by a vector field u^μ which should be thought of as the minimal structure one must impose to be able to determine a locally preferred rest frame [22, 23, 136, 137]. This vector field u^μ known as the aether is ubiquitous throughout spacetime and is named after the famed lumeniferous aether of turn of the century physics[23].

We are ultimately interested in applying our numerical techniques (with some modifications) to construct black holes in Einstein-Aether theory, a subject we will turn to in chapter 4. This section serves as an introduction to the theory. We present the action and field equations of Einstein-Aether in various forms and then discuss the various field redefinitions one can use to somewhat simplify the highly complex field equations. We then investigate the propagating degrees of freedom contained in the theory, demonstrating that there are a total of five modes - the

[23]There has also been more recent work on 'aether theories', notably the vector-tensor theories of the 1970s [138, 139, 140]. These differ from the version we present in this thesis in that we will require our aether field to be normalised. Early work has also been done by Gasperini in this context using the tetrad formalism [136]. In cosmology, vector-tensor theories have been studied by Clayton and Moffatt [141, 142] as well as Bassett et al [143] and shocks have been studied by Clayton [144]. More recently, Arkani-Hamed et al [145, 146] have proposed a string-inspired mechanism for Lorentz symmetry breaking in a similar 'spirit' to Einstein-Aether (whereby the gradient of a scalar is fixed to be of constant norm) and finally we note also the systematic analysis of Lorentz violation in general gravitational settings of Kostelecky [147].

two gravitational waves of general relativity, together with a further three coupled aether-metric modes. We close with a brief discussion of the current experimental bounds on the theory that come from a variety of sources including post-Newtonian analysis and cosmology.

1.4.1. Action and Field Equations

Einstein-Aether theory is a diffeomorphism invariant model for Lorentz violation in the gravitational sector. In this theory, Lorentz symmetry is spontaneously broken by the inclusion of a dynamical vector field known as the aether $u^\mu(x)$. This aether field acquires a unit timelike vacuum expectation value (VEV) that is enforced dynamically at the level of the action through a Lagrange multiplier constraint (for a review, see [24]). Whilst the field content of the theory is simply gravity and a vector field (*not* a gauge field), as we shall discuss, the broken Lorentz symmetry leads to a complex spectrum of propagating degrees of freedom and an intricate causal structure governed by multiple 'light' cones (and hence effective metrics). As one might expect, this makes the nature of its black hole solutions rather different from in general relativity.

In much of the literature on Einstein-Aether theory, the authors discuss the theory in mostly minus $(+,-,-,-)$ signature. In this thesis, we will however use the mostly plus $(-,+,+,+)$ signature, in which the action (in the absence of matter) takes the form

$$S = \frac{1}{16\pi G}\int d^4x\sqrt{-g}\left[R - K^{\mu\nu}{}_{\alpha\beta}\left(\nabla_\mu u^\alpha\right)\left(\nabla_\nu u^\beta\right) + \lambda(g_{\mu\nu}u^\mu u^\nu + 1)\right]\ , \quad (1.4.59)$$

where R is the Ricci scalar, G is the gravitational coupling constant (that is generically different from the Newton constant G_N in pure general relativity as the terms quadratic in the gradient of the aether field ∇u change the kinetic terms for the metric). The tensor $K^{\mu\nu}{}_{\alpha\beta}$ is defined as

$$K^{\mu\nu}{}_{\alpha\beta} := c_1 g^{\mu\nu}g_{\alpha\beta} + c_2\delta^\mu{}_\alpha\delta^\nu{}_\beta + c_3\delta^\mu{}_\beta\delta^\nu{}_\alpha - c_4 u^\mu u^\nu g_{\alpha\beta}\,, \quad (1.4.60)$$

where the c_i $(i = 1, 2, 3, 4)$ are dimensionless arbitrary coupling constants, and the term proportional to the Lagrange multiplier λ enforces the constraint that the aether field lie on the unit hyperboloid. It is this Lagrange multiplier together with the c_4 term that distinguishes the theory from the vector tensor theories of [148]. The tensor $K^{\mu\nu}{}_{\alpha\beta}$ should be thought as the most general polynomial in u that is irreducible under the constraint, in the sense that it contains no u terms that can be covariantly reduced by imposing the constraint equation. (One example of a reducible object would be a term that is proportional to $u^\mu \nabla_\sigma u_\mu$). Moreover, terms of the form $R_{ab}u^a u^b$ are also not included as these are proportional to the difference between the c_2 and c_3 terms by integration by parts. It will be convenient in what follows to introduce the quantity

$$J^{\mu\nu} \equiv K^{\mu\alpha\nu\beta}\nabla_\alpha u_\beta = c_1 \nabla^\mu u^\nu + c_2 g^{\mu\nu}\nabla.u + c_3 \nabla^\nu u^\mu - c_4 u^\mu u^\nu \,, \qquad (1.4.61)$$

where we note that $J^{\mu\nu}$ is *not* symmetric in its indices. The action may then be written more succinctly as

$$S = \frac{1}{16\pi G}\int d^4x\sqrt{-g}\left(R - J^{\mu\nu}\nabla_\mu u_\nu + \lambda(u^2+1)\right) . \qquad (1.4.62)$$

The field equations are obtained by varying the action and one finds that

$$\begin{aligned} G_{\mu\nu} = & - \nabla_\alpha\left[J^\alpha{}_{(\mu}u_{\nu)} + J_{(\mu}{}^\alpha u_{\nu)} - J_{(\mu\nu)}u^\alpha\right] - \frac{1}{2}g_{\mu\nu}J^{\alpha\beta}\nabla_\alpha u_\beta \\ & + c_1\left[(\nabla_{(\mu}u^\alpha)\nabla_{\nu)}u_\alpha + (\nabla_\alpha u_{(\mu})\nabla^\alpha u_{\nu)}\right] \\ & + 2c_2(\nabla.u)\nabla_{(\mu}u_{\nu)} \\ & + c_3\left[(\nabla_{(\mu}u^\alpha)\nabla_{|\alpha|}u_{\nu)} + (\nabla^\alpha u_{(\mu})\nabla_{\nu)}u_\alpha\right] \\ & - c_4\left[2a_\alpha u_{(\mu}\nabla_{\nu)}u^\alpha + a_\mu a_\nu\right] \\ & - \lambda\left(u_\mu u_\nu - \frac{1}{2}g_{\mu\nu}(u^2+1)\right) , \end{aligned} \qquad (1.4.63)$$

where $G_{\mu\nu} = R_{\mu\nu} - \frac{1}{2}g_{\mu\nu}R$ is the Einstein tensor, $J = J^\mu{}_\mu$ and we have defined the 'acceleration' $a_\mu = u^\alpha\nabla_\alpha u_\mu$. For the vector equation we have

$$\nabla^\alpha J_{\alpha\mu} + c_4 a^\alpha \nabla_\mu u_\alpha + \lambda u_\mu = 0\,, \qquad (1.4.64)$$

and finally the scalar (constraint) equation is

$$g^{\mu\nu}u_\mu u_\nu + 1 = 0\,. \qquad (1.4.65)$$

In view of the fact that we will later be interested in solving the Harmonic Einstein equation in order to find black hole solutions, it will be useful to rewrite the gravitational equations in terms of the Ricci tensor

$$\begin{aligned}
R_{\mu\nu} = & - \nabla_\alpha \left[J^\alpha{}_{(\mu}u_{\nu)} + J_{(\mu}{}^\alpha u_{\nu)} - J_{(\mu\nu)}u^\alpha\right] \\
& + \frac{1}{2}g_{\mu\nu}\nabla_\alpha \left[(J^{\alpha\beta} + J^{\beta\alpha})u_\beta - Ju^\alpha\right] + \frac{1}{2}g_{\mu\nu}J^{\alpha\beta}\nabla_\alpha u_\beta \\
& + c_1 \left[(\nabla_{(\mu}u^\alpha)\nabla_{\nu)}u_\alpha + (\nabla_\alpha u_{(\mu})\nabla^\alpha u_{\nu)} - g_{\mu\nu}(\nabla^\alpha u^\beta)(\nabla_\alpha u_\beta)\right] \\
& + c_2(\nabla.u)\left[2\nabla_{(\mu}u_{\nu)} - g_{\mu\nu}(\nabla.u)\right] \\
& + c_3 \left[(\nabla_{(\mu}u^\alpha)\nabla_{|\alpha|}u_{\nu)} + (\nabla^\alpha u_{(\mu})\nabla_{\nu)}u_\alpha - g_{\mu\nu}(\nabla^\alpha u^\beta)(\nabla_\beta u_\alpha)\right] \\
& - c_4 \left[2a_\alpha u_{(\mu}\nabla_{\nu)}u^\alpha + a_\mu a_\nu - \frac{3}{2}g_{\mu\nu}a^2\right] \\
& - \lambda\left(u_\mu u_\nu + \frac{1}{2}g_{\mu\nu}\right) . \qquad (1.4.66)
\end{aligned}$$

The equations ((1.4.63), (1.4.66)) are what one finds on directly varying the action, and we will use this form (when supplemented by a DeTurck term) in our later calculations. We note for completeness however that the equations of Einstein-Aether theory are often presented in a somewhat different way in the literature (see for example [149, 150]). One can arrive at this alternate (and simplified) form by directly substituting the aether and scalar equations into (1.4.63), to arrive at

$$\begin{aligned}
G_{\mu\nu} = & \nabla_\alpha \left[J_{(\mu\nu)}u^\alpha + J^\alpha{}_{(\mu}u_{\nu)} - J_{(\mu}{}^\alpha u_{\nu)}\right] - \frac{1}{2}g_{\mu\nu}J^{\alpha\beta}(\nabla_\alpha u_\beta) \\
& + c_1\left[(\nabla_{(\mu}u^\alpha)(\nabla_{\nu)}u_\alpha) - (\nabla_\alpha u_{(\mu})(\nabla^\alpha u_{\nu)})\right] + c_4 a_\mu a_\nu \\
& + \lambda u_\mu u_\nu , \qquad (1.4.67)
\end{aligned}$$

or equivalently

$$\begin{aligned}
R_{\mu\nu} = & \nabla_\alpha \left[J_{(\mu\nu)}u^\alpha + J^\alpha{}_{(\mu}u_{\nu)} - J_{(\mu}{}^\alpha u_{\nu)}\right] \\
& - \frac{1}{2}g_{\mu\nu}\nabla_\alpha\left[J^{(\beta}{}_{\beta)}u^\alpha + J^{\alpha(\beta}u_{\beta)} - J^{(\beta|\alpha|}u_{\beta)}\right] + \frac{1}{2}g_{\mu\nu}J^{\alpha\beta}(\nabla_\alpha u_\beta) \\
& + c_1\left[(\nabla_{(\mu}u^\alpha)(\nabla_{\nu)}u_\alpha) - (\nabla_\alpha u_{(\mu})(\nabla^\alpha u_{\nu)})\right] \\
& + c_4\left[a_\mu a_\nu - \frac{1}{2}g_{\mu\nu}a^2\right] \\
& + \lambda\left(u_\mu u_\nu + \frac{1}{2}g_{\mu\nu}\right) . \qquad (1.4.68)
\end{aligned}$$

One may further eliminate the Lagrange multiplier λ if desired from these equations by considering the trace of the aether equation (1.4.64) which reveals that

$$\lambda = c_4(a^\alpha a_\alpha) + (\nabla_\alpha J^\alpha{}_\beta)u^\beta . \qquad (1.4.69)$$

Metric Redefinitions

It can sometimes be convenient to re-express the theory (1.4.59) in terms of different variables. Indeed as we shall see, the introduction of a transformed metric and aether field can be particularly useful in the discussion of black holes as it allows us to simplify their otherwise very complex multi-horizon structure[24]. Let us define

$$\begin{aligned} g'_{\mu\nu} &= g_{\mu\nu} + (\sigma - 1) u_\mu u_\nu \,, \\ u'^\mu &= \frac{1}{\sqrt{\sigma}} u^\mu \,. \end{aligned} \tag{1.4.70}$$

We conventionally choose the constant $\sigma > 0$ so that the new metric remains Lorentzian (although of course the Euclidean theory one would otherwise obtain is implicitly still the same theory). Physically the effect of this field redefinition is to stretch the metric tensor in the aether direction by a factor of σ. It can then be shown that the action (1.4.59) for $(g'_{\mu\nu}, u'^\mu)$ takes the same form as that for $(g_{\mu\nu}, u^\mu)$ up to the values of the coefficients c_i. These transform as follows [151],

$$\begin{aligned} c'_1 &= \frac{\sigma}{2}\left((1+\sigma^{-2})c_1 + (1-\sigma^{-2})c_3 - (1-\sigma^{-1})\right) \,, \\ c'_2 &= \sigma(c_2 + 1 - \sigma^{-1}) \,, \\ c'_3 &= \frac{\sigma}{2}\left((1-\sigma^{-2})c_1 + (1+\sigma^{-2})c_3 - (1-\sigma^{-2})\right) \,, \\ c'_4 &= c_4 - \frac{\sigma}{2}\left((1-\sigma^{-1})^2 c_1 + (1-\sigma^{-2})c_3 - (1-\sigma^{-1})^2\right) \,. \end{aligned} \tag{1.4.71}$$

It is useful to note that this implies that certain combinations of the c_i scale rather simply. If we introduce the notation $c_{ij} = c_i + c_j$, $c_{ijk} = c_i + c_j + c_k$, we then find in particular that

$$\begin{aligned} & c'_{14} = c_{14} \,, \\ & c'_{123} = \sigma c_{123} \,, \\ & c'_{13} - 1 = \sigma(c_{13} - 1) \,, \\ & c'_1 - c'_3 - 1 = \sigma^{-1}(c_1 - c_3 - 1) \,. \end{aligned} \tag{1.4.72}$$

[24]Note that in pure Einstein-Aether theory this metric redefinition is not to be viewed as physical but merely a change of variables. If one couples the theory to matter, then there is coupling between the aether and matter sector through the effective metric $g'_{\mu\nu} = g_{\mu\nu} + (\sigma - 1)u_\mu u_\nu$. As described in the main text, such a redefinition relabels the aether parameters c_i and one generally assumes that this procedure has already been done so that $g_{\mu\nu}$ is the metric to which matter couples. Whilst experiments can constrain the values of the c_i parameters, one cannot distinguish between the two metrics by real or gedankenexperiments.

The parameter redefinitions defined by (1.4.71), (1.4.72) may be used to relate solutions of the field equations coming from the original and scaled actions. They may also be used to simplify (1.4.59) itself by eliminating one of the c_i, or some combination of the c_i. As an example of this, if we choose $\sigma = (s_2)^2 = 1/(1 - c_{13})$, then one finds c'_{13} vanishes i.e $c'_3 = -c'_1$. Another useful choice is to arrange for the new metric (1.4.70) to coincide with the effective metric for one of the wave modes in the theory by choosing $\sigma = s_i^2$ (see section (1.4.2)). In this way, in the context of black hole solutions, one can transform to a frame where one of the horizons for the spin-2, spin-1 or spin-0 modes coincides with the metric horizon, thereby simplifying discussions of the horizon structure.

A final extremely useful simplification arises in the discussion of *static*, spherically symmetric solutions of Einstein-Aether theory. In such cases, the aether may be taken to be hypersurface orthogonal and hence the square of the twist $\omega_\alpha = \epsilon_{\alpha\beta\gamma\delta} u^\beta \nabla^\gamma u^\delta$ vanishes [150, 152]. As far as such solutions are concerned, any multiple of $\omega_\alpha \omega^\alpha$ may be added to the action (1.4.59) without changing the physics. Since we have that

$$\omega_\alpha \omega^\alpha = -(\nabla_\alpha u_\beta)(\nabla^\alpha u^\beta) + (\nabla_\alpha u_\beta)(\nabla^\beta u^\alpha) + (u^\beta \nabla_\beta u_\alpha)(u^\gamma \nabla_\gamma u^\alpha) \,, \qquad (1.4.73)$$

the addition of $c_1 \omega_\alpha \omega^\alpha$ will result in the new couplings $c'_1 = 0, c'_3 = c_{13}$ and $c'_4 = c_{14}$. Alternatively one could subtract $c_4 \omega_\alpha \omega^\alpha$ from the action eliminating the c_4 term entirely. In practice, the latter choice is extremely useful and effectively means that when considering static solutions we can ignore c_4 without loss of generality[25].

We close this section by noting briefly that whilst in our introduction to Einstein-Aether we have presented the theory in a somewhat 'ad-hoc' manner, in cases where the aether may be taken to be hypersurface orthogonal it can be shown that the theory is in fact the IR limit of Horava-Lifshitz gravity [153, 154, 155] (see [156] for an introduction to Horava-Lifshitz gravity). The latter has much stronger physical motivation coming from quantum gravity. In particular, it is not supposed to be simply an effective field theory of gravity but may constitute a full UV completion of general relativity as it has been demonstrated to be power counting renormalisable [156]. Of course one may still view Einstein-Aether theory as merely a toy model for Lorentz violation in the gravitational sector; In particular when viewed as a low energy effective field theory [157] it can be thought of as a way to systematically capture the Lorentz violating phenomenology of some more fundamental theory, but

[25]Note that elimination of the c_4 term must of course be done *after* any rescaling of the metric and aether field, as otherwise application of (1.4.70) will regenerate the c_4 term that one sought to remove.

in our opinion its study is perhaps given greater weight when framed in the light of Horava-Lifshitz gravity.

1.4.2. Wave Modes and Physical Degrees of Freedom

In this section, we study the linearised theory of the aether coupled to gravity, discussing its wave modes and calculating their speeds in terms of the c_i parameters that appear in the action (1.4.59). We find that in addition to the two usual transverse traceless modes of general relativity, there are a further three coupled aether-metric modes. The discussion we present is our own and is somewhat different to that explicitly found in the literature [149]. In particular, our presentation is perhaps somewhat more covariant in the sense that we explicitly calculate the 'effective metrics' that govern the propagation of each of the modes as they will prove useful later. Since ultimately we will be interested in applying our numerical methods to construct Einstein-Aether black holes as a proof of principle as opposed to performing an exhaustive exploration of the full phase space of solutions, we shall set $c_3 = c_4 = 0$ in our calculations. Moreover, with a view to our later numerical calculations and in the light of the discussion of the previous section, we will add a DeTurck term to the Einstein equations and compute the wave speeds in this setting. (Note however that we do not analytically continue time and so are working in Lorentzian signature, where the harmonic Einstein equations are hyperbolic).

Altogether, we have the Harmonic Einstein equation:

$$\begin{aligned} J_{\mu\nu} &= c_1 \nabla_\mu u_\nu + c_2 g_{\mu\nu} \left(\nabla \cdot u\right) , \\ R^H_{\mu\nu} &= -\nabla_\sigma \left(J^\sigma{}_{(\mu} u_{\nu)} + J_{(\mu}{}^\sigma u_{\nu)} - J_{(\mu\nu)} u^\sigma\right) \\ &\quad + \frac{1}{2} g_{\mu\nu} \nabla_\sigma \left(\left(J^{\sigma\rho} + J^{\rho\sigma}\right) u_\rho - J u^\sigma\right) + \frac{1}{2} g_{\mu\nu} J^{\sigma\rho} \nabla_\sigma u_\rho \\ &\quad + c_1 \left(\left(\nabla_{(\mu} u^\sigma\right) \nabla_{\nu)} u_\sigma + \left(\nabla_\sigma u_{(\mu}\right) \nabla^\sigma u_{\nu)} - g_{\mu\nu} \left(\nabla^\sigma u^\rho\right) \nabla_\sigma u_\rho\right) \\ &\quad + c_2 \left(\nabla \cdot u\right) \left(2 \nabla_{(\mu} u_{\nu)} - g_{\mu\nu} \left(\nabla \cdot u\right)\right) \\ &\quad + \lambda \left(u_\mu u_\nu + \frac{1}{2} g_{\mu\nu}\right) , \end{aligned} \tag{1.4.74}$$

the vector equation,

$$\nabla^\sigma J_{\sigma\mu} + \lambda u_\mu = 0 \, , \tag{1.4.75}$$

and the constraint,

$$u^2 = -1 \, , \tag{1.4.76}$$

where

$$R^H_{\mu\nu} = R_{\mu\nu} - \nabla_{(\mu}\xi_{\nu)} \ , \quad \xi^\mu = g^{\alpha\beta}\left(\Gamma^\mu{}_{\alpha\beta} - \bar{\Gamma}^\mu{}_{\alpha\beta}\right) \ . \tag{1.4.77}$$

The Lagrange multiplier may be eliminated by way of the relation,

$$\lambda = u^\alpha \nabla^\sigma J_{\sigma\alpha} \, . \tag{1.4.78}$$

We now consider perturbing these equations about some background solution $\bar{g}_{\mu\nu}$ and $\bar{u}_\mu$. We let the value of ξ^μ be $\bar{\xi}^\mu$ on this background and so it may be a soliton. In detail, we linearise as,

$$u_\mu = \bar{u}_\mu + a_\mu \ , \quad g_{\mu\nu} = \bar{g}_{\mu\nu} + h_{\mu\nu} \ , \quad \xi^\mu = \bar{\xi}^\mu + \chi^\mu \, , \tag{1.4.79}$$

so that

$$\chi_\mu = \bar{\nabla}^\alpha h_{\alpha\mu} - \frac{1}{2}\partial_\mu h \, , \tag{1.4.80}$$

where indices are now raised/lowered with respect to the background $\bar{g}_{\mu\nu}$. Linearisation of the constraint equation shows that

$$2\bar{u} \cdot a = \bar{u}^\mu \bar{u}^\nu h_{\mu\nu} \, . \tag{1.4.81}$$

Since we are interested in the characteristics of the equations, governed by the principal symbol we now assume that a_μ and $h_{\mu\nu}$ are very short wavelength perturbations and work to two derivative order (in the vector and Einstein equations). It is useful at this point to introduce some new notation. We define

$$\phi = \bar{u} \cdot a \ , \quad j_\mu = \bar{u}^\alpha h_{\alpha\mu} \, , \tag{1.4.82}$$

in terms of which the constraint becomes $\bar{u} \cdot j = 2\phi$. Eliminating λ and linearising the vector equation then gives

$$\begin{aligned} 0 &= c_1 \left[\partial^2 a_\mu - \frac{1}{2}\partial^2 j_\mu + \frac{1}{2}\bar{u} \cdot \partial \chi_\mu - \frac{1}{2}\partial_\mu \left(\bar{u} \cdot \chi\right)\right] \\ &\quad + c_2 \left[\left(\partial_\mu + \bar{u}_\mu \left(\bar{u} \cdot \partial\right)\right)\left(\partial \cdot a - \bar{u} \cdot \chi\right)\right] \ . \end{aligned} \tag{1.4.83}$$

Similarly the linearised Einstein equations read,

$$0 = \frac{1}{2}\partial^2 h_{\mu\nu} + c_1 B^{(1)}_{\mu\nu} + c_2 B^{(2)}_{\mu\nu} \, , \tag{1.4.84}$$

with

$$
\begin{aligned}
B^{(1)}_{\mu\nu} &= \left(\frac{1}{2}\left(\bar{u}\cdot\partial\right)^2 h_{\mu\nu} + \left(\bar{u}\cdot\partial\right)\left(\partial_{(\mu}a_{\nu)} - \partial_{(\mu}j_{\nu)}\right)\right) + \bar{u}_{(\mu}\left(\partial^2 j_{\nu} - \partial^2 a_{\nu} - \left(\bar{u}\cdot\partial\right)\xi_{\nu)}\right) \\
&\quad - \bar{u}_{(\mu}\partial_{\nu)}\left(\partial\cdot a - \bar{u}\cdot\chi\right) - \frac{1}{2}\bar{g}_{\mu\nu}\left(\partial^2\phi - \left(\bar{u}\cdot\partial\right)\left(\bar{u}\cdot\chi\right)\right) \,, \\
B^{(2)}_{\mu\nu} &= -2\bar{u}_{(\mu}\partial_{\nu)}\left(\partial\cdot a - \bar{u}\cdot\chi\right) - \left(\bar{u}_{\mu}\bar{u}_{\nu} + \frac{1}{2}\bar{g}_{\mu\nu}\right)\left(\bar{u}\cdot\partial\right)\left(\partial\cdot a - \bar{u}\cdot\chi\right) \,. \qquad (1.4.85)
\end{aligned}
$$

To derive the wave modes, it is useful at this point to contract the Einstein equations (1.4.84) with $\bar{u}^{\mu}$ and combine this with the vector equation (1.4.83) to eliminate j_{μ}. Following this prescription, one obtains a second vector equation

$$
\begin{aligned}
0 &= c_1\left(2 - c_1\right)\left(\partial^2 a_{\mu} - \partial_{\mu}\left(\bar{u}\cdot\chi\right)\right) + \left(2c_2 - 3c_1c_2 - c_1^2\right)\bar{u}_{\mu}\left(\bar{u}\cdot\partial\right)\left(\partial\cdot a - \bar{u}\cdot\chi\right) \\
&\quad + \left(2c_2 + c_1^2\right)\partial_{\mu}\left(\partial\cdot a - \bar{u}\cdot\chi\right) + c_1^2\left(\left(\bar{u}\cdot\partial\right)^2 a_{\mu} - \left(\bar{u}\cdot\partial\right)\partial_{\mu}\phi\right) \\
&\quad + c_1\left(\partial_{\mu}(\bar{u}.\chi) + \bar{u}.\partial\chi_{\mu}\right) . \qquad (1.4.86)
\end{aligned}
$$

One may explicitly check that $S_{\mu\nu} = c_1 B^{(1)}_{\mu\nu} + c_2 B^{(2)}_{\mu\nu}$ is conserved

$$
\partial^{\alpha} S_{\alpha\mu} - \frac{1}{2}\partial_{\mu} S = 0 \,, \qquad (1.4.87)
$$

and since the Einstein equations are

$$
\partial^2 h_{\mu\nu} = -2S_{\mu\nu} \,, \qquad (1.4.88)
$$

this implies that

$$
0 = \partial^2\left(\partial^{\alpha} h_{\alpha\mu} - \frac{1}{2}\partial_{\mu} h\right) = \partial^2 \chi_{\mu} \,. \qquad (1.4.89)
$$

This equation has a very important consequence that simplifies calculations considerably. As we shall discuss shortly, the various perturbation modes in the theory obey wave equations of the form

$$
\left(\partial^2 + q\left(\bar{u}\cdot\partial\right)^2\right)\Phi_{\mu\ldots} = 0 \,, \qquad (1.4.90)
$$

for constants q that depend on the spin of the perturbation $\Phi_{\mu\ldots}$ and translate into a wave speed s according to

$$
s^2 = \frac{1}{1-q} \,, \qquad (1.4.91)
$$

where $s = 1$ is the speed of light. Equation (1.4.89) implies that only for perturbations with $q = 0$, (so $s = 1$), such that ∂^2 annihilates the perturbation can we have a non-vanishing ${\chi_\mu}$[26]. As we now demonstrate, the physical spin-2, spin-1 and spin-0 perturbations generically all have $q \neq 0$ (unless one chooses specific c_i parameters) and hence must all have vanishing χ_μ. In fact only the gauge perturbations have $q = 0$ and in this case one may explicitly calculate that $\chi_\mu = 0$ as well so that then *all* modes satisfy this condition. We may now proceed to study the different perturbations in some detail, beginning with gauge modes.

Gauge Transformations:

A gauge transformation is given by a perturbation of the form,

$$h_{\mu\nu} = \partial_\mu v_\nu + \partial_\nu v_\mu \ , \quad a_\mu = \partial_\mu \left(\bar{u} \cdot v \right) \ , \tag{1.4.92}$$

where v^μ generates the diffeomorphism, and $\chi_\mu = \partial^2 v_\mu$ for this perturbation.

One may show by direct calculation that the vector equation (1.4.83) vanishes on gauge transformations as it is composed solely of gauge invariant terms (such as $\partial \cdot a - \bar{u} \cdot \chi$). Similarly, $B^{(1)}_{\mu\nu}$ and $B^{(2)}_{\mu\nu}$ are gauge invariant as well. The Harmonic Einstein tensor on such a perturbation therefore yields

$$\partial^2 \left(\partial_{(\mu} v_{\nu)} \right) = 0 \, , \tag{1.4.93}$$

where this derivative structure arises as a consequence of the DeTurck term (recall (1.3.47)). We see from this that gauge perturbations acquire a kinetic term and obey a wave equation that is governed by the metric $g^{\alpha\beta}$. Note also that the gauge modes have $q = 0$ in the notation of equation (1.4.90). Finally, since we have that $\chi_\mu = \partial^2 v_\mu$, we may conclude that $\chi_\mu = 0$ and so the latter is unperturbed. (Once again to see this, expand the perturbation χ_μ in harmonics).

Physical Degrees of Freedom

We now consider the propagating spin-2, spin-1 and spin-0 degrees of freedom in the theory. To proceed, we may set $\chi_\mu = 0$ (preempting the fact that these modes will all have $q = 0$) and consider two further contractions of the vector equation 1.4.86.

[26] To see this explicitly, expand the perturbations in a plane wave basis $\chi_\mu = \sum_a \alpha^{(a)}_\mu e^{ik^{(a)}.x}$, $\Phi_{\mu\nu\ldots} = \sum_a \phi^{(a)}_{\mu\nu\ldots} e^{ik^{(a)}.x}$ and substitute into (1.4.89), (1.4.90). We see from (1.4.90) that when $q \neq 0$, we must have $k \neq 0$ and (1.4.89) then implies that $\alpha_\mu = 0 \implies \chi_\mu = 0$.

- **Spin-0**

We may contract with ∂^μ and $\bar{u}^\mu$ to obtain,

$$
\begin{aligned}
0 &= 2\left(c_1+c_2\right)\partial^2\left(\partial\cdot a\right)+\left(2c_2-3c_1c_2\right)\left(\bar{u}\cdot\partial\right)^2\left(\partial\cdot a\right)-c_1^2\left(\bar{u}\cdot\partial\right)\partial^2\phi\,, \\
0 &= \left(2-c_1\right)\partial^2\phi+\left(2c_1+3c_2\right)\left(\bar{u}\cdot\partial\right)\left(\partial\cdot a\right)
\end{aligned}
\tag{1.4.94}
$$

respectively. Eliminating $\partial^2\phi$ between these equations we then obtain

$$
\left(\partial^2+q_{(0)}\left(\bar{u}\cdot\partial\right)^2\right)\left(\partial\cdot a\right)=0\,,\quad q_{(0)}=\frac{c_1^3+2c_2-4c_1c_2+3c_1^2c_2}{\left(c_1+c_2\right)\left(2-c_1\right)}\,. \tag{1.4.95}
$$

We see from this that the degree of freedom $\partial.a$ propagates with speed $s_{(0)}^2 = 1/(1-q_{(0)})$. It is the spin-0 degree of freedom.

- **Spin-2**

If we now consider a perturbation with $a_\mu = 0$ (and hence $\phi = 0$) we see that it automatically satisfies the vector equation (1.4.86). The Einstein equation (1.4.84) for such a mode becomes

$$
-\frac{1}{2}\left(\partial^2+q_{(2)}\left(\bar{u}\cdot\partial\right)^2\right)h_{\mu\nu}=0\,,\quad q_{(2)}=c_1\,. \tag{1.4.96}
$$

We therefore see that this is a mode with $q_{(2)} = c_1$ and speed $s_{(2)}^2 = 1/(1-c_1)$. Note that when $c_1 = 0$, this mode propagates at the speed of light and hence corresponds to the usual spin-2 degree of freedom in general relativity.

- **Spin-1**

Finally we discuss vector perturbations where $\partial.a = 0$. Note that if this quantity does not vanish, the wave speed of such a perturbation would of course be constrained to propagate with speed $q_{(0)}$ as in (1.4.95), but in the vanishing case, the wave speed may be different. Note also that provided $q \neq 0$, then $\phi = 0$. We consider a mode of the form,

$$
a_\mu = n_\mu\,,\quad \bar{u}\cdot n=\partial\cdot n=0\,,\qquad \chi_\mu=0\,, \tag{1.4.97}
$$

where n_μ has two polarization states after the constraints $\bar{u} \cdot a = 0$ and $\phi = \partial \cdot a = 0$ are imposed. The vector equation (1.4.86) then implies

$$0 = c_1 (2 - c_1) \partial^2 n_\mu + c_1^2 (\bar{u} \cdot \partial)^2 n_\mu \,, \tag{1.4.98}$$

so that

$$0 = \left(\partial^2 + q_{(1)} (\bar{u} \cdot \partial)^2\right) n_\mu \,, \quad q_{(1)} = \frac{c_1}{2 - c_1} \,. \tag{1.4.99}$$

These are the two spin-1 vector modes.

In summary, we have displayed the five physical degrees of freedom that are present in Einstein-Aether theory. Our choice of DeTurck term results in the gauge modes acquiring a kinetic term governed solely by the metric $g^{\alpha\beta}$, in other words $q_{(gauge)} = 0$. All the physical perturbations on the other hand are governed by effective metrics of the form $(g^{\mu\nu} + q_{(physical)} u^\mu u^\nu)$ with $q_{(physical)} \neq 0$ (generically), so that $\chi_\mu = 0$. Recalling the definition of the perturbation χ_μ, this essentially means that they are in Lorentz gauge. We close by noting that this behaviour is of course related to our choice of DeTurck term. One could envision choosing a 'modified' DeTurck term involving the aether

$$R^H_{\mu\nu} = R_{\mu\nu} - \nabla_{(\mu}\xi_{\nu)} + k_1 (\bar{u} \cdot \partial) \left(\bar{u}_{(\mu}\xi_{\nu)}\right) + k_2 \bar{u}_{(\mu}\partial_{\nu)} (\bar{u} \cdot \xi) + (k_3 \bar{g}_{\mu\nu} + k_4 u_\mu u_\nu) (\partial \cdot \xi) \,,$$

for some constants k_1, k_2, k_3, k_4 in the hopes that the equations of motion might simplify further. The difficulty with this however is that the effective metric governing the gauge fluctuations would no longer simply be $g^{\mu\nu}$ and thus it becomes difficult to distinguish gauge fluctuations from physical modes. Indeed, the two may mix in this case whilst with our choice of DeTurck term, there is no such mixing and it is straightforward to distinguish the two.

1.4.3. Constraints on the Parameter Space

To close our introduction to Einstein-Aether theory, we briefly review for completeness some of the experimental and theoretical constraints on the parameters c_i. Whilst for the purposes of this thesis, we have not always restricted the black hole solutions we construct in chapter 4 to lie in phenomenologically allowed regions of parameter space, in our forthcoming paper it would be interesting to do so.

Special Points in Parameter Space

The first significant observation concerning the parameter space of Einstein-Aether theory is that it reduces to general relativity at two distinct points,

- When $c_1 = c_2 = c_3 = c_4 = 0$.
- When $c_{14} = c_{123} = 2c_1 - c_1^2 + c_3^2 = 0$ (in the absence of matter) .

The second of these is non-trivial and was found by making use of the field redefinitions (1.4.70) in [158].

Another special point in parameter space corresponds to $c_{13} = c_2 = c_4 = 0$, yielding a theory whose vector kinetic term becomes that of Maxwell [22]. This region of parameter space however is known to be pathological due to the formation of caustic singularities and should likely not be thought of as a typical representation of the dynamics of Einstein Aether theory [159].

Weak Fields and PPN

A convenient technique for systematically capturing how metric theories of gravity compare against each other or with experiment is provided by way of the parameterised post-Newtonian (PPN) formalism. This formalism encapsulates the weak-field, slow motion limit (known as the post-Newtonian limit) by way of an expansion about flat spacetime in a set of potentials. The so called 'PPN parameters' of a given theory are the coefficients of these potentials and in the current formalism, there are ten such coefficients [148].

The PPN parameters for Einstein-Aether theory were computed in [160, 161, 162]. It was found there that eight out of ten of these (The Eddington-Robertson-Schiff parameters, the Whitehead parameters and the energy momentum conservation parameters) take on their general relativity values, whilst the remaining two, namely the preferred frame parameters are given by,

$$\begin{aligned} \alpha_1 &= \frac{-8(c_3^2 + c_1 + c_4}{2c_1 - c_1^2 + c_3^2} , \\ \alpha_2 &= \frac{\alpha_1}{2} - \frac{(c_1 + 2c_3 - c_4)(2(c_1 + 3c_2 + c_3 + c_4))}{c_{123}(2 - c_{14})} . \end{aligned} \tag{1.4.100}$$

These are then subject to the current experimental bounds $\alpha_1 < 10^{-4}$ and $\alpha_2 < 10^{-7}$ [163]. Needless to say, these constraints are rather stringent and it is then natural to expect that on expanding (1.4.100), one might find similar bounds on the c_i themselves. Since the c_i parameter space is four dimensional however, it is in fact possible to set $\alpha_1 = \alpha_2 = 0$ identically by eliminating c_2, c_4 as,

$$\begin{aligned} c_2 &= \frac{-2c_1^2 - c_1c_3 + c_3^2}{3c_1}, \\ c_4 &= \frac{-c_3^2}{c_1}, \end{aligned} \tag{1.4.101}$$

and hence reducing to a 2D parameter space. Quite remarkably, the values of the c_i parameters in this 2D space can then be made $\mathcal{O}(1)$ and still satisfy the PPN constraints. In this regime, one can then argue that the theory contains potentially large Lorentz-violating gravitational modifications but nevertheless remains indistinguishable from general relativity within the framework of PPN [157].

Cherenkov Radiation

The derivation of the speeds of the 5 massless wavemodes obtained by perturbing around flat space was presented in section (1.4.2). These squared speeds must remain non-negative to ensure that they remain oscillatory and do not become exponentially growing. Imposing the lower bound $s^2 > 0$, translates into a bound on the c_i parameters.

As a consequence of the fact that matter couples universally to gravitation (consisting now of a mixture of graviton and aether modes), there are new possibilities for radiative emission from matter particles. Of particular importance is the possibility of gravitational Cherenkov radiation. Recall that the usual (electromagnetic) Cherenkov effect arises when a charged particle moves faster than the effective speed of light in a medium, resulting in the radiation of photons by the charged particle. Gravitational Cherenkov radiation should be thought of as the analogous effect in this setting where a massive particle moves faster than the speed of the gravitational wave mode and hence will radiate these graviton/aether wave modes. By consideration of the energy loss from high energy cosmic rays, one can obtain very stringent constraints on aether theory by way of Cherenkov radiation. When the PPN conditions (1.4.101) have been imposed, the bounds on the remaining parameters due to gravitational Cherenkov radiation become [164],

$$\begin{aligned} 0 &\leq c_1 + c_3 \leq 1, \\ 0 &\leq c_1 - c_3 \leq \frac{c_1 + c_3}{3(1 - c_1 - c_3)}. \end{aligned} \tag{1.4.102}$$

The calculation is similar to what has been done in pure general relativity to set a lower bound on the speed of gravitational waves [165].

Cosmology

The 'Newton constant' in Einstein-Aether theory which appears in cosmological solutions turns out to be different to that found through perturbative analysis about Minkowski space

$$G_{cosmo} = \frac{2G_N}{2 + c_{13} + 3c_2} \,. \tag{1.4.103}$$

This observation leads to an interesting class of tests for Einstein-aether. The difference between these two constants is bounded by for example nucleosynthesis (as discussed in the recent cosmological analysis of [166], where an investigation of the two dimensional parameter space that remains after the imposition of (1.4.101) was conducted). Further astrophysical and cosmological constraints on the theory come from the primordial power spectrum and the CMB [167, 168], radiation damping [169, 170], the masses of neutron stars [171, 172] as well as dynamical stability [173]. A much more complete discussion can be found in the review article [24].

2. Bosonic Fractionalisation in AdS/CFT

2.1. Introduction

In this chapter we will discuss a particular class of phase transition in condensed matter physics known as fractionalisation transitions using the techniques of gauge gravity duality. (The reader is referred to section 1.2.5 of the introductory chapter of this thesis for an overview of the relevant aspects of applied holography). We shall take a relativist's approach to the subject, where the problem amounts to the construction of particular classes of black hole solutions in general relativity and an examination of their thermodynamics (so as to demonstrate the existence or non-existence of a phase transition). In detail, we will have to solve the Einstein equations in asymptotically AdS spacetime, in the presence of matter (which in our setting will consist of an Abelian gauge field, together with a real and complex scalar). The construction of such solutions is in general analytically intractable and one must appeal to numerics. In this sense, this chapter constitutes our simplest example of numerical relativity - the black holes that we construct are static and planar, depending non-trivially only on a single (radial) coordinate so that the equations of motion are ODEs. We will therefore not need the full elliptic formalism reviewed in section 1.3 of the introduction, although we note extensions of this work where such methods are invaluable. We proceed by solving the system using shooting methods, constructing the black holes in a near horizon and asymptotic region respectively and connecting the two. We begin with some condensed matter motivation and an overview of what is meant by 'bosonic fractionalisation' before turning to the problem of constructing the gravitational solutions.

In the context of condensed matter theory, given a field theory at finite density (with respect to some $U(1)$ symmetry), it is of interest to study the physical nature of its ground states. In particular, one might be interested under what conditions the $U(1)$ symmetry is broken, corresponding to superfluid or superconducting phases, if there are Fermi surfaces present and how their properties compare with those of the conventional Fermi liquid theory that underlies much of modern solid state physics. Such questions have attracted considerable interest recently, in particular with regard to a classic result in condensed matter known as the Luttinger theorem and a holographic generalisation thereof [174, 175, 176]. This result relates the sum of the volumes of all Fermi surfaces V_i (associated to fermionic operators carrying electric charge q_i) to the total charge density Q[1]

$$Q = \sum_i q_i V_i \, . \tag{2.1.1}$$

These studies were guided by the observation that the finite charge density of a field theory, as encoded holographically by the electric flux in some dual gravitational geometry can be sourced in two distinct ways: By explicit charged matter sources in the bulk such as neutral 'hairy black holes' supporting *charged* scalar hair or alternatively by the presence of charged black hole horizons with no hair[2]. (Note that this distinction can be made technically sharp by virtue of the fact that the large N limit of field theories that have gravity duals naturally involves a hierarchy between a small number of charged fields and a large quantity of black hole microstates [177]). The case of a bulk charged horizon is of particular interest for condensed matter - a fact that can be understood as a consequence of the holographic observation by Witten that the presence of a black hole horizon in the bulk geometry is dual to deconfined phases of matter [178]. Using this as motivation, it has been conjectured that electrically charged horizons may be used to describe field theories in condensed matter where some of the electric charge density is tied up in 'gauge-variant' operators, the flux from the horizon being associated with these deconfined or 'fractionalised' charge carriers [8, 174]. The study of dual gravity geometries with bulk horizons then serves as a powerful holographic tool to investigate such systems, particularly when direct analysis of the field theory is intractable.

A useful system independent description of fractionalisation has been provided by the Luttinger theorem [8]. In essence, since only Fermi surfaces corresponding to gauge invariant degrees of freedom are experimentally observable (notably by photoemission spectroscopy [174]), fractionalised gauge charge will show up as a mismatch in the Luttinger theorem,

$$\mathcal{F} = Q - \sum_i q_i V_i \, , \tag{2.1.2}$$

[1]We note for completeness that there is also an analogous bosonic result that relates the total charge to the 'Magnus force' felt by some test vortex in the dual field theory [176].

[2]We stress in this latter case that these black holes are *not* hairy black holes. The charge is entirely 'behind' the black hole horizon with the charged scalar being zero outside.

where the amount the theorem is violated by corresponds to the electric flux $\mathcal{F}$ emanating from a bulk horizon. Further support has been lent to this viewpoint recently by the identification of the corresponding Green function singularities associated to these 'hidden', fractionalised fermionic degrees of freedom in the work of Faulkner and Iqbal [179].

A natural question to ask now is whether transitions can occur in physical systems between phases which are fractionalised and phases which are not and it is this which we now turn to for the remainder of this chapter. In gravitational language, we seek transitions between solutions of the Einstein equations where the electric flux is sourced entirely by a horizon (corresponding to full fractionalisation) and those where it originates entirely due to charged matter in the bulk (corresponding to what we call a cohesive phase) [174, 180, 181]. In the former case, this corresponds to electrically charged bulk black holes *without* scalar hair and in the latter case to a neutral black hole supporting charged scalar hair[3]. In addition to the aforementioned phases one might also expect the existence of a partially fractionalised phase as intermediate between these two extremes that corresponds on the gravity side to a charged (as opposed to neutral) black hole supporting charged scalar hair. Since the presence of non-singlet matter will always break the $U(1)$ symmetry, such phases have broken symmetry and hence the transition between a cohesive and partially fractionalised phase must occur in the superfluid phase. In view of this, we will term the two kinds of ordered phase in our subsequent work as the 'superfluid cohesive phase' and the 'superfluid fractionalised phase'.

Whilst violation of the Luttinger theorem as presented in equation (2.1.2) phrases fractionalisation in terms of fermionic systems, for the remainder of this chapter we will in fact discuss gravitational duals to *bosonic* fractionalisation transitions that serve as bosonic analogues of the fermionic transitions discussed in [174, 182]. That is to say, the holographic gravitational actions we consider will consist of only bosonic fields. In detail, we shall discuss fractionalisation both in an ad-hoc ('bottom-up') Einstein-Maxwell-dilaton-charged scalar theory as well as (briefly) in a top-down' model that arises as a reduction of 11D supergravity (the low energy limit of M-theory). As we shall see, the fractionalisation transitions that can occur in these settings constitute rather striking zero temperature quantum phase transitions that leave a marked imprint on finite temperature physics[4]. We note also that the

[3]Such a transition has already been observed in the literature, namely the M-theory superconductor transition from finite temperature charged black hole to zero temperature charged domain wall with no horizon. We shall discuss this in further detail in what follows.

[4]Indeed the study of such $T = 0$ quantum critical points is of great theoretical interest in condensed matter more generally as they are believed to play a role in various ill understood phenomena notably high temperature superconductivity [7].

gravitational theories we consider share a structural similarity to those discussed in the electron star literature [183] with the charged scalar taking the place of the fermion fluid found there. Some of the infrared (IR) geometries considered there will also feature in our work. Similar solutions have also previously found use in the description of QCD like theories [184, 185, 186] and in the description of quantum criticality at finite density [187, 188, 189, 190, 191, 192, 193, 194].

In detail, we begin by introducing the class of Einstein-Maxwell-dilaton-charged scalar theories we will consider for the remainder of this chapter. We then develop the holographic renormalisation and thermodynamics of these models in some detail with a view to calculating the free energy which is of crucial importance for phase transition physics. We then provide a detailed description of a class of bottom-up models which illustrate the concepts underlying fractionalisation and use shooting methods to construct $T = 0$ solutions of these models that are dual to fractionalised, partially fractionalised and cohesive phases in field theory. Finally, we close by outlining aspects of fractionalisation at finite temperature and in a top-down M-theory setting. (The latter two topics are discussed in much greater length in the paper on which this chapter is based [2]).

The main results of our analysis are summarised in Fig. 2.1. In particular, as we shall see, the phase diagram is governed by the structure of the IR zero temperature states. Depending on the nature of the effective gauge coupling which is controlled by the neutral scalar field, we find either a fully or partially fractionalised phase, if the coupling goes to zero and a cohesive phase if it remains finite. In the latter two cases, as explained above, the $U(1)$ symmetry is manifestly broken, so we end up with superfluid states of matter. In addition to the aforementioned phases, there is one further neutral phase that arises in the M-theory case, where the ground state does not depend on the chemical potential (it is 'incompressible'). In fact, the only $T = 0$ phase transition in the M-theory case is governed by a $z = 2$ quantum critical point and is from cohesive to neutral (and is not a fractionalisation transition).

2.2. General Features, Action and Field Content

In this section, we introduce the gravitational theories we will be concerned with in a setting general enough to cover both bottom-up and top-down constructions. At zero temperature we will analyse the possible IR geometries admitted by these theories as well as the deformations about these solutions that allow them to be connected to the desired AdS asymptotics (that will be universal to everything we shall consider in this chapter). As we shall see, these IR geometries are zero

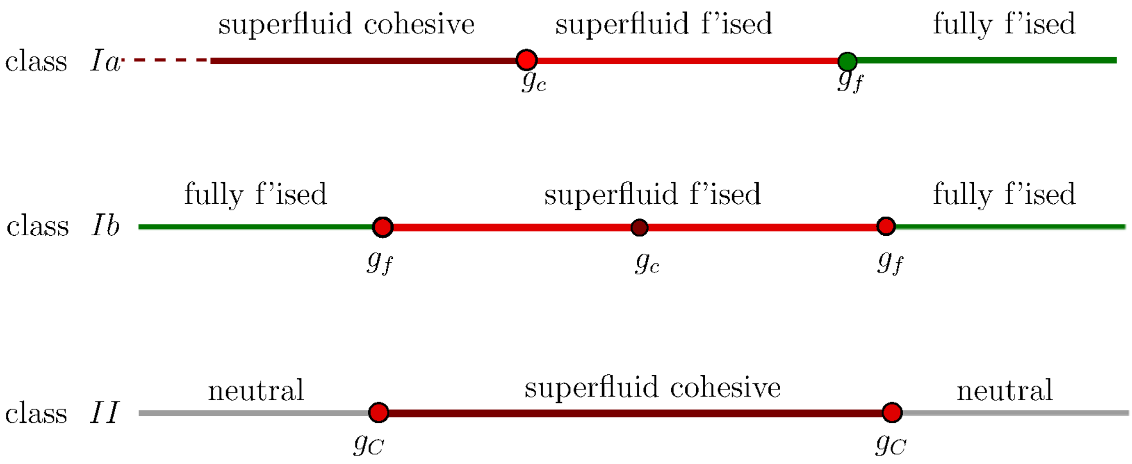

Figure 2.1.: Zero-temperature phase structure of the models considered in this chapter plotted as a function of $\frac{\Phi_1}{\mu}$ where Φ_1 is a UV deformation parameter and μ is the chemical potential corresponding to the finite density of the dual field theory (both are explained in the text in section 2.3). Shades of red indicate broken symmetry, with dark red symbolising the cohesive states and bright red the superfluid fractionalised ones. The $U(1)$ symmetry is unbroken in the green fully fractionalised and grey neutral phases. Class Ib is even in Φ_1, while the class Ia example has no particular reflection symmetry associated with the dilaton. The M-theory discussion of section 2.7 is in class II.

temperature charged domain walls[5] and determine the low energy physics of the dual field theory and thus whether one is in a fractionalised or cohesive phase.

The class of theories we will be interested in can be encompassed by the following action[6]:

$$\begin{aligned} S \;=\; & \int d^{d+1}x\sqrt{-g}\Big[R - \tfrac{1}{4}Z_F(\Phi)F_{MN}F^{MN} - \tfrac{1}{2}(\nabla\Phi)^2 - Z_S(S)|DS|^2 - V(\Phi,|S|)\Big] \\ & + S_{\mathrm{CS}}\,, \end{aligned} \tag{2.2.3}$$

where we denote the $d+1$ bulk directions with upper-case Latin indices $M, N, \ldots$, whilst the dual field-theory coordinates will be denoted with lower-case Greek indices $\mu, \nu, \ldots$. The field Φ is a neutral scalar field, which we will refer to as a 'dilaton' (in

[5]We note as a technical aside that these 'domain wall' solutions are in fact nakedly singular. This is rather generic in AdS/CMT and they are nevertheless considered 'well behaved' by virtue of the fact that when heated up infinitesimally, the singularity becomes clothed by a horizon. See for instance [195].

[6]Note that this action is written in units where $16\pi G_N = 1$.

the spirit of string theory), whereas S is a charged scalar field with the usual $U(1)$ covariant derivative $DS = (\nabla - iqA)S$. We have also included a term S_{CS}, which stands for a possible Chern-Simons contribution. These are often found in consistent supergravity reductions and are relevant in top-down constructions. Whilst the solutions we construct will not depend on S_{CS}, we note that in certain cases the phase structure may be altered by its presence, and spatial modulation and striped phases become possible [196, 197, 198, 199]. This will not be discussed further here although we note that in these cases, the black hole ansatz that must be solved for results in PDEs and the elliptic techniques of section 1.3 have recently taken centre stage in this area of holography (see for example [200]).

The coupling coefficients $Z_F(\Phi), Z_S(S)$ as well as the potential term $V(\Phi, |S|)$ in the action (2.2.3) depend explicitly on the neutral and complex scalar fields. (Note that we have not considered the most general action of this form here, but it is sufficient to capture the physics we wish to discuss). In a 'bottom-up' setting, these quantities are not specified by some underlying fundamental theory and must be chosen 'by hand'. Much of the interesting behaviour we will exhibit in these theories depends on this choice and arises as a consequence of the interplay between the potential and couplings. It will be convenient to recast the kinetic terms for the scalars in canonical form, (although this is in fact only possible for the magnitude of the complex field). We can rewrite the kinetic term for the charged scalar S using a polar decomposition as $S = \eta' e^{iq\varphi}$ and compute that

$$Z_S(|S|)|DS|^2 = Z_S(\eta')(\nabla\eta')^2 + q^2 Z_S(\eta')\eta'^2(\nabla\varphi - A)^2 \,. \tag{2.2.4}$$

On changing variables to η, defined as $\int d\eta' \sqrt{Z_s(\eta')} = \int d\eta$, one then arrives at

$$Z_S(|S|)|DS|^2 = (\nabla\eta)^2 + q^2 X(\eta)^2(\nabla\varphi - A)^2 \,, \tag{2.2.5}$$

where we have introduced a function $X(\eta)$ which arises due to the aforementioned change of variables. It is required to have the small-η expansion $X(\eta) \sim \eta + \mathcal{O}(\eta^2)$. We now make some further simplifications to the action (2.2.3). In the 'bottom-up' analysis that follows, $X(\eta)$ must be specified (this is of course equivalent to specifying $Z_S(S)$). We may in fact capture all the physics we wish to discuss by retaining only the first term in the above small-η expansion and shall do so in what follows. (We discuss the more general case here as in the 'top-down' M-theory case, a closed form expression for $Z_S(S)$ and hence $X(\eta)$ is known from dimensional reduction which may then be included in full in calculations). We may now use the local $U(1)$ gauge symmetry in the theory to transform $S \to e^{i\theta}S$ (equivalently $\eta \to \eta$, $\varphi \to \varphi + \theta/q$)

together with $A \to A + \partial\theta/q$. Using this we can (by a suitable choice of θ) fix a gauge where $\varphi = 0$ and we shall do this in what follows.

The general action we consider (in terms of real fields) is then of the form,

$$
\begin{aligned}
S \;=\; & \int d^{d+1}x\sqrt{-g}\Big[R - \tfrac{1}{4}Z_F(\Phi)F_{MN}F^{MN} - \tfrac{1}{2}(\nabla\Phi)^2 - (\nabla\eta)^2 \\
& -q^2X(\eta)^2A^2 - V(\Phi,|S|)\Big]\,, \qquad (2.2.6)
\end{aligned}
$$

where $X(\eta) = \eta$ by choice in the 'bottom-up' case with $Z_F(\Phi)$ and $V(\Phi,|S|)$ to be specified later. All these aforementioned quantities are fixed by dimensional reduction in 'top-down' constructions.

Of particular interest in holography are the so called hyperscaling geometries. These are defined in terms of the following scaling symmetry which should be thought of as a generalisation of the Lifshitz scaling reviewed in the introduction (see section 1.2.5):

$$
\begin{aligned}
\mathbf{x} &\to \lambda\mathbf{x}\,, \\
t &\to \lambda^z t\,, \\
r &\to \lambda^{(\theta-2)/2} r\,, \qquad (2.2.7)
\end{aligned}
$$

under which $ds \to \lambda^{\theta/2}ds$. Here, z is the dynamical critical exponent present in the Lifschitz case, and θ is the new hyperscaling violation parameter. Hyperscaling is physically significant, influencing the thermodynamics of gravitational solutions. Recently it has also been realised that theories with hyperscaling violation can exhibit intriguing violations of area laws for entanglement entropy (intermediate between linear and logarithmic violation) perhaps indicating the existence of duals to novel, exotic phases of matter [194]). Hyperscaling geometries are generated by an IR divergent dilaton ($\Phi \longrightarrow \pm\infty$)[191, 192, 193], and so in classifying solutions of our theory it will be important to first classify the possible behaviours of the dilaton in the IR (and hence the behaviour of the coupling $Z_F(\Phi)$). We consider two possibilities defined as follows:

$$
\begin{aligned}
\text{class } I: &\qquad Z_F(\Phi) \xrightarrow{\text{IR}} \infty\,, \\
\text{class } II: &\qquad Z_F(\Phi) \xrightarrow{\text{IR}} \text{Constant}\,. \qquad (2.2.8)
\end{aligned}
$$

We emphasise that we do not require $Z_F(\Phi)$ to be even in Φ. In particular, this is of importance in class I, where one can envision a scenario where $Z_F(\Phi)$ diverges as say $\Phi \longrightarrow \infty$, but remains finite as $\Phi \longrightarrow -\infty$. As we shall see, it is in this sense that Φ is able to drive fractionalisation type transitions.

Finally, we must specify the potential, which we require to have an expansion of the following form

$$\ell^2 V(\eta, \Phi) = -6 - \Phi^2 - 2\eta^2 + \cdots \tag{2.2.9}$$

The first term is chosen to ensure that we have an AdS_4 vacuum solution with AdS length l^2 when all fluxes vanish (it is essentially a cosmological constant term) and the remaining terms can be thought of as fixing the conformal dimension ($\Delta = 2$) of the dual operators to the Φ and S fields.

For the remainder of this chapter we work in $D = 4$ bulk dimensions, so that the boundary field theory is $d = 3$ dimensional. We will use the following ansatz for the metric, gauge and scalar fields. Note that all functions depend only on the radial coordinate r. $\{t, x, y\}$ are field theory coordinates and we remind the reader, that the r coordinate corresponds to the 'extra' dimension in the bulk geometry which has a holographic interpretation in terms of field theory energy scale (as discussed previously in section 1.2.5),

$$\begin{gathered} ds^2 = -f(r)e^{-\beta(r)}dt^2 + \frac{dr^2}{f(r)} + \frac{r^2}{\ell^2}\left(dx^2 + dy^2\right) \,, \\ A = A_t(r)dt \,, \qquad \Phi = \Phi(r) \,, \qquad \eta = \eta(r) \,. \end{gathered} \tag{2.2.10}$$

The metric above has a horizon at $r = r_h$ defined by $f(r_h) = 0$, and on this hypersurface we must also impose the condition $A_t(r_h) = 0$[7]. Evaluated on our ansatz (2.2.10), the equations of motion following from (2.2.6) are found to be:

$$\begin{aligned} 0 &= \Phi'' + \left(\frac{f'}{f} - \frac{1}{2}\beta' + \frac{2}{r}\right)\Phi' + \frac{(\partial_\Phi Z_F)A'^2 e^\beta}{2f} - \frac{\partial_\Phi V}{f} \,, \\ 0 &= \eta'' + \left(\frac{f'}{f} - \frac{1}{2}\beta' + \frac{2}{r}\right)\eta' + \frac{q^2 A^2 e^\beta}{f^2}\eta - \frac{\partial_\eta V}{2f} \,, \\ 0 &= A'' + \left(\frac{Z_F'}{Z_F} + \frac{1}{2}\beta' + \frac{2}{r}\right)A' - \frac{2q^2\eta^2}{fZ_F}A \,, \\ 0 &= \Phi'^2 + 2\eta'^2 + \frac{2q^2A^2\eta^2 e^\beta}{f^2} + \frac{2}{r}\beta' \,, \\ 0 &= \Phi'^2 + 2\eta'^2 + \frac{2q^2A^2\eta^2 e^\beta}{f^2} - \frac{2V}{f} - \frac{4}{r}\left(\frac{f'}{f} - \beta' + \frac{1}{r}\right) - \frac{2A'^2 e^\beta}{f} \,. \end{aligned} \tag{2.2.11}$$

[7]One way to understand this condition is by continuing to Euclidean signature as we shall do in our discussion of thermodynamics. One can then argue that we would obtain a singular gauge connection on integrating the gauge field around the Euclidean time circle if we did not have $A_t \to 0$ as the Euclidean time circle shrinks to zero at the horizon.

2.3. Ultraviolet Expansions and Asymptotic Charges

Following standard AdS/CFT technology, we require solutions that asymptote to AdS_4 at large values of r. From the field equations that follow from (2.2.3) one finds that such solutions admit the large r expansions:

$$\begin{aligned}
f &= \frac{r^2}{\ell^2} + \frac{1}{2}\left(\eta_1^2 + \tfrac{1}{2}\Phi_1^2\right) + \frac{\ell G_1}{r} + \cdots\,, \\
\beta &= \beta_a + \frac{\ell^2\left(\eta_1^2 + \tfrac{1}{2}\Phi_1^2\right)}{2r^2} + \cdots\,, \\
\Phi &= \frac{\ell\Phi_1}{r} + \frac{\ell^2\Phi_2}{r^2} + \cdots\,, \\
\eta &= \frac{\ell\eta_1}{r} + \frac{\ell^2\eta_2}{r^2} + \cdots\,, \\
A_t &= \ell e^{-\beta_a/2}\left(\mu - \frac{Q}{r} + \cdots\right)\,,
\end{aligned} \tag{2.3.12}$$

where there are eight undetermined integration constants $\{\Phi_1, \Phi_2, \eta_1, \eta_2, \mu, Q, G_1, \beta_a\}$ known as UV data in these expansions. The ellipses denote terms higher order in $1/r$, the coefficients of which are determined entirely in terms of the aforementioned eight pieces of UV data. By application of the holographic dictionary, we can relate the data that enters the leading and subleading fall-offs of the $\Phi(r)$ and $\eta(r)$ equations to the source and VEVs of the operators dual to these fields in the boundary theory. The data μ and Q correspond respectively to the chemical potential and charge density associated to the finite density of the field theory. Finally, by constructing the boundary stress tensor one can deduce the exact relationship between the remaining UV data in these expansions and thermodynamic quantities such as the energy and pressure of the dual theory. This procedure is knows as holographic renormalisation as it involves as a first step the addition of counterterms to (2.2.3) to render the full on shell action finite. There is no ambiguity in the 'gravitational part' of this counterterm action, however, for the scalars one must make a choice (corresponding to whether one imposes Dirichlet or Neumann conditions for the second order scalar equation). We choose counterterms for the scalar fields such that the fixed η_1, Φ_1 ensemble has a well defined variational principle. The specific counterterm action we choose is

$$S_{\rm ct} = 2\int_{\partial\Sigma}\sqrt{-\gamma}\left(\mathcal{K} - \frac{2}{\ell}\right) - \int_{\partial\Sigma}\sqrt{-\gamma}\frac{1}{\ell}\left(|S|^2 + \tfrac{1}{2}\Phi^2\right)\,, \tag{2.3.13}$$

where $\mathcal{K} = \gamma^{\mu\nu}\mathcal{K}_{\mu\nu}$ is the trace of the extrinsic curvature of a constant r hypersurface with unit normal $n^r = f(r)^{\frac{1}{2}}$ and $\gamma_{\mu\nu}$ is the induced metric on such a slice. We then find that the total renormalised action

$$S_{\text{ren}} = S + S_{\text{ct}} \tag{2.3.14}$$

is finite, as is the renormalised stress tensor (obtained by functional differentiation of the renormalised action)

$$T_{\mu\nu} = -2\frac{\delta S_{ren}}{\delta\gamma_{\mu\nu}} = 2\left(\mathcal{K}_{\mu\nu} - \mathcal{K}\gamma_{\mu\nu} - \frac{2}{\ell}\gamma_{\mu\nu}\right) - \frac{1}{\ell}\left(|S|^2 + \tfrac{1}{2}\Phi^2\right)\gamma_{\mu\nu}\,. \tag{2.3.15}$$

From the stress tensor, we can then extract the energy density[8] of the field theory defined as

$$\varepsilon = \frac{re^{\beta_a}}{\ell}T_{00} = -\frac{2}{\ell}\left(G_1 - \eta_1\eta_2 - \tfrac{1}{2}\Phi_1\Phi_2\right)\,. \tag{2.3.16}$$

We pause at this point to emphasise the very different roles played by the two scalar fields in our theory. The dilaton Φ introduces an explicit deformation parameter into the theory. More explicitly, we can switch on a relevant operator by sourcing it in the dual theory - in other words by choosing a non-zero value for the UV expansion parameter Φ_1. In contrast, we do not want to allow the second scalar η to act as a source as we would like to consider situations where it can condense *spontaneously* (corresponding to superconductivity in field theory) and hence shall ultimately impose $\eta_1 = 0$ in what follows.

2.4. Thermodynamics

We now turn to a discussion of the thermodynamics of gravitational solutions and relate this to the asymptotic charges of the previous section. In order to do this we begin by analytically continuing to Euclidean signature[9]

$$t = -i\tau\,, \qquad I_E = -iS_{\text{ren}}\,, \qquad A^E_\tau(r) = -iA_t(r)\,, \tag{2.4.17}$$

[8] The quantity $e^{-\beta_a}$ is the boundary speed of light (squared), and so the conversion between ADM mass and energy, and correspondingly energy density, involves a factor of $e^{-\beta_a}$. For this and related reasons it is convenient to set $\beta_a = 0$, which we will assume to be the case from now on.

[9] We emphasise in the interest of clarity that all calculations in this section will be Euclidean but the discussion in this chapter up to this point has of course been Lorentzian and in subsequent sections will return to that signature.

where the index E stands for Euclidean. As a starting point for thermodynamics, we work in the grand canonical ensemble where the Euclidean action I_E is related to the (Gibbs) free energy $\Omega(\mu, T)$ as

$$I_E = \beta\Omega(\mu, T) := \beta \mathrm{vol}_2 \omega(\mu, T)\,, \tag{2.4.18}$$

where the second equality is to be regarded as a definition of the quantity $\omega(\mu, T)$. The key result from which all the thermodynamic relations we are interested in follow is that when evaluated on-shell (i.e. assuming that the equations of motion are satisfied), the above action can be written as a total derivative. We now outline how one can arrive at this fact: one begins by observing after a direct calculation that the (x, x) component of the stress energy tensor $T_{\mu\nu} = -2\frac{\delta\mathcal{L}_M}{\delta g^{\mu\nu}}$ can be written as

$$T_{xx} = \frac{r^2}{l^2}(\mathcal{L} - R)\,, \tag{2.4.19}$$

where R is the Ricci scalar for the geometry (2.2.10) and $\mathcal{L}$ is the Lagrangian density (defined by $S = \int d^4x\sqrt{|g|}\mathcal{L} = \int d^4x\sqrt{|g|}\,(R + \mathcal{L}_M))$ for the action (2.2.3). The corresponding component of the Einstein tensor $G_{\mu\nu} = R_{\mu\nu} - \frac{1}{2}g_{\mu\nu}$ is then given by

$$G^x{}_x = g^{xx}G_{xx} = \frac{1}{2}(\mathcal{L} - R)\,, \tag{2.4.20}$$

where we have used the Einstein equations $G_{xx} = \frac{1}{2}T_{xx}$ (and we remind the reader that the factor of $\frac{1}{2}$ arises as we are working in units where $16\pi G = 1$). Using the result that $R = -G^\mu{}_\mu$, we then arrive at

$$\mathcal{L} = -(G^\tau{}_\tau + G^r{}_r), \tag{2.4.21}$$

and hence

$$\mathcal{S}_{\mathrm{OS}} = -\int \sqrt{|g|}\,(G^\tau{}_\tau + G^r{}_r)\,d^dx\,, \tag{2.4.22}$$

where S_{OS} is the on-shell action. One may now show by explicit calculation of the Einstein tensor (on our ansatz (2.2.10)) that

$$\int \sqrt{|g|}\,(G^\tau{}_\tau + G^r{}_r)\,d^dx = -i\beta\mathrm{vol}_2\int_{r_+}^{\infty}\frac{d}{dr}\left[\frac{2}{r}\sqrt{|g|}g^{rr}\right]dr\,, \tag{2.4.23}$$

from which we see that the on shell action is indeed a total derivative as claimed. We have introduced a lower limit in the above integral to account for a possible black hole horizon in the IR of the geometry at $r = r_+$. (We are implicitly assuming we are using bulk coordinates which are only valid exterior to a horizon and hence the lower limit of the integration should be cut off at this radial position). In fact (2.4.23) vanishes when evaluated there as $g^{rr} = 0$, and hence the integral only has an asymptotic contribution at infinity.

Using the above expression for I_{OS}, one can now calculate quantities such as the pressure of the system using standard thermodynamic relations

$$\omega(\mu, T) = -P\,. \tag{2.4.24}$$

We conclude our discussion of thermodynamics with a derivation of the Smarr relation for our system. We may exploit the symmetries of the background metric, to show that this follows from the vanishing of another total derivative on shell. In particular, note that we have two commuting Killing vectors $T = \partial_\tau$, $\nu = \partial_y$. For κ Killing, we have the Ricci identity $R_{MN}k^M = \nabla_M \nabla_N k^M$, from which we conclude that

$$\sqrt{|g|} R^M{}_N k^N = -\partial_r(\sqrt{|g|} g^{rN} \nabla_N k^M)\,, \tag{2.4.25}$$

where we have used the Killing equation as an intermediate step.

In this way, we construct

$$\begin{aligned}
\sqrt{|g|} R^\tau{}_\tau &= \sqrt{|g|} R^\tau{}_M T^M = -\partial_r \left[\frac{e^{-\beta/2} r^2}{2l^2} (f\beta' - f') \right], &(2.4.26)\\
\sqrt{|g|} R^y{}_y &= \sqrt{|g|} R^y{}_M \nu^M = \partial_r \left[\frac{e^{-\beta/2} r f}{l^2} \right], &(2.4.27)
\end{aligned}$$

and hence

$$\sqrt{|g|}\,(R^\tau{}_\tau - R^y{}_y) = -\partial_r \left[\frac{e^{-\beta/2} r^2}{2\ell^2} \left(f\beta' - f' + \frac{2f}{r} \right) \right]. \tag{2.4.28}$$

The trace reversed Einstein equations can now be used to obtain the following (on shell) relation

$$\sqrt{|g|}\,(R^\tau{}_\tau - R^y{}_y) = -\frac{1}{2} \partial_r \left[\sqrt{|g|} Z_F(\Phi) A^E_\tau F^{\tau r} \right]. \tag{2.4.29}$$

Note that whilst the construction of (2.4.28) is carried out systematically using the symmetries of the background spacetime, in the derivation of (2.4.29), it is a matter of trial and error to find the correct linear combination to give a total derivative. Integration from the black hole horizon at $r = r_+$ to the UV boundary at $r = \infty$

gives the result

$$\frac{e^{-\beta/2}r^2}{\ell^2}\left(f\beta' - f' + \frac{2f}{r}\right)\Bigg|_{r_+}^{\infty} = \sqrt{|g|}Z_F(\Phi)A_\tau^E F^{\tau r}\Big|^{\infty}, \tag{2.4.30}$$

where the bottom limit on the right hand side vanishes as $A_\tau^E(r_h) = 0$ as discussed previously. Evaluated on our UV expansions, we then obtain the Smarr-Gibbs-Duhem relation

$$\frac{3}{2}\varepsilon = \mu Q + Ts - \ell^{-1}\left(\eta_1\eta_2 + \frac{1}{2}\Phi_1\Phi_2\right), \tag{2.4.31}$$

which can be rewritten in terms of the pressure P, charge density Q, and Hawking temperature T as

$$\varepsilon + P = \mu Q + Ts\,, \tag{2.4.32}$$

where we have used that the fact that the temperature is given by

$$T = \frac{e^{(\beta_a-\beta_+)/2}}{4\pi\ell^2}f'(r)\Big|_{r=r_+} \qquad (\beta_a = 0)\,, \tag{2.4.33}$$

and moreover, the entropy density is given in terms of the horizon radius as

$$s = \frac{r_+^2}{4G_N} \qquad (\text{note} \quad 16\pi G_N = 1)\,. \tag{2.4.34}$$

Whilst we have performed the above thermodynamic calculations at finite temperature, it is important to emphasise that they continue to hold at zero temperature (where $r_+ \to 0$). Indeed it is this case that is of most relevance for the discussion that follows in this thesis where the expression for the pressure (and hence Gibbs free energy) is important in demonstrating the existence of $T = 0$ phase transitions.

2.5. Class I: Bottom Up Model and $T = 0$ Shooting Problem

Having analysed the asymptotic AdS_4 expansions and thermodynamics of the solutions we are concerned with for the last two sections, we will now begin our discussion of how to set up the numerical problem of connecting this AdS_4 structure to IR geometries that describe fractionalised and cohesive phases of matter. This will constitute a shooting problem and we will have to develop IR expansions of the field equations (in analogy to what was done in the UV) about leading order geometries that describe fractionalised or cohesive phases respectively. We will perform this analysis at zero temperature where these leading order geometries are singular, charged domain walls. (They are 'well-behaved' nevertheless in the sense that they are the zero temperature limit of non-singular black holes with horizons at finite temperature [2]). Before turning to their construction, however, we first make precise the class of models we will be interested in by a further specialisation of the action (2.2.3).

In the case where $Z_F(\Phi)$ is not symmetric in Φ, there are two qualitatively different behaviours associated with a divergent dilaton. When the dilaton diverges to plus (minus) infinity, the effective gauge coupling $e^2 \sim Z^{-1}$ goes to zero (infinity) in the IR. This behaviour is crucial in our discussion, and in particular as we shall see, it is this that gives rise to a continuous phase transition between a superfluid fractionalised phase and a cohesive phase, via a quantum critical point with finite dilaton. (The transition being driven by the asymptotic (UV) value of the dilaton Φ_1). We will also demonstrate that the gravitational solutions on either side of this solution are of hyperscaling form. In addition to the aforementioned fractionalisation transition, there is also a further transition between a partial and fully fractionalised phase that we shall also discuss.

In order to proceed with our analysis we will now specialise our theory to a particular sub-class of models, sufficient to display the physics we are interested in, by specification of the coupling functions $Z_F(\Phi)$ and $V(\Phi, \eta)$. We choose,

$$Z_F(\Phi) = Z_0^2 e^{a\Phi/\sqrt{3}}\,, \qquad \ell^2 V(\Phi,\eta) = -V_0^2 \cosh\left(b\Phi/\sqrt{3}\right) - 2\eta^2 + g_\eta^2 \eta^4\,, \quad (2.5.35)$$

where $a, b > 0$ (the latter condition is of course without loss of generality). The η^4 term allows for soliton solutions that interpolate between the AdS_4 maximum at $\eta = 0$ and the AdS_4 minimum at $\eta^2 = g_\eta^{-2}$. We will study IR geometries for general values of a and b (see also [174, 182]). All our numerical results will however be for the particular case $a = b = g_\eta^2 = 1$, $V_0^2 = 6$ and $Z_0^2 = 1$.

2.5.1. T=0 Infrared Expansions

We now develop IR expansions of the equations of motion that follow from (2.2.3) about geometries describing fractionalised and cohesive states of matter. We work at $T = 0$ and following Hartnoll [174] expand all fields in a Frobenius expansion about $r = 0$. Moreover, we search for solutions that have a logarithmically divergent dilaton[10]. In summary, we look for expansions about $r = 0$ of the form:

$$\begin{aligned}
f(r)e^{-\beta(r)} &= r^\alpha\left(1+\sum_{n=1}^{\infty}\beta_n r^{sn}\right)\,,\\
f(r) &= f_0 r^\beta\left(1+\sum_{n=1}^{\infty}f_n r^{sn}\right)\,,\\
A_t(r) &= A_0 r^\gamma\left(1+\sum_{n=1}^{\infty}A_n r^{sn}\right)\,,\\
\Phi(r) &= \sqrt{3}\left(\delta\log r+\sum_{n=1}^{\infty}\Phi_n r^{sn}\right)\,,\\
\eta(r) &= \eta_0 r^\tau\left(1+\sum_{n=1}^{\infty}\Pi_n r^{sn}\right)\,,
\end{aligned}\tag{2.5.36}$$

where $\{\alpha,\beta,\gamma,\delta,\tau,f_0,A_0,\eta_0,\beta_n,f_n,A_n,\Phi_n,\Pi_n\}$ are constants to be determined by solving the equations of motion order by order and $s\in\mathbb{Q}$ is the step-size of the series. We note that we have used a rescaling of the t coordinate to remove a constant prefactor in the $f(r)e^{-\beta(r)}$ expansion together with an r rescaling to remove a constant term in the $\Phi(r)$ expansion. The quantities $\{\alpha,\beta,\gamma,\delta,\tau,f_0,A_0,\eta_0\}$ characterise the leading order solution. As we shall see in the next subsection, in the case of a fractionalised IR solution (where the IR horizon flux is non-vanishing), the quantities $\{\alpha,\beta,\gamma,\delta,\tau,f_0,A_0\}$ are explicitly determined by the equations of motion at leading order. On the other hand, η_0 is not determined at this order and is data. The remaining coefficients in the expansions $\{\beta_n,f_n,A_n,\Phi_n,\Pi_n\}$ are fully determined at higher orders and no new data enters the system. In the case of a cohesive solution, together with the equations of motion, we impose that the horizon flux vanishes in the IR ($\lim_{r\to 0}\sqrt{-g}Z(\Phi)F^{rt}=0$). One finds then that $\{\alpha,\beta,\delta,\tau,f_0\}$ are determined by the leading order equations of motion, whilst A_0 and η_0 are data (γ which is free at this order gets fixed in terms of η_0 when including perturbations as we explain below). In order to ensure the IR horizon flux vanishes, we set $A_0 = 0$ for our cohesive solutions. (Note we will later introduce a non-zero flux into these solutions by including deformations about them as we describe in the next paragraph). As with the fractionalised solutions, all the higher order coefficients $\{\beta_n,f_n,A_n,\Phi_n,\Pi_n\}$ are determined order by order and there is no more data.

Having developed the IR expansions above, we need to connect them to the AdS_4 asymptotics of section (2.3). In order to do this, we proceed by perturbing the IR

[10] As explained above, the heuristic motivation for choosing this behaviour is that the divergence of Φ controls the behaviour of $Z_F(\Phi)$ and thus the effective gauge coupling and bulk IR electric flux, which is intimately tied to fractionalisation.

expansions above[11]. This perturbed expansion can then be integrated outwards (to large values of r) and connected to the UV expansion (that is integrated inwards) by tuning a subset of the IR and UV data as a shooting problem. (The shooting problem itself will be described in much greater detail in the next section). We perturb the equations (2.5.36) as follows,

$$\begin{aligned}
f(r)e^{-\beta(r)} &= r^{\alpha}\left(1+\sum_{n=1}^{\infty}\beta_n r^{sn}\right)+\epsilon r^{\alpha}\,\delta\beta\left(\sum_{ij=1}^{\infty}\beta_{ij}r^{iN+s(j-1)}\right)\,,\\
f(r) &= f_0 r^{\beta}\left(1+\sum_{n=1}^{\infty}f_n r^{sn}\right)+\epsilon r^{\beta}\,\delta f\left(\sum_{ij=1}^{\infty}f_{ij}r^{iN+s(j-1)}\right)\,,\\
A_t(r) &= A_0 r^{\gamma}\left(1+\sum_{n=1}^{\infty}A_n r^{sn}\right)+\epsilon r^{\gamma}\,\delta A\left(\sum_{ij=1}^{\infty}A_{ij}r^{iN+s(j-1)}\right)\,,\\
\Phi(r) &= \sqrt{3}\left(\delta\log r+\sum_{n=1}^{\infty}\Phi_n r^{sn}\right)+\epsilon\sqrt{3}\,\delta\Phi\left(\sum_{ij=1}^{\infty}\Phi_{ij}r^{iN+s(j-1)}\right)\,,\\
\eta(r) &= \eta_0 r^{\tau}\left(1+\sum_{n=1}^{\infty}\Pi_n r^{sn}\right)+\epsilon r^{\tau}\,\delta\eta\left(\sum_{ij=1}^{\infty}\eta_{ij}r^{iN+s(j-1)}\right)\,, \qquad (2.5.37)
\end{aligned}$$

where ϵ is the expansion parameter and $\{N,\delta\beta,\delta f,\delta A,\delta\Phi,\delta\eta,\beta_{ij},f_{ij},A_{ij},\Phi_{ij},\eta_{ij}\}$ are constants. The leading perturbations about our original IR background are characterised by an exponent N and amplitudes $\{\delta\beta,\delta f,\delta A,\delta\Phi,\delta\eta\}$. (Without loss of generality, we have assumed that $\beta_{11}=f_{11}=A_{11}=\Phi_{11}=\eta_{11}=1$). These quantities can be determined by the *linearisation* of the equations of motion, about the background (2.5.36) including only the *leading* perturbation in (2.5.37). (More than the leading term should of course be included when shooting later). In more detail, if we substitute this expansion into the equations of motion, which we write as a vector E_i (consisting of the Einstein, Maxwell and scalar equations) and then expand as a power series in ϵr^N, one finds (at leading order)

$$M_{ij}\delta v_j = 0\,, \qquad (2.5.38)$$

where $v_j=\{\beta(r),f(r),A_t(r),\Phi(r),\eta(r)\}$, $\delta v_j=\{\delta\beta,\delta f,\delta A,\delta\Phi,\delta\eta\}$ and the linearisation of the equations $M_{ij}=\frac{\delta E_i}{\delta v_j}$. The exponent N is then determined by the condition $\det M_{ij}=0$ and the vector δv_j is given by the zero eigenvectors of M_{ij}. The equation governing the perturbations (2.5.38) admits two non-trivial solutions for the IR backgrounds we discuss. In the fractionalised case, for the first deformation

[11] In holographic language, we would like to characterise the possible irrelevant deformations about the IR solution (2.5.36) and use these to induce an RG flow to the UV.

one finds that N is determined explicitly, all perturbation modes except the charged scalar are excited ($\delta\eta = 0$) and δv_j is given in terms of a single free parameter c^{IR}. The second deformation on the other hand has $N = 0$ and perturbs only the IR value of the charged scalar. In total therefore, there are two pieces of IR data in fractionalised solutions: η_0 and c^{IR}. For cohesive solutions, the situation is somewhat more complex and one finds for the first perturbation that $N = N(\eta_0)$, and furthermore $\gamma = \gamma(\eta_0)$ (recall γ was not fixed at leading order in the cohesive case). The only mode that is excited is the Maxwell field mode, (so $\delta\beta = \delta f = \delta\Phi = \delta\eta = 0$). The second perturbation has $N = 0$ and shifts the IR value of the charged scalar only. In total, as with the fractionalised case, there are hence two pieces of IR data: η_0 and δA. We now present in more detail the IR geometries that we have found.

Fractionalised IR Solutions

The first class of solutions we discuss are fractionalised solutions, where some or all of the flux is sourced by a black hole horizon. In this case, one must demand that the horizon flux $\sqrt{-g}Z(\Phi)F^{rt}$ is a non-zero constant as $r \to 0$. This is most easily engineered by substituting the expansions (2.5.36) into the horizon flux, to find at leading order $\sqrt{-g}Z(\Phi)F^{rt} \sim r^{1+\frac{1}{2}(\alpha-\beta)+\delta+\gamma}$. To ensure a non-zero horizon flux, we then impose that $1+\frac{1}{2}(\alpha-\beta)+\delta+\gamma = 0$. The fractionalised IR solutions are found to be

$$
\begin{aligned}
f(r)e^{-\beta(r)} &= r^{\frac{2(12+a^2-b^2)}{(a+b)^2}}\left(1+\sum_{n=1}^{\infty}\beta_n r^{sn}\right), \\
f(r) &= f_0 r^{\frac{2(a-b)}{a+b}}\left(1+\sum_{n=1}^{\infty}f_n r^{sn}\right), \\
A_t(r) &= A_0 r^{\frac{12+(3a-b)(a+b)}{(a+b)^2}}\left(1+\sum_{n=1}^{\infty}A_n r^{sn}\right), \\
\Phi(r) &= \sqrt{3}\left(\frac{-4}{a+b}\log r+\sum_{n=1}^{\infty}\Phi_n r^{sn}\right), \\
\eta(r) &= \eta_0 r^{\tau}\left(1+\sum_{n=1}^{\infty}\Pi_n r^{sn}\right),
\end{aligned}
\tag{2.5.39}
$$

where

$$
\begin{aligned}
f_0 &= \frac{(a+b)^4 V_0^2}{4(6+a(a+b))(12+(3a-b)(a+b))}, \\
A_0^2 &= \frac{4(6-b(a+b))}{(12+(3a-b)(a+b))Z_0^2}.
\end{aligned}
\tag{2.5.40}
$$

In a fully fractionalised phase one has by definition $\eta_0 = 0$, but the latter is non-zero in a partially fractionalised solution. We do not explicitly show the higher order terms $\{\beta_n, f_n, A_n, \Phi_n, \Pi_n\}$ although we note once again that they are determined explicitly and no new data enters the system. The step size s in the series above is in general a complicated function of the parameters in the theory $\{a, b, V_0, Z_0, g_\eta\}$ (and we were not able to find a general formula for it). In the case of relevance for us however, $\{a = b = 1, V_0^2 = 6, Z_0^2 = 1\}$ (for which we do all our numerics), one finds for these fractionalised solutions that $s = 4$.

From the above leading order expansion, we can extract the dynamical critical and hyperscaling exponents which we find to be equal to,

$$z = \frac{12 + (a - 3b)(a + b)}{a^2 - b^2}\,, \qquad \theta = \frac{4b}{b - a}\,. \tag{2.5.41}$$

We pause here to explain an important point. Both of these scaling quantities are infinite for our choice of parameters defined above. Despite this fact, however, their ratio remains finite (see also [182]) and the solution is well-behaved. This observation is important as many thermodynamic quantities in the vicinity of the quantum critical point are governed by this ratio (as we shall discuss briefly in what follows) and hence will have finite (as opposed to unbounded) scaling exponents with temperature.

Having found the above IR expansions, one may now study the perturbations (deformations) about this background as in (2.5.37). For these fractionalised solutions there are two such deformations. For the first perturbation, N is determined explicitly in terms of the theory parameters as follows. (We present the results in the case where $a = b$ as they are extremely unsightly in the general case). One finds

$$N = \frac{3 + b^2}{6b^4}\left(-3 + \sqrt{81 - 24b^2}\right)\,. \tag{2.5.42}$$

Since in the case of relevance for us $\{a = b = 1, V_0^2 = 6, Z_0^2 = 1\}$, we have $N > 0$, this perturbation is what is known in AdS/CFT language as an irrelevant deformation. It is negligible as $r \to 0$, but becomes important in the ultraviolet as r becomes large. It is this irrelevant deformation that allows us to connect the IR solutions here to new asymptotics (i.e. AdS_4). All perturbation modes, except the charged scalar are excited ($\delta\eta = 0$) and one may show that they are determined up to an overall amplitude c^{IR} as

$$\{\delta\beta\,, \delta f\,, \delta A\,, \delta\Phi\} = c^{IR}\left\{1\,, -f_0\,, \frac{Nb^2 A_0}{2(3 - b^2)}\,, -\frac{b}{\sqrt{3}}\right\}\,. \tag{2.5.43}$$

This mode is of a similar structure to what has been found in studies of fractionalisation in a fermionic context [174].

The second deformation is much simpler, having $N = 0$, and only the charged scalar mode is excited (i.e. $\{\delta\beta, \delta f, \delta A, \delta\Phi\} = \mathbf{0}$). One may think of this perturbation as simply a redefinition of the IR data η_0. In summary, the IR data in fractionalised solutions is η_0 and c^{IR}.

Critical IR Solution

We now describe the so called 'critical' IR solution which by definition has a non-divergent dilaton and in fact has $\Phi = 0$. Physically, the solution is just the AdS_4 solution that arises when the charged scalar field is fixed to lie at the minimum of its potential and the gauge field vanishes $A_t(r) = 0$. The solution is of physical interest as the transition from fractionalised to cohesive phases takes place via this critical solution. (This was shown in detail in the finite temperature discussions of fractionalisation in the paper on which this chapter is based [2], but will not be discussed here and we merely mention this solution for completeness). The solution takes the form

$$\begin{aligned} f(r)e^{-\beta(r)} &= r^2\,, \\ f(r) &= \frac{r^2}{R_{IR}^2}\,, \\ \eta(r) &= \pm g_\eta^{-1}\,, \\ A_t(r) &= 0\,, \end{aligned} \tag{2.5.44}$$

with

$$R_{IR}^2 = \frac{6g_\eta^2\ell^2}{1+g_\eta^2V_0^2}\,, \tag{2.5.45}$$

where R_{IR} is the AdS length scale. We stress that unlike the other IR geometries we consider in this section, the critical solution is an *exact* solution - there are no subleading corrections to it.

Once again, there are two irrelevant deformations about this background. The first deformation excites only the Maxwell field ($A_t(r) \to A_t(r) + \delta A_t(r)$), and the second only the charged scalar field ($\eta(r) \to \eta(r) + \delta\eta(r)$). At leading order, they take the form

$$\delta A_t(r) = \delta A\, r^{N_1}\,, \qquad \delta\eta(r) = \delta\eta\, r^{N_2}\,, \tag{2.5.46}$$

with

$$
\begin{aligned}
N_1 &= \frac{1}{2}\left(-1+\sqrt{1+\frac{48\ell^2 q^2}{Z_0^2\left(1+g_\eta^2 V_0^2\right)}}\right)\,, \\
N_2 &= \frac{3}{2}\left(-1+\sqrt{1+\frac{32 g_\eta^2}{3\left(1+g_\eta^2 V_0^2\right)}}\right)\,.
\end{aligned} \tag{2.5.47}
$$

Cohesive IR Solutions

The final class of IR geometries that we look for are the cohesive solutions. These are defined by demanding that the IR horizon flux $\lim_{r\to 0}\sqrt{-g}Z(\Phi)F^{rt}$ vanishes which we engineer by choosing $A_0 = 0$. The solution is found to be,

$$
\begin{aligned}
f(r)e^{-\beta(r)} &= r^2\left(1+\sum_{n=1}^{\infty}\beta_n r^{sn}\right)\,, \\
f(r) &= f_0 r^{\frac{2(3-b^2)}{3}}\left(1+\sum_{n=1}^{\infty} f_n r^{sn}\right)\,, \\
A_t(r) &= 0\,, \\
\Phi(r) &= \sqrt{3}\left(\frac{2b}{3}\log r+\sum_{n=1}^{\infty}\Phi_n r^{sn}\right)\,, \\
\eta(r) &= \eta_0\left(1+\sum_{n=1}^{\infty}\Pi_n r^{sn}\right)\,,
\end{aligned} \tag{2.5.48}
$$

with

$$
f_0 = \frac{3V_0^2}{4(9-b^2)}\,. \tag{2.5.49}
$$

Once again, the stepsize s of the series is a complicated function of the theory parameters, but in the case of relevance for our numerics $\{a = b = 1, V_0^2 = 6, Z_0^2 = 1\}$, one finds $s = 2/3$. These solutions have dynamical critical exponent z and hyperscaling parameter θ given by

$$
z = 1\,, \quad \theta = -\frac{2b^2}{3-b^2}\,. \tag{2.5.50}
$$

As in the previous two cases, we now discuss the perturbations that one finds about this IR background. Once again there are two such perturbations: The first deformation excites only the Maxwell field ($A_t(r) \to A_t(r) + \delta A_t(r)$), so that $\{\delta\beta = \delta f = \delta\Phi = \delta\eta = 0\}$. The corresponding exponent N is given as $N = N(\eta_0)$ for these solutions. Explicitly, in the case where $a = b$, the perturbation takes the form

$$\delta A_t = \delta A r^{\gamma(\eta_0)} = \delta A r^{\frac{3+b^2}{6}+N(\eta_0)}\,, \tag{2.5.51}$$

with

$$N(\eta_0) = \frac{3+b^2}{6}\left(-2+\sqrt{1+\frac{72q^2\eta_0^2}{Z_0^2 f_0(3+b^2)^2}}\right)\,. \tag{2.5.52}$$

We note also that consistency of the series expansion requires that $N > 0$ and for these cohesive solutions this produces the following constraint

$$\eta_0^2 \; > \; \frac{(3+b^2)^2 f_0 Z_0^2}{72q^2}\,. \tag{2.5.53}$$

The reader is referred also to [201], where a similar constraint is seen to arise.

The second deformation is analogous to that found for fractionalised solutions, having $N = 0$, and only the charged scalar mode is excited (i.e. $\{\delta\beta, \delta f, \delta A, \delta\Phi\} = \mathbf{0}$). One may think of this perturbation as simply a redefinition of the IR data η_0. In summary for cohesive solutions, we again have two pieces of data, δA and η_0.

2.5.2. Overview of the Numerical Shooting Problem

As we have discussed, in order to construct the fractionalised and cohesive geometries we are searching for, we must connect the IR expansions of section (2.5.1) to the desired AdS_4 asymptotics. To do this, we perturbed these IR geometries by their irrelevant deformations and then the procedure of integrating these perturbations to the correct UV is an ODE shooting problem. We solve this shooting problem by providing data in the IR of the geometry and integrating to the UV and providing data in the UV and using this to integrate into the IR. We then require that these two solutions match correctly at some arbitrary point in between. In the UV, the data is given by the free parameters in the large r asymptotic expansions of section (2.3). In the IR, the data is determined by an expansion about the horizon in the case of a black hole solution, and of particular relevance for us at $T = 0$, by the data in the perturbed IR expansions of section (2.5.1).

Due to the nature of our ansatz (2.2.10), we only have two non-trivial Einstein equations. One can show in particular that the $G_{xx} = G_{yy}$ equation is satisfied automatically when both the G_{tt} and G_{rr} equations hold, and by considering two appropriate linear combinations of the G_{tt} and G_{rr} equations, the two Einstein equations can be taken to be first order ODEs for the functions $f(r)$ and $\beta(r)$. The remaining three equations, for the Maxwell field $A_t(r)$ together with the neutral and charged scalars $\Phi(r), \eta(r)$ are second order. Altogether, we will therefore need eight pieces of data $(1+1+2+2+2)$ to specify a unique solution. In detail, if we match the solutions integrated from the IR up to some intermediate position $r = r_0$ and from the UV down to $r = r_0$, we must match eight integration constants associated to our equations. Let us denote the IR data as x_i and UV data as y_a. We introduce a vector $\Psi^{IR}(x)$ defined as

$$\Psi^{IR}(x) = \left(f_x(r_0), \beta_x(r_0), A_x(r_0), A'_x(r_0), \Phi_x(r_0), \Phi'_x(r_0), \eta_x(r_0), \eta'_x(r_0)\right), \quad (2.5.54)$$

which is obtained by integrating the differential equations to some fixed radius r_0 by evolving the given IR data x_i. We can also define an analogous vector that is obtained from evolving given UV data y_a inwards to the same radius

$$\Psi^{UV}(y) = \left(f_y(r_0), \beta_y(r_0), A_y(r_0), A'_y(r_0), \Phi_y(r_0), \Phi'_y(r_0), \eta_y(r_0), \eta'_y(r_0)\right). \quad (2.5.55)$$

We now construct a quantity dependent on the whole set of initial data (IR and UV)

$$V(x,y) = \Psi^{IR}(x) - \Psi^{UV}(y). \quad (2.5.56)$$

In order to have a solution to our differential equations, we must now have

$$V(x,y) = 0, \quad (2.5.57)$$

which is eight conditions. We will consequently require that eight elements of the data (x_i, y_a) be tuned in order to satisfy this constraint. We denote the tuning variables as α and the remainder of the data that fixes the solution of interest as λ. In summary, for some λ, we will need to tune the α such that $V(\alpha;\lambda) = 0$.

To illustrate the above discussion, we consider our case in some detail. The UV expansion we use is common to all the geometries under consideration and initially consists of eight pieces of data $\{G_1, \beta_a, \Phi_1, \Phi_2, \eta_1, \eta_2, \mu, Q\}$, but we require that $\eta_1 = 0$ for solutions of interest (since we are only interested in scenarios where the charged scalar spontaneously breaks the $U(1)$ symmetry in the theory) which reduces this to seven pieces of UV data. In the IR, in all cases (cohesive, fully fractionalised and partially fractionalised) we have two pieces of data $\{\eta_0, c\}$ where $c = c^{IR}$ for fractionalised solutions and $c = \delta A$ for cohesive solutions (refer to section (2.5.1)). Altogether, we therefore have a total of nine pieces of data and eight constraints to satisfy. We therefore expect a one parameter family of solutions of all three types, where each family can be parameterised by some element of the IR or UV data which we are free to choose. We choose to use Φ_1 and hence we write $\lambda = \{\eta_1 = 0, \Phi_1\}$ and $\alpha = \{G_1, \beta_a, \Phi_2, \eta_2, \mu, Q, \eta_0, c\}$. One must choose some initial value for the parameter Φ_1 and some initial guess for the data α. Following the prescription outlined above, we must then tune the α such that $V(\alpha; \lambda) = 0$ and this is done by a Newton Raphson method. One then repeats this procedure for a variety of choices of the parameter Φ_1 to generate a line of solutions. (Of course, what one might find (and we do find) is that solutions of all types don't exist for all values of the parameter Φ_1). We close this section by noting that although one could in principle shoot from just one end of the geometry (either the UV or the IR), it is much easier for our purposes to shoot from both ends to encode automatically from the start the asymptotic structures we are interested in.

2.5.3. T=0 Fractionalisation Transition

In this section, we show the results of deforming the zero temperature geometries of section (2.5.1) by their irrelevant deformations and shooting to the UV to construct solutions which asymptote to AdS_4. All numerics associated with the shooting problem were performed in Mathematica, integrating the IR expansions outwards from $r_{min} = 0.1$ to $r_{mid} = 3$, and the UV expansions from $r_{max} = 70$ to $r_{mid} = 3$. What one finds are one parameter families of full geometries of all three phases: superfluid cohesive, superfluid (partially) fractionalised and fully fractionalised. In more detail, if we parameterise solutions by the dimensionless UV ratio, $\frac{\Phi_1}{\mu}$ the superfluid cohesive phase is found to exist for $\frac{\Phi_1}{\mu} < \frac{\Phi_1}{\mu}(g_m) \sim -0.131$. The superfluid fractionalised phase exists for $\frac{\Phi_1}{\mu}(g_m) < \frac{\Phi_1}{\mu} < \frac{\Phi_1}{\mu}(g_f)$ and meets the fully fractionalised branch smoothly at $\frac{\Phi_1}{\mu}(g_f) \sim 0.621$.

In figures (2.2),(2.3) and (2.4) respectively we plot examples of the full shooting solutions in a fractionalised phase (showing two cases with different degrees of fractionalisation) and in the mesonic phase. The norm of the vector V (as defined in equation (2.5.56)) serves as a measure of the accuracy of a shooting solution. We find for that $\sqrt{V(r_{mid})} \sim 10^{-9}$ for all three of the aformentioned solutions. On the same graphs, we also overlay the UV and IR expansions of the relevant functions, in this way demonstrating that the full solution has the appropriate asymptotics.

The holographic quantity we use as a measure of fractionalisation is the ratio of the flux emanating from the deep IR of the solution $\mathcal{A}$ to the total charge Q. As a consequence of Gauss's law, this must interpolate between zero in the cohesive phase and unity in the fully fractionalised case [174, 176, 192]

$$\frac{\mathcal{A}}{Q} \equiv \frac{1}{Q}\left(\sqrt{-g}Z(\Phi)F^{rt}\Big|_{r_+}\right) . \tag{2.5.58}$$

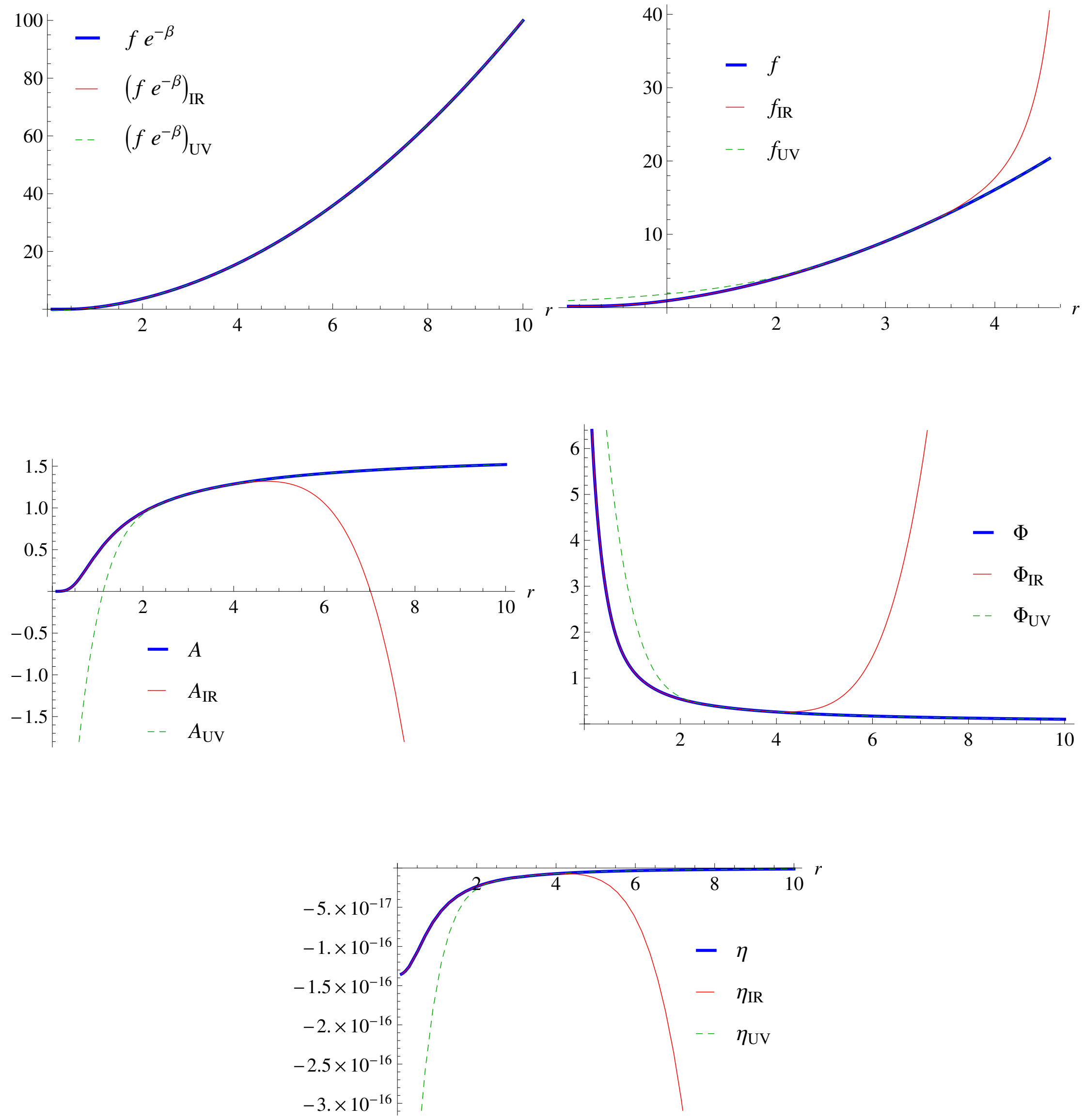

Figure 2.2.: Full shooting solutions $\{f(r), \beta(r), A(r), \Phi(r), \eta(r)\}$ for an (almost) fully fractionalised phase found using the methods described in the text. We overlay on the same plots, the UV and IR expansions to demonstrate the solutions have the correct asymptotics. The solution displayed was computed with $r_{mid} = 0.1, r_{mid} = 3, r_{max} = 70$ and has $\frac{\Phi_1}{\mu} = 0.607$. Notice the sign of the dilaton divergence is as in (2.5.39) and moreover observe that the charged scalar is essentially zero everywhere. One finds from analysis of the ratio of the total flux emanating from the IR to the total charge that for $\frac{\Phi_1}{\mu} \sim 0.621$, solutions become fully fractionalised.

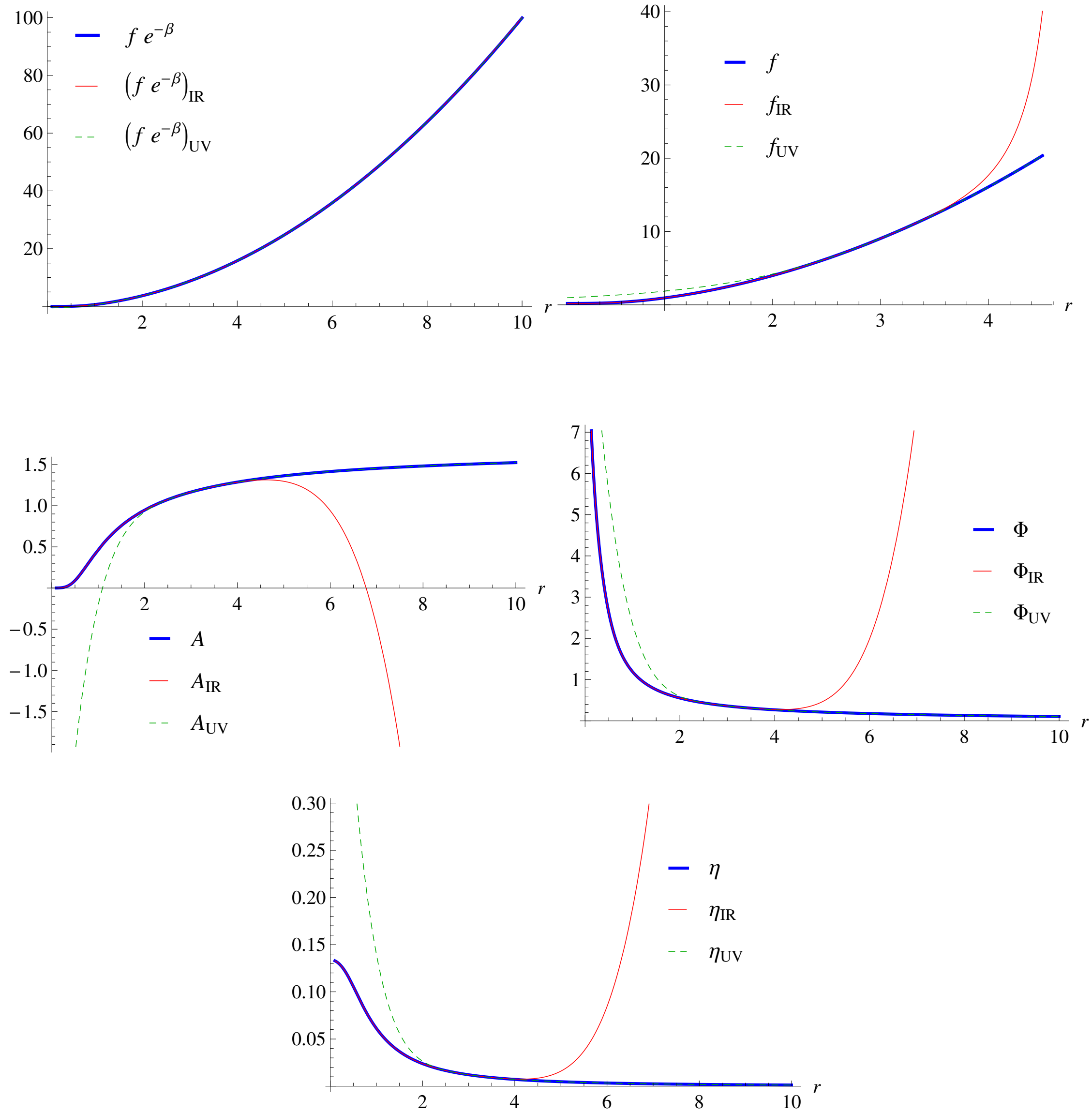

Figure 2.3.: Full shooting solutions $\{f(r), \beta(r), A(r), \Phi(r), \eta(r)\}$ for a partially fractionalised phase found using the methods described in the text. We overlay on the same plots, the UV and IR expansions to demonstrate the solutions have the correct asymptotics. The solution displayed was computed with $r_{mid} = 0.1, r_{mid} = 3, r_{max} = 70$ and has $\frac{\Phi_1}{\mu} = 0.0964$. Notice the sign of the dilaton divergence is as in (2.5.39) and moreover observe that the charged scalar is non-zero. One finds that this partially fractionalised phase persists until $\frac{\Phi_1}{\mu} \sim -0.131$.

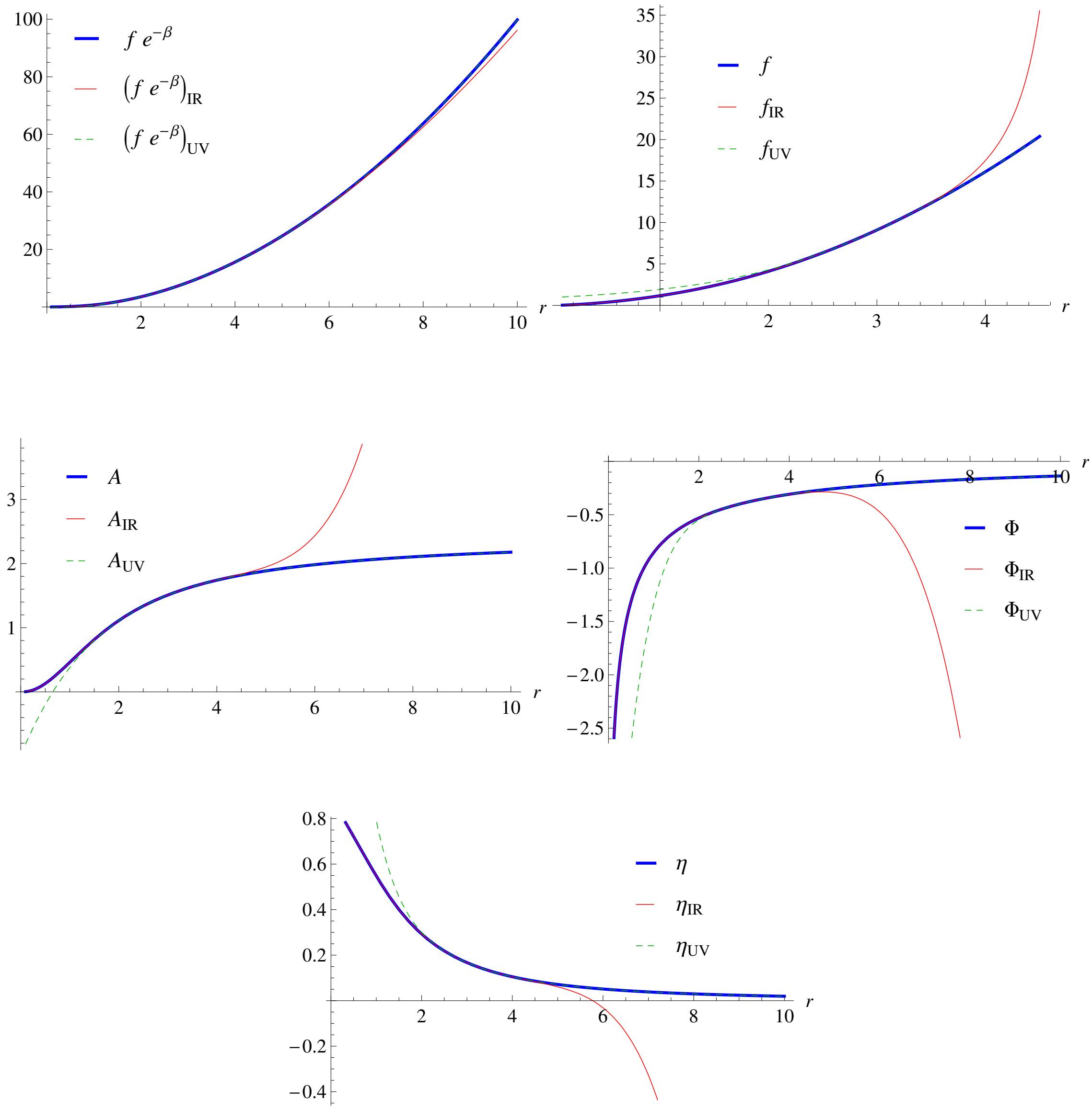

Figure 2.4.: Full shooting solutions $\{f(r), \beta(r), A(r), \Phi(r), \eta(r)\}$ for a cohesive phase found using the methods described in the text. We overlay on the same plots, the UV and IR expansions to demonstrate the solutions have the correct asymptotics. The solution displayed was computed with $r_{mid} = 0.1, r_{mid} = 3, r_{max} = 70$ and has $\frac{\Phi_1}{\mu} = -0.598$. Notice the sign of the dilaton divergence is as in (2.5.48) and is opposite to the fractionalised solutions. The charged scalar is of course non-zero in the cohesive phase.

In Fig. 2.5 we plot this measure for the three solution branches found and it is this that allows us to identify which phase corresponds to superfluid cohesive, superfluid fractionalised and fully fractionalised respectively. In addition to this measure of

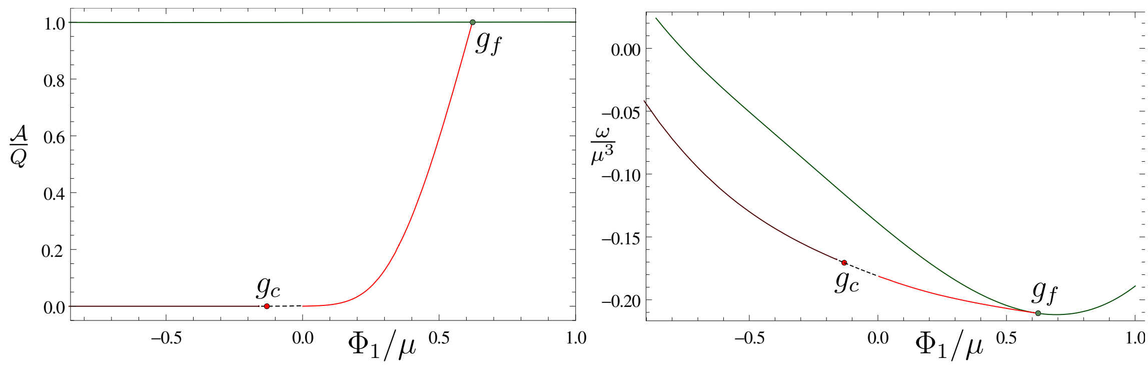

Figure 2.5.: Dependence of the $T = 0$ domain walls on the parameter Φ_1/μ. As in Fig 2.1, shades of red indicate broken $U(1)$ symmetry, with dark red indicating a superfluid cohesive and bright red a superfluid fractionalised phase. Fully fractionalised geometries are shown in green. Supplementary low temperature data ($T \simeq 10^{-3}\mu$) in the vicinity of the fractionalisation transition g_c is indicated by black dashes.

fractionalisation, we also plot in 2.5 the free energy ω (more precisely the dimensionless quantity ω/μ^3 obtained by dividing out the chemical potential) of the various branches. As discussed previously, this is crucial in exhibiting a phase transition. We demonstrate explicitly that the free energy of the fractionalised phase is always greater than the superfluid phase whenever they coexist and hence the transition does indeed occur. We note also that it proved numerically extremely challenging to calculate the zero temperature free energies very near the critical point. To this end, in this region we supplement these figures with low temperature data ($T \simeq 10^{-3}\mu$) calculated using the methods outlined in section (2.5.4). Note the close agreement this demonstrates between our $T = 0$ and low temperature analyses.

The behaviour of the free energy in Fig. 2.5 strongly suggests that the phase transition is continuous. Using the same data, one can also compute the first derivative of the free energy which appears to be smooth also. We can therefore rule out a first order transition, but we are unable to make further definitive statements about the order of the transition and in particular, it is likely that more robust numerics would be needed to determine this.

2.5.4. Comments on Finite Temperature

We now make some remarks on fractionalisation at finite temperature. This was discussed in greater depth in the paper on which this chapter is based [2], but was not the work of the author of this thesis and thus is not included in detail here. What was done there was to extrapolate the known finite temperature solutions to low temperature in order to demonstrate that they connect to the $T = 0$ geometries considered in the preceding sections. The analysis reveals some important physics: the process of lowering the temperature can result in an instability that leads to a superconducting phase below some critical temperature T_C. This critical temperature is a function of the parameters (data) in the theory and can be dialed to zero by tuning these parameters beyond certain threshold values. The effect of this is to produce a structure in phase space under which the theory is superconducting, known as a 'superconducting dome'. The position of the edge of this dome was argued to constrain when $T = 0$ fractionalisation transitions can occur and in particular accounts for the absence of a $T = 0$ fractionalised phase in M-theory as we shall explain in the next section. The finite temperature analysis is also very illuminating, as through it, one can study various low temperature signatures of quantum criticality, notably the dynamical critical exponent z and the hyperscaling violation exponent θ, in terms of which the thermodynamic entropy scales as

$$S \sim T^{\frac{d-\theta}{z}} \,. \tag{2.5.59}$$

Using equation (2.5.59), it was shown in the aforementioned paper [2] how one can identify z and θ from numerical fits of the low-temperature analysis. From these calculations, one sees strikingly the quantum critical nature of the $T = 0$ fractionalisation transition which leaves a distinctive 'wedge imprint' on thermodynamic observables at finite temperature that is characteristic of quantum phase transitions. Moreover, one can compare the values of θ and z on either side of this wedge to find that at low temperatures they match extremely closely with the analytic $T = 0$ values for the cohesive and fractionalised geometries of section (2.5.1), lending further support for the picture of a $T = 0$ fractionalisation transition and verifying the validity of our $T = 0$ IR geometries. (Further strength for this picture is also provided by examining the behaviour of the dilaton which is a finite at $T \neq 0$, having no divergence but starts to diverge to either plus or minus infinity as the temperature is lowered, again agreeing with what was found at $T = 0$).

2.6. Class Ib: Bottom - Up Model

Thus far, we have presented a model which falls under class Ia of the classification introduced through Fig. 2.1. Qualitatively the key point governing its phenomenology is the fact that the coupling $Z_F(\Phi)$ remains finite for an interval of UV scalar deformations Φ_1. It is this fact that allows the model to support a superfluid fractionalised phase (and hence to exhibit a phase transition as these solutions become thermodynamically preferred).

In this small section, we make a few brief remarks about a model in class Ib. We consider a theory with the same potential that we have used previously, but will consider now an *even* gauge coupling $Z_F(\Phi) = Z_0^2 \cosh\left(\frac{a\Phi}{\sqrt{3}}\right)$. With this new coupling, if we have an IR divergent dilaton, then $Z_F(\Phi)$ must diverge irrespective of the sign of the dilaton blowup. Qualitatively, we therefore expect the interval of cohesive solutions exhibited by this theory to be reduced to a single point corresponding to $\Phi_1 = 0$. Note that at this point, the solution has $\Phi(r) = 0$ everywhere and corresponds to an AdS_4 to AdS_4 charged domain wall.

We conjecture that this model will exhibit a transition from a superfluid cohesive phase at the point $\Phi_1 = 0$, to a superfluid fractionalised phase that persists for some region $0 < \Phi_1 < \Phi_1(g_f)$, eventually becoming fully fractionalised when $\Phi_1 \geq \Phi_1(g_f)$.

2.7. Class II: M Theory

In this section, we will now discuss a model in class II, which arises as a consistent truncation of $11D$ supergravity on an arbitrary Sasaki-Einstein 7-manifold [202, 203]. (Whilst, the details of the compactification and truncation are fascinating we need not discuss them further here). Structurally, this model shares even gauge coupling with class Ib, but differs in that it has finite Z everywhere. The equations of motion of the theory can be obtained from the four dimensional action

$$\begin{aligned} S_M \;=\; & \frac{1}{16\pi G}\int d^4x\sqrt{-g}\Big[R - \frac{(1-h^2)^{3/2}}{1+3h^2}F_{MN}F^{MN} - \frac{3}{2(1-\frac{3}{4}|\chi|^2)^2}|D\chi|^2 \\ & -\frac{3}{2(1-h^2)^2}(\nabla h)^2 - \frac{6}{\ell^2}\frac{(-1+h^2+|\chi|^2)}{(1-\frac{3}{4}|\chi|^2)^2(1-h^2)^{3/2}}\Big] + \frac{1}{16\pi G}\int \frac{2h(3+h^2)}{1+3h^2}F\wedge F\,. \end{aligned} \tag{2.7.60}$$

By defining $\chi = \xi e^{iq\varphi}$ and performing the transformation

$$h = \tanh\left(\frac{\Phi}{\sqrt{3}}\right)\,, \qquad \xi = \frac{2}{\sqrt{3}}\tanh\left(\frac{\eta}{\sqrt{2}}\right)\,, \tag{2.7.61}$$

this action falls into the class II of models of Fig. 2.1 and is of the form (2.2.3) with the specific choices

$$
\begin{aligned}
Z_F(\Phi) &= \frac{4}{\cosh^3\left(\frac{\Phi}{\sqrt{3}}\right)\left(1+3\tanh^2\left(\frac{\Phi}{\sqrt{3}}\right)\right)}\,, \\
V(\Phi,\eta) &= \frac{\frac{4}{3}\tanh^2\left(\frac{\eta}{\sqrt{2}}\right)-\cosh^{-2}\left(\frac{\Phi}{\sqrt{3}}\right)}{\cosh^{-4}\left(\frac{\eta}{\sqrt{2}}\right)\cosh^{-3}\left(\frac{\Phi}{\sqrt{3}}\right)}\,, \\
X(\eta) &= \frac{1}{\sqrt{2}}\sinh\left(\sqrt{2}\eta\right)\,,
\end{aligned}
$$

and charge $q\ell = 1$ [204]. (Note that this theory has a Chern Simons term which as we mentioned previously is common in top down constructions). We now briefly give an overview of the phase structure of this theory when held at finite density. This has been discussed extensively in the holography literature and more details can be found there [202, 204].

2.7.1. Phase Structure

The theory (2.7.60) exhibits a superfluid branch of black hole solutions that emerges as an instability of the charged Reissner-Nordstrom family of solutions which exists with zero deformation $h = 0$. Once again, under dilaton deformation we see the emergence of a superconducting dome structure whose zero temperature limit corresponds to a charged AdS_4 to AdS_4 domain wall [202, 204]. Whenever the $U(1)$ symmetry is unbroken, the zero temperature limit of the neutral and charged black hole solutions does not depend on the chemical potential μ and hence the entire region outside the dome at $T = 0$ is in fact degenerate (for constant μ). In addition, the $T \to 0$ limits of the neutral and charged solutions meet at a unique point, corresponding to an unbroken $T = 0$ solution which can be shown to uplift to an eleven dimensional Schrodinger solution of M theory [205]. We present a schematic phase diagram illustrating the above discussion in Fig. 2.6. Note that we have chosen to plot this at fixed mass (energy) in view of the degeneracy of the ground state.

In the light of our earlier analysis in the bottom up case, we expect that as we tune the dilaton deformation, we eventually reach a transition from a broken $U(1)$ solution to a (partially) fractionalised phase. Interestingly, as we shall see, this is in fact *not* the case for this class of theories because the superconducting and neutral domes coincide. Said in another way, there is transition from the broken $U(1)$ phase directly to a neutral solution.

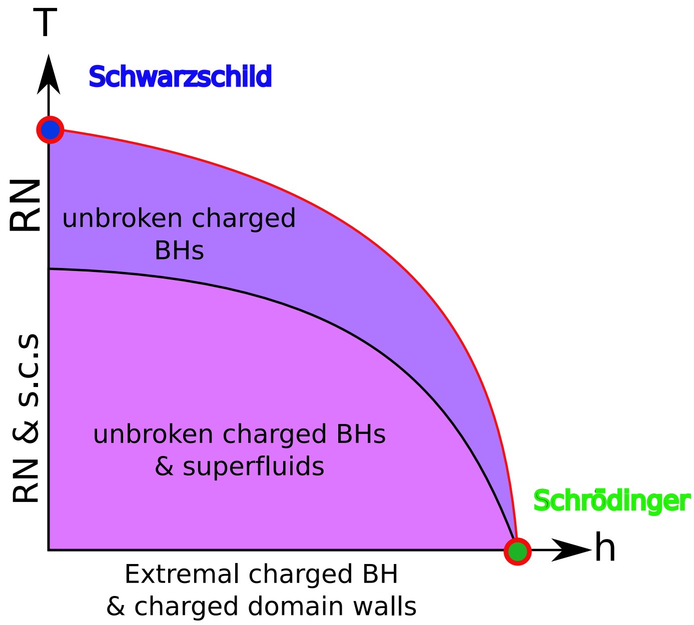

Figure 2.6.: The existence of bulk solutions at fixed mass. The red line denotes neutral solutions terminating in the *Schr* zero-termperature fixed point. Note that the neutral dome meets the superconducting dome at precisely this fixed point, showing that there is no fractionalised phase in this model.

2.7.2. Neutral Top-Down Solutions

We now discuss the structure of the neutral solutions outside the dome in which the neutral scalar h attains the singular value $h = 1$ in the IR at $T = 0$ (to see this is somewhat involved and one must appeal to the equations of motion). Note that in the parameterisation of equation (2.7.61), this corresponds to a logarithmically divergent dilaton (which likely comes as no surprise at this point!)

To proceed, we rewrite (2.7.60) adapted to the case of interest where we set the charged scalar to zero (as by definition we are looking for solutions outside the superconducting dome, for which the $U(1)$ symmetry is unbroken). In the variables of (2.7.61), the action can be rewritten as

$$S = \int d^4x\sqrt{-g}\Big[R - \frac{\operatorname{sech}^3\left(\frac{\Phi}{\sqrt{3}}\right)}{1 + 3\tanh^2\left(\frac{\Phi}{\sqrt{3}}\right)}F^2 - \frac{1}{2}(\nabla\Phi)^2 + \frac{6}{\ell^2}\cosh\left(\frac{\Phi}{\sqrt{3}}\right)\Big] . \quad (2.7.62)$$

At finite temperature, the theory admits a one parameter family of (non-singular) neutral 'dilatonic' black holes. At zero temperature however, the situation is somewhat different and there is strong numerical evidence (from studying the zero temperature limit of non-extremal black holes) to suggest that the isometries of the metric are enhanced from the $\mathbb{R} \times SO(2)$ symmetry above to the full $SO(1,2)$ Lorentz symmetry [2]. Consequently, and choosing a convenient radial gauge we take,

$$ds^2 = \frac{d\rho^2}{F(\rho)} + \rho^2 \text{sech}\left(\Phi(\rho)/\sqrt{3}\right) \eta_{\mu\nu} dx^\mu dx^\nu \,. \tag{2.7.63}$$

This expression is convenient for the current purposes, but we note that we can convert it into the form (2.2.10) via

$$r^2 = \rho^2 \,\text{sech}\left(\Phi/\sqrt{3}\right) , \qquad e^{-\beta} f = r^2 \,, \qquad \sqrt{F} = \frac{d\rho}{dr}\sqrt{f} \,. \tag{2.7.64}$$

Singular IR Solutions

We may now proceed to construct the IR solution in question by dimensional reduction. First observe that if ϕ diverges as $\phi \to \infty$[12] in the IR, then the action approaches

$$S_{\text{sing}} = \int d^4x \sqrt{-g}\Big[R - 2e^{-\sqrt{3}\Phi} F^2 - \frac{1}{2}(\nabla\Phi)^2 + \frac{3}{\ell^2} e^{\Phi/\sqrt{3}}\Big] \,, \tag{2.7.65}$$

which can be obtained by reduction of a pure Einstein-Hilbert (with cosmological constant) action in five dimensions:

$$S_5 = \int d^5x \sqrt{-\hat{g}}\Big[\hat{R} + \frac{3}{\ell^2}\Big] \,, \tag{2.7.66}$$

using a graviphoton ansatz

$$d\hat{s}^2 = e^{\Phi/\sqrt{3}} ds^2(M) + e^{-2\Phi/\sqrt{3}} \left(dz + 2\sqrt{2}A\right)^2 \,. \tag{2.7.67}$$

Under this reduction, pure five-dimensional AdS with metric

$$d\hat{s}_5^2 = \ell_5^2 \left[\frac{d\rho^2}{\rho^2} + \rho^2 \left(-dt^2 + d\mathbf{x}^2\right) + \rho^2 dz^2\right] \,, \qquad \left(\ell_5^2 = 4\ell^2\right) \,, \tag{2.7.68}$$

reduces to a logarithmic dilaton solution in four dimensions, that is:

$$ds^2 = \ell_5^2 \left[\frac{d\rho^2}{\rho} + \rho^3(-dt^2 + d\mathbf{x}^2)\right] \,, \quad \text{with} \quad \Phi = -\sqrt{3}\log(\rho) \,. \tag{2.7.69}$$

[12] The case $\Phi \to -\infty$ is equivalent by the $\Phi \to -\Phi$ symmetry of the lagrangian coming from 11D.

As we now discuss, this solution plays the role of the singular IR we are seeking. (Note that in this case, the graviphoton field A is trivial, and so we have a standard circle reduction).

On substituting the metric ansatz (2.7.63) into the equations that follow from (2.7.65) (with $A_t = \mu =$ constant), one obtains a single, fully decoupled ODE for the scalar field Φ

$$\begin{aligned} \rho^2\Phi''(\rho) \;\; &= \;\; \frac{-1}{2\sqrt{3}}\tanh\left(\tfrac{\Phi(\rho)}{\sqrt{3}}\right)\left[12-\rho^2\Phi'(\rho)^2\left(4+3\,\mathrm{sech}^2\left(\tfrac{\Phi(\rho)}{\sqrt{3}}\right)\right)\right] \\ &\quad -\left[1+3\,\mathrm{sech}^2\left(\tfrac{\Phi(\rho)}{\sqrt{3}}\right)\right]\rho\,\Phi'(\rho) \\ &\quad +\frac{1}{12}\mathrm{sech}^4\left(\tfrac{\Phi(\rho)}{\sqrt{3}}\right)\rho^3\Phi'^3(\rho)\,. \end{aligned} \tag{2.7.70}$$

Note that for any solution, the chemical potential in the boundary theory is arbitrary, as A is pure gauge in the bulk and if A is to be well-defined, one should choose the gauge $A_t = 0$. The Einstein equations then determine $F(\rho)$ algebraically

$$F(\rho) = \frac{4\ell^{-2}\rho^2\cosh\left(\Phi/\sqrt{3}\right)}{4-(\rho\Phi'/\sqrt{3})^2\mathrm{sech}^2\left(\Phi/\sqrt{3}\right)-4\rho\Phi'/\sqrt{3}\tanh\left(\Phi/\sqrt{3}\right)}\,, \tag{2.7.71}$$

where the prime denotes a derivative with respect to the radial direction ρ. The Φ equation admits an IR expansion, which reproduces (2.7.69) to leading order. It takes the form

$$\Phi(\rho) = -\sqrt{3}\log\rho + \frac{3\sqrt{3}}{2}\rho^2 + \cdots \tag{2.7.72}$$

and notably has no free parameters. Furthermore, rescaling the ρ coordinate has no physical effect on the solution. This IR expansion can be integrated directly to the UV and one finds that it connects to the desired AdS_4 solution. Reading off the UV data, one finds complete agreement with the analytic values corresponding to the exact solution found in [202]. One can furthermore check that the chemical potential $\mu(r_\infty) - \mu(r_{\mathrm{IR}})$ vanishes. We have therefore demonstrated that the unique neutral $T = 0$ solution of (2.7.60) with logarithmically diverging dilaton is the analytic solution given in Eq (8.2) of [202].

One can also study the approach to zero temperature in further detail. In particular one observes linear temperature scaling consistent with a $z = 2$ quantum critical point. Furthermore, as mentioned briefly above, it can also be demonstrated that this solution, when lifted to eleven dimensions, is a Schrödinger solution $\mathrm{Schr}_5 \times KE_6$ of the full M theory.

2.8. Discussion

In summary, we have demonstrated in this chapter how to construct bosonic analogues of so called 'fractionalisation transitions' by way of a suitably engineered bottom-up gravitational action. In addition, we examined the phase diagram of the M-theory superconductor equipped with these new insights. In particular, we demonstrate how at zero temperature there is no fractionalisation transition in the latter case, as one proceeds directly from the broken superfluid cohesive phase to a neutral phase.

The qualitative structure of the transitions studied in this chapter can be understood by studying the IR behaviour of the dilaton and in particular also the coupling between the dilaton and the gauge kinetic term. All examples we have encountered thus far support the conjecture that one cannot have a cohesive phase if the dilaton coupling to the gauge kinetic term diverges in the infrared ($Z \to \infty$). Physically this can be explained by observing simply that a diverging Z implies that the effective gauge coupling vanishes. (This is most easily seen by recalling the form of the gauge kinetic terms which in a conventional normalisation read $\sim \frac{1}{e^2}F^2$ and hence the coupling constant is the reciprocal of the coefficient). Since the electromagnetic coupling vanishes, matter in the IR cannot source any flux and consequently any flux there must be sourced by a black hole horizon, resulting in a fractionalised phase. Note also that our arguments for this behaviour are purely holographic, using only the properties of the bulk gravitational solutions. Although this physical reasoning seems rather strong, we know of no rigorous argument that could prove the aforementioned conjecture. It would also be interesting to understand better whether one can use bulk arguments to shed light on a possible order parameter for fractionalisation. This could in principle be rather powerful as one could translate this into a field theoretic quantity which could then prove useful in entirely different settings (that could for example be unrelated to holography).

In asymptotically AdS spacetimes, one commonly finds that the near horizon geometries of zero temperature black holes contain an AdS_2 factor, the signature of which is a diverging critical exponent. It is well known that such geometries have the rather curious property of finite entropy at zero temperature and consequently violate the third law of thermodynamics (Nernst's postulate). Interestingly, however, they are often unstable when embedded in top-down models and hence the laws of thermodynamics appear once again to be upheld by the classical solutions [196, 202, 204]. Note also that although we can often trace finite entropy singularities at zero temperature to divergent critical exponents, this alone will not necessary result in singular solution. In particular a divergent critical exponent can be compensated for by an equally divergent hyperscaling parameter resulting in a vanishing entropy at $T = 0$ [182]. In this manner, one can avoid finite entropy singularities and this is precisely the mechanism employed by our bottom-up model. In the M theory case, there is as discussed no fractionalised phase and in particular the 'would be fractionalised' Reissner- Nordstrom solutions ultimately end up masked by a superconducting dome. It could be very interesting to investigate precisely what conditions must be met for any entropic singularity (i.e. any AdS_2 IR geometry) to be unstable [206] to new phases cloaking it at low temperatures.

3. Stationary Elliptic Numerical Relativity

3.1. Introduction

The Harmonic Einstein equation as introduced in chapter (1.3) is the vacuum Einstein equation together with a gauge fixing term that is taken to be that of DeTurck. For static black holes that have been analytically continued to Euclidean signature, this equation was shown in the introduction to be elliptic and hence can be tackled as an elliptic boundary value problem, where Ricci flow and Newton's method constitute good numerical algorithms to solve the system. In this chapter, we extend these results to the stationary case which must be treated in the full Lorentzian signature as there exists no analytic continuation of a general stationary spacetime to a smooth, real geometry.

We will begin our discussion by reviewing the approach to construct static solutions using the Harmonic Einstein equation, but this time recasting the analysis entirely from a Lorentzian perspective, demonstrating that the equation is elliptic. The key observation to proceed, is that as a consequence of the static symmetries, the Harmonic Einstein equations give precisely the same equations for the metric components in either Euclidean or Lorentzian signature (provided that we use coordinates adapted to the static symmetry). Whilst in general then the Lorentzian Harmonic Einstein equation is hyperbolic, this useful observation shows that when restricted to static metrics, it is in fact elliptic and can thus be solved as a boundary value problem. We then proceed to the full stationary case and consider the character of the general Lorentzian Harmonic Einstein equation. We demonstrate that for the case of a globally timelike stationary Killing field, the associated equations are still in fact elliptic and moreover from this analysis it becomes clear that the threat to ellipticity is physically due to ergo-regions, where the timelike Killing field becomes spacelike. Since ultimately, we are most interested in the construction of black holes, we will need to relax the globally timelike restriction. To do this, we make a Kaluza-Klein ansatz for stationary black holes, motivated by the rigidity theorem [35], that has also been used by Harmark in the classification of higher dimensional black holes [207]. As a direct consequence of rigidity, Killing symmetries in the directions of angular or linear motion of the horizon are assumed and it turns out that this is crucial in maintaining ellipticity in the presence of ergoregions. At this point, based on the analytic treatment of the uniqueness theorems for stationary problems, we make the assumption that the base manifold is Riemannian and that the horizons and axes of symmetry constitute (physical) boundaries on this base manifold (we will clarify the meaning of 'base manifold' in the next section). With these conditions, we are able to conclude the Harmonic Einstein equation restricted to our class of stationary spacetimes is in fact elliptic and we determine suitable boundary conditions at any horizons and axes in a manner analogous to the Lorentzian static case. These are shown to be compatible with Ricci flat (as opposed to soliton) solutions, but unfortunately the maximum principle of the static case does not readily generalise to stationary geometries. Finally, we end this chapter by showing how the Kerr solution satisfies the aforementioned boundary conditions.

3.2. Static Spacetimes from a Lorentzian Perspective

Instead of immediately studying stationary spacetimes, it will be instructive to first revisit the static case, this time in Lorentzian signature. That is to say, we will *not* perform an analytic continuation in time to arrive at a Riemannian geometry. The Harmonic Einstein equation, however, is not elliptic for a general Lorentzian manifold and without ellipticity, as we have discussed now at length, one would not expect to be able to impose the various boundary conditions that we require physically in a well posed manner. All is not lost however as we shall now discuss. Consider a chart away from the horizon which manifests the static symmetry,

$$ds^2 = g_{\mu\nu}dx^\mu dx^\nu = -N(x)dt^2 + h_{ij}(x)dx^i dx^j \,, \tag{3.2.1}$$

so that $N > 0$. This form of the metric will be very important for the discussion that follows. We should regard the time coordinate as fibered over a base manifold $\mathcal{M}$ with Riemannian metric $ds^2_{\mathcal{M}} = h_{ij}(x)dx^i dx^j$. Furthermore, if we assume a similar structure for the reference metric, namely that it is static with respect to $\partial/\partial t$ so that

$$\bar{ds}^2 = \bar{g}_{\mu\nu} dx^\mu dx^\nu = -\bar{N}(x) dt^2 + \bar{h}_{ij}(x) dx^i dx^j \,, \tag{3.2.2}$$

again with $\bar{N} > 0$ and $\bar{h}_{ij}$ a smooth Riemannian metric, then we can guarantee that $R^H_{\mu\nu}$ also shares this static isometry. Now due to this static isometry, the Harmonic Einstein equation thought of as PDEs for the metric components of g is invariant under an analytic continuation $t \to \tau = it$. Hence we see immediately that the Harmonic Einstein equations restricted to Lorentzian static metrics and reference metrics must be elliptic (even though the full manifold is not Riemannian). A simple consequence of this discussion is that Ricci-DeTurck flow yields precisely the same flow equations for the metric functions N and h_{ij} independent of whether we are in Lorentzian signature or in the analytically continued Euclidean case of the previous chapter.

Explicitly the Ricci-DeTurck equations for the metric (3.2.1) take the form

$$\begin{aligned} R^H_{tt} &= -\frac{1}{2}\hat{\nabla}^i(\partial_i N) + \frac{1}{2N}(\partial^i N)(\partial_i N) - \frac{1}{2}\hat{\xi}^k \partial_k N - \frac{1}{4N}\bar{h}^{mi}_{(-1)}(\partial_m \bar{N})(\partial_i N)\,, \\ R^H_{ti} &= 0\,, \\ R^H_{ij} &= \hat{R}_{ij} - \hat{\nabla}_{(i}\hat{\xi}_{j)} - \frac{1}{4N^2}(\partial_i N)(\partial_j N) - \frac{1}{2}h_{k(i}\hat{\nabla}_{j)}\left(\frac{1}{N}\bar{h}^{km}_{(-1)}\partial_m \bar{N}\right)\,. \end{aligned} \tag{3.2.3}$$

In these equations, indices are contracted and crucially covariant derivatives $\hat{\nabla}$ are with respect to the Riemannian base metric. To avoid any possible confusion we use the notation $\bar{h}^{ij}_{(-1)}$ for the inverse metric to $\bar{h}_{ij}$, so that $\bar{h}_{ik}\,\bar{h}^{kj}_{(-1)} = \bar{h}^{(-1)ij}\bar{h}_{jk} = \delta^i_k$. The vector field $\xi = \{0, \hat{\xi}^i\}$, where $\xi^t = 0$ on the ansatz (3.2.1) and $\hat{\xi}^i$ is the DeTurck vector of the base metric, namely

$$\hat{\xi}^i = h^{jk}\left(\hat{\Gamma}^i{}_{jk} - \bar{\hat{\Gamma}}^i{}_{jk}\right)\,, \tag{3.2.4}$$

where $\hat{\Gamma}^i{}_{jk}$ is the connection for h_{ij} and $\bar{\hat{\Gamma}}^i{}_{jk}$ is the connection for $\bar{h}_{ij}$. From the form of these equations, we see explicitly how the Ricci-DeTurck components are symmetric under the static isometry and moreover that the equations are elliptic provided that the base metric h_{ij} is Riemannian. (The two derivative structure is controlled by for example $\hat{R}_{ij} - \hat{\nabla}_{(i}\hat{\xi}_{j)}$).

Provided that we are in the exterior region to any horizons, we have that $N, \bar{N} > 0$. In the case of a non-extremal horizon however where $\partial/\partial t$ has fixed action, we have that N and $\bar{N}$ vanish there. Exactly as with our discussions in the introduction, we require that the base manifold h_{ij} nevertheless retains a smooth Riemannian geometry where $N = 0$ in order for the spatial horizon to have a well defined geometry. We choose the same structure for the reference metric $\bar{h}_{ij}$. In that Riemannian setting, we know from our previous analyses that when we have a single non-extremal horzion, or alternatively multiple horizons with the same surface gravity κ, then we can make Euclidean time periodic $\tau \sim \tau + 2\pi/\kappa$, for some appropriate choice of κ (which is fixed by the procedure and depends both on the near horizon geometry and the asymptotic structure) so that there is no boundary at the horizon(s) and the geometry is perfectly smooth there. Moreover, the Ricci-DeTurck tensor will be a smooth tensor on this geometry (as it is constructed from smooth functions of this smooth metric) and hence both Ricci-DeTurck flow and the Newton method will preserve this smoothness property under evolution (or equivalently in this interpretation the lack of boundary at the Euclidean horizon). However, there is one subtlety - in the chart above with $t \to \tau = it$, the metric becomes

$$ds^2 = +N(x)d\tau^2 + h_{ij}(x)dx^i dx^j \,, \tag{3.2.5}$$

and the chart does not cover the horizon where $N = 0$. Such coordinates adapted to the static symmetry are analogous to polar coordinates, and fail at the polar origin - the horizon. Essentially, to manifest the smoothness of the Riemannian manifold, one must pass to Cartesian coordinates. We write the line element in the base adapted to the horizon such that $x^i = (r, x^a)$ (with the horizon at $r = 0$) as

$$ds^2 = +r^2 V d\tau^2 + U\,(dr + r\,U_a dx^a)^2 + h_{ab}dx^a dx^b \,, \tag{3.2.6}$$

where the metric components are functions of r and x^a. Changing to coordinates

$$a = r \sin \kappa\tau \,, \quad b = r \cos \kappa\tau \tag{3.2.7}$$

provides a good chart covering the horizon, such that the metric components are smooth functions, provided that V, U, U_a, h_{ab} are smooth (C^∞) functions of r^2 and x^a, and

$$V = \kappa^2 U \tag{3.2.8}$$

at the horizon $r = 0$ [21, 121]. Equation (3.2.8) follows from the definition of surface gravity κ (given by equation (1.2.7), or equivalently $\xi^\nu \nabla_\nu \xi^\mu = \kappa \xi^\mu$, where ξ is the Killing vector normal to the horizon [35]) applied to (3.2.6), together with the boundary behaviours of the metric functions at the horizon required by regularity. Exactly the same conditions will also apply to the reference metric. The point is that instead of using the 'good' chart (which is inconvenient practically as it does not make manifest the isometries in the problem), we can use our polar chart and simply treat the horizon as a fictitious boundary. We then determine the boundary conditions there using the regular chart, namely that V, U, U_a, h_{ab} are smooth in r^2 and x^a, and that $V = \kappa^2 U$ at $r = 0$ where κ determines the temperature of the solution. As noted above, provided that we take smooth coordinates we know that $R^H_{\mu\nu}$ preserves this smoothness property and lack of boundary at the horizon. The same conclusions must hold in the adapted coordinates even though there is now a horizon 'boundary'. In fact one can explicitly check by brute force that we have

$$R^H = +r^2 f d\tau^2 + g\left(dr + r\, g_a dx^a\right)^2 + r_{ab} dx^a dx^b\,, \tag{3.2.9}$$

where the functions f, g, g_a and r_{ab} are smooth in r^2, x^a, and in addition $f = \kappa^2 g$ at $r = 0$. However, the simpler way to see that this must be the case is to remember that in the smooth Cartesian coordinates (a, b, x^a) then $g_{\mu\nu}$ is smooth and hence $R^H_{\mu\nu}$ will be too, and since $R^H_{\mu\nu}$ with our reference metric preserves the static isometry, then it follows that $R^H_{\mu\nu}$ must have the behaviour stated above.

We can now turn our attention back to the analysis in Lorentzian signature. If we are to study only the region exterior to the horizon, then we must regard the horizon now as a physical (rather than fictitious) boundary. This is fundamentally distinct from the Riemannian case where the boundary can be smoothly removed by a suitable choice of chart without introducing the black hole interior. However, as we mentioned at the start of this chapter, due to the static isometry, the Harmonic Einstein equations and the solutions for the metric components are in fact invariant under analytic continuation. The equations are therefore the same in either signature and the same boundary conditions for regularity will apply in the Lorentzian case (3.2.1) as in the Euclidean case (3.2.5). In detail, we may therefore work directly in Lorentzian signature where the equations are elliptic, and we provide the same boundary conditions for the metric components at the horizon taking

$$ds^2 = -r^2 V dt^2 + U\left(dr + r\, U_a dx^a\right)^2 + h_{ab} dx^a dx^b\,, \tag{3.2.10}$$

where $r = 0$ at the horizon and $V > 0$ outside the horizon and vanishes smoothly on it. We will also (as before) have the boundary conditions at the horizon that V, U, U_a, h_{ab} are smooth in r^2 and x^a, and that $V = \kappa^2 U$. Once again the constant κ gives the surface gravity of the horizon. Should we wish to, we can manifest the regularity of the horizon in a similar manner to what we have done in the Euclidean case, this time by performing a hyperbolic change of coordinates

$$a = r \sinh \kappa t \,, \quad b = r \cosh \kappa t \,, \tag{3.2.11}$$

giving a chart with coordinates a, b, x^a that now covers the $t = 0$ slice of the Killing horizon and whose metric components are smooth functions. The key difference with the Euclidean case however is that even in these coordinates the horizon is still to be viewed as a boundary. That is to say, we cannot remove the horizon boundary as we could there.

A further consequence of the invariance of the metric components under $t \to \tau = it$ is that the tensor $R^H_{\mu\nu}$ shares the same regularity properties of the metric in the Lorentzian context too and hence takes the form,

$$R^H = -r^2 f dt^2 + g \left(dr + r\, g_a dx^a\right)^2 + r_{ab} dx^a dx^b \tag{3.2.12}$$

near the chart boundary at $r = 0$ where again f, g, g_a and r_{ab} are smooth in r^2, x^a, and in addition $f = \kappa^2 g$. We then arrive at the picture that in the Riemannian case, Ricci flow and the Newton method preserve smoothness and the lack of boundary at the horizon, whilst in the Lorentzian context Ricci flow and the Newton method preserve the surface gravity of the solution.

We close this section by mentioning some interesting points. Firstly in the Riemannian elliptic boundary problem, the asymptotic data that we are required to impose for well-posedness of the elliptic problem lead us to fix the size of the time circle. This has the beautiful interpretation of fixing a piece of physical data associated to a solution, namely the inverse temperature (recall that the Euclidean continuation of the time coordinate removes the horizon boundary and essentially corresponds to working in the canonical ensemble). An elegant feature of the Lorentzian analysis that we have just described in this section is that whilst we now have a horizon boundary, we are again led to fix physical data this time corresponding to the surface gravity with respect to $\partial/\partial t$. In practice the way one can do this is to fix the value of the function N asymptotically (or on some boundary away from the horizon). This fixes the normalisation of the Killing vector $\partial/\partial t$ and thus the surface gravity governed by κ. Furthermore, just as the smoothness and absence of boundary are preserved in the Riemannian case, the data associated to the surface gravity is preserved in our Lorentzian case under any Newton method of Ricci flow updates.

A second point to note is that in practice, even in the Euclidean context we will generally choose to use adapted coordinates so as to manifest any isometries present (as this becomes crucial for numerics [21]) and hence operationally the mechanics of solving this static problem are in fact exactly the same in either signature. For the purposes of implementation, whether regularity is imposed at a 'real' or fictitious boundary where some set of coordinates degenerates is of no consequence. That said, it turns out that there is in fact one important advantage that one gains by thinking about even the purely static problem in a Lorentzian signature, namely that in this case one is able to consider multiple Killing horizons with respect to $\partial/\partial t$ with *different* associated surface gravities, each of which is separately preserved by the Newton method/Ricci flow. We could not consider such situations in a purely Euclidean framework of course as we may only use analytic continuation to remove a single horizon boundary, and in the process of doing so, any remaining horizons become conical singularities.

Having revisited the framework of static elliptic numerical relativity in Lorentzian signature, we now turn to a discussion of stationary solutions where no Riemannian description is possible and we will be required to treat the problem in Lorentzian signature from the outset.

3.3. Stationary Spacetimes with Globally Timelike Killing Vector

We now wish to use the methods above to find stationary vacuum solutions. In this section, we will begin this task by studying the case of stationary solutions with a globally timelike Killing vector and will show that the associated Harmonic Einstein equation is elliptic. Consequently all our techniques from the static case will carry over with only small modification. Whilst a good first step, this situation corresponds physically to a scenario where there are no horizons or ergo-regions present in the spacetime. Since ultimately we wish to construct stationary black holes, in subsequent sections we will need to discuss how to relax the requirement of a globally timelike Killing field.

Consider the most general stationary metric with Killing vector $T = \partial/\partial t$, which we may write using coordinates adapted to the stationary isometry as

$$g = -N(x)\left(dt + A_i(x)dx^i\right)^2 + h_{ij}(x)dx^i dx^j. \tag{3.3.13}$$

Under our starting assumption that T is a globally timelike vector field, we have that $N > 0$ everywhere and we may furthermore assume that N is bounded. Physically, as alluded to above this means that our spacetime has no Killing horizons and moreover no ergo-region. One may calculate that $\det g_{\mu\nu} = -N \det h_{ij}$ and we then see that provided the metric g is Lorentzian and smooth, so that $\det g_{\mu\nu} < 0$ and bounded, we have that the base $\det h_{ij} > 0$. We then have the useful result that we may regard the metric (3.3.13) as a smooth fibration of time over a base manifold $\mathcal{M}$, so that $(\mathcal{M}, h)$ is a smooth Riemanian manifold with *Euclidean* signature metric h_{ij}.

It is interesting to note that whilst one might imagine that for a stationary spacetime, the natural way to think of the metric would be through the ADM ansatz, (3.3.13) is in fact not of this form. Rather, it is a Kaluza-Klein ansatz where we have reduced over the time direction. Consequently the base manifold $(\mathcal{M}, h)$ is *not* the submanifold obtained by taking a constant t slice of the full geometry. We can now put all of this together to show that

$$R^H_{\mu\nu} \sim -\frac{1}{2} g^{\alpha\beta} \partial_\alpha \partial_\beta g_{\mu\nu} + \ldots = -\frac{1}{2} h^{ij} \partial_i \partial_j g_{\mu\nu} + \ldots \tag{3.3.14}$$

where as usual $\ldots$ denote terms with less than two derivatives. Critically, despite the fact that $g_{\mu\nu}$ is Lorentzian, since the metric components have no t dependence, the character of the two derivative terms is governed entirely by the Euclidean metric h^{ij}. (In arriving at this conclusion, we have implicitly used the fact that for the metric (3.3.13), $g^{ij} = h^{ij}$ which is a well-known property of the Kaluza-Klein ansatz). This immediately implies that the Harmonic Einstein equations are elliptic and hence this stationary problem reduces to an elliptic problem on the Riemannian base manifold $\mathcal{M}$.

It is also very important that $R^H_{\mu\nu}$ is itself a tensor that is symmetric with respect to the stationary isometry. This is an important constraint as without this, Ricci-DeTurck flow and the Newton method will not consistently truncate to the class of stationary metrics. Said in another way, without this, under Ricci flow/Newton method updates a metric which is initially stationary would not in general remain stationary (preserve the stationary symmetries). In order that $R^H_{\mu\nu}$ preserves the stationary isometries we will require that the reference metric $\bar{g}$ is also a smooth Lorentzian metric which is itself stationary with respect to the vector field T, so that

$$\bar{g} = -\bar{N}(x) \left(dt + \bar{A}_i(x) dx^i \right)^2 + \bar{h}_{ij}(x) dx^i dx^j \,, \tag{3.3.15}$$

where we also assume here that T is globally timelike and bounded with respect to $\bar{g}$ so that $\bar{N} > 0$ and bounded. Then $\bar{h}_{ij}$ gives a second Riemannian metric on the same manifold $\mathcal{M}$. Since $R^H_{\mu\nu}$ preserves the stationary symmetry, the Ricci-DeTurck flow can be consistently truncated to a parabolic flow on the space of Lorentzian stationary metrics. Since this flow remains diffeomorphic to Ricci flow (subject at least to the normal component of ξ vanishing on any boundaries), we arrive at the interesting result that we may apply Ricci flow to Lorentzian stationary spacetimes. Likewise the Newton method will preserve the symmetry.

To summarise then, this section contains the key ideas and techniques that underly our whole approach to recasting the stationary case as an elliptic problem. The procedure is straightforward - one writes the metric in Kaluka-Klein form (3.3.13) whereupon it becomes clear that the character of the equations is then governed by the base metric h^{ij}. By proving that this metric is Riemannian, one may then prove ellipticity of the equations. To do this one needs to make assumptions about the nature of the spacetime under study. In a situation where the solution we wish to find has a stationary Killing vector that is globally timelike and bounded then nearby to that solution, h_{ij} is Riemannian and the character of the Harmonic Einstein equation will be elliptic. Subject to imposing suitable (elliptic) boundary conditions on any boundaries/asymptotic regions, we may use the Lorentzian Ricci-DeTurck flow or Newton method to solve for the solution in essentially the same manner as in the static case[1].

There is however one very important caveat compared with the static case which is worth mentioning. Whilst there, we had the vacuum maximum principle of [121] which subject to suitable boundary conditions was able to rule out the existence of soliton solutions, we do not know of how to prove an analogous result in this new stationary setting. The essence of the problem is easy to see. Whilst in the (vacuum) static case, we had the inequality $\nabla^2\phi + \xi^\mu\partial_\mu\phi = 2\nabla_\mu\xi_\nu\nabla^\mu\xi^\nu > 0$, where $\phi = |\xi|^2$, in the stationary case, this inequality does not appear to hold since in Lorentzian signature, with only stationary symmetry, $\nabla_\mu\xi_\nu\nabla^\mu\xi^\nu$ is of indefinite sign. It is unclear therefore how to formulate a maximum principle for the stationary case

[1] For completeness we include here a discussion of boundary conditions in the case of 'finite' (i.e. not necessarily asymptotic) boundary. We recall that for a solution to the Harmonic Einstein equation to be Ricci flat we require that $\xi = 0$. Whatever boundary conditions we choose must therefore compatible with vanishing ξ. Let us briefly consider the case of Dirichlet conditions and consider taking adapted coordinates to the boundary so that we have

$$ds^2 \;=\; -N(x)\left(dt + A_r(x)dr + A_a(x)dx^a\right)^2 + Vdr^2 + V_a dr dx^a + h_{ab}(x)dx^a dx^b\,, \tag{3.3.16}$$

where $x^i = (r, x^a)$ and the boundary is at $r = 0$. Fixing the induced metric specifies Dirichlet conditions for N, A_a and h_{ab}. Requiring that ξ^t, ξ^r and ξ^a vanish then provides conditions for V, V_a, and A_r. We have hence fixed *all* the metric components on the boundary. (Naively this might seem like 'too much data' but of course the key point here is that we are also imposing $\xi = 0$). For the reasons outlined above and presented in [121], we expect that this will constitute a well-posed elliptic boundary value problem. Then, subject to imposing suitable conditions at any other boundaries in the problem (e.g. asymptotically) that are consistent with vanishing ξ, we can hope to obtain solutions with globally vanishing DeTurck vector as desired.

(the proof certainly doesn't seem to proceed in the same relatively straightforward manner as before). In principle there could therefore be soliton solutions even when we have boundary conditions compatible with vanishing ξ. In practice, as alluded to before, this rarely presents problems and what one has to do is simply test a solution that is found to see whether is a true Ricci flat solution or a soliton. (The only scenarios we can envision where this could be a problem would be when one is looking for a particular Ricci flat solution amidst a whole slew of solitons, but aside from these situations the pragmatic approach will suffice).

For completeness and to close this section we now explicitly show the stationary Ricci-DeTurck flow equations (which give the Harmonic Einstein equations at a fixed point $\partial/\partial\lambda = 0$). These are the equations which one has to solve numerically to find a solution. The key point to notice, pertaining to our earlier discussions is the two derivative structure, indicated by way of an over-brace:

$$
\begin{aligned}
\frac{\partial N}{\partial \lambda} = & \overbrace{\hat{\nabla}^i(\partial_i N)}^{=h^{km}\partial_k\partial_m N+\ldots} -\frac{1}{N}(\partial^i N)(\partial_i N) - \frac{N^2}{2}F^{ij}F_{ij} + \hat{\xi}^k\partial_k N \\
& + \frac{1}{2N}\bar{h}^{km}_{(-1)}(\partial_m\bar{N})(\partial_k N) + \bar{h}^{km}_{(-1)}\bar{N}(A^i - \bar{A}^i)\bar{F}_{jm}\partial_k N \\
& + \frac{1}{2}(A_i - \bar{A}_i)^2\bar{h}^{km}_{(-1)}(\partial_m N)(\partial_k N)\,,
\end{aligned}
$$

$$
\begin{aligned}
\frac{\partial A_i}{\partial \lambda} = & \overbrace{\hat{\nabla}^k F_{ik} + \hat{\nabla}_i(A_k\hat{\xi}^k) + \hat{\nabla}_i(\hat{\nabla}^p A_p - \hat{\bar{\nabla}}^p\bar{A}_p)}^{=h^{km}\partial_k\partial_m A_i+\ldots} - \frac{1}{N}F_{ij}\partial^j N \\
& + \hat{\xi}^k F_{ki} + \frac{1}{2N}\bar{h}^{km}_{(-1)}F_{ki}\partial_m\bar{N} - \bar{h}^{km}_{(-1)}\bar{N}(A^j - \bar{A}^j)F_{ik}\bar{F}_{jm} \\
& + \frac{1}{2}\bar{h}^{km}_{(-1)}(A_p - \bar{A}_p)^2 F_{ki}\partial_m\bar{N} \\
& + \hat{\nabla}_i\Bigg(\Bigg(\frac{1}{2N}\bar{h}^{mp}_{(-1)}(A_m - \bar{A}_m) \\
& + \frac{1}{\bar{N}}(A^p - \bar{A}^p) + \frac{1}{2}\bar{h}^{kp}_{(-1)}(A_m - \bar{A}_m)^2(A_k - \bar{A}_k)\Bigg)\,\partial_p\bar{N}\Bigg) \\
& + \hat{\nabla}_i(\bar{h}^{km}_{(-1)}\bar{N}(A^j - \bar{A}^j)(A_k - \bar{A}_k)\bar{F}_{jm})\,,
\end{aligned}
$$

$$
\begin{aligned}
\frac{\partial h_{ij}}{\partial \lambda} = & \overbrace{-2\hat{R}_{ij} + 2\hat{\nabla}_{(i}\hat{\xi}_{j)}}^{=h^{km}\partial_k\partial_m h_{ij}+\ldots} + \frac{1}{2N^2}(\partial_i N)(\partial_j N) - NF^k_j F_{ki} \\
& \Bigg(\frac{1}{2}h_{ik}\hat{\nabla}_j(\frac{1}{N}\bar{h}^{km}_{(-1)}\partial_m\bar{N}) + h_{ik}\hat{\nabla}_j(\bar{h}^{km}_{(-1)}\bar{N}\bar{F}_{qm}(A^q - \bar{A}^q)) \\
& + \frac{1}{2}h_{ik}\hat{\nabla}_j(\bar{h}^{km}_{(-1)}(A^p - \bar{A}^p)^2\partial_m\bar{N}) + (i \leftrightarrow j)\Bigg)\,.
\end{aligned}
\tag{3.3.17}
$$

In the above, indices are contracted and covariant derivatives $\hat{\nabla}$ are with respect to the base metric h_{ij}, and we have defined the antisymmetric tensors $F_{ij} \equiv \partial_i A_j - \partial_j A_i$ and $\bar{F}_{ij} \equiv \partial_i \bar{A}_j - \partial_j \bar{A}_i$ in a manner analogous to electrodynamics. Again $\hat{\xi}^i$ is the DeTurck vector of the base metric defined as before in (3.2.4).

We note also that the individual components of the DeTurck tensor $R^H_{\mu\nu}$ may be derived from the above equations using the fact that

$$\begin{aligned} \frac{\partial N}{\partial \lambda} &= -2R^H_{tt}\,, \\ \frac{\partial A_i}{\partial \lambda} &= -\frac{2}{N}(R^H_{it} - R^H_{tt}A_i)\,, \\ \frac{\partial h_{ij}}{\partial \lambda} &= -2(R^H_{ij} + R^H_{tt}A_iA_j - R^H_{it}A_j - R^H_{jt}A_i)\,. \end{aligned} \tag{3.3.18}$$

3.4. Stationary Black Holes

We are now in a position to consider the case of Ricci flat, non-extremal stationary black holes. In this situation, in contrast to the discussion above, the norm of T will vanish either at the horizon itself (if T is a globally timelike vector, such as for certain Kerr-AdS black holes [208]), or alternatively outside the horizon at the boundary of an ergo-region. Since we are (at least for now) interested only in the region outside the horizon, in the first of these cases, we may treat the system as for globally timelike T, with the horizon regarded as a boundary of the base manifold $\mathcal{M}$ where suitable data is to be imposed. In the latter more general case however, outside the horizon but within the ergo-region we will have that the norm of $T > 0$, and hence $\det h_{ij} < 0$. Our arguments in the previous section will then require modification as the base manifold fails to be Riemannian.

In order to make progress here we will need to make use of the so called Rigidity Theorem for stationary black holes, proved in $D > 4$ by Ishibashi, Hollands and Wald [54] and by Moncrief and Isenberg [209] for various asymptotics including asymptotic flatness. This theorem states that given a stationary Killing vector T, and a rotating non-extremal Killing horizon with topology $\mathbb{R} \times \Sigma$, (for Σ compact), there exists a Killing vector K that commutes with T, and is normal to the horizon. Note that of course the stationary Killing vector T will not be normal to the horizon in the presence of rotation. Moreover, there also exist some further number $N \geq 1$ of commuting Killing vectors R_a, which also commute with T and generate closed orbits with period 2π so that K may be written in terms of these as

$$K = T + \Omega^a R_a \tag{3.4.19}$$

for some constants Ω^a. What this means is that rotation of the horizon is generated by an isometry of the spacetime. The horizon moves rigidly with respect to the orbits of K in its exterior and hence with respect to the asymptotic rotation generators R_a. If this were not the the case, then one could argue on physical grounds that we should see gravitational radiation emitted from a region near the horizon, ultimately violating the assumption of stationarity.

Motivated by the Rigidity Theorem, we will assume that our stationary spacetime with Killing vector T has in addition a further N 'rotational' Killing vectors R_a for $a = 1, 2, \ldots, N$. The $\{R_a\}$ commute amongst themselves and with the stationary Killing field T and physically should be thought of as the generators of rotational or translational isometries. (In the former case, they generate closed orbits with some fixed period, whilst in the latter case the associated orbits are non-compact). In the interest of generality, let us assume that there are a number of disconnected horizon components, $\mathcal{H}_1, \ldots, \mathcal{H}_k$. The Rigidity Theorem then tells us that each component is separately a Killing horizon with as associated Killing vector that is given by some linear combination of the stationary and rotational Killing vectors. We write this in the form $K_{\mathcal{H}_m} = T + \Omega^a_{\mathcal{H}_m} R_a$ for some constants $\Omega^a_{\mathcal{H}_m}$, which we stress may be different for each component. (Physically one should think of these constants as corresponding to the angular velocity of the associated Killing horizon).

In view of these assumptions, let us now consider a new metric ansatz using coordinates adapted to the isometries $y^A = \{t, y^a\}$, so that

$$ds^2 = g_{\mu\nu} dX^\mu dX^\nu \;\; = \;\; G_{AB}(x) \left(dy^A + A^A_i(x) dx^i \right) \left(dy^B + A^B_j(x) dx^j \right) + h_{ij}(x) dx^i dx^j \tag{3.4.20}$$

where $T = \partial/\partial t$ and $R_a = \partial/\partial y^a$. (Note physically, this metric describes rotation or linear motion *in a Killing direction*). Just as with the case of a stationary solution with globally timelike Killing vector, this new geometry is best thought of as a fibration of the Killing vector directions over a base manifold $\mathcal{M}$ with associated metric h_{ij}. As we shall see, it is once again this base metric which controls the character of the associated equations. The base manifold $\mathcal{M}$ is mathematically the orbit space of the full Lorentzian manifold with respect to T and R_a. In particular, if R_a generates a compact orbit, then we can normalise the period to be 2π and hence the coordinate y^a will be periodic as $y^a \sim y^a + 2\pi$. Note also as before that the metric h_{ij} is *not* induced on a constant y hypersurface as once again (3.4.20) is of the Kaluza-Klein form.

Our full spacetime is Lorentzian and thus exterior to any horizons we must have (regardless of ergo-regions) $\det g_{\mu\nu} = \det G_{AB} \det h_{ij} < 0$. On any physical boundaries or asymptotic regions we have that T is timelike, the R_a are spacelike and hence the fiber metric G_{AB} is Lorentzian there and the base metric is consequently Euclidean. On the other hand at a Killing horizon $\mathcal{H}_m$, by definition the norm of $K_{\mathcal{H}_m} = T + \Omega^a_{\mathcal{H}_m} R_a$ vanishes, and hence $\det G_{AB} = 0$. Similarly, at axes of symmetry associated to the fixed action of the rotatational Killing vectors R_a we will also have that $\det G_{AB} = 0$.

In other to make further progress we will now need to make one final assumption. We emphasise that here what we are really trying to do is to find a useful constructive numerical technique for finding black hole solutions, as opposed to proving general results and theorems. Therefore, motivated by the uniqueness theorem treatment of $D = 4$ black holes as an elliptic boundary value problem on a Riemannian base (see for instance [53] and the D dimensional generalisations [106, 107]), we will simply make the following assumption:

Assumption: $(\mathcal{M}, h)$ is a smooth Riemannian manifold with boundaries given by the horizons and axes of symmetry of the R_a that generate rotational isometries.

A consequence of $\det h_{ij} > 0$ everywhere on $\mathcal{M}$, including in particular on the horizon and axis boundaries is that $\det G_{AB} \leq 0$ everywhere on $\mathcal{M}$, with it vanishing only at the horizon or axis boundaries of $\mathcal{M}$. (Note in particular that $\det g_{\mu\nu} = 0$ there as one should have anticipated by virtue of the fact that the coordinates of (3.4.20) break down there). It is of interest to note also that the same ingredients of relevance in our analysis, namely the structure of the base $\mathcal{M}$, together with the data associated with the Killing horizon boundaries $\Omega^a_{\mathcal{H}_m}$ and specification of which R_a vanish at the axis boundaries has been conjectured to provide at least a partial classification of higher dimensional black holes in terms of their rod structure [207].

3.4.1. Ellipticity of the Harmonic Einstein Equation

In the above analysis it is important to stress that we have not assumed that the stationary Killing field T is timelike and indeed it is not. In the presence of horizons, it will become null and in an ergoregion it will become spacelike. Indeed as shown in (3.4), it was precisely when T failed to be timelike that ellipticity broke down as the base metric then failed to be Riemannian. Equipped now with our assumption above on the base metric, the crucial observation we make is that for the class of stationary solutions (3.4.20) we have

$$R^H_{AB} = -\frac{1}{2} g^{\alpha\beta}\partial_\alpha\partial_\beta g_{AB} + \ldots = -\frac{1}{2} h^{mn}\partial_m\partial_n G_{AB} + \ldots\,,$$
$$R^H_{ij} = -\frac{1}{2} g^{\alpha\beta}\partial_\alpha\partial_\beta g_{\mu\nu} + \ldots = -\frac{1}{2} h^{mn}\partial_m\partial_n h_{ij} + \ldots\,, \qquad (3.4.21)$$

where again the ellipses represent terms with less than two derivatives. We hence see explicitly that the equations have character determined solely by the metric h_{ij}, and since $\mathcal{M}$ is Riemannian (by assumption), these are elliptic.

In analogy with the previous section, we should also ensure that $R^H_{\mu\nu}$ shares the same isometries as the metric (3.4.20) so that we correctly truncate to this class of stationary solutions under Ricci Flow/Newton method updates. Consequently we choose for the reference metric

$$ds^2 = \bar{g}_{\mu\nu} dX^\mu dX^\nu = \bar{G}_{AB}(x)\left(dy^A + \bar{A}^A_i(x)dx^i\right)\left(dy^B + \bar{A}^B_j(x)dx^j\right) + \bar{h}_{ij}(x)dx^i dx^j \qquad (3.4.22)$$

where T, R_a are again Killing with respect to it and we furthermore assume that $(\mathcal{M}, \bar{h})$ is a smooth Riemannian manifold. (Since we are free to choose the reference metric, which is then fixed, this does not truly impose any further restrictions on our method).

The final matter to address is boundary conditions. In addition to the asymptotic boundary, all horizons and axes of symmetry constitute real physical boundaries and we will need to impose data there. We will discuss this in detail in the next section. The picture is then that using Ricci-DeTurck flow or the Newton method and beginning with initial data in our stationary class, for small flow times (at least) we expect to remain in this class and importantly the base $(\mathcal{M}, h)$ remains Riemannian. Subject to choosing suitable initial conditions and provided the aforementioned condition is not violated we should then be able to use this method to find a stationary black hole.

As in the last section, we now explicitly write down the flow equations that would need to be solved to carry out such a task. The components of the Harmonic Einstein equation may be also deduced from these, using the equations

$$\frac{\partial G_{AB}}{\partial\lambda} = -2R^H_{AB}\,,$$
$$\frac{\partial A^C_j}{\partial\lambda} = -2G^{AC}(R^H_{jA} - R^H_{AB}A^B_j)\,,$$
$$\frac{\partial h_{ij}}{\partial\lambda} = -2(R^H_{ij} + R^H_{AB}A^A_i A^B_j - R^H_{iA}A^A_j - R^H_{jA}A^A_i)\,. \qquad (3.4.23)$$

Contracting indices and taking covariant derivatives $\hat{\nabla}$ with respect to the base metric h_{ij}, one finds after a rather long calculation

$$\begin{aligned}
\frac{\partial G_{AB}}{\partial\lambda} &= \overbrace{\hat{\nabla}^i(\partial_i G_{AB})}^{=h^{mp}\partial_m\partial_p G_{AB}+\dots} -G^{CD}(\partial^i G_{AD})(\partial_i G_{CB}) + \frac{1}{2}\bar{h}^{km}_{(-1)}G^{CD}(\partial_m\bar{G}_{CD})(\partial_k G_{AB}) \\
&\quad -\frac{1}{2}G_{BE}G_{AF}F^{Eij}F^F_{ij} + \hat{\xi}^k\partial_k G_{AB} + \bar{h}^{km}_{(-1)}\bar{G}_{CD}(A^{Di}-\bar{A}^{Di})\bar{F}^C_{im}\partial_k G_{AB} \\
&\quad +\frac{1}{2}\bar{h}^{km}_{(-1)}(A^{Ci}A^D_i + \bar{A}^{Ci}\bar{A}^D_i - 2A^{Ci}\bar{A}^D_i)(\partial_m\bar{G}_{CD})(\partial_k G_{AB}),
\end{aligned}$$

$$\begin{aligned}
\frac{\partial A^C_i}{\partial\lambda} &= \overbrace{-\hat{\nabla}^k F^C_{ik} + \hat{\nabla}_i(A^C_k\hat{\xi}^k) + \hat{\nabla}_i(\hat{\nabla}^p A^C_p - \bar{\hat{\nabla}}^p\bar{A}^C_p)}^{=h^{mp}\partial_m\partial_p A^C_i+\dots} - G^{AC}F^B_{ij}\partial^j G_{AB} + \hat{\xi}^k F^C_{ki} \\
&\quad +\frac{1}{2}\bar{h}^{km}_{(-1)}G^{DE}F^C_{ki}\partial_m\bar{G}_{DE} - \bar{h}^{km}_{(-1)}\bar{G}_{DE}(A^{jD}-\bar{A}^{jD})F^C_{ik}\bar{F}^E_{jm} \\
&\quad +\frac{1}{2}\bar{h}^{km}_{(-1)}(A^{pD}A^E_p + \bar{A}^{pD}\bar{A}^E_p - 2A^{pD}\bar{A}^E_p)F^C_{ki}\partial_m\bar{G}_{DE} \\
&\quad +\hat{\nabla}_i\Bigg(\bigg(\frac{1}{2}\bar{h}^{mp}_{(-1)}G^{DE}(A^C_m - \bar{A}^C_m) + \bar{G}^{CE}(A^{pD}-\bar{A}^{pD}) \\
&\quad +\frac{1}{2}\bar{h}^{kp}_{(-1)}(A^{mD}A^E_m + \bar{A}^{mD}\bar{A}^E_m - 2A^{mD}\bar{A}^E_m)(A^C_k - \bar{A}^C_k)\bigg)\,\partial_p\bar{G}_{DE}\Bigg) \\
&\quad +\hat{\nabla}_i(\bar{h}^{km}_{(-1)}\bar{G}_{DE}(A^{jE}-\bar{A}^{jE})(A^C_k - \bar{A}^C_k)\bar{F}^D_{jm}),
\end{aligned}$$

$$\begin{aligned}
\frac{\partial h_{ij}}{\partial\lambda} &= \overbrace{-2\hat{R}_{ij} + 2\hat{\nabla}_{(i}\hat{\xi}_{j)}}^{=h^{mp}\partial_m\partial_p h_{ij}+\dots} + \frac{1}{2}G^{AB}G^{CD}(\partial_i G_{CB})(\partial_j G_{AD}) - G_{AB}F^{Ak}_j F^B_{ki} \\
&\quad +\Bigg(\frac{1}{2}h_{ik}\hat{\nabla}_j(G^{AB}\bar{h}^{km}_{(-1)}\partial_m\bar{G}_{AB}) + h_{ik}\hat{\nabla}_j(\bar{h}^{km}_{(-1)}\bar{G}_{AB}\bar{F}^B_{qm}(A^{qA}-\bar{A}^{qA})) \\
&\quad +\frac{1}{2}h_{ik}\hat{\nabla}_j(\bar{h}^{km}_{(-1)}(A^{pA}A^B_p + \bar{A}^{pA}\bar{A}^B_p - 2A^{pA}\bar{A}^B_p)\partial_m\bar{G}_{AB}) + (i\leftrightarrow j)\Bigg)\,,
\end{aligned} \tag{3.4.24}$$

where as before the base DeTurck vector field $\hat{\xi}^i$ is defined as in (3.2.4) and we analogously define $F^A_{ij} \equiv \partial_i A^A_j - \partial_j A^A_i$ and similarly, $\bar{F}^A_{ij} \equiv \partial_i\bar{A}^A_j - \partial_j\bar{A}^A_i$. In appendix (B) of this thesis we present useful intermediate results that lead to these expressions.

3.4.2. Reduced Stationary Case

We will now make an observation that allows us to truncate the equations above to a much simpler class of stationary spacetimes. For many examples, this 'reduced' stationary system will in fact by sufficient as we shall discuss shortly. We proceed by requiring the metric to have invariance under the discrete symmetry

$$t \to -t\,, \quad y^a \to -y^a\,. \tag{3.4.25}$$

This allows for a consistent truncation of the Harmonic Einstein equation in the sense that the Ricci-DeTurck tensor $R^H_{\mu\nu}$ is also invariant. Note in particular that this discrete symmetry requires all the A^A_i to vanish, leading to a dramatic simplification of the equations

$$\begin{aligned} R^H_{AB} &= -\frac{1}{2}\hat{\nabla}^i(\partial_i G_{AB}) + \frac{1}{2}G^{CD}(\partial^i G_{AD})(\partial_i G_{CB}) - \frac{1}{4}\bar{h}^{km}G^{CD}(\partial_m \bar{G}_{CD})(\partial_k G_{AB}) \\ &\quad -\frac{1}{2}\hat{\xi}^k \partial_k G_{AB}\,, \\ R^H_{ij} &= \hat{R}_{ij} - \hat{\nabla}_{(i}\hat{\xi}_{j)} - \frac{1}{4}G^{AB}G^{CD}(\partial_i G_{CB})(\partial_j G_{AD}) - \frac{1}{2}h_{k(i}\hat{\nabla}_{j)}(G^{AB}\bar{h}^{km}\partial_m \bar{G}_{AB})\,, \end{aligned} \tag{3.4.26}$$

and R^H_{Ai} vanishes (as it must do for the equations to truncate to this reduced stationary class consistently). One can also show by explicit calculation that automatically $\xi^A = 0$ for this class. The specification of boundary conditions proceeds in a manner that is likely now familiar. In the case of a Dirichlet boundary, one imposes the induced metric by fixing G_{AB} together with the tangential components of h_{ij}. The remaining components of the base metric h_{ij} are then determined by requiring $\xi^i = 0$.

It is worth emphasising that equations (3.4.26) really do represent a marked simplification of the full equations. One might imagine that this 'reduced stationary case' would hence be extremely restrictive in physical contexts but remarkably this turns out not to be so. In particular, in $D = 4$, the 'circularity' theorem allows all asymptotically flat stationary black holes to be recast in the form [35], meaning that the reduced stationary class is sufficient for any $4D$ problem. The situation is less clear for $D > 4$, but interestingly all known analytic solutions (to us) are also of this reduced stationary form.

3.4.3. Horizon and Axis Boundaries

We now explicitly give the boundary conditions for the components of our stationary ansatz (3.4.20) and the reference metric at any Killing horizons and axes of rotational symmetry. In the $4D$ case, recall that the horizon and axes of symmetry play the role of boundaries of the Riemannian base manifold (orbit space) and what we shall discuss here can be viewed as a higher dimensional generalisation of that picture.

That is to say, we may regard the results we will present in this section on the metric behaviour at the horizons and axes as generalising the boundary conditions in that context [53]. It is also worth noting that they are also consistent with the boundary conditions found by Harmark using a particular choice of coordinates on the base manifold [207].

As discussed in the previous chapter, the problem of determining boundary conditions can be viewed as analogous to that of deducing the smoothness condition for a spherically symmetric function in spherical polar coordinates at the origin. By definition, such a function can only depend on r in the polar chart, but since we require it to smooth, meaning that in Cartesian coordinates x^i, it is a C^∞ function of the x^i's, we know that it cannot be a smooth function of r, but rather must be a smooth function of r^2. This is simply because $r^2 = \sqrt{x^i x^i}$ and hence if it were a function of r that would violate our assumption that the function is smooth in the x^i coordinates. We can also relax the requirement of C^∞ smoothness, and require only C^2 (this is the minimum required of course for a solution to the Einstein equations, being second order in derivatives). In that case, the smoothness requirement can be simply be thought of as a Neumann boundary condition at the origin $\partial f/\partial r|_{r=0} = 0$. A similar analysis can be performed for a tensor, the only difference being now that the components transform on shifting from a chart that manifests smoothness, but not the isometries, to a chart where the opposite is true, in other words, the symmetry is manifest, but smoothness is not. We give the details in an appendix (A). We may now apply the same logic to our spacetime metric and reference metric.

Let us begin first with the situation of a single Killing horizon, or multiple horizons that share a common normal Killing vector $K = T + \Omega^a R_a$. It is convenient to change coordinates as

$$t\,,\ y^a \quad \to \quad \tilde{t} = t\,, \quad \tilde{y}^a = y^a - \Omega^a t\,, \tag{3.4.27}$$

so that $K = \partial/\partial\tilde{t}$ and $R_a = \partial/\partial\tilde{y}^a$. Note that if R_a generates a compact orbit, then the coordinate $\tilde{y}^a$ is periodic $\tilde{y}^a \sim \tilde{y}^a + 2\pi$. We now consider a boundary which as usual can be due to either vanishing norm of K or a compact R_a. Choosing coordinates adapted to the boundary ($r = 0$), we can then split the base metric as

$$h_{ij}dx^i dx^j = N dr^2 + r\, N_{\tilde{i}} dr dx^{\tilde{i}} + h_{\tilde{i}\tilde{j}} dx^{\tilde{i}} dx^{\tilde{j}}\,, \tag{3.4.28}$$

and likewise for the reference metric where $N \to \bar{N}$, $N_{\tilde{i}} \to \bar{N}_{\tilde{i}}$ and $h_{\tilde{i}\tilde{j}} \to \bar{h}_{\tilde{i}\tilde{j}}$.

Horizon: For a Killing horizon we write the following metric components as

$$G_{\tilde{t}A} = -r^2 f_A\,, \quad A^A_r = r g^A\,, \tag{3.4.29}$$

for $y^A = (\tilde{t}, \tilde{y}^a)$ and then let $X = \left\{ f_A\,,\ g^A\,,\ G_{\tilde{y}^a\tilde{y}^b}\,,\ A^A_{\tilde{i}}\,,\ N\,,\ N_{\tilde{i}}\,,\ h_{\tilde{i}\tilde{j}} \right\}$ be the set of functions describing our metric. Let $\bar{X}$ be the analogous set describing the reference metric. Then the results of appendix A imply that for the metric and reference metric to be smooth we require the following behaviour; the functions X and $\bar{X}$ must be smooth functions of r^2 and $x^{\tilde{i}}$ at $r = 0$, and furthermore obey the regularity conditions

$$\left(f_{\tilde{t}} - \kappa^2 N \right)|_{r=0} = 0\,, \quad \left(\bar{f}_{\tilde{t}} - \kappa^2 \bar{N} \right)|_{r=0} = 0\,, \tag{3.4.30}$$

where κ is constant and determines the surface gravity. Note also that since both the metric and the reference metric are smooth with respect to the *same* Killing field, the same constant appears in both the conditions (3.4.30). So physically multiple horizons considered in this analysis must have the same surface gravity.

Axis: Now consider one of the axes associated to one of the vanishing compact rotational Killing vectors R_a. Without loss of generality choose this to be R_N. Then we write

$$G_{\tilde{y}^N A} = r^2 f_A\,, \quad A^A_r = r g^A\,, \tag{3.4.31}$$

and let $Y = \left\{ f_A\,,\ g^A\,,\ G_{\tilde{t}\tilde{t}}\,,\ G_{\tilde{t}\tilde{y}^{\tilde{a}}}\,,\ G_{\tilde{y}^{\tilde{a}}\tilde{y}^{\tilde{b}}}\,,\ A^A_{\tilde{i}}\,,\ N\,,\ N_{\tilde{i}}\,,\ h_{\tilde{i}\tilde{j}} \right\}$ be the set of functions describing our metric (where $\tilde{a} = 1, \ldots, N-1$). Let $\bar{Y}$ be the set of functions that analogously describe the reference metric. Appendix A implies that for a smooth metric and reference metric we must have that the metric functions Y and $\bar{Y}$ are smooth functions of r^2 and $x^{\tilde{i}}$ at $r = 0$, and in addition we require,

$$\left(f_{\tilde{y}^N} - N \right)|_{r=0} = 0\,, \quad \left(\bar{f}_{\tilde{y}^N} - \bar{N} \right)|_{r=0} = 0\,. \tag{3.4.32}$$

Unsurprisingly one obtains analogous conditions for any choice of axis with respect to a different R_a.

In summary we see that in the situation where one has a single Killing vector $K = T + \Omega^a R_a$ normal to all horizons, we may use the coordinates $(\tilde{t}, \tilde{y}^a)$ and obtain boundary conditions. One may rewrite these in terms of the original (t, y^a) as desired. If multiple Killing horizons are present with different normals, then the boundary conditions for each should be obtained in turn by taking coordinates as in (3.4.27) with Ω^a appropriate to each horizon. To complete our discussion of boundary conditions we note that one should also ensure consistency in regions where a horizon and axis of symmetry intersect.

A horizon meeting an axis: It is possible to check that the boundary conditions at the intersection point between a horizon with an axis, or two axes are compatible with each other by a brute force calculation. We outline this for the case of a metric intersecting the axis R_N, noting that similar results would be found in the other cases and that the calculation proceeds in a similar manner. We take coordinates on the base such that the horizon lies at $r = 0$ and the axis is at $\theta = 0$. In detail, we have

$$h_{ij}dx^i dx^j = N dr^2 + M d\theta^2 + r\theta A dr d\theta + r\, B_{\tilde{i}} dr dx^{\tilde{i}} + \theta\, C_{\tilde{i}} d\theta dx^{\tilde{i}} + h_{\tilde{i}\tilde{j}} dx^{\tilde{i}} dx^{\tilde{j}} \,, \tag{3.4.33}$$

where now $\tilde{i} = 1, \ldots, D-3$. Then writing,

$$\begin{aligned} G_{\tilde{t}\tilde{t}} &= -r^2 f \,, \quad G_{\tilde{t}\tilde{y}^{\tilde{a}}} = r^2 f_{\tilde{a}} \,, \quad G_{\tilde{y}^N \tilde{y}^N} = \theta^2 g \,, \quad G_{\tilde{y}^N \tilde{y}^{\tilde{a}}} = \theta^2 g_{\tilde{a}} \,, \quad G_{\tilde{t}\tilde{y}^N} = r^2\theta^2 k \,, \\ A^A_r &= r\, p^A \,, \quad A^A_\theta = r\, q^A \,, \end{aligned} \tag{3.4.34}$$

our arguments from appendix A applied to the horizon $r = 0$ and to the axis $\theta = 0$ then imply that the set of functions characterising the metric found in the equations (3.4.33) and (3.4.34) above, $N, M, \ldots, k, p^A, q^A$, together with the remaining components $G_{\tilde{y}^a \tilde{y}^b}$ and $A^A_{\tilde{i}}$, must all be smooth functions in r^2, θ^2 and $x^{\tilde{i}}$ near the meeting point $r = \theta = 0$. Furthermore regularity requires

$$\left(f - \kappa^2 N\right)|_{r=0} = 0 \,, \quad \text{and} \quad (g - M)\,|_{\theta=0} = 0 \,. \tag{3.4.35}$$

We see then that the conditions above are indeed consistent where two boundaries meet (a horizon and axis, or two axes).

We now address a crucial point. Having introduced boundary conditions for the metric, it is very important to check that they lead to conditions on the vector ξ that are at least consistent with ensuring the elliptic boundary value problem for the Harmonic Einstein equations is compatible with the trivial solution. (We may yet find Ricci solitons, but we need to ensure there is at least the possibility of Ricci flat solutions). To investigate this, we need only use the structure of our metric and reference metric to explicitly check that

$$\xi^r|_{r=0} = 0\,, \quad \partial_r \xi^{\tilde{i}}|_{r=0} = 0\,, \quad \partial_r \xi^A|_{r=0} = 0\,, \tag{3.4.36}$$

both at a horizon and axis of symmetry, which is indeed consistent with a trivial solution. (Note that unsurprisingly, in deriving these results, one must use the boundary behaviours of the metric at axes/horizons that has just been discussed at length. In other words which metric functions go to zero and how quickly they go to zero at the fixed points is important in obtaining the required behaviour for the ξ vector).

In summary, one may now proceed to consider Ricci-De Turck flow or the Newton method operating on the metric g near a horizon or axis. With our choice of reference metric that has the same isometry K and is also regular at the boundaries, the Ricci-DeTurck tensor will be symmetric in K as well. In particular, the Ricci-DeTurck flow and Newton method will preserve regularity and therefore as a consequence of the discussion above leave the surface gravity constant.

We close this section with a final technical point. For the C^∞ (or the C^2 case when we do not require a restriction as strong as smoothness), the metric functions may be viewed as having Neumann boundary conditions. In addition to this however, we also have the additional constraints $f_{\tilde{t}} = \kappa^2 N$ for horizons, and $f_{\tilde{y}^N} = N$ for axes. One might fear that these latter conditions should not be imposed in addition to the Neumann conditions as this would then constitute 'too much data' for an elliptic problem. The system would become overconstrained in other words. However the resolution of this is simply that this 'fictitious boundary' of the equations should be viewed as a regular singular point of the equations as a consequence of the singular terms that arise from the vanishing norm of the Killing vector and thus the usual enumeration of boundary conditions for the elliptic problem does not in fact apply. Instead we emphasise again that these additional regularity conditions are preserved under Ricci flow/Newton method and thus it is perhaps best to think of them not as boundary conditions at all but rather as a restriction on the class of regular metrics. Our Ricci Flow/Newton method will then act to update the solution within this class.

3.5. Example of Boundary Conditions: Kerr

In this section, we discuss the Kerr solution in the context of the framework that has been introduced in this chapter, in particular showing that the boundary behaviours of the metric functions detailed in the previous sections are satisfied. Further details of interest can be found in [1]. Of particular note there is the worked example detailing an application to $D = 4$ rotating black holes in a cavity, which serves as the first practical use of the stationary methods developed here.

The Kerr solution may be written in a reduced stationary form so that $A_i^A = 0$. In the textbook Boyer-Lindquist coordinates this is already manifest and the metric takes the form

$$ds^2 = G_{tt}dt^2 + 2G_{t\phi}dtd\phi + G_{\phi\phi}d\phi^2 + h_{rr}dr^2 + h_{\theta\theta}d\theta^2 \,, \tag{3.5.37}$$

with fiber metric

$$\begin{aligned} G_{tt} &= -\frac{\left(\Delta - a^2\sin^2\theta\right)}{\Sigma}\,, \quad G_{\phi\phi} = \sin^2\theta\frac{\left((r^2+a^2)^2 - \Delta a^2\sin^2\theta\right)}{\Sigma}\,, \\ G_{t\phi} &= -a\sin^2\theta\frac{(r^2+a^2-\Delta)}{\Sigma}\,, \end{aligned} \tag{3.5.38}$$

and base

$$h_{rr} = \frac{\Sigma}{\Delta}\,, \quad h_{\theta\theta} = \Sigma\,, \tag{3.5.39}$$

where the functions Δ, Σ are defined as $\Delta = r^2 + a^2 - 2Mr$ and $\Sigma = r^2 + a^2\cos^2\theta$. The stationary Killing vector is $T = \frac{\partial}{\partial t}$ and the rotational Killing vector is $R = \frac{\partial}{\partial\phi}$.

The base manifold has coordinates (r, θ) and as can be seen from above, the metric components depend explicitly on these. There are two horizons, and only the outermost will concern us. This outer horizon is a boundary of this base $\mathcal{M}$ and is located at $\Delta = 0$ where $r \equiv r_h = M + \sqrt{M^2 - a^2}$, and the remaining boundaries are associated with the single axis of rotation at $\theta = 0, \pi$. One may calculate explicitly that

$$\det G_{AB} = -(a^2 + r(r - 2M))\sin^2\theta\,. \tag{3.5.40}$$

Note that this determinant vanishes at these boundaries, in agreement with the behaviour discussed in the previous section. Everywhere in the exterior of the black hole, we have that $r_h < r$ and $0 < \theta < \pi$ and hence G_{AB} has Lorentzian signature and h_{ij} is Euclidean and smooth. The stationary Killing field is not normal to the horizon as the solution is rotating, but one may show that the Killing field $K = T + \Omega R$ is normal (and therefore tangent as its a null hypersurface) to the horizon and timelike near there, where the angular velocity of the horizon is computed to be $\Omega = \frac{a}{a^2+r_h^2}$.

Whilst the θ coordinate is regular everywhere (and in particular at the rotation axis), the Boyer-Lindquist r coordinate is not at the horizon as $\Delta \to 0$ there. It is therefore essential that we define a new regular radial coordinate ρ such that $d\rho = dr/\sqrt{\Delta}$ and $\rho = 0$ at the horizon giving

$$r = M + \sqrt{M^2 - a^2} \cosh \rho \,, \tag{3.5.41}$$

so that the components of the base metric h_{ij} are smooth at the horizon boundary. In particular in these coordinates the determinant of the base metric,

$$h_{ij} dx^i dx^j = \frac{\Sigma}{\Delta} dr^2 + \Sigma d\theta^2 = \Sigma \left(d\rho^2 + d\theta^2 \right) \implies \det h_{ij} = \Sigma^2 \geq r_h^2 \,, \tag{3.5.42}$$

and hence since $r_h^2 > 0$, the base is indeed a smooth Riemannian manifold everywhere on and in the exterior of the horizon (and hence satisfies the key assumption of the previous section). It is useful to change to a corotating system of coordinates

$$\tilde{t} = t \,, \quad \tilde{\phi} = \phi - \Omega t \,, \tag{3.5.43}$$

and then we may confirm that near the horizon $\rho = 0$ we have

$$G_{\tilde{t}\tilde{t}} = -\kappa^2 \left(h_{\rho\rho}|_{\rho=0} \right) \rho^2 + \mathcal{O}(\rho^4) \,,$$

$$G_{\tilde{t}\tilde{\phi}} = \mathcal{O}(\rho^2) \,, \quad G_{\tilde{\phi}\tilde{\phi}} = \mathcal{O}(1) \,,$$

$$h_{\rho\rho} = h_{\theta\theta} = (r_h^2 + a^2 \cos^2 \theta) + \mathcal{O}(\rho^2) \,,$$

in accord with our boundary behaviour above. Note also that the constant κ is indeed the surface gravity of the Kerr solution

$$\kappa^2 = \frac{M^2 - a^2}{4 M^2 r_h^2} \,. \tag{3.5.44}$$

At the axis of symmetry $\theta = 0$ we have,

$$G_{\tilde{t}\tilde{t}} = \mathcal{O}(1) \,, \quad G_{\tilde{t}\tilde{\phi}} = \mathcal{O}(\theta^2) \,,$$

$$G_{\tilde{\phi}\tilde{\phi}} = \left(h_{\theta\theta}|_{\theta=0} \right) \theta^2 + \mathcal{O}(\theta^4) \,,$$

$$h_{\rho\rho} = h_{\theta\theta} = (a^2 + (M + \sqrt{M^2 - a^2} \cosh \rho)^2) + \mathcal{O}(\theta^2) \,,$$

which again agrees with our calculation of axis boundary behaviour. Likewise the same agreement is seen at $\theta = \pi$.

3.6. Discussion

In this chapter we have developed the theoretical foundations to set up the Harmonic Einstein equation for the case of Lorentzian static and stationary spacetimes as an elliptic boundary value problem. Ricci Flow or the Newton method acting on these spacetimes may then be used as algorithms to solve this equation, ultimately yielding solutions to the static and stationary vacuum Einstein equations.

We have shown in particular, how to view the static problem, previously solved in a Riemannian context [21] from a Lorentzian perspective. In this case, it is relatively straightforward to observe that the Lorentzian Harmonic Einstein equation truncates to the static case and gives an elliptic system as a consequence of the independence of the metric functions on the time coordinate. Whilst the horizon must now be viewed as a physical boundary in Lorentzian signature, one may determine suitable boundary conditions for regularity at the horizon by a suitable change of coordinates.

Having treated the static case from a fully Lorentzian perspective, we then proceeded to discuss the stationary case, beginning as a warm-up with stationary spacetimes with a globally timelike Killing vector. As in the static Lorentzian case, it was possible to demonstrate that for a suitable choice of reference metric, the Lorentzian Harmonic Einstein equation again truncates to such stationary spacetimes giving the desired elliptic system of equations. Indeed the analysis also demonstrated that ellipticity would furthermore fail in regions where the stationary Killing field became spacelike, physically corresponding to black hole ergo-regions - something we needed to be able to cover with our analysis.

Heuristically, one may also regard the challenge to ellipticity in the Lorentzian setting as arising as a consequence of spatial gradients in the direction of motion of the horizon. In order for a spacetime to be stationary, there can be no such gradients and the motion of the horizons must be solely in an isometry direction, a statement that is formalised in the Rigidity theorems. Drawing on these general theorems, we proceeded to consider a broad class of stationary spacetimes which were written as fibrations of the orbits of the stationary Killing vector, together with the orbits of other mutually commuting Killing vectors associated with rotation or translation over a base manifold. This class was also considered by Harmark in his classification of higher dimensional black holes [207]. Further motivated by stationary uniqueness theorems, we then made the key assumption that this base manifold was Riemannian. Together now with a reference metric of the same form and the observation that a particular combination of the stationary and rotational Killing vectors lies normal to the horizon, it was possible to show the Harmonic Einstein equation once again consistently truncates to this class of stationary spacetimes and is in fact elliptic. We provided the necessary boundary conditions at the Killing horizons or axes of symmetries which physically constitute true boundaries on the Riemannian base (orbit space) manifold. These were then shown to be consistent with obtaining true Ricci flat solutions to the Einstein equations as opposed to solitons. The Ricci-DeTurck flow is then parabolic on this class of Lorentzian stationary spacetimes, and gives an explicit algorithm to solve the system, as does of course Newton's method. We finally revisited the famous Kerr metric in the light of our stationary elliptic discussions and motivated how several of the results derived in this chapter apply in that case.

In the remainder of this thesis we shall turn to a discussion of Einstein-Aether theory. After introducing this modified theory of gravity and providing some historical context we turn to the rather complex matter of its black hole solutions. We will in particular be interested in stationary black holes and will use a generalisation of the methods introduced in this chapter to numerically construct them. These are the first stationary solutions of this type in the literature and in order to construct them we will need to understand how to generalise the methods outlined in this chapter to handle the interior of the black hole where the equations are not elliptic. Said in another way, we will need to understand how to solve the Harmonic Einstein equations as a mixed hyperbolic-elliptic system and moreover will need to add matter (as Einstein aether theory by definition must include an aether vector field).

4. Black Holes in Einstein-Aether Theory

4.1. Introduction

As discussed in the introduction, Einstein-Aether theory is a modified theory of gravity that exhibits spontaneously broken Lorentz symmetry in the gravitational sector. It consists of general relativity coupled to a dynamical, unit timelike vector field u^μ called the aether. The dynamics of the latter alters the metric dynamics and hence the coupled system differs significantly from more standard examples of general relativity coupled to matter fields. In this chapter we turn to a discussion of black holes in Einstein-Aether theory. Ultimately, we will show how to use a modification of the numerical techniques of previous chapters to construct both static and stationary aether black holes. Our intention is not to provide an in depth exploration of the full parameter space of solutions (a task left for future work), but instead is more of a proof of principle to demonstrate that we can indeed find such solutions using our methods. We shall demonstrate that the static solutions we construct (using new techniques) agree with what has been discussed in the literature [150, 152]. The stationary solutions however are new and are the first examples of such solutions in Einstein-Aether theory[1].

The study of solutions to the Einstein-Aether field equations began in [171]. In the spherical symmetric situations discussed there, the aether has one degree of freedom, and restricting to the time independent case, the authors found a three parameter family of spherical star solutions, a two parameter family of which is asymptotically flat. This work in particular, focused on a sub-family of these for which the aether field coincides with the static Killing vector. A study of black holes was then initiated in [150]. It was first necessary for the authors to define precisely what is meant by a black hole in Einstein-Aether theory, as with multiple characteristic degrees of freedom it is not immediately obvious. It was argued that

[1] We note that *slowly* rotating black hole solutions in Einstein-Aether theory have also recently been found [210], but our solutions are more general, having no such slow rotation restrictions.

a generic Einstein-Aether black hole will have multiple horizons, corresponding to trapping each of the spin-2, 1 and 0 wave modes and a 'true' black hole should have an outer horizon that traps the fastest of these. With these definitions one can indeed construct static, spherically symmetric black holes and the authors showed by way of series expansion of the field equations about the metric horizon and infinity, that there is a three-parameter family of regular solutions. This initially appeared rather mysterious as one expects only a one parameter family as there are no conserved charges (beyond the mass) in the theory that could account for the additional two. The resolution of this was explained to be due to singular behaviour at the spin-0 horizon. Whilst [211] have argued that this singularity is permitted as it is 'cloaked' by the metric horizon[2], Eling at al [150] note that imposing regularity at this spin-0 horizon as an additional constraint reduces the three parameter family to a two parameter family, which is further reduced to the expected one parameter family on requiring asymptotic flatness. In practice, they used shooting methods to find their solutions in a manner analogous to what was done in a holographic setting in chapter 2 of this thesis. Regularity at the spin-zero horizon can be imposed in two ways, firstly by tuning shooting data at infinity until a regular solution is found or alternatively by explicitly expanding the equations (in the near horizon region) as a series about a *regular* spin-zero horizon. The complexity of the equations is such that this could not be done in complete generality and a subset of the c_i was analysed.

Qualitatively these Einstein-Aether black holes share many features in common with the Schwarzchild solution of pure general relativity (at least in the exterior region), and in particular both have a curvature singularity at $r = 0$. Unlike the spherical star solutions of [171], the aether field in these black holes is not everywhere aligned with the static Killing vector. Since the aether field is constrained to be timelike but the static Killing vector becomes null on the black hole metric horizon, the aether field actually flows into the black hole. In the interior regions, some of these black holes solutions were found to exhibit oscillatory behaviour both in the metric and aether components, in a manner similar to what occurs in Einstein-Yang-Mills black holes [212]. A more detailed analysis of these static Einstein-Aether black holes can be found in [152], where in particular, phenomenologically allowed areas of parameter space were analysed (in contrast to [150]), and comparison of physical quantities such as the radius of the innermost stable circular orbit are

[2]Whilst generically it is true that the spin-zero horizon is inside the metric horizon and therefore cloaked, one can perform a field redefinition to make these two horizons coincide and it is this that really demonstrates that regularity at the spin-zero horizon should be imposed as an additional constraint [150].

made with pure general relativity. An analysis of the gravitational perturbations and quasinormal modes of these static aether black holes has also been undertaken in [213, 214], where it was argued that the oscillation frequency and damping rates are larger than for the Schwarzchild solution, hence opening up the possibility for experimental discrimination between them with the next generation of gravitational wave experiments.

As discussed briefly in the introduction, Einstein-Aether theory is in fact the IR limit of Horava-Lifshitz theory when the aether field is hypersurface orthogonal. All spherically symmetric aether fields are hypersurface orthogonal, and hence all the black hole solutions of [150, 152] are also solutions of Horava-Lifshitz gravity (see also [215] for a discussion of spherically symmetric star solutions in Horava-Lifshitz gravity). The converse has been argued to hold for solutions with a 'regular centre' [161], but it is likely that additional Horava-Lifshitz solutions exist without this condition. Whilst there has been relatively little work on black holes in Einstein-Aether theory, much more attention has been directed at black holes in Horava-Lifshitz gravity. We note however that this is not in a regime where the theory is related to what we consider here. In particular, Horava-Lifshitz black holes have been studied where a projectability condition is imposed [216] (that the lapse function is space independent) and where only a reduced set of terms in the full action are retained [217, 218, 219].

There remain many aspects of black hole physics in Einstein-Aether theory that remain almost completely unexplored. A study of black hole mechanics has been undertaken in [220] but many questions remain unanswered. In particular, whilst it has been possible to derive a relation similar to a first law of black hole mechanics, relating variations of energy and angular momentum to a surface integral at the horizon, no thermodynamic interpretation has been found as of yet. A definitive expression for the black hole entropy in the theory also remains elusive. The issue of stationary black holes in Einstein-Aether has also thus far been completely untouched (although we will address this in this chapter). It is worth noting however that there have been some studies pertaining to stationary black holes in Horava-Lifshitz gravity. Notably, Barausse et al [221] derived a 'no-go' theorem, ruling out slowly rotating, stationary, axisymmetric black holes in the infrared limit of Horava-Lifshitz gravity, provided that they are regular everywhere except at the central singularity. This result would likely have ruled out the theory entirely due to the strong astrophysical evidence that exists for rotating black holes were it not for the fact that the same authors actually found such slowly rotating black holes in a later work [210]. They modified their previous claim, arguing that whilst there are in fact slowly rotating black holes in Horava-Lifshitz gravity, there are no slowly rotating solutions that are *also* solutions of Einstein-Aether theory. This is perhaps quite surprising given the relationships that exist between the static solutions in the two theories.

In this chapter we will first discuss various general features of black holes in Einstein-Aether theory. We then explain how to extend the numerical techniques we have discussed in previous chapters to the interior of a horizon, following the work of [222]. Since as explained previously, Einstein-Aether black holes have multiple horizons, we will need to construct at least part of the interior solution to exhibit their structure faithfully. Moreover as we shall see, the Einstein equations are not elliptic in the interior region, so one must now solve a mixed elliptic-hyperbolic PDE problem. We describe this procedure in some detail and then apply it to construct static, spherically symmetric black hole solutions in Einstein-Aether theory, discussing how the solutions we have found by these new techniques agree with the solutions found in the literature. We then go on to describe how we can construct stationary solutions.

4.2. Structure and Regularity of Einstein-Aether Black Holes

As alluded to in the preceding section, the definition of 'black hole' in Einstein-Aether theory is not immediately clear as we now explain in more detail. In order for a black hole to be able to trap matter signals it must have a horizon that is defined with respect to the metric which matter couples to universally. This is the metric $g_{\mu\nu}$ of (1.4.59) and we shall henceforth refer to the horizon with respect to this as the 'metric horizon'. Einstein-Aether theory, however, has multiple characteristic hypersurfaces, corresponding to spin-2, spin-1 and spin-0 wave modes and hence there are additional notions of causality that one must consider. We previously performed a linearised analysis in section (1.4.2) to calculate the squared speeds s_i^2 of the wave modes when $c_3 = c_4 = 0$. As we saw, these speeds are generically different from each other and from the metric speed of light. To be causally isolated, a black hole interior must trap matter fields, but also all of these aether and metric modes. In particular it must be bounded by a horizon corresponding to the fastest speed. Having now established what is meant by a black hole in the theory one must now turn to the question of whether such solutions exist and are regular. As we have demonstrated, the characteristic surfaces for a mode of speed s_i, are null with respect to the effective metric

$$g^{\mu\nu}_{(i)} = g^{\mu\nu} + q_{(physical)} u^\mu u^\nu = g^{\mu\nu} + \left(\frac{s_i^2 - 1}{s_i^2}\right) u^\mu u^\nu \,. \tag{4.2.1}$$

At such a characteristic surface, by definition the coefficient of a second derivative term in the equations goes to zero. This may then allow for a solution where some second derivative grows without bound, leading to singular behaviour. Whilst this does not appear to happen at the spin-2 or spin-1 horizons (at least in spherically symmetric solutions of Einstein-Aether theory), it does occur at the spin-0 horizon and these are generically singular. As discussed previously, it was found in [150] using shooting methods that with the additional requirement of spin-0 regularity, the field equations allow a one parameter family of asymptotically flat, spherically symmetric black hole solutions, sharing many qualitative features in common with the Schwarzchild solutions of pure general relativity. In the next two sections, we will show how to construct these solutions using new methods and demonstrate that these solutions are the same as those in the literature.

We close this section by emphasising that as pointed out in [150], it is perhaps somewhat surprising a-priori that regular black hole solutions to Einstein-Aether theory can be found at all, as there are some results that would at first sight appear to be obstructions to their existence. Firstly, it has been argued in the literature [223], that whilst the aether field may be regular at an arbitrary point on the horizon, it cannot smoothly extend to the bifurcation surface $\mathcal{B}$. (The latter is defined as the intersection of the past and future horizons). The essence of the argument is that the Killing flow acts as a Lorentz boost at any point on $\mathcal{B}$, and therefore the aether cannot be invariant there. In particular, it must become an infinite null vector as the fixed point set of the isometry at $\mathcal{B}$ is approached. This raises concerns as regularity on the future event horizon has been directly linked to regularity at $\mathcal{B}$ due to a theorem of Racz and Wald [224] (that is independent of any field equations), and hence it seems that we might have an obstruction to constructing regular solutions. The key point and resolution to this is that whilst the metric satisfies all the conditions of the theorem, the aether vector field breaks the required time reflection symmetry and so it need not be regular at the bifurcation surface. In other words, there may exist solutions in Einstein-Aether theory that have regular future horizon but which blow-up at the bifurcation surface, in contrast to what one might normally expect.

A second potential obstruction to the existence of regular Einstein-Aether black holes comes from the form of the stress tensor. At a *regular* stationary metric horizon, we have as a consequence of the Raychaudhuri equation (applied to the null geodesic congruence that generates the horizon) that $R_{\mu\nu}k^\mu k^\nu = 0$, where k^μ is the null horizon generator. It then immediately follows from the Einstein equations that, $T_{\mu\nu}k^\mu k^\nu = 0$. For most matter content this can be shown to hold by an explicit examination of the stress tensor. Interestingly, this property does not appear to hold kinematically for the aether stress tensor. The very fact though that one can construct regular solutions means that it *must* hold and hence must be imposed by the field equations in some non-obvious way. (Note that for the case of stationary black holes in general relativity, $T_{\mu\nu}k^\mu k^\nu = 0$ on the horizon is guaranteed in the non-extremal case by the observation that $T_{\mu\nu}k^\mu k^\nu$ is invariant under the flow generated by k^μ, that k^μ vanishes at $\mathcal{B}$ and that $T_{\mu\nu}$ is regular there. This argument fails in the presence of the aether as we need not have regularity at $\mathcal{B}$ as argued previously).

4.3. Ingoing Stationary Methods

The stationary techniques that we have reviewed in chapter 3 are applicable to construct solutions exterior to a metric horizon. We would now however like to turn to a generalisation of the aforementioned methods that allow us to build the interior black hole solution as well. We shall follow the methods introduced in [222] and this will be an essential ingredient in constructing Einstein-Aether black holes, since as we have explained, together with the metric horizon, black holes in this theory also have additional horizons associated to the spin-2, spin-1 and spin-0 modes. A key new feature in this analysis is that interior to the metric horizon, the associated PDE problem we need to solve will also no longer be purely elliptic and we will need to explain how to deal with this.

We begin with the familiar general stationary ansatz

$$ds^2 = -N(x)(dt + A_i(x)dx^i)^2 + b_{ij}(x)dx^i dx^j \, , \tag{4.3.2}$$

where as usual, the stationary Killing vector $T = \partial/\partial t$. (The spacetime is Lorentzian so $\det g_{\mu\nu} = -N \det b_{ij} < 0$ and we recall that in cases where T is globally timelike so that $N(x) > 0$, we have that b_{ij} is Riemannian). As usual, in order to obtain a well-posed problem we should eliminate the coordinate invariance associated with general relativity and thus following previous chapters, we solve the Harmonic Einstein (or Einstein DeTurck) equations

$$R^H_{\mu\nu} \equiv R_{\mu\nu} - \nabla_{(\mu}\xi_{\nu)} = T_{\mu\nu} + \dots \tag{4.3.3}$$

The strategy now is to take the stationary ansatz (4.3.2) and pose the Harmonic Einstein equations on an ingoing slice that intersects the future event horizon and extends *into* the black hole interior. This is to be thought of as analogous to writing our ansatz in an ingoing Eddington-Finkelstein coordinate chart. The metric (4.3.2) in ingoing coordinates, is by definition regular at the future horizon. Since we have that $\det g_{\mu\nu} = -N \det b_{ij} < 0$ everywhere, we conclude that b_{ij} is Riemmian outside a horizon (or ergoregion if one is present) where $N > 0$ and hence by our previous discussions, the Harmonic Einstein equations will be elliptic there. On the other hand, b_{ij} is Lorentzian in the interior of a horizon (or ergoregion) where $N < 0$ and thus the equations become hyperbolic. This problem therefore constitutes a mixed elliptic-hyperbolic PDE system. (Such systems are not uncommon physically, arising for example in the context of transonic flow in fluid dynamics). Although the rigorous mathematical analysis of this system is in principle quite different to what we have previously considered, we will not need the formal details of this as the practicalities will be very similar to what we have done before. In particular, we proceed by solving the system of equations using the Newton method exactly as one would do in the 'old method' (the only difference being boundary conditions as we will shortly discuss in detail). Ricci flow methods could also be used in principle, but this shall not be pursued further here. As usual, we will have to impose $\xi^\mu = 0$ by a suitable choice of metric boundary behaviour.

The key difference with the old stationary methods concerns boundary conditions and moduli. Since the PDE system becomes hyperbolic in the region interior to the metric horizon, our old boundary conditions are no longer suitable there. (One cannot treat a hyperbolic system as a boundary value problem). We therefore impose only the Harmonic Einstein equation but *no* boundary conditions at the innermost points of our domain. This is to be contrasted with the methods of chapter 3 where regularity demanded that certain additional conditions be imposed at the innermost points of the domain (there the horizon). Moreover, in those methods, the choice of reference metric fixed the surface gravity and angular velocity of the solutions that one finds (again on regularity grounds). Said in another way, any moduli associated to a solution are automatically fixed. In contrast, in these ingoing methods, the constraint that the metric be smooth everywhere within the domain is sufficient to ensure regularity at the metric horizon in ingoing coordinates and that is why no additional conditions need to be imposed. It is important to stress though that now solutions will only be specified up to any moduli. The practicalities of solving the system however remain unchanged, starting with a smooth initial guess near a solution, one updates according to the Newton method and since the Harmonic

Einstein tensor is smooth the resulting solution should remain so as well. We note as a technical aside that in the above text, we have made the tacit assumption that the asymptotic boundary conditions together with regularity at the future horizon are sufficient to define a locally unique stationary black hole solution, up to any moduli. In the previous cases, this was guaranteed by virtue of the ellipticity of the Harmonic Einstein equations, but in these mixed hyperbolic-elliptic cases we know of no general proof. On physical grounds, it seems highly likely however that this remains true as it forms the basis for some well-known physical principles such as the fluid-gravity correspondence [225, 226].

The moduli associated to solutions in these ingoing methods are fixed by the specification of additional boundary conditions. In particular we fix a single function value at z_{max}, (the 'innermost point' of the domain) per modulus. Specification of these quantities should of course not really be thought of as 'boundary' conditions but merely the procedure by which one selects a particular solution out of some family. They should also not be thought of as regularity conditions. The procedure is best illustrated by way of example and hence we shall now apply it to both static and stationary black holes in Einstein-Aether theory.

4.4. Spherically Symmetric Black Hole Solutions

To construct spherically symmetric, static[3] black holes in Einstein-Aether theory, we begin with the ansatz

$$ds^2 = -T(z)dv^2 - \frac{2V(z)}{z^2}dvdz + \frac{A(z)}{z^4}dz^2 + \frac{S(z)}{z^2}(d\theta^2 + \sin^2\theta d\phi^2)\,, \tag{4.4.4}$$

where we stress again that v is an ingoing Eddington-Finkelstein coordinate. Note also that we have used an inverse radial coordinate $z = 1/r$, as it is convenient for numerical purposes to compactify the domain of interest so that $0 \leq z \leq z_{max} = \frac{11}{10}$[4] (corresponding to $\frac{10}{11} \leq r \leq \infty$). Following the prescription outlined in the previous section, this is the metric on an ingoing slice of the spacetime that intersects the future (metric) horizon and extends inside the black hole. We emphasise that it is important (for our method to work) that this slice extends into the *interior* of the black hole, that is to say that the metric horizon lies within the z interval $[0, z_{max}]$. (In practice as we shall discuss shortly, this is engineered by making a suitable choice

[3]The term *static* Einstein-Aether black holes is something of a misnomer as the solutions are not static - the aether field is infalling and flows into the black hole. These solutions are however not new and we will use the terminology that is often found in the literature [150, 152] despite the possible confusion.

[4]The reason for this (perhaps) somewhat unusual value of z_{max} will be explained shortly.

of reference metric in our numerical analysis that satisfies this and essentially hoping for the best!)

We take as an ansatz for the aether field

$$U = P(z)dv - \frac{Q(z)}{z^2}dz\,, \tag{4.4.5}$$

(where by spherical symmetry we have set any potential angular terms to zero identically).

We choose the reference metric to be of the same form as in (4.4.4) (but with $T \to \bar{T}$, $V \to \bar{V}, \dots$), and from this we compute the reference connection and hence the associated DeTurck vector ξ.

The field equations that one obtains on substituting (4.4.4), and (4.4.5) into (1.4.63) (where the latter is supplemented by a DeTurck term) are highly complicated and we do not present them explicitly here. We simply note that in our implementation we did not eliminate the constraint $\lambda(z)$ (as doing so seems to complicate the numerical form of the equations further) and thus in addition to the metric and aether components, we also have $\lambda(z)$ as a quantity to be solved for, that is of course not an independent function. In fact, it turns out to be numerically advantageous to define a new function $L(z)$ such that $\lambda(z) = z^3 L(z)$ and solve for $L(z)$. In order to make progress, since we are interested (at least initially) in simply demonstrating that our techniques may be used to find solutions as opposed to scanning the whole range of parameter space, we shall set the aether parameters $c_3 = c_4 = 0$. Furthermore, we shall make use of the metric redefinitions described in (1.4.1) to make the metric horizon coincide with the spin-0 horizon. We see that this corresponds to the choice

$$c_2 = -\frac{c_1^3}{2 - 4c_1 + 3c_1^2}\,, \tag{4.4.6}$$

and hence out of the four dimensional aether parameter space, we focus only on the parameter c_1.

Since this is a static, spherically symmetric problem, the Harmonic Einstein equations are a coupled system of nonlinear ordinary differential equations in z for the metric and aether components. To solve them we shall use the Newton method and proceed by discretising the metric, aether and constraint functions on our z interval. In detail, we shall use a Chebyshev grid to perform the discretisation and spectral methods to represent the first and second derivatives of these functions on the grid. The calculations in the static case were done using Mathematica and thus we had to work at low resolution. In the stationary case described in the next section, we work at higher resolution by using C++ to calculate the equations explicitly and also to implement the Newton method.

We partition the interval $0 \leq z \leq z_{max}$, using a Chebyshev grid with $N = 12$ points

$$z_i = \left\{ \frac{z_{max}}{2} \left(1 + \cos\left(i \frac{\pi}{N-1} \right) \right) \right\} \quad \text{for } \; i = \{0, \ldots, (N-1)\} \,, \tag{4.4.7}$$

in terms of which the metric and aether fields are discretised as $\mathcal{F}_i = \mathcal{F}(z_{(N-1)-i})$ with $\mathcal{F}(z_i) = \{T(z_i), V(z_i), \ldots, L(z_i)\}$. From this discrete lattice, we may calculate a matrix $\mathcal{D}$, that approximates the continuum derivative operator that acts in the z direction. This matrix is defined by

$$\mathbf{V}' = \frac{1}{z_{max}} \mathcal{D}.\mathbf{V} \,, \tag{4.4.8}$$

with

$$\mathbf{V}' = \begin{pmatrix} T'_0 & V'_0 & \ldots & L'_0 \\ T'_1 & V'_1 & \ldots & L'_1 \\ \vdots & \vdots & \ddots & \vdots \\ T'_{N-1} & V'_{N-1} & \ldots & L'_{N-1} \end{pmatrix} , \qquad \mathbf{V} = \begin{pmatrix} T_0 & V_0 & \ldots & L_0 \\ T_1 & V_1 & \ldots & L_1 \\ \vdots & \vdots & \ddots & \vdots \\ T_{N-1} & V_{N-1} & \ldots & L_{N-1} \end{pmatrix} ,$$

and it can be shown (see for instance [227]) that the components of the $N \times N$ matrix $\mathcal{D}$ are constructed as

$$\begin{aligned} \mathcal{D}_{00} &= -\frac{2(N-1)^2+1}{3} \,, & \mathcal{D}_{N-1,N-1} &= \frac{2(N-1)^2+1}{3} \,, \\ \mathcal{D}_{jj} &= -\frac{(z_j - \frac{1}{2})}{2(1-z_j)z_j} & &\text{for } \; i,j = \{1, \ldots, (N-2)\} \,, \\ \mathcal{D}_{ij} &= \frac{c_i}{c_j} \frac{(-1)^{i+j}}{(z_i - z_j)} & &\text{for } \; i \neq j \,, \end{aligned} \tag{4.4.9}$$

where

$$c_i = \begin{cases} 2 & \text{if } i = 0 \text{ or } i = N-1 \\ 1 & \text{otherwise} \,. \end{cases}$$

As an example, in our case of $N = 12$, the matrix looks like,

$$\frac{\mathcal{D}}{z_{max}} = \begin{pmatrix} -74. & 90. & -23. & 11. & -6.2 & 4.2 & -3.2 & 2.6 & -2.2 & 2. & -1.9 & 0.91 \\ -22. & 11. & 15. & -6. & 3.3 & -2.2 & 1.7 & -1.3 & 1.1 & -1. & 0.95 & -0.46 \\ 5.7 & -15. & 2.6 & 9.8 & -4.3 & 2.6 & -1.8 & 1.4 & -1.2 & 1.1 & -1. & 0.49 \\ -2.6 & 6. & -9.8 & 1. & 7.6 & -3.5 & 2.3 & -1.7 & 1.4 & -1.2 & 1.1 & -0.55 \\ 1.6 & -3.3 & 4.3 & -7.6 & 0.46 & 6.7 & -3.3 & 2.2 & -1.7 & 1.4 & -1.3 & 0.64 \\ -1.1 & 2.2 & -2.6 & 3.5 & -6.7 & 0.13 & 6.4 & -3.3 & 2.3 & -1.8 & 1.7 & -0.8 \\ 0.8 & -1.7 & 1.8 & -2.3 & 3.3 & -6.4 & -0.13 & 6.7 & -3.5 & 2.6 & -2.2 & 1.1 \\ -0.64 & 1.3 & -1.4 & 1.7 & -2.2 & 3.3 & -6.7 & -0.46 & 7.6 & -4.3 & 3.3 & -1.6 \\ 0.55 & -1.1 & 1.2 & -1.4 & 1.7 & -2.3 & 3.5 & -7.6 & -1. & 9.8 & -6. & 2.6 \\ -0.49 & 1. & -1.1 & 1.2 & -1.4 & 1.8 & -2.6 & 4.3 & -9.8 & -2.6 & 15. & -5.7 \\ 0.46 & -0.95 & 1. & -1.1 & 1.3 & -1.7 & 2.2 & -3.3 & 6. & -15. & -11. & 22. \\ -0.91 & 1.9 & -2. & 2.2 & -2.6 & 3.2 & -4.2 & 6.2 & -11. & 23. & -90. & 74. \end{pmatrix}$$

(We have displayed the matrix $\mathcal{D}$ for completeness, showing its elements to only two significant figures in the interest of compactness. In our actual calculations we worked to machine precision in Mathematica). The second derivative matrix is obtained by simply acting again on $\mathbf{V}'$ with $\frac{\mathcal{D}}{z_{max}}$, and is therefore given by the matrix $\frac{\mathcal{D}^2}{z_{max}^2}$. Using these matrices we may construct a vector representing the Harmonic Einstein equations E_A at each point along our one-dimensional grid. The effect of the spectral representation has been to transform the set of differential equations into a system of nonlinear algebraic equations that must be solved to determine $\{T_i, V_i, \ldots, L_i\}$. To do this we use the Newton method and proceed by expanding the Harmonic Einstein equations about some initial guess. We write the true solution to the equations as a vector v_A, (which should be thought of as obtained from flattening the matrix $\mathbf{V}$). This is then written in terms of an initial guess $v_A^{(0)}$ as $v_A = v_A^{(0)} + \delta v_A$ and we expand the Harmonic Einstein equations as

$$E_A = E_A^{(0)} + \mathcal{O}_{AB}\delta v_B + O(\delta v^2) = 0\,, \tag{4.4.10}$$

where $E_A^{(0)}$ represent the Harmonic Einstein equations evaluated on the initial guess $v_A^{(0)}$. The matrix $\mathcal{O}_{AB} = \frac{\partial E_A}{\partial v_B}|_{v^{(0)}}$ is the *linearisation* of the Harmonic Einstein equations, given by the derivative of the equation vector with respect to the variables $\{T_i, V_i, \ldots, L_i\}$. We now proceed by solving the problem $\mathcal{O}_{AB}\delta v_B = -E_A^{(0)}$ for δv_B.

Using this solution one may then iteratively update the guess vector $v_A^{(0)}$, ultimately obtaining a solution to the full nonlinear problem $E_A = 0$. We must now turn to a discussion of our choice for this initial guess and moreover how to implement the boundary conditions for the original differential equation system in this discretised framework.

We choose the background (reference) metric to be Schwarzchild with horizon at $z = 1$

$$
\begin{aligned}
\bar{T}(z) &= 1 - z\,, \\
\bar{V}(z) &= 1\,, \\
\bar{A}(z) &= 0\,, \\
\bar{S}(z) &= 1\,.
\end{aligned}
\tag{4.4.11}
$$

Notice that the horizon of the reference metric is at $z = 1$ and this is ultimately the reason we chose our grid to cover the interval $[0, z_{max}]$. (Although in this ingoing formalism, the position of the reference metric horizon does *not* coincide with the horizon of solutions, they should be close to one another and by choosing the reference horizon to be within our grid, we can hope that this will also be true for the solutions we seek).

As an initial data, we take throughout the domain

$$
\begin{aligned}
T^{init}(z) &= \bar{T}(z)\,, \\
V^{init}(z) &= \bar{V}(z)\,, \\
A^{init}(z) &= \bar{A}(z)\,, \\
S^{init}(z) &= \bar{S}(z)\,, \\
P^{init}(z) &= \frac{-1 + (-1 + z)Q^{init}(z)^2}{2Q^{init}(z)}\,, \\
Q^{init}(z) &= 1 - 0.6z\,, \\
L^{init}(z) &= -0.8z\,,
\end{aligned}
\tag{4.4.12}
$$

where in summary we have chosen the initial guess for the metric to equal the reference metric. For the aether we chose a guess consistent with it being asymptotically coincident with the timelike Killing vector and smooth at the metric horizon. Having chosen this behaviour for $Q^{init}(z)$, the function $P^{init}(z)$ is then fixed by requiring that the aether constraint $(u^2 + 1) = 0$ is satisfied. The Lagrange multiplier is not independent (see (1.4.69)) so in principle one can calculate a suitable initial guess (as well as its asymptotic behaviour) from what we have already chosen. We simply engineered that it vanish sufficiently quickly at infinity.

All that remains is to impose appropriate boundary data. We impose asymptotic flatness at $z = 0$ as well as the requirement that the aether field coincide with the static Killing vector asymptotically. Moreover, it is important to ensure the initial guess satisfies the boundary conditions and hence the asymptotic behaviour of the Lagrange multiplier is chosen also to match the above, so that we have

$$\mathcal{F}_0 \quad = \quad \mathcal{F}^{init}(z = 0)\,, \tag{4.4.13}$$

where $\mathcal{F}^{init}(z) = \{T^{init}(z), V^{init}(z), \ldots L^{init}(z)\}$ and $\mathcal{F}_0$ is as defined below equation (4.4.7). All these boundary variables are hence fixed to equal their initial values and need not be updated in the Newton method iterations. (They should hence be left out of the computation of the linearised Harmonic Einstein equations $\mathcal{O}_{AB}$).

As explained in the previous section where the ingoing methods were introduced, we will also need to impose a single additional boundary condition at the innermost point of the domain. This fixes the single modulus of these spherically symmetric solutions, namely the mass. We choose

$$T_{N-1} = T^{init}(z = z_{max})\,, \tag{4.4.14}$$

and hence T_{N-1} should also not be updated during the iterations. (Note that if one does not impose this extra condition to fix the mass modulus, what one finds is that the linearised operator in the Newton method $\mathcal{O}_{AB}$ has zero modes indicating that not enough data has been fixed. This can be seen even at the level of using the ingoing methods to setup the problem of finding the Schwarzchild solution in pure general relativity). We have now specified the problem completely and can proceed to solve the equation system (4.4.10) iteratively using Mathematica. We found that if one attempts to immediately solve the full problem as specified above, the iterative procedure generically fails to converge to a solution. It turns out to be extremely useful to first relax the aether field on a fixed gravitational background. That is to say, it is useful to first solve the problem

$$E^{ae}_{\alpha} = 0\,, \tag{4.4.15}$$

where E^{ae}_{α} schematically represents the aether and constraint equations on a fixed gravitational background. (We use the index α rather than A to stress the fact that this index is not running over all the variables but only the aether and constraint variables). This 'preparatory' problem is then solved as before using the

Newton method (updating the aether guess on the fixed gravitational background corresponding to the initial guess (4.4.12)). Having done this, we may then use the solution to this relaxation as initial data for the full problem which then quickly converges to a solution.

Numerical Results

We now turn to a discussion of the results of our calculations. We solved equation (4.4.10) iteratively by the Newton method, relaxing the aether first according to (4.4.15) and then proceeding with the full problem. From the resulting vector that solves the system, one can compute interpolating polynomials that approximate the functions $\{T(z), V(z), \ldots, L(z)\}$. These are displayed in Figure 4.1 and together constitute the metric and aether functions of a numerical static, spherically symmetric black hole in Einstein-Aether theory. The solution displayed corresponds to a black hole with $c_1 = 0.4$ and has a mass that is implicitly determined by our choice of boundary data at the innermost point T_{NN}. That is to say, changing the data there, will change the mass of the solution, thus moving along the one-parameter family of solutions.

The mass M_T of this black hole solution can be computed by the usual ADM prescription by examining the coefficient of the $\mathcal{O}(z)$ term in the $g_{\nu\nu}$ component of the metric [228]. We then have that

$$2GM_{ADM} = -T'(0)\,, \tag{4.4.16}$$

where G is the gravitational constant that appears in the Einstein-Aether action. For the solution of Figure 4.1, we may readily compute that $2GM_{ADM} = 1.03(3)$ and the metric horizon is at $z_h = 0.997(4)$, (defined by $T(z_h) = 0$).

To highlight some of the qualitative differences between black holes in Einstein-Aether and general relativity, it is instructive to consider a plot of the function $\sqrt{S(z)}(T(z) - 1)/2$. We display this in Figure 4.3 for the static aether black hole of Figure 4.1. For Schwarzchild solutions in pure general relativity, this quantity is a constant that is proportional to the mass of the black hole. In contrast, in Einstein-Aether theory we see that it varies as a function of z (and moreover one can show the deviation from general relativity is dependent on c_1). We also plot $\phi = \xi^\mu \xi_\mu$ for our static aether black hole in Figure 4.2 to verify that it vanishes on our solutions and hence that we have a true (as opposed to solitonic) solution.

We may now repeat the procedure outlined above, changing c_1 to investigate the structure of black holes in Einstein-Aether theory for different values of this

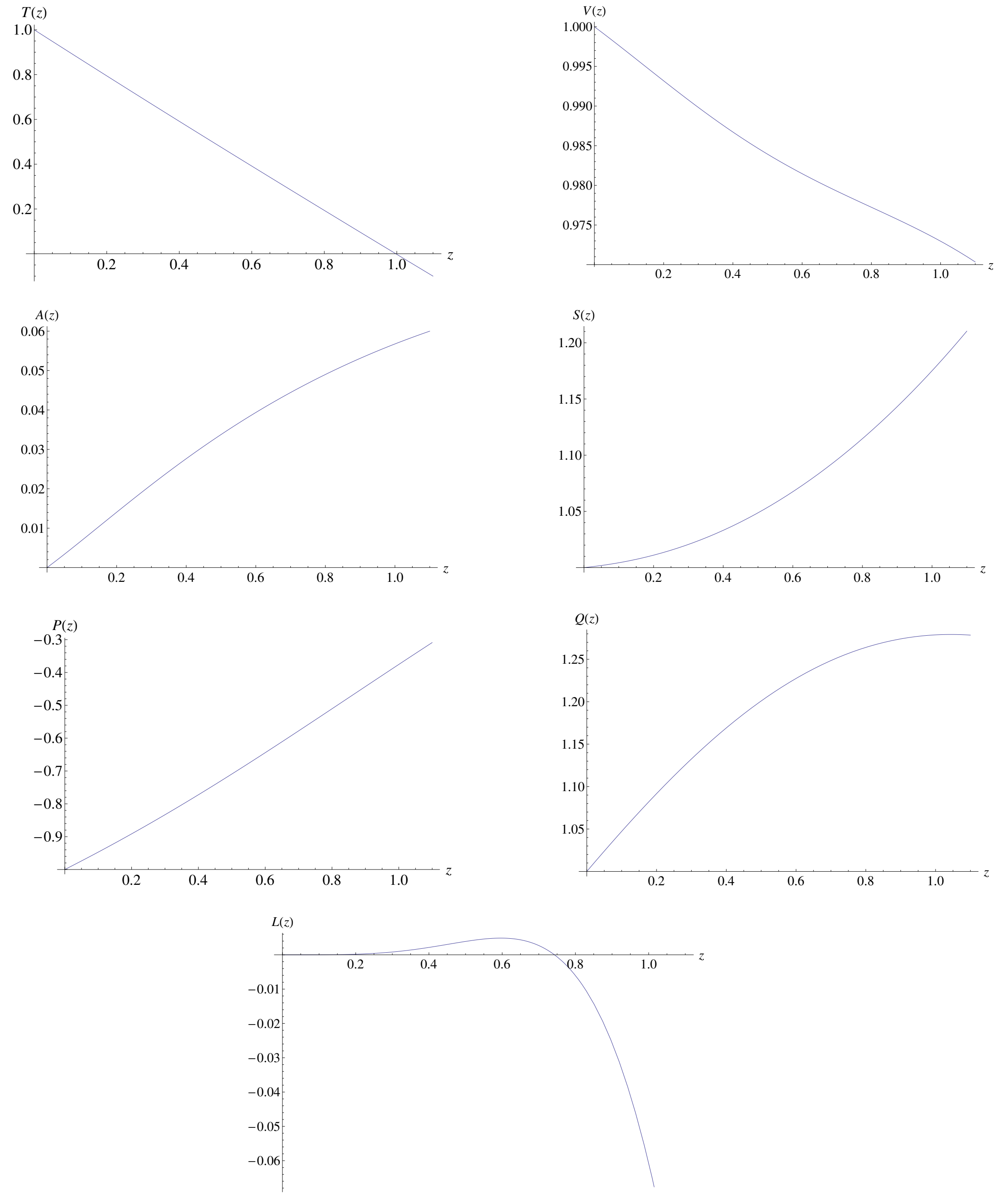

Figure 4.1.: Interpolating functions $\{T(z), V(z), \ldots, L(z)\}$ with $N = 12$ points, computed from the vector that solves (4.4.10). These constitute the metric, aether and constraint variables for a spherically symmetric, static Einstein-Aether black hole with aether parameters $\{c_1 = 0.4, c_2 = -0.0727, c_3 = 0, c_4 = 0\}$ and mass $2GM_{ADM} = 1.03(3)$.

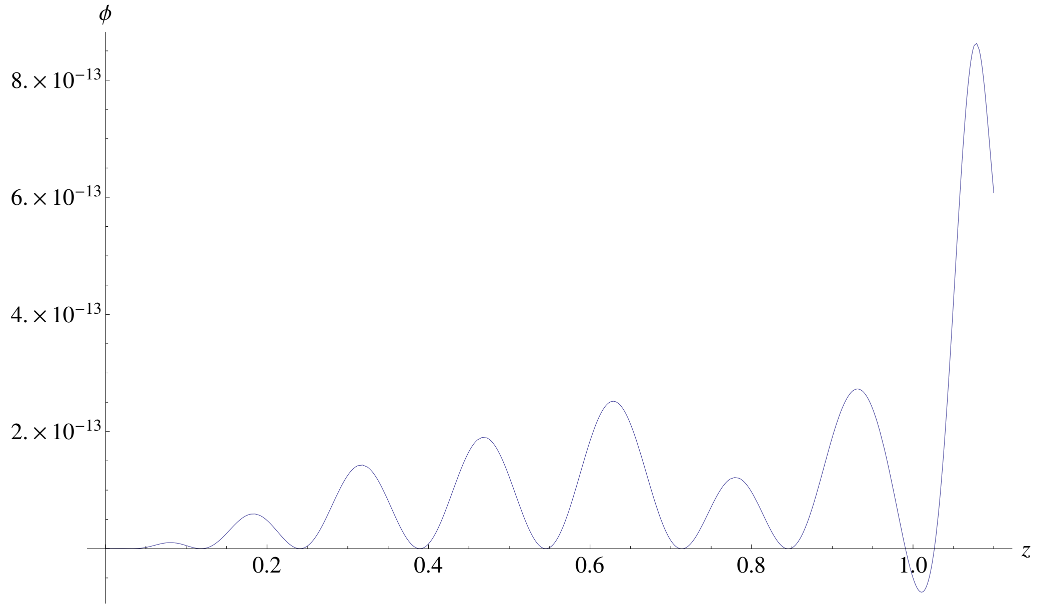

Figure 4.2.: Plot of $\phi = \xi^{\mu}\xi_{\mu}$ for the static Einstein aether black hole of Figure 4.1. We see that the function is zero throughout the grid, indicating that we have a true solution and not a soliton

parameter. One finds qualitatively similar results to what we have displayed in Figure 4.1, but the theory becomes 'further' from general relativity with increasing c_1 and solving the Newton method steps to find a solution becomes harder. It is helpful to use the results for lower values of c_1 as initial data when attempting to solve the problem for large values of c_1, ($c_1 > 0.5$). One cannot find solutions when $c_1 \geq 1$, a fact that that can be understood by observing that the theory becomes singular in this regime (at least when we restrict to $c_3 = c_4 = 0$, and with c_2 chosen such that the spin-0 and metric horizons coincide). This is most easily seen by studying the expressions for the wave speeds in section (1.4.2)). Due to the considerable complexity of the Einstein-Aether equations of motion and since the aforementioned calculations were performed in Mathematica, we were forced to work at rather low resolution ($N = 12$). It hence becomes rather difficult to proceed to very high values of c_1 (> 0.9), but this problem could be somewhat resolved by performing the calculations at higher resolution, using for example C++ code to implement the Newton Method.

We shall now demonstrate that the static solutions presented here are in fact the same as those in the literature [150, 152]. The authors of the latter works used a different spacetime metric and aether ansatz to what we have used and hence to establish equivalence we must first study the transformation between their quantities and our own. Up to a change in signature, the line element they considered is of the

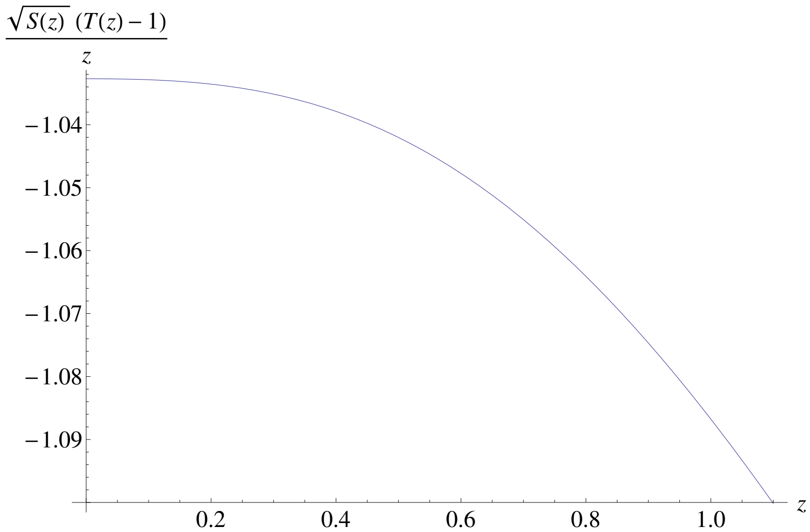

Figure 4.3.: Plot of $\sqrt{S(z)}(T(z)-1)/2$ as a function of z for the black hole of Figure 4.1. This function is a constant for Schwarzchild in general relativity proportional to the mass. We see in Einstein-Aether theory this is no longer the case.

form

$$\begin{aligned} ds^2 &= -M(\bar{r})d\bar{v}^2 + 2B(\bar{r})d\bar{v}d\bar{r} + \bar{r}^2 d\Omega^2_{(2)} \\ &= -\bar{M}(\bar{z})d\bar{v}^2 - \frac{2\bar{B}(\bar{z})}{\bar{z}^2}d\bar{v}d\bar{z} + \frac{1}{\bar{z}^2}d\Omega^2_{(2)}\,, \end{aligned} \tag{4.4.17}$$

and their aether ansatz is[5]

$$\begin{aligned} U &= -\frac{1+a(\bar{r})^2M(\bar{r})}{2a(\bar{r})}d\bar{v} + a(\bar{r})B(\bar{r})d\bar{r} \\ &= -\frac{1+\bar{a}(\bar{z})^2\bar{M}(\bar{z})}{2\bar{a}(\bar{z})}d\bar{v} - \frac{\bar{a}(\bar{z})\bar{B}(\bar{z})}{\bar{z}^2}d\bar{z}\,, \end{aligned} \tag{4.4.18}$$

where we have introduced the coordinate $\bar{z} = 1/\bar{r}$. To make contact with (4.4.4) and (4.4.5), we see that we should define

$$\bar{z} = \frac{z}{\sqrt{S(z)}}\,, \qquad \bar{v} = v + F(z)\,, \tag{4.4.19}$$

[5]Note that in [150], the aether field was defined with its vector index upstairs and so one must be cautious to remember to lower that index when comparing with (4.4.18)

for some function $F(z)$, and equality of the two forms then requires that

$$\begin{aligned}
T(z) &= \bar{M}\left(\frac{z}{\sqrt{S(z)}}\right), && (4.4.20)\\
V(z) &= \bar{M}\left(\frac{z}{\sqrt{S(z)}}\right)F'(z)z^2 + \bar{B}\left(\frac{z}{\sqrt{S(z)}}\right)\sqrt{S(z)}\left(1-\frac{zS'(z)}{2S(z)}\right), && (4.4.21)\\
A(z) &= z^2F'(z)\left(-\bar{M}\left(\frac{z}{\sqrt{S(z)}}\right)F'(z)z^2 - 2\bar{B}\left(\frac{z}{\sqrt{S(z)}}\right)\sqrt{S(z)}\right.\\
&\quad \left.\times\left(1-\frac{zS'(z)}{2S(z)}\right)\right), && (4.4.22)\\
P(z) &= -\frac{1}{2\bar{a}\left(\frac{z}{\sqrt{S(z)}}\right)^2}\left(1+\bar{a}\left(\frac{z}{\sqrt{S(z)}}\right)^2\bar{M}\left(\frac{z}{\sqrt{S(z)}}\right)\right), && (4.4.23)\\
Q(z) &= \frac{1}{2\bar{a}\left(\frac{z}{\sqrt{S(z)}}\right)^2}\left(1+\bar{a}\left(\frac{z}{\sqrt{S(z)}}\right)^2\bar{M}\left(\frac{z}{\sqrt{S(z)}}\right)F'(z)z^2\right)\\
&+ \bar{a}\left(\frac{z}{\sqrt{S(z)}}\right)\bar{B}\left(\frac{z}{\sqrt{S(z)}}\right)\sqrt{S(z)}\left(1-\frac{zS'(z)}{2S(z)}\right). && (4.4.24)
\end{aligned}$$

Having established these transformations, we repeated the shooting calculations of [150], to obtain their static aether black holes[6]. In detail, for the aether parameters $\{c_1 = 0.4,\, c_2 = -0.0727,\, c_3 = c_4 = 0\}$, we integrated inwards from $\bar{z} = 1/100$ to $\bar{z} = 1000$ to obtain a solution. (Note once again that the metric horizon has been chosen to coincide with the spin-0 horizon). The asymptotic expansions of the field equations contain two pieces of data

$$\begin{aligned}
\bar{M}(\bar{z}) &= 1 + M_1\,\bar{z} + \frac{c_1\,M_1^3}{48}\bar{z}^3 + \dots\,,\\
\bar{B}(\bar{z}) &= 1 + \frac{c_1\,M_1^2}{16}\bar{z}^2 - \frac{c_1 M_1^3}{12}\bar{z}^3 + \dots\,,\\
\bar{a}(\bar{z}) &= 1 - \frac{M_1}{2}\bar{z} + a_2\,\bar{z}^2 - \frac{M_1\,(96\,a_2 + (-6+c_1)M_1^2)}{96}\bar{z}^3 + \dots\,, && (4.4.25)
\end{aligned}$$

namely M_1 and a_2. We fixed $M_1 = -1.00327(0)$[7], and tuned a_2 so as to achieve regularity at the spin-0 horizon. In more detail, regularity at the spin-zero horizon is implemented by observing that $\bar{B}(\bar{z})$ satisfies $\bar{B}'(\bar{z}) = \frac{b_0}{\bar{M}(\bar{z})} + \dots$ and thus at the horizon, where $\bar{M}(\bar{z}) \to 0$, we require as a 'regularity condition' that the function $b_0 = 0$ [150]. (The ellipses denote terms that are finite in this limit). Given M_1,

[6]There is a slight subtlety here, namely that unlike in the shooting of [150], we did not scale our $\bar{r}$ coordinate such that the horizon lies precisely at $\bar{r} = 1$. One needs to make this additional transformation if a comparison of observables (such as with Table I of [150]) is desired.

[7]We used our spectral solutions to read off M_1 to high precision. This was then held fixed at this value, with the remaining piece of data a_2 being used as our shooting parameter.

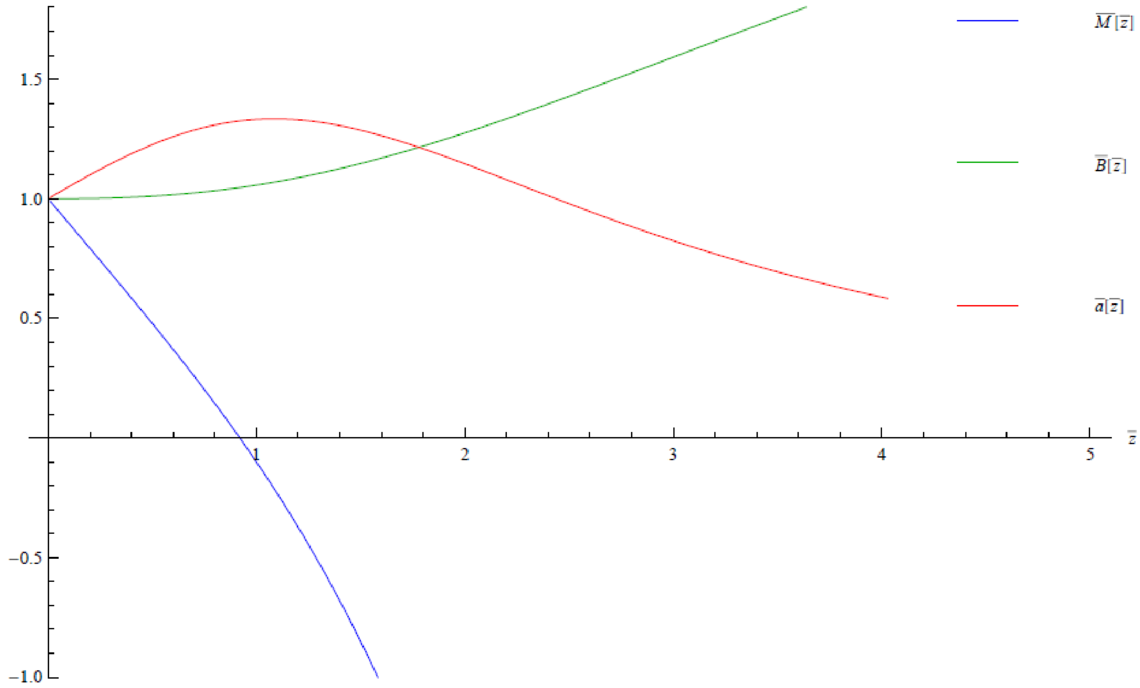

Figure 4.4.: Metric functions of a static Einstein-Aether black hole constructed by shooting methods with $\{c_1 = 0.4,\ c_2 = -0.0727,\ c_3 = c_4 = 0\}$. These are identical to the solutions of [150, 152] except we do not use their radial scaling that shifts the position of the horizon to be at $\bar{r} = 1$.

our shooting algorithm tunes a_2 so as to satisfy this condition. (One will find of course that until a_2 is tuned to a critical value, the integration will not continue on inside the horizon). These shooting solutions for $\{\bar{M}(\bar{z}), \bar{B}(\bar{z}), \bar{a}(\bar{z})\}$ are displayed in Figure 4.4. Given these shooting solutions, we then demonstrated that application of (4.4.20) reproduced our metric functions found by spectral methods in the coordinates defined by (4.4.4), (4.4.5), hence verifying the equivalence of the two solutions. In detail, we assumed that the expression for $Q(z)$ in (4.4.20) held and then used this to compute $F'(z)$. We were then able to verify that all the remaining relations in (4.4.20) held with this $F'(z)$. We show this in Figure 4.5 where we plot $F'(z)$ together with the difference of each of the equations in (4.4.20) (with the exception of $Q(z)$ which is used to compute $F'(z)$). Moreover, taking into account a radial scaling to shift the horizon to unit radius, we can reproduce exactly the results of Table I of [152]

The results of this section, constitute a rediscovery of the static Einstein-Aether black holes found in [150, 152], by way of completely different techniques. Our methods are in many ways considerably simpler to use in practice than the shooting methods considered there (in that we don't have to tune anything to find solutions).

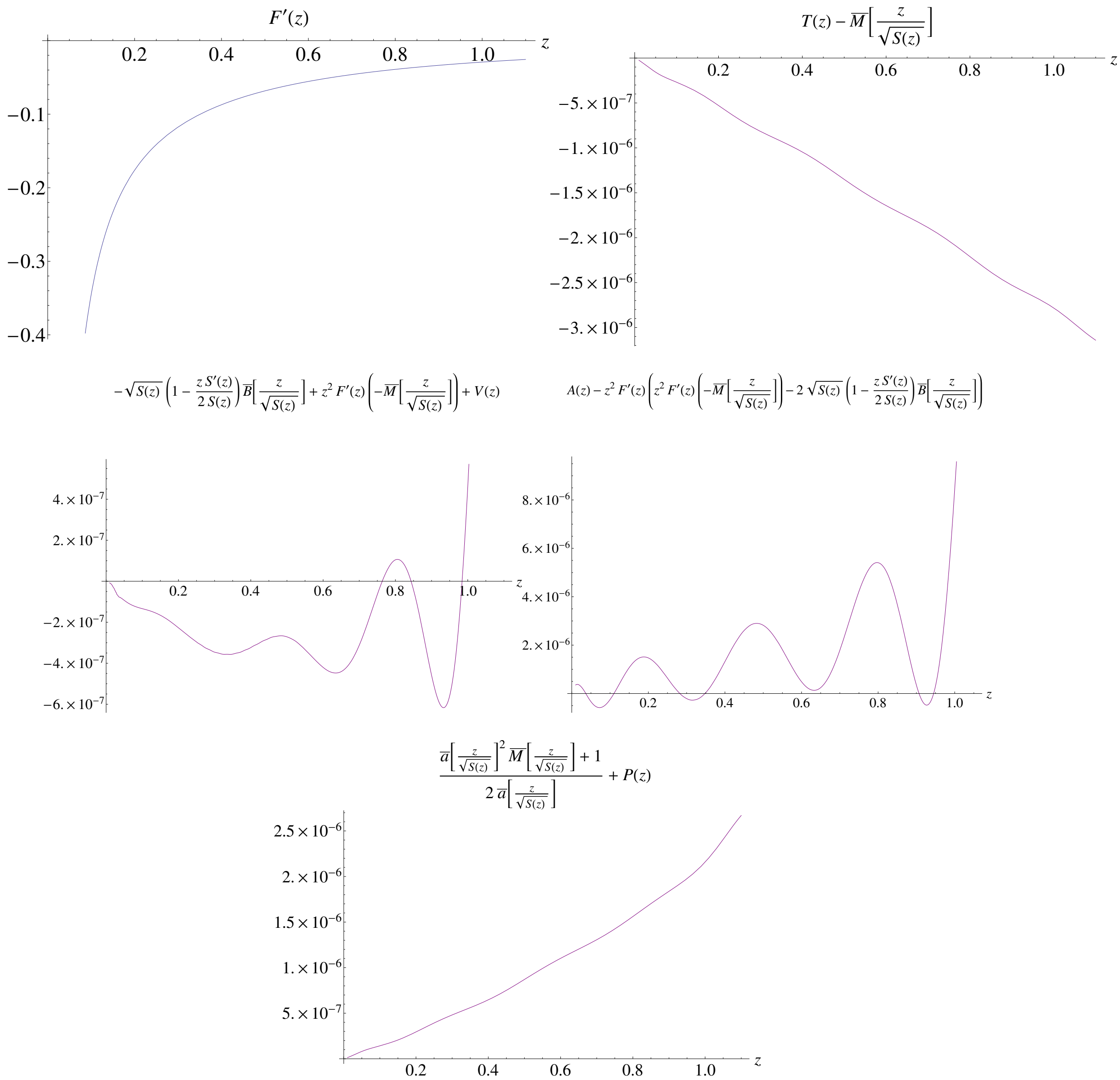

Figure 4.5.: Demonstration of the equivalence of our static Einstein-Aether black holes constructed by spectral methods and those found by shooting methods. We plot the function $F'(z)$ introduced in the text as well as the difference of each of the relations in (4.4.20). In all cases, we see that the difference between the two solutions is consistent with being zero.

Moreover, regularity at the spin-zero horizon is encoded from the start in our approach by use of the ingoing techniques detailed in the previous section and we do not need to impose this a-posteriori. The real power of these new techniques however is that they readily extend (with little more than technical differences) to the stationary case.

4.5. Stationary Black Hole Solutions

We may now proceed to apply the techniques of the previous section to the more complex problem of constructing stationary, rotating black holes in Einstein-Aether theory. We begin with the metric

$$\begin{aligned} ds^2 &= -T(z,\theta)\,dv^2 - 2W(z,\theta)\sin^2\theta\,dvd\phi - \frac{2V(z,\theta)}{z^2}dvdz \\ &+ \frac{2U(z,\theta)\sin\theta}{z}dvd\theta + \frac{S(z,\theta)\sin^2\theta}{z^2}d\phi^2 + \frac{2P(z,\theta)\sin^2\theta}{z^2}d\phi dz \\ &+ \frac{2Q(z,\theta)\sin\theta}{z^2}d\phi d\theta + \frac{A(z,\theta)}{z^4}dz^2 + \frac{B(z,\theta)}{z^2}d\theta^2 \\ &+ \frac{2F(z,\theta)\sin\theta}{z^2}dzd\theta\,, \end{aligned} \tag{4.5.26}$$

together with the aether ansatz,

$$U = H(z,\theta)dv + J(z,\theta)\sin^2\theta d\phi - \frac{X(z,\theta)}{z^2}dz + \frac{Y(z,\theta)\sin\theta}{z}d\theta\,, \tag{4.5.27}$$

where once again, v is an ingoing time coordinate and z is an *inverse* radial coordinate. By the assumption of stationarity, $\frac{\partial}{\partial v}$ and $\frac{\partial}{\partial \phi}$ are Killing vectors and hence the functions that appear in both (4.5.26) and (4.5.27) depend non-trivially on only the (z,θ) coordinates. We still however have the full number of ten metric components and four aether components to determine together with the Lagrange multiplier constraint $\lambda(z,\theta) = z^3 L(z,\theta)$. The equations of motion that follow from this ansatz constitute a complicated PDE problem in two variables and the shooting techniques that have been used thus far in the literature to construct static solutions are not applicable outside the case of ODEs. Fortunately, the numerical methods discussed in the previous section naturally extend to multivariate problems.

To proceed, we begin as before, this time discretising both the z and θ directions to form a tensor product grid structure with $N_z \times N_\theta$ points [227]. We shall describe two distinct discretisation procedures and present the results that follow from each in turn. As usual, with our ingoing methods, it is important to choose coordinates such that the radial patch extends into the interior of the metric horizon. We shall consider the radial range $0 \leq z \leq z_{max} = 0.6$, with $z = 0$ corresponding to infinity (and by a suitable choice of background metric, we can ensure that the aforementioned constraint is satisfied and the metric horizon lies inside our grid). By symmetry, we can without loss of generality consider the polar angle in the range $0 \leq \theta \leq \theta_{max} = \pi/2$. The first discretisation scheme we consider is analogous to that used in the static case and uses Chebyshev grids independently in both the z and θ directions and spectral representations of derivative operators. In detail we consider a $2D$ tensor product grid with $N_z = N_\theta = 20$

$$\begin{aligned} z_i &= \left\{ \frac{z_{max}}{2} \left(1 + \cos\left(i \frac{\pi}{N_z - 1} \right) \right) \right\} \qquad \text{for } i = \{0, \ldots, (N_z - 1)\} \ , \\ \theta_j &= \left\{ \frac{\theta_{max}}{2} \left(1 + \cos\left(j \frac{\pi}{N_\theta - 1} \right) \right) \right\} \qquad \text{for } j = \{0, \ldots, (N_\theta - 1)\} \ , \end{aligned} \tag{4.5.28}$$

in terms of which the metric, aether and constraint functions are discretised as $\mathcal{F}_{ij} = \mathcal{F}(z_{(N_z-1)-i}, \theta_{(N_\theta-1)-j})$, with $\mathcal{F}(z_i, \theta_j) = \{T(z_i, \theta_j), W(z_i, \theta_j), \ldots, L(z_i, \theta_j)\}$. One may then construct the $1D$ Chebyshev differentiation matrices $\mathcal{D}_z$ and $\mathcal{D}_\theta$ (of sizes $N_z \times N_z$ and $N_\theta \times N_\theta$ respectively), as before using the definition (4.4.9). The full $2D$ derivative matrices may then be computed from these matrices as tensor products. That is to say, if we represent our functions across the grid as an array of the form $\mathcal{F}^c_{ij}$, (where the new index $c = \{0, \ldots, 14\}$ labels which metric/aether/constraint component we are considering), then we have that

$$\begin{aligned} \frac{\partial}{\partial z} \mathcal{F}^c_I &= (\mathbb{1} \otimes \mathcal{D}_z)_{IJ} \mathcal{F}^c_J \, , \\ \frac{\partial}{\partial \theta} \mathcal{F}^c_I &= (\mathcal{D}_\theta \otimes \mathbb{1})_{IJ} \mathcal{F}^c_J \, , \\ \frac{\partial^2}{\partial z^2} \mathcal{F}^c_I &= (\mathbb{1} \otimes \mathcal{D}^2_z)_{IJ} \mathcal{F}^c_J \, , \\ \frac{\partial^2}{\partial \theta^2} \mathcal{F}^c_I &= (\mathcal{D}^2_\theta \otimes \mathbb{1})_{IJ} \mathcal{F}^c_J \, , \\ \frac{\partial^2}{\partial z \partial \theta} \mathcal{F}^c_I &= (\mathcal{D}_z \otimes \mathcal{D}_\theta)_{IJ} \mathcal{F}^c_J \, . \end{aligned} \tag{4.5.29}$$

The $\mathcal{F}^c_I$ are the components of the vector that are obtained from flattening the matrix $\mathcal{F}^c_{ij}$[8]. From (4.5.29), one may then assemble the equations of motion across the $2D$ grid, which are then turned into a vector which we write schematically as E_A. We may then proceed to solve the system by the Newton method, exactly as before in the

[8]The ordering of the tensor products in (4.5.29) depends on the ordering of the flattening operation, that is to say the ordering of the multiplication in the tensor product may be reversed from what is written here depending on whether flattening is done row by row or column by column.

static case: One begins by expanding the equations as $E_A = E_A^{(0)} + \mathcal{O}_{AB}\delta v_B + \mathcal{O}(v^2)$, (where in analogy with the static case, v_A is the flattened vector constructed from $\mathcal{F}_J^c$ viewed as an array in (c, J) and using the same notation as we used there, $v_A^{(0)}$ is some initial guess and $E_A^{(0)}$ the equations evaluated on this initial guess). We then solve $\mathcal{O}_{AB}\delta v_B = -E_A^{(0)}$ [9] iteratively updating v_A, eventually converging to a solution of the full non-linear problem $E_A = 0$. As before in the static case, in our experience it is essential to first relax the aether field and constraint equations on a fixed gravitational background before tackling the full problem.

The second discretisation scheme we consider is finite differencing (6th order). The only difference compared with the spectral methods outlined above is in the splitting of the (z, θ) intervals and the construction of the derivative matrices $\mathcal{D}_z$ and $\mathcal{D}_\theta$. Instead of (4.5.28), we use a tensor product grid defined by

$$\begin{aligned} Z_i &= z_{min} + i\left(\frac{z_{max} - z_{min}}{N_z - 1}\right), \\ \Theta_i &= \theta_{min} + i\left(\frac{\theta_{max} - \theta_{min}}{N_z - 1}\right) \qquad \text{for } i = 0, \ldots, N_z - 1, \end{aligned} \tag{4.5.30}$$

(where we recall that in our case, $z_{min} = \theta_{min} = 0$, $z_{max} = 0.6$, and $\theta_{max} = \pi/2$). Notice that unlike the Chebyshev grids where points cluster at the end points of the intervals, finite difference grids consist of evenly spaced points. The derivative matrices $\mathcal{D}_z, \mathcal{D}_\theta$ are then constructed by way of a polynomial interpolation of order m ($m = 6$ for 6th order differencing). (Note that the precise details of the stencils we use are described in [229] and in the Mathematica tutorial "Numerical Solution to Partial Differential Equations". Schematically, these methods work by constructing a stencil with general coefficients and using Padé approximations to compute these coefficients so as to make the stencil accurate for as high degree polynomials as possible. Moreover these methods automatically minimise errors at any boundaries in the problem).

The mechanics of solving the system then proceeds exactly as in the spectral case, constructing the $2D$ derivative matrices as tensor products, assembling the equations of motion from these and solving the system by the Newton method. Whilst spectral methods have the advantage of being able to achieve high accuracy even at relatively low resolution (any loss of accuracy that can arise there due to the Runge phenomena can in practice be minimised by using a Cheyshev as opposed to an even grid), the difficulty with them is that they only work well when the

[9] Instead of symbolically differentiating the equations with respect to the discretised variables as in the static case to calculate $\mathcal{O}_{AB}$, we found it much more efficient here to compute it as a central difference $\mathcal{O}_{AB} = \frac{E_A(\mathbf{v}+\delta\mathbf{v}) - E_A(\mathbf{v}+\delta\mathbf{v})}{2\Delta}$ where the vector $\delta\mathbf{v}_A = \Delta\delta_{AB}$.

functions to be solved for are very smooth (formally $\mathbb{C}^\infty$). In the case of black holes in Einstein-Aether theory, one can show that the metric functions are not $\mathbb{C}^\infty$ at $z = 0$ due to log terms in the expansion (specifically terms of the form $z^2 \log z$ and higher order contributions). Indeed we find as a consequence of this that for large deviations from general relativity $c_1 > 0.6$, spectral methods seem to struggle to converge to solutions. It therefore appears that finite difference techniques are more robust for our purposes.

Having specified our discretisation schemes, all that remains to be done to solve the system is to choose a suitable background metric and initial guess together with appropriate boundary conditions for the PDE problem in question. We must also fix two pieces of boundary data at $z = z_{max}$ to fix the angular velocity and mass moduli associated to stationary solutions.

In the regime where c_1 is small, the theory is parametrically close to general relativity and thus any stationary black holes should resemble the Kerr solution. We therefore choose Kerr for the reference metric, that is to say, we choose a reference line element of the form (4.5.26) with

$$\begin{aligned}
\bar{T}(z,\theta) &= 1 - \frac{2M^2 z}{\Sigma(z,\theta)}\,, \\
\bar{V}(z,\theta) &= M\,, \\
\bar{W}(z,\theta) &= \frac{2aM^2 z}{\Sigma(z,\theta)}\,, \\
\bar{S}(z,\theta) &= \frac{1}{\Sigma(z,\theta)}\left((M^2 + a^2 z^2)^2 - z^2 \Delta(z) a^2 \sin^2\theta\right)\,, \\
\bar{P}(z,\theta) &= Ma\,, \\
\bar{B}(z,\theta) &= \Sigma(z,\theta)\,, \\
\bar{U}(z,\theta) &= 0\,, \\
\bar{Q}(z,\theta) &= 0\,, \\
\bar{A}(z,\theta) &= 0\,, \\
\bar{F}(z,\theta) &= 0\,,
\end{aligned} \tag{4.5.31}$$

where $\Sigma(z,\theta) = M^2 + a^2 z^2 \cos^2\theta$ and $\Delta(z) = M^2 - 2M^2 z + a^2 z^2$. Moreover as an initial guess, we begin with metric functions equal to those of the Kerr metric $\{T^{init}(z,\theta) = \bar{T}(z,\theta), \ldots, F^{init}(z,\theta) = \bar{F}(z,\theta)\}$. For the aether functions

$X^{init}(z,\theta), Y^{init}(z,\theta)$ and constraint $L^{init}(z,\theta)$ we choose

$$\begin{aligned} X^{init}(z,\theta) &= M(1+0.4z)\,, \\ Y^{init}(z,\theta) &= 0\,, \\ L^{init}(z,\theta) &= -0.01z^2\,, \end{aligned} \tag{4.5.32}$$

whilst for the remaining aether components, we take $J^{init}(z,\theta) = -aH^{init}(z,\theta)$, and solve for $H^{init}(z,\theta)$ by demanding that the aether constraint $u^2+1=0$ is satisfied by the initial guess. (The precise form of the function $H^{init}(z,\theta)$ is rather unsightly and hence we do not include it here).

As with the static case, we impose Dirichlet boundary conditions at $z=0$ (infinity), and demand that all functions equal their initial values there

$$\mathcal{F}_{0j} = \mathcal{F}^{init}(z=0, \theta=\theta_{(N_\theta-1)-j}) \qquad \forall j\,, \tag{4.5.33}$$

(where $\mathcal{F}_{ij}$ is as defined below equation (4.5.29)). This condition is of course equivalent to imposing asymptotic flatness for the metric components. These components should not be updated during the Newton method iterations. The new feature in the stationary case is that we must also impose appropriate boundary conditions at the axis of rotational symmetry. By the regularity analysis of section 3.4.3, we know that all functions in the problem should have expansions with no terms linear in θ at this axis, and thus we impose Neumann boundary data for all the metric, aether and constraint components at $\theta=0$

$$\frac{\partial}{\partial\theta}\mathcal{F}_{i0} = 0 \qquad \forall i\,. \tag{4.5.34}$$

On the other hand, we must ensure that all functions are even about the 'mirror plane' corresponding to the $\theta=\pi/2$ boundary (which is of course an artificial construction that we introduced as the region $\pi/2 < \theta \leq \pi$ carries no new information). This is achieved by imposing Dirichlet conditions for all functions that appear in the metric/aether ansatze as odd in $d\theta$

$$\mathcal{G}_{i\,(N_c-1)} = \mathcal{G}^{init}(z=z_{(N_z-1)-i}, \theta=\pi/2) = 0 \qquad \forall i\,, \tag{4.5.35}$$

where $\mathcal{G}_{ij} = \{F_{ij}, U_{ij}, Q_{ij}, Y_{ij}\}$, and imposing Neumann conditions for the remaining variables

$$\frac{\partial}{\partial\theta}\mathcal{H}_{i\,(N_c-1)} = 0 \qquad \forall i\,, \tag{4.5.36}$$

where $\mathcal{H}_{ij} = \{T_{ij}, V_{ij}, W_{ij}, S_{ij}, P_{ij}, B_{ij}, A_{ij}, X_{ij}, L_{ij}, J_{ij}, H_{ij}\}$.

There is an additional subtlety at the axis in these ingoing methods. Whilst regularity at the horizon is automatic in our chart, at the axis we would expect to have to impose the additional regularity condition of section 3.4.3, namely that $B(z, \theta = 0) = S(z, \theta = 0)$. Recall though that this condition should be thought of as a arising as a consequence of smoothness at the axis and since our initial guess for the metric (Kerr) is smooth and the Newton method updates preserve smoothness we expect that this condition is automatically satisfied and need not be imposed. Indeed we will explicitly check that this is so and that it is satisfied for the numerical solutions we find.

Finally, following the ingoing horizon prescription, we must fix the two moduli associated to our solution by imposing two additional conditions at the innermost points of our domain. We do this by imposing

$$\begin{aligned} T_{(N_z 1)(N_c-1)} &= T^{init}(z = z_{max}, \theta = \theta_{max}) \,, \\ W_{(N_z 1)(N_c-1)} &= W^{init}(z = z_{max}, \theta = \theta_{max}) \,, \end{aligned} \tag{4.5.37}$$

which fixes the mass and angular momentum moduli of the system. Note that one can in principle fix *any* two functions at $\{z_{max}, \theta_{max}\}$, but we choose $T(z, \theta)$, and $W(z, \theta)$ as they work well. As with the static case, if one does not impose these conditions to fix the moduli, the linearisation of the equations $\mathcal{O}_{AB}$ has zero modes and one will not find a solution. We may now turn to a discussion of the results we have found on implementing the numerical setup described in this section. We performed all calculations in C++, outputting data to Mathematica (and using this to display our interpolations). The Einstein-Aether equations were built systematically in a subroutine in C++ that calculates them at a given point in our domain. In detail we broke these equations down into their constituent zero, one and two derivative pieces involving the metric and aether. These pieces (schematically $\partial g, \partial\partial g, \partial u, \partial\partial u$ etc) were then computed symbolically in Mathematica on our ansatz and then outputted to C++ as arrays that the subroutine assembles into the full equations. By calling this subroutine throughout the grid (given initial data) one can then calculate the Einstein-Aether equations throughout the domain. (Note that in places where Dirichlet boundary conditions are imposed, such as at $z = 0$, the routine does not need to be called as those points are not updated in the Newton method iterations. Moreover, on boundaries which have Neumann conditions, instead of calling the Einstein-Aether equations we impose the Neumann boundary condition explicitly as an equation in the equation-vector E_A). Our code uses this routine to compute the linearisation $\mathcal{O}_{AB}$ of these equations and then uses the linear algebra package LAPACK to solve the problem $\mathcal{O}_{AB}\delta v_B = -E_A^{(0)}$ which we use to update our initial guess. This procedure is then iterated until a solution is found which is determined by requiring that the norm of the equation vector be below some threshold value, here $\sqrt{\sum_A E_A} < 10^{-12}$. As explained in the preceding sections, we first relax the aether and constraint variables on the Kerr background, before relaxing the full system. This appears to be essential to find solutions (at least with out initial data).

Numerical Results

With the aforementioned initial data and boundary conditions, the Harmonic Einstein equations may be solved iteratively by the Newton method relaxing the aether first on a fixed gravitational background before attacking the full problem. We display the results of finite differencing, which is ultimately the more robust of the two discretisation methods we have discussed; Whilst the spectral methods also work well for this value of $c_1(= 0.4)$, they fail at higher values and the metric functions are indistinguishable by eye from the finite differencing case so we shall not display them here. From the vector that solves the system, we compute interpolations that approximate the metric, aether and constraint variables respectively. The first five metric variables $\{T(z,\theta, V(z,\theta), W(z,\theta), S(z,\theta), P(z,\theta)\}$ are displayed in Figure 4.6, and the remainder, $\{B(z,\theta), U(z,\theta), Q(z,\theta), A(z,\theta), F(z,\theta)\}$ in Figure 4.7, whilst the aether and constraint $\{H(z,\theta), J(z,\theta), X(z,\theta), Y(z,\theta), L(z,\theta)\}$ are shown in Figure 4.8. These results constitute the first example of a stationary, rotating black hole in Einstein-Aether theory. The black hole in question was constructed on a $N_z \times N_\theta = 20 \times 20$ grid from initial data (as specified in (4.5.31)), using a reference metric with $\{M = 1,\ a = 0.3\}$. The aether parameters are $\{c_1 = 0.4,\ c_2 = -0.0727,\ c_3 = c_4 = 0\}$, where c_2 has been chosen as before so that the spin-0 horizon coincides with the metric horizon[10]. We also verify in Figure 4.9 that axis regularity holds (as discussed previously in this chapter) for this solution by plotting $\left(1 - \frac{S(z,\theta=0)}{B(z,\theta=0)}\right)$ and observing that this quantity is indeed zero as required.

One may repeat the calculations described above for increasing c_1 to construct

[10]Note that with these choices of aether parameters, solutions are labeled by c_1 and the background parameters $\{M, a\}$ (which we remind the reader are not the same as the mass and angular momentum of solutions). Having fixed c_1 and a, solutions of different M are related by a rescaling of the z coordinate and so one can choose any value of M and we choose $M = 1$. For a we choose the value $a = 0.3$ so that we can find solutions at large c_1 with relative ease. Finding solutions with both very large a and large c_1 is quite difficult and is left to future (higher resolution) work.

rotating black holes that are increasingly deformed from their general relativistic counterparts. As before in the static case, for $c_1 > 0.5$, it is essential to use the results of previous runs for lower c_1 as initial data for these calculations as our initial guess (4.5.31) will fail to converge directly. One finds that these solutions look qualitatively similar to what we have displayed for $c_1 = 0.4$, and as a first step towards characterising the space of solutions we plot in Figure 4.10, the mass of these black holes as a function of c_1, as well as in Figure 4.11, their angular momentum per unit mass. We note for clarity that the mass $\mathcal{M}$ of a *solution* (not the reference!) is given by $\mathcal{M} \sim \partial_z g_{vv}|_{z=0}$, and the angular momentum a by $a \sim \frac{1}{\mathcal{M}} \partial_z g_{t\phi}|_{z=0}$ and we use these equations to create the latter two figures. Note also that in Figure 4.10, we have normalised our results by dividing out the mass $\mathcal{M}$ of the solution that is found when $c_1 = 0$.

We postpone a more in depth of analysis of these stationary rotating black holes together with an examination of the full parameter space of solutions to our forthcoming publication. We will also include in that work results at higher resolution together with a discussion of some of the physical quantities characterising these solutions. In particular, we will compute the full embeddings of the metric, spin1 and spin-2 horizons to exhibit their geometry and contrast it with that of the Kerr solution of classical general relativity. It could also be of interest to compute physical quantities such as the radius of the innermost stable circular orbit for these stationary aether black holes with a view to performing a phenomenological analysis of the space of solutions in the spirit of [152]. In this thesis we nevertheless show some preliminary results pertaining to the aforementioned horizon embeddings. In particular, we plot the proper angular size $\sqrt{g_{\phi\phi}}(z, \theta)$ of the horizon at $\theta = \pi/2$ for the metric, spin-1 and spin-2 horizons respectively as a function of c_1 and contrast this with the same quantity plotted for the Kerr solution in general relativity. The position of the metric horizon in the equatorial plane is given simply by the equation $g^{zz}(z, \theta) = 0$. (To see this we define a function f which vanishes on the horizon, $f = z - z_h(\theta)$. The vector $\partial_\mu f$ is normal to the horizon, and since it is therefore a null vector, one has that $g^{\mu\nu}(\partial_\mu f)(\partial_\nu f) = 0$. In the mirror plane $\theta = \pi/2$ however, there are no gradients in θ by symmetry and so the the null condition above reduces to $g^{zz}(z, \theta) = 0$ as claimed). For the other horizons, one need only solve an analogous equation but using the effective metrics governing the spin-1 and spin-2 modes that were discussed in the introductory chapter of this thesis (see section 1.4.2). That is to say, we should solve $g^{zz}_{(eff)}\left(z, \theta = \frac{\pi}{2}\right) = g^{zz} + q u^z u^z = 0$ where $q = \frac{c_1}{2-c_1}$ for the spin-1 horizon, and $q = c_1$ for the spin-2 horizon. To compare with Kerr, we ran our code at a given value of c_1, and computed the mass $\mathcal{M}$ of the resulting aether

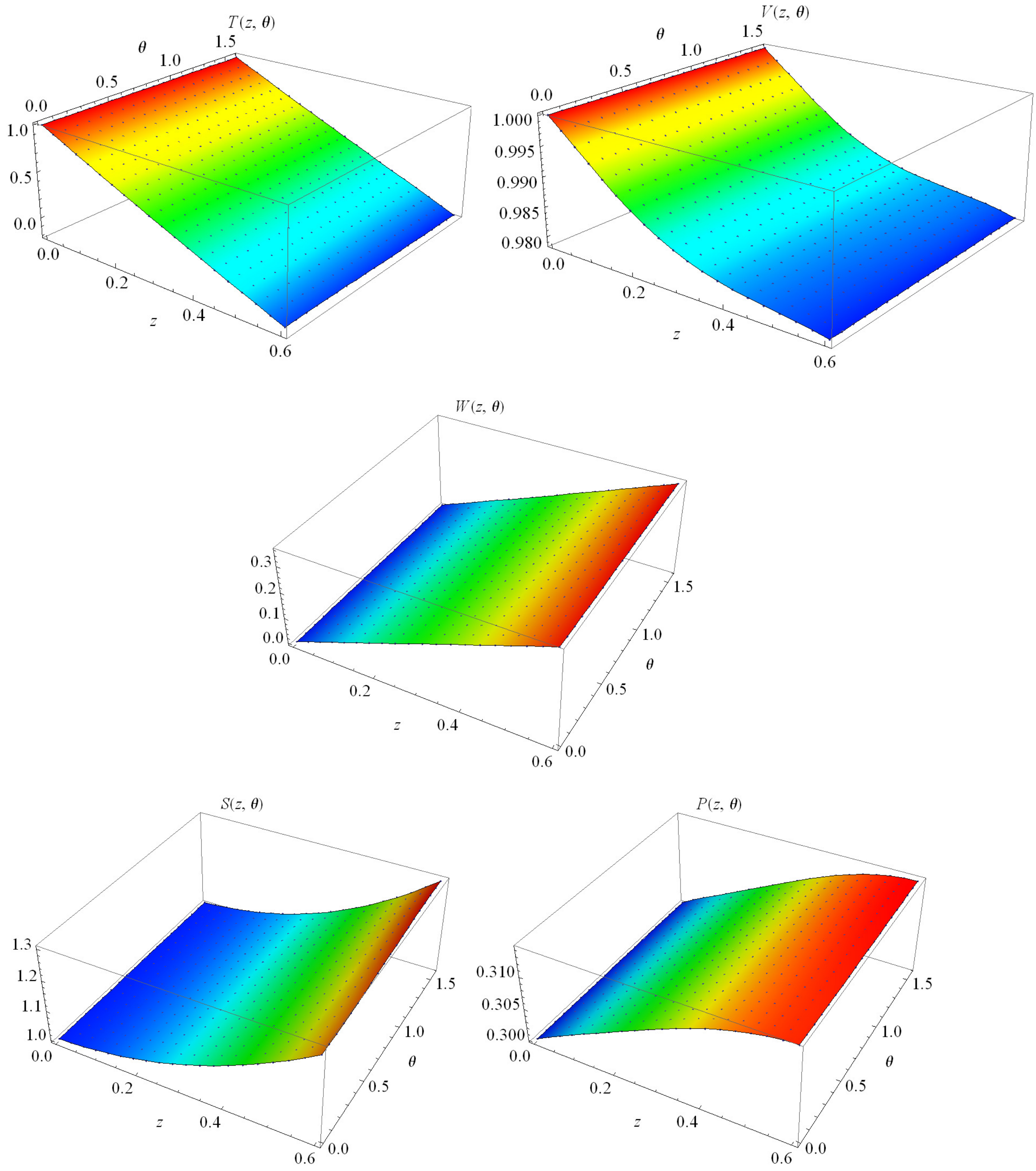

Figure 4.6.: Interpolating functions for the metric variables of a stationary black hole in Einstein-Aether theory, $\{T(z,\theta, V(z,\theta), W(z,\theta), S(z,\theta), P(z,\theta)\}$, computed using 6th order finite differencing from initial data and reference metric as specified in (4.5.31) with $\{M = 1, a = 0.3\}$ on an $N_z \times N_\theta = 20 \times 20$ grid, with $\{c_1 = 0.4,\ c_2 = -0.0727,\ c_3 = c_4 = 0\}$. The spin-0 horizon has been chosen to coincide with the metric horizon.

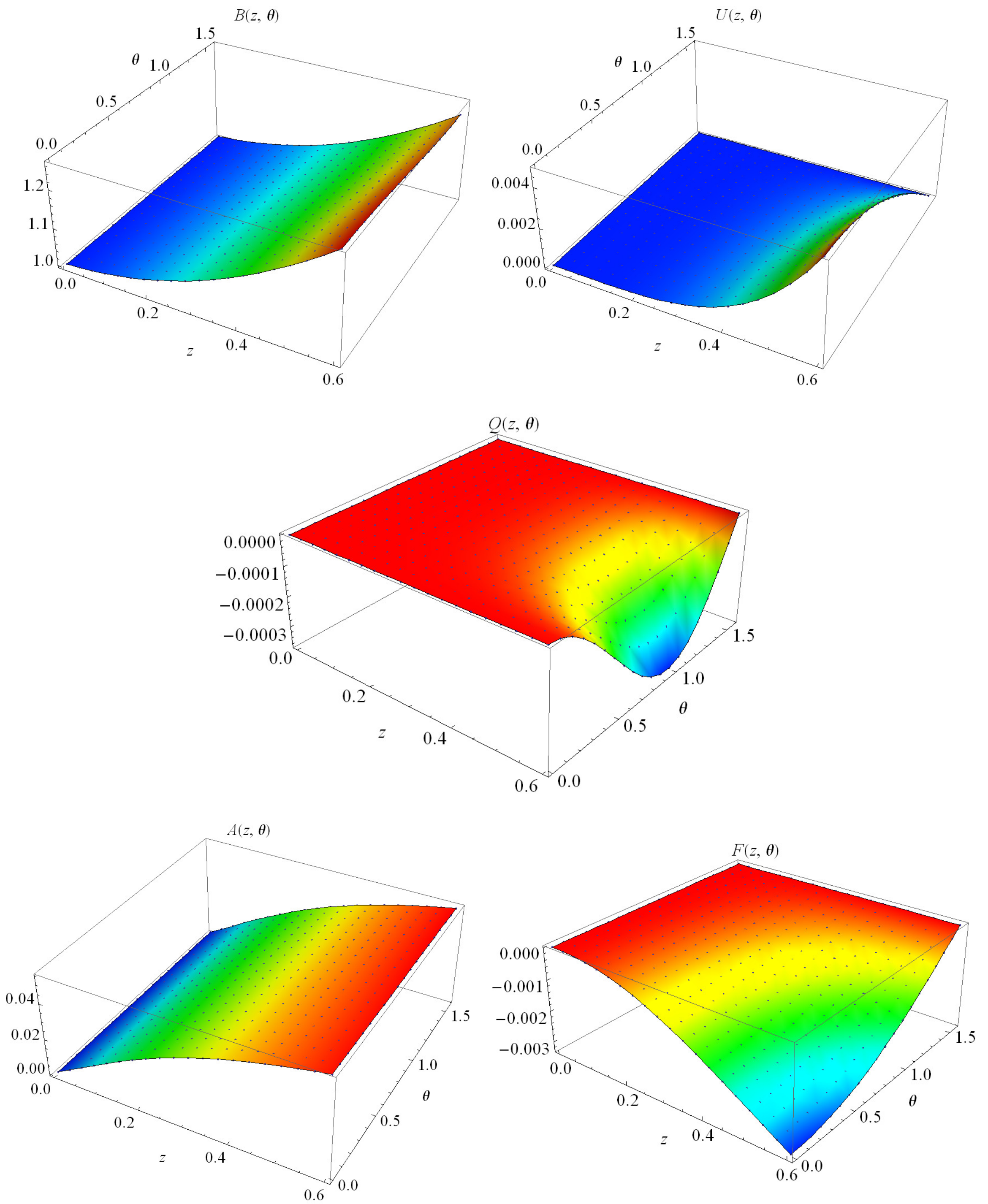

Figure 4.7.: The remaining metric variables for the rotating Einstein-Aether black hole described in the text, $\{B(z,\theta), U(z,\theta), Q(z,\theta), A(z,\theta), F(z,\theta)\}$, computed using 6th order finite differencing from initial data and reference metric as specified in (4.5.31) with $\{M = 1, a = 0.3\}$ on an $N_z \times N_\theta = 20 \times 20$ grid, with $\{c_1 = 0.4,\ c_2 = -0.0727,\ c_3 = c_4 = 0\}$. The spin-0 horizon has been chosen to coincide with the metric horizon.

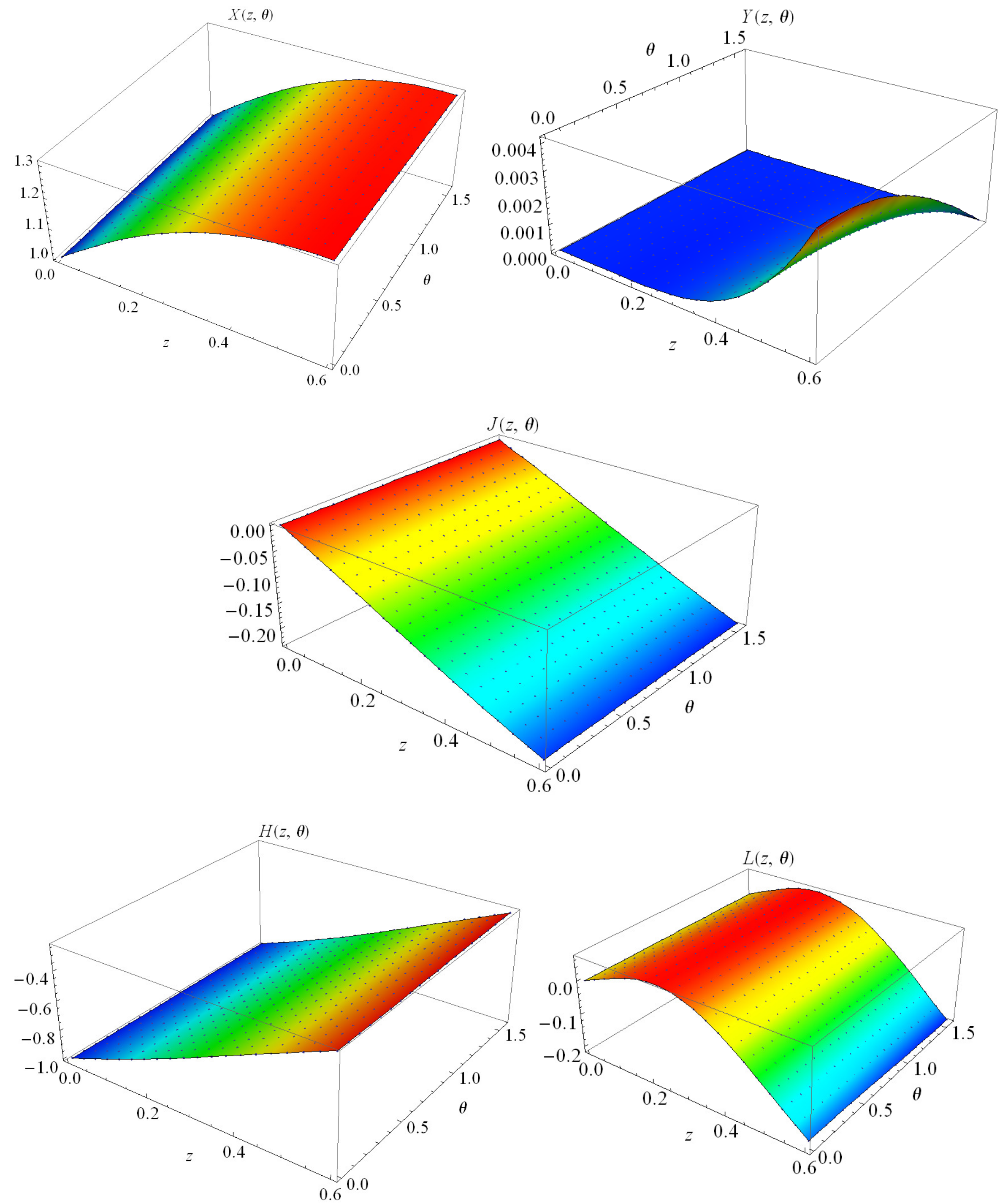

Figure 4.8.: Interpolating functions for the aether and constraint variables $\{X(z,\theta), Y(z,\theta), \dots, L(z,\theta)\}$ of the stationary rotating black hole in Einstein-Aether theory described in the text, computed using 6th order finite differencing from initial data and reference metric as specified in (4.5.31) with $\{M = 1, a = 0.3\}$ on an $N_z \times N_\theta = 20 \times 20$ grid, with $\{c_1 = 0.4,\ c_2 = -0.0727,\ c_3 = c_4 = 0\}$.

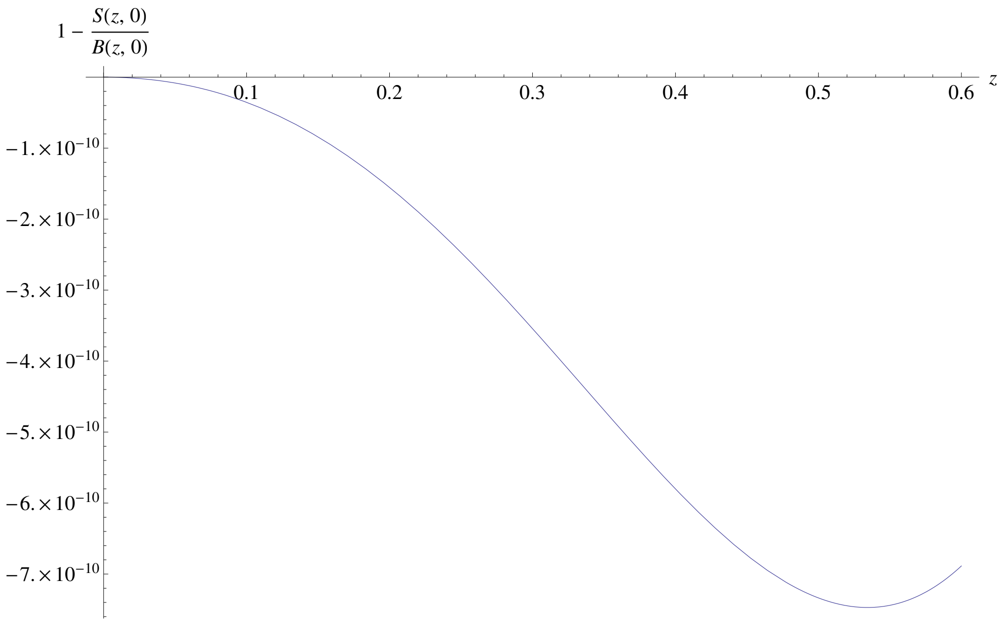

Figure 4.9.: Plot of $1-\frac{S(z,\theta=0)}{B(z,\theta=0)}$ to check axis regularity for the stationary aether black hole described in the text with $\{c_1 = 0.4,\ c_2 = -0.0727,\ c_3 = c_4 = 0\}$ on a $N_z \times N_\theta = 20 \times 20$ grid. We see that as required by regularity, this quantity is consistent with being zero.

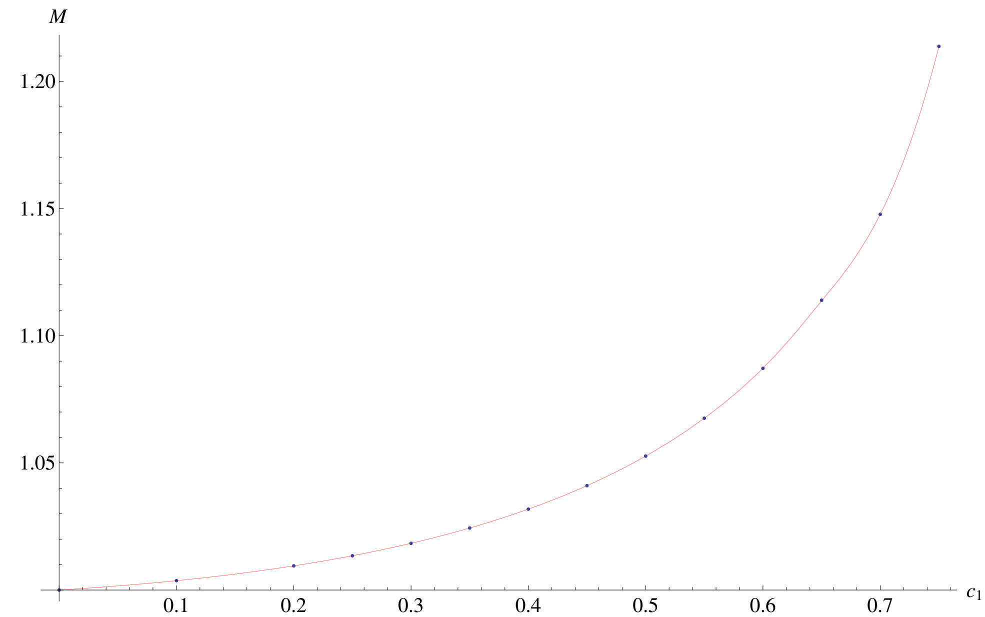

Figure 4.10.: Mass $\mathcal{M}$ of the stationary aether black holes found by the procedure outlined in the text as a function of c_1. We use initial data and reference metric as specified in (4.5.31) with $\{M = 1, a = 0.3\}$ and work on a $N_z \times N_\theta = 15 \times 15$ grid. (We remind the reader that in these ingoing methods, the mass and angular momentum of the reference metric does not constrain the mass and angular momentum of a solution). The parameter $c_2 = \frac{-c_1^3}{3c_1^2-4c_1+2}$, so that the spin-0 horizon coincides with the metric horizon and we take $c_3 = c_4 = 0$.

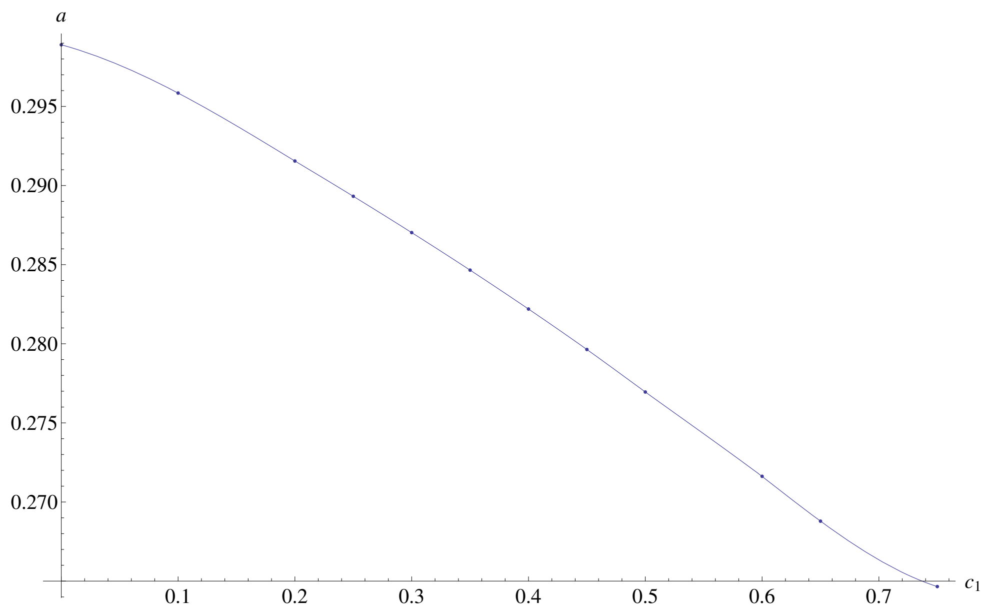

Figure 4.11.: Angular momentum per unit mass a of the stationary aether black holes found by the procedure outlined in the text as a function of c_1. We use initial data and reference metric as specified in (4.5.31) with $\{M = 1, a = 0.3\}$ and work on a $N_z \times N_\theta = 15 \times 15$ grid. (We remind the reader again that in these ingoing methods, the mass and angular momentum of the reference metric does not constrain the mass and angular momentum of a solution). The parameter $c_2 = \frac{-c_1^3}{3c_1^2 - 4c_1 + 2}$, so that the spin-0 horizon coincides with the metric horizon and we take $c_3 = c_4 = 0$.

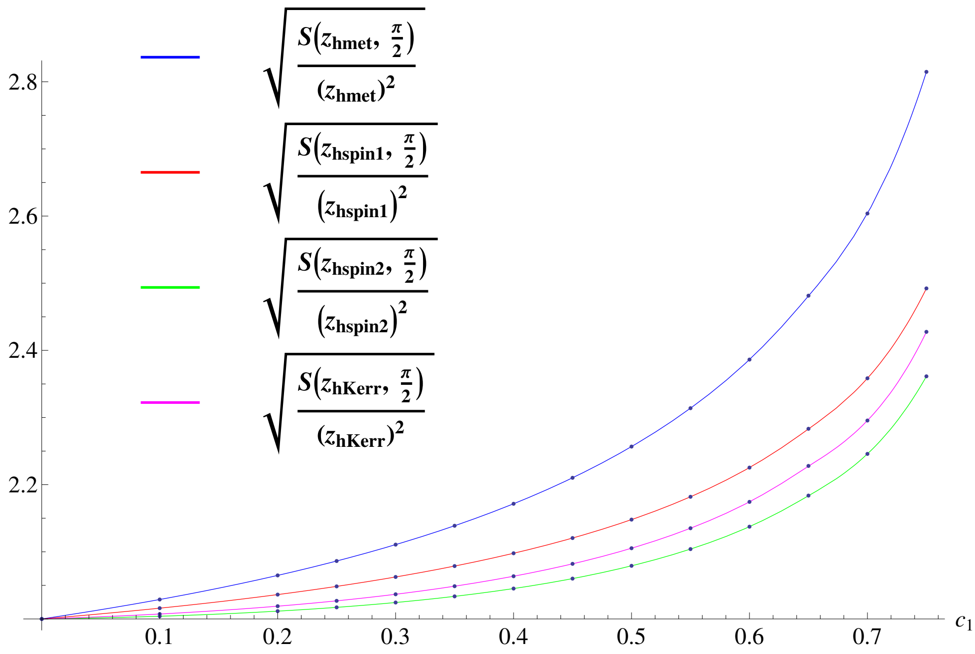

Figure 4.12.: Plot of the proper size of the metric (blue), spin-1 (red) and spin-2 (green) horizons in the equatorial plane ($\theta = \pi/2$) for the stationary aether black holes discussed in the text as a function of c_1. The proper size of each horizon is given by $\sqrt{\frac{S(z,\theta)}{z^2}}$, with $\theta = \pi/2$ and z satisfying $g^{zz} + qu^z u^z = 0$ with $q = 0$ for the metric horizon, $q = \frac{c_1}{2-c_1}$ for the spin-1 horizon and $q = c_1$ for the spin-2 horizon. The corresponding quantity for a Kerr black hole of the same mass (for a given c_1) is also shown on the same graph in magenta. As before, calculations were done on an $N_z \times N_\theta = 15 \times 15$ grid with $c_2 = \frac{-c_1^3}{3c_1^2-4c_1+2}$ and $c_3 = c_4 = 0$.

black hole solution. The quantity $\sqrt{g_{\phi\phi}}(z, \theta = \pi/2)$ for a Kerr solution of the same mass is then given by twice the mass of the aether black hole (as can be seen from the analytic expressions for the Kerr in (4.5.31)). One may repeat the procedure varying c_1. The results of this analysis are shown in Figure 4.12, where the proper sizes of each horizon in the equatorial plane are plotted and overlaid on the same graph.

Finally, in order to check that the solutions we have found are not solitons, we demonstrate that the ξ vector vanishes everywhere on them. We would also like to discuss whether our numerics are converging to a true continuum solution of the Harmonic Einstein equations with $\xi = 0$. To that effect, in Figure 4.13 we show a plot of the maximum value of $\phi = \xi^\mu \xi_\mu$ as a function of the the number of grid points $N = N_z = N_\theta$ for the numerical black hole with the parameters described above found using 6th order finite differencing. In Figure 4.14, we show the same quantity but this time for spectral differencing. In both cases whilst the ξ vector is everywhere extremely small (in particular if we regard $\sqrt{\xi^\mu \xi_\mu}$ as a global measure of error, we see that in both cases $\sqrt{\xi^\mu \xi_\mu} \sim 10^{-6}$), it is difficult to make any definitive statements with regard to convergence at this low resolution. In order to analyse convergence in more detail, we also include higher resolution plots of the maximum value of $\phi = \xi^\mu \xi_\mu$ across the grid for both finite and spectral differencing. These are the results of my collaborator Figueras and in order to effectively illustrate convergence one has to proceed to considerably higher resolutions than our desktop resources were capable of. These calculations were therefore performed on the supercomputer COSMOS. They also make use of more efficient packages to deal with sparse matrices. (The LAPACK package that was used in my own code is more suited to spectral techniques where the differentiation matrices are not sparse, but is wasteful for finite differencing; rapidly leading to memory issues on large grids). Note we have also checked that these COSMOS results are consistent with our results at low resolution.

In Figure 4.15 we show the results of these high resolution 6th order finite differencing and in Figure 4.16 we show the spectral results. In the former case, convergence is analysed for stationary black hole solutions with $\{c_1 = 0.3, a = 0.3, M = 1\}$ on grid sizes $\{N_z, N_\theta = 2N_z\}$ with $\{N_z = 15, 20, 25, 30, 35, 40\}$. In the latter spectral plots, we show solutions at the same resolutions as finite differencing but we also explicitly overlay the results for three separate values of the aether and rotation parameters $\{c_1 = a = 0.1, 0.3, 0.5\}$. The reason for this is we want to illustrate that spectral methods are not converging anywhere in parameter space. Indeed it is clear from Figure 4.16 that for spectral methods, whilst the ξ vector is extremely small everywhere, there is no sense in which one sees convergence to a continuum solution with vanishing ξ as the resolution is increased. This is indicative of the arguments discussed earlier that spectral methods fail completely for this problem as a result of the non-analyticity of the metric functions at infinity. In contrast, for the finite differencing in Figure 4.15 we see indication of convergence with ϕ decreasing by five orders of magnitude as the grid size is increased from $N_z = 15$ to $N_z = 25$. Whilst the ξ vector stops decreasing with increasing resolution at $\phi \sim 10^{-16}$ corresponding to $\xi \sim 10^{-8}$ this is to be expected and is not an indication of failure to converge to a continuum solution but instead can be understood as arising due to loss of numerical precision. In detail, the condition number of the matrix that appears in the Newton method (i.e. the ratio of its smallest to largest eigenvalue) becomes of order $\sim 10^{-16}$ at this point (i.e. the same order as machine precision) and hence one cannot reliably invert the problem.

To close our discussion of convergence we also plot the value of $A(z_{max}, \theta_{max})$ as a function of resolution in Figure 4.17 for finite differencing and in Figure 4.18 for spectral methods. (These are for the original low resolution solutions described in the text with $c_1 = 0.4, a = 0.3$). This is a measure of whether one is converging to a continuum solution of the *Harmonic* Einstein equations, whilst the previous plots are concerned with convergence to a solution of the original Einstein equations (i.e. a solution of the Harmonic Einstein equations for which $\xi = 0$). Once again at this low resolution, it is difficult to see clear convergence behaviour and whilst our results are not incompatible with convergence at higher resolution, it is not clearly indicated and further analysis would be necessary to check this. Some evidence can be obtained by virtue of the fact that in Figure 4.15 we see that (for finite differencing) the constraint $\xi = 0$ appears to converge in the maximum norm and thus it is plausible that the solution does as well. (This is of course not guaranteed; convergence of the constraint is a necessary but not sufficient condition for convergence of the solution itself). Further support for convergence of the solution itself is provided by monitoring $||A0 - A(z_{max}, \theta_{max}, N)||$ in a suitable norm (where $A0$ is the guess for the continuum value and $A(z_{max}, \theta_{max}, N)$ is the approximation to this on an $N \times N$ grid). To this effect, in Figure 4.19 we show a plot of $log_{10}(N)$ against $log_{10}(\int dz\, d\theta\, |A0 - A(z_{max}, \theta_{max}, N)|)$ for $N = \{8, 10, 12, 16, 20, 22, 24, 26, 28, 30, 32\}$. (We approximate $A0 = A(z_{max}, \theta_{max}, N_{max})$ with $N_{max} = 34$). The data used to create this plot are for a solution with $a = c_1 = 0.3$ and are courtesy of Wiseman. The gradient of the line of best fit that is displayed in the aforementioned Figure is ~ -4.5. (One expects the slope to be ~ -6 for 6th order finite differencing, but the data is not high resolution enough to display asymptotic scaling). We see from this plot that there is some evidence for convergence to a continuum solution at higher resolution, but further work would be required to confirm this. We do not analyse the spectral solution further as we know from Figure 4.16 that the constraint is not converging and thus neither can the solution itself.

4.6. Discussion

In this section, we have discussed aspects of black hole physics in Einstein-Aether theory, a modified theory of gravity that introduces a preferred frame in the universe, spontaneously breaking the Lorentz symmetry of classical general relativity. This theory is currently compatible with all observational constraints from both solar system and cosmological tests and provides a very instructive toy model within which to explore the interesting phenomenology of Lorentz violation in the gravitational

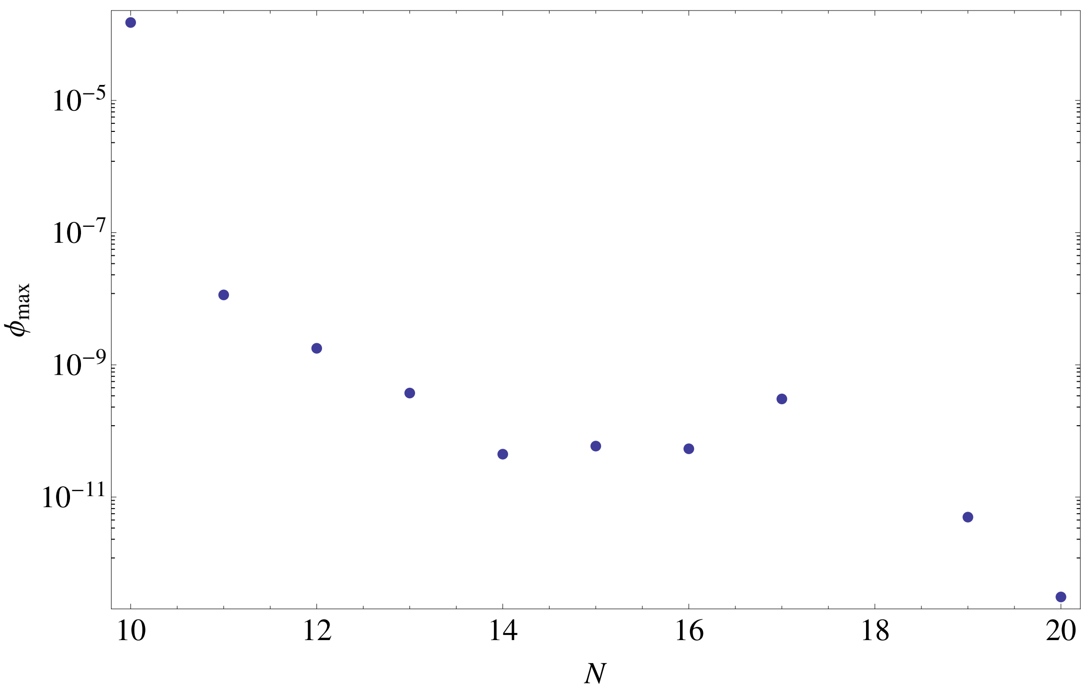

Figure 4.13.: Plot of the maximum value of $\phi = \xi^\mu \xi_\mu$ as a function of the number of grid points N for the black hole described in the text with parameters $\{c_1 = 0.4, a = 0.3, M = 1\}$ found using 6th order finite differencing. The ξ vector is everywhere small ($\sqrt{\xi^\mu \xi_\mu} \sim 10^{-6}$). Convergence to a continuum solution with $\xi = 0$ seems plausible and further support for this may be found by proceeding to higher resolution as shown in Figure 4.15.

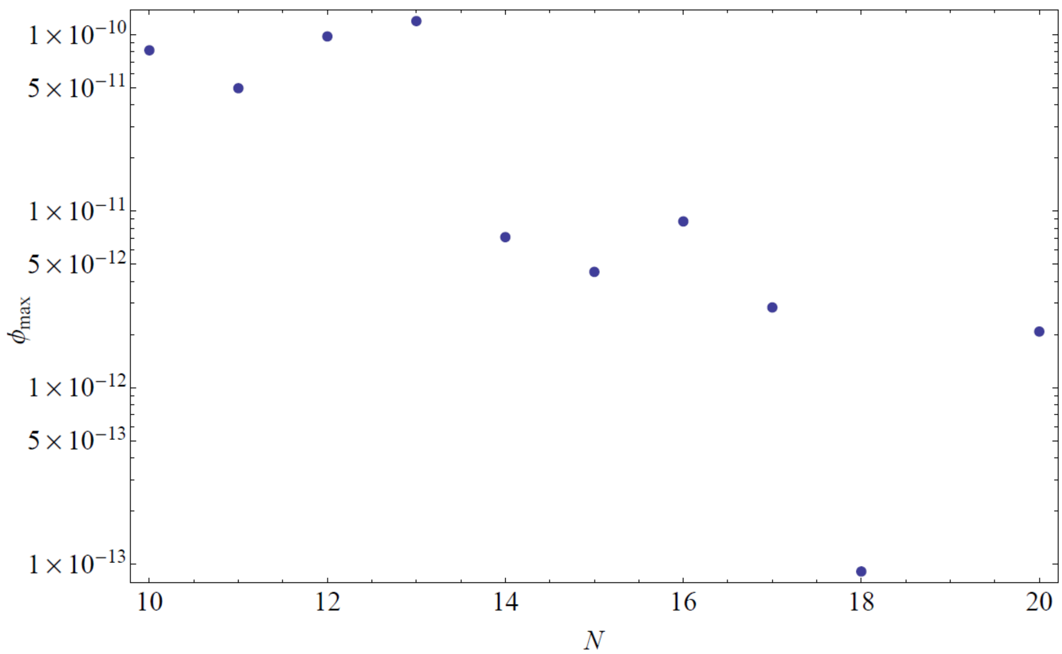

Figure 4.14.: Plot of the maximum value of $\phi = \xi^\mu \xi_\mu$ as a function of the number of grid points N for the black hole described in the text with parameters $\{c_1 = 0.4, a = 0.3, M = 1\}$ found using spectral differencing. As with the finite differencing case, whilst ξ is everywhere small, the convergence to a well-behaved continuum solution is unclear at this resolution and by proceeding to higher resolution as in Figure 4.16, one in fact sees that spectral methods do not converge.

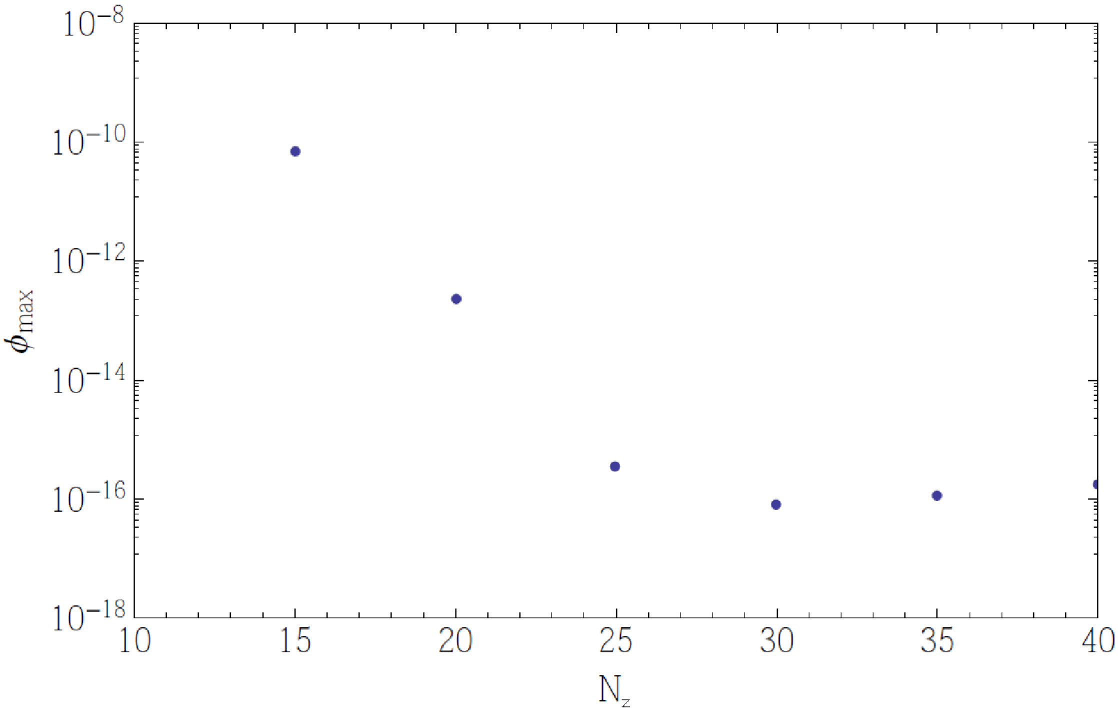

Figure 4.15.: Plot of the maximum value of $\phi = \xi^\mu \xi_\mu$ as a function of resolution for 6th order finite differencing. The solutions displayed are for $\{c_1 = 0.3, a = 0.3, M = 1\}$ on grid sizes $\{N_z, N_\theta = 2N_z\}$ with $\{N_z = 15, 20, 25, 30, 35, 40\}$. The ξ vector is everywhere small, consistent with a true solution of the Einstein equations. We also see good convergence behaviour with ξ decreasing by five orders of magnitude as the grid size is increased from $N_z = 15$ to $N_z = 25$. As we proceed to even higher resolutions we no longer see a drop in ϕ (below $\sim 10^{-16}$), but this is not an indication of failure to converge but rather due to reaching the limit of machine precision as described in the main text. *Figure courtesy of Dr Pau Figueras*

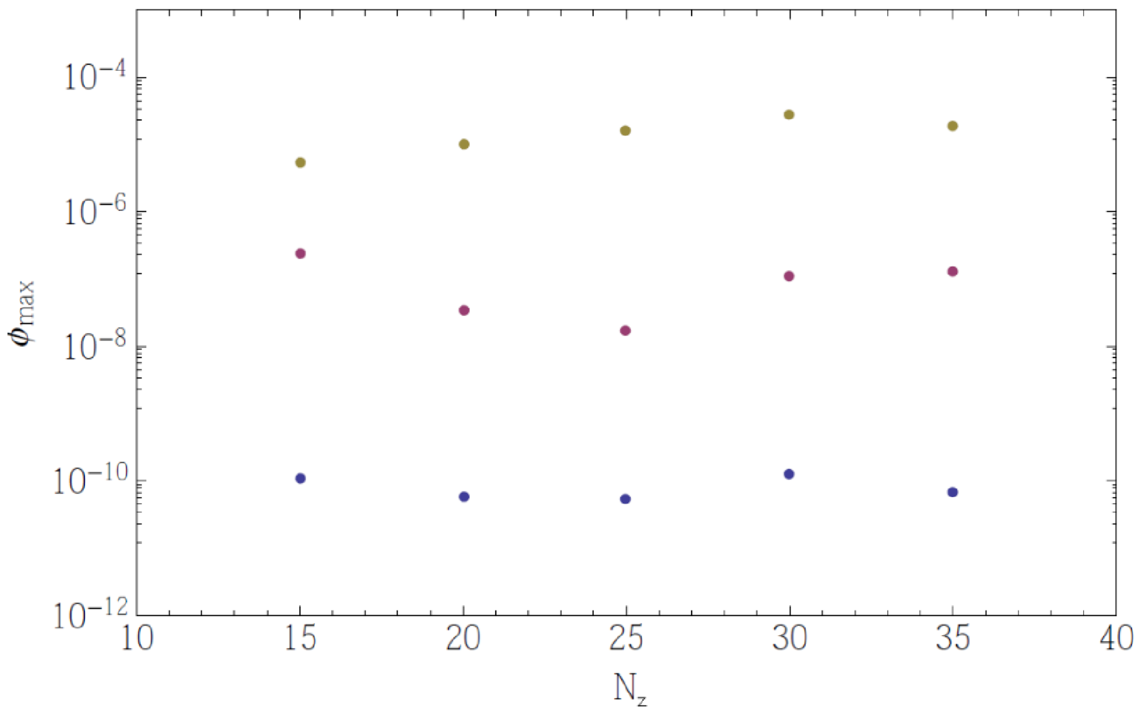

Figure 4.16.: Plot of the maximum value of $\phi = \xi^{\mu}\xi_{\mu}$ as a function of resolution for spectral differencing. The solutions displayed are on grid sizes $\{N_z, N_\theta = 2N_z\}$ with $\{N_z = 15, 20, 25, 30, 35, 40\}$. We plot three solutions for different values of the aether parameters for $\{c_1 = a = 0.1\}$ (in blue), $\{c_1 = a = 0.3\}$ (in red) and $\{c_1 = a = 0.5\}$ (in yellow). All solutions have $M = 1$. In contrast to the finite differencing case, whilst ξ is everywhere small, there is no clear convergence to a continuum solution with $\xi = 0$ indicating that spectral methods are failing for this problem. Notice this failure to converge occurs even in the case where $c_1 = 0.1$ corresponding to small deformations from Einstein gravity. *Figure courtesy of Dr Pau Figueras*

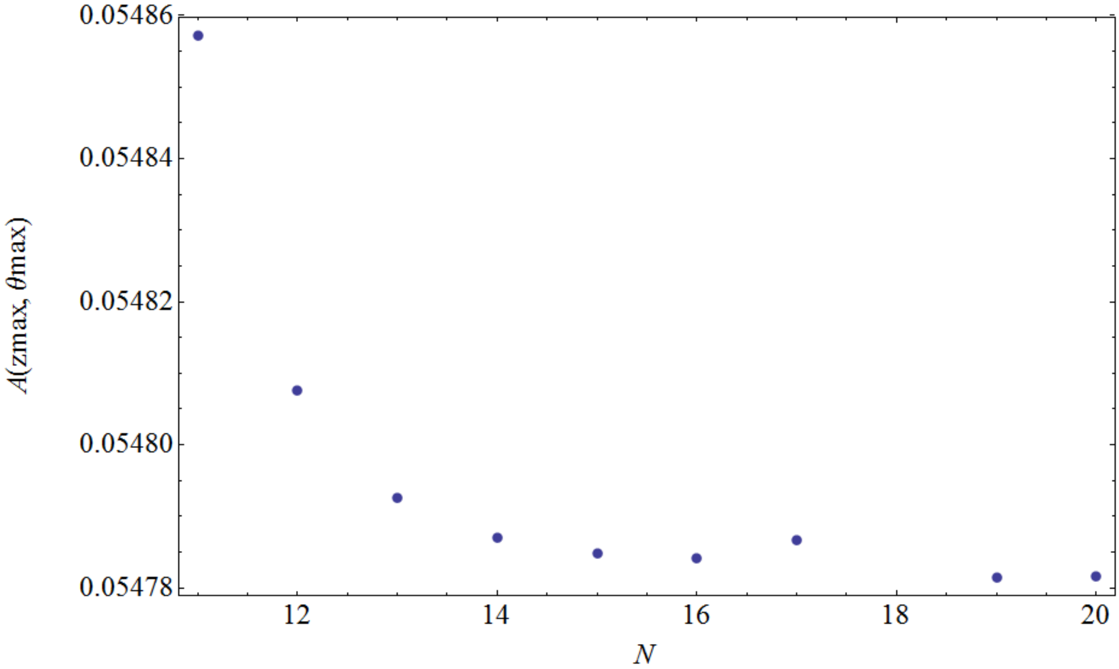

Figure 4.17.: Plot of $A(z_{max}, \theta_{max})$ as a function of resolution for the black hole described in the text with parameters $\{c_1 = 0.4, a = 0.3, M = 1\}$ found using finite differencing. The convergence to a constant continuum value of $A(z_{max}, \theta_{max})$ is unclear at this relatively low resolution and is analysed further in Figure 4.19 at higher resolution where we see better evidence that the solution itself is converging.

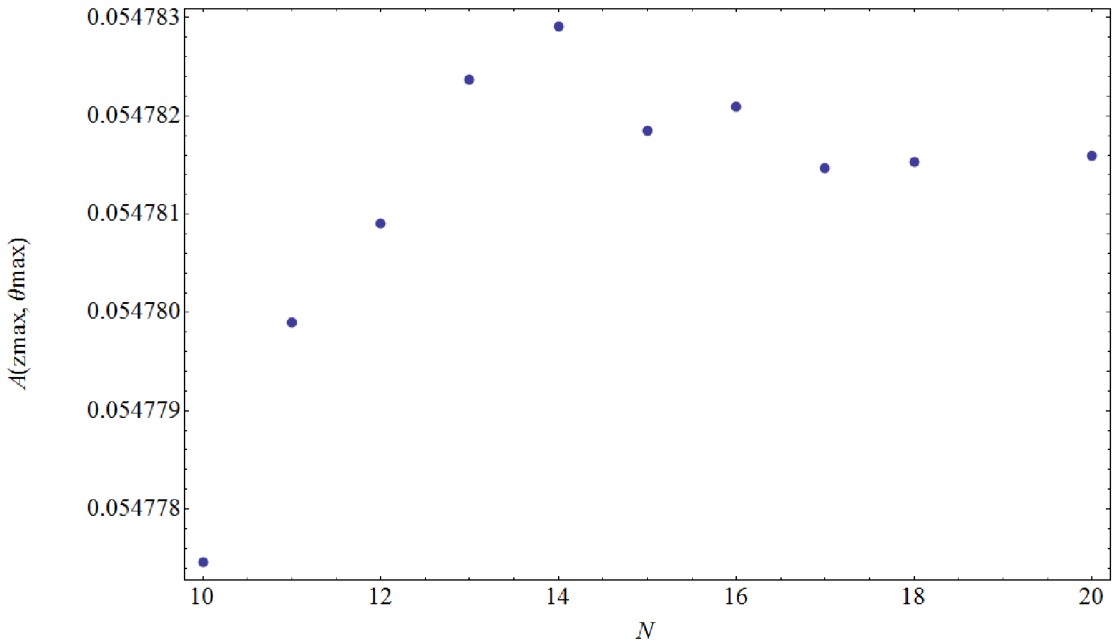

Figure 4.18.: Plot of $A(z_{max}, \theta_{max})$ as a function of resolution for the black hole described in the text with parameters $\{c_1 = 0.4, a = 0.3, M = 1\}$ found using spectral methods. Convergence to a continuum value of $A(z_{max}, \theta_{max})$ is not clear and indeed we know that since the constraint does not converge in the spectral case (Figure 4.16), the solution cannot either.

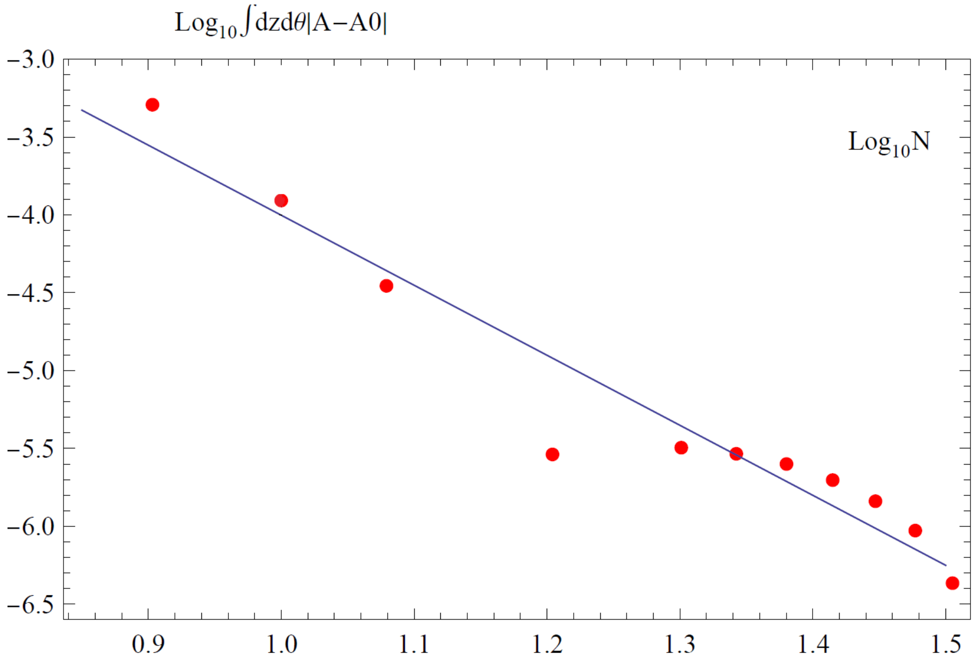

Figure 4.19.: Plot of $log_{10}(N)$ against $log_{10}(\int dz\, d\theta\, |A0 - A(z_{max}, \theta_{max}, N)|)$ for $N = \{8, 10, 12, 16, 20, 22, 24, 26, 28, 30, 32\}$. (We approximate the continuum value $A0 = A(z_{max}, \theta_{max}, N_{max})$ with $N_{max} = 34$). The data was found using finite differencing for a black hole with $a = c_1 = 0.3$. The gradient of the line of best fit is found to be ~ -4.5, (one expects ~ -6 in the regime of asymptotic convergence for 6th order differencing but this data is not at high enough resolution to see this). This plot shows some evidence in support of convergence of the solution itself at high resolution to a non-zero continuum value, although further work would be needed to confirm this. *Figure courtesy of Dr Toby Wiseman*

sector. As a consequence of the spontaneously broken Lorentz symmetry, the theory has multiple propagating degrees of freedom, each governed by a different characteristic hypersurface (that it is null with respect to). The notion of a black hole in such theories is hence quite subtle and in particular must trap all these additional causal influences together with the more conventional matter influences that couple directly to the metric $g_{\mu\nu}$ itself. Having fixed some definitions, we demonstrated how to construct spherically symmetric black holes in Einstein-Aether theory using a modification of the methods of elliptic numerical relativity discussed in 3. In particular, as a consequence of the layered multi-horizon structure that these black holes possess, it was necessary to construct numerical solutions interior to the metric horizon to exhibit their full structure. We therefore posed the Harmonic Einstein equations on an ingoing slice of the spacetime that extended into the interior of the black hole. These equations cease to be elliptic in this region (and in fact within an ergoregion if one exists) and thus the equations we had to solve constitute a mixed hyperbolic elliptic problem. The technical procedure of solving these equations nevertheless carries over from the elliptic procedures discussed previously in this thesis with little modification, aside from the prescription of boundary conditions. Whilst in the fully elliptic case, data is imposed on all interior and asymptotic boundaries in the problem, in the mixed elliptic hyperbolic case it needs only to be imposed asymptotically. Moreover, since in the latter case specification of a reference metric no longer fixes any moduli associated to a solution, these had to be fixed separately leading to specification of additional conditions at the innermost point of the domain (one additional constraint in the static case to fix the mass and two in the stationary case to fix mass and angular momentum). Within this framework, we were able to construct static, spherically symmetric black holes in Einstein-Aether theory, solving the Harmonic Einstein equations by the Newton method and demonstrating that these solutions were the same as what had previously been found in the literature using different (shooting) techniques. Furthermore, we were able to extend our techniques to construct the first examples of stationary, rotating black holes in Einstein-Aether theory. We performed our calculations using a field redefinition to make the metric and spin-0 horizons in the theory coincide and regularity at the spin-0 horizon was hence encoded from the outset by virtue of the fact that smoothness at the metric horizon is guaranteed in our ingoing chart with our boundary conditions.

There are a number of directions in which the work we have discussed in this chapter could be extended. In addition to simply providing a more in depth analysis of the space of stationary solutions in Einstein-Aether theory that we will discuss in a forthcoming publication, it is of interest to explore the horizon structure of the theory and describe the embeddings of the metric, spin-0, 1 and 2 horizons and study how their structure varies as a functions of the aether parameters c_i. Furthermore, in the interest of simplicity we restricted our analysis here to the subspace of parameter space for which $c_3 = c_4 = 0$, and it would be interesting to relax this requirement to investigate whether one finds qualitatively similar solutions in those cases to what we have found here. It is of course also of interest to explore black holes in the regions of aether parameter space that are phenomenologically viable. Beyond Einstein-Aether theory, the techniques we have discussed in this chapter would also be useful to shed light on the study of black holes in various other theories of modified gravity, notably Horava-Lifshitz theory and it would be interesting to investigate the phase space of stationary solutions there, in particular to further investigate the results of Barausse [210, 221], that suggest there are no slowly rotating solutions common to both theories. Finally, we note that it would be very interesting to explore in greater detail the thermodynamics of these black holes, and in particular to investigate the first law of thermodynamics that is applicable in these static and stationary settings.

5. Conclusions and Summary

Since its creation, general relativity has gradually established itself as one of the cornerstones of modern physics. Despite its abstract and highly theoretical beginnings, drawing on the nascent areas of pure mathematics of the time, (notably differential geometry), the theory today has remarkably become as significant in applied science as theoretical physics, having practical applications to satellite and GPS technology. In theoretical physics, general relativity underlies almost all of modern cosmology together with large portions of stellar astrophysics as well as serving as a powerful arena in which to study aspects of fundamental theories of quantum gravity, notably string and M-theory. It has become the pinnacle of elegance in modern physics to which we aspire to and to which we compare new gravitational theories that attempt to go beyond Einstein's theory. In this thesis we have studied a variety of different aspects of relativity in four and higher dimensions and in particular, we have highlighted how numerical relativity especially is invaluable in studying phenomena as diverse as a phase transitions in condensed matter and Lorentz violation in modified gravity. We note though that despite discussing a broad and exotic range of topics, we have in truth barely scratched the surface of the enormous field that is numerical relativity, restricting our discussion to stationary systems and remaining almost silent on the fascinating and complex problem of dynamical gravity.

In chapter 1, we introduced the prerequisite background theory of relevance to this thesis, discussing in particular various important aspects of the theory of black holes which to a large extent served as the unifying theme throughout our work. We reviewed the various uniqueness and 'no-hair' theorems that constrain solutions in four and higher dimensions where it became clear that whilst black holes in $D = 4$ are rather well-behaved objects, their higher dimensional cousins have no such manners highlighting the importance of numerics in higher dimensional gravity. Having introduced aspects of black hole theory, we went on to discuss the remarkable topic of black hole thermodynamics and reviewed gravitational aspects of holography. In particular, we explained how one can study very complicated (and strongly coupled) field theories at finite temperature and density by simple dual geometries describing hairy black holes, where heuristically the Hawking temperature of the horizon accounts for the temperature of the field theory, and the hair for the matter content of the theory. The second part of the introduction introduced elliptic methods for static numerical relativity and the all important Harmonic Einstein equation. Without gauge fixing, the Einstein equations $R_{\mu\nu} = 0$ are of indefinite signature which can be inconvenient for numerics. By following DeTurck, and adding $-\nabla_{(\mu}\xi_{\nu)}$ to this, one can recast the Euclidean Einstein equations as an elliptic boundary value problem. The remainder of this section consisted of a detailed treatment of the boundary conditions appropriate to this elliptic problem together with an explanation of how subject to choosing boundary conditions compatible with $\xi^\mu = 0$ one is likely (and sometimes guaranteed by maximum principles) to find solutions of the original Einstein equations. We then outlined two numerical algorithms to solve the Harmonic Einstein equation, namely Ricci flow and the Newton method. We ended the introduction with an overview of Einstein-Aether theory, a modified theory of gravity that spontaneously breaks Lorentz symmetry by the inclusion of a dynamical timelike vector field of unit norm. We presented the action and discussed various non-trivial field redefinitions and transformations of the parameters defining the theory $\{c_1, c_2, c_3, c_4\}$ that can be used to simplify the equations of motion. We then briefly discussed constraints on the theory from a number of solar system and cosmological tests and finally presented a detailed analysis of the propagating degrees of freedom in the theory. The latter analysis is our own and does not appear in the literature and in particular used the *Harmonic* Einstein equations to compute the effective metrics governing each of the wavemodes in the theory which were later used in our discussion of Einstein-Aether black holes in the final chapter of this thesis.

In chapter 2 we discussed our first and simplest application of numerical relativity, developing a holographic description of bosonic fractionalisation transitions in condensed matter physics. We began with some motivation for the subject, introducing the concept of fractionalised phases of matter where composite particles split apart into their gauge charged constituents and argued that this is dual in gravity to geometries where electric flux is sourced by an electrically charged horizon as opposed to bulk charged matter. The gravitational description of fractionalisation then amounts to studying transitions between electrically charged black holes and neutral black holes supporting charged scalar hair. We considered a simple class of theories consisting of gravity and a Maxwell field together with a real and charged scalar and used a simple planar, static ansatz to construct black hole solutions. On this ansatz, the Einstein equations reduced to ODEs and the problem of constructing our solutions was framed as a shooting problem where $T = 0$ IR geometries describing fractionalised, cohesive or partially fractionalised states of matter had to be connected to a universal AdS_4 asymptotic structure. We constructed one parameter families of each class of solutions and exhibited transitions between them, arguing that the existence or non-existence of a fractionalisation transition can be attributed to the IR behaviour of the real scalar which controls the Maxwell coupling. In cases where this coupling vanishes, charged matter is unable to source any flux, meaning a cohesive phase becomes impossible and full fractionalisation is the only possibility. Although the analysis here was restricted to $T = 0$, we made some comments on finite temperature and in the light of our newfound insights studied also M-theory. We explained the absence of a $T = 0$ fractionalised phase there as being a consequence of the finiteness of the effective gauge coupling in this theory in the IR. There are various interesting directions in which this work could be taken further: It would be of interest to study fractionalisation in a more general ansatz than (2.2.10), in particular to allow for the presence of spatial modulation and stripes. This problem is also of general interest in the context of this thesis as the elliptic PDE methods explored here provide a natural framework to solve the equations that result in such cases. It would also be of interest to study the order of such fractionalisation transitions. A more open ended and complex problem is to shed light on a possible field theory order parameter for fractionalisation and its relation to entanglement entropy [230].

In chapter 3 we discussed the stationary generalisation of the elliptic PDE methods of the introductory chapter of this thesis. Unlike for static spacetimes where there exists a well defined analytic continuation to a smooth real Riemannian geometry, in stationary situations the problem must be treated directly in Lorentzian signature. We argued that for stationary spacetimes with globally timelike Killing vector, the Harmonic Einstein equations are straightforwardly elliptic. In the presence of horizons and ergo-regions however the situation is less obvious and the analysis of such situations constituted the bulk of this chapter. Motivated by the Rigidity Theorem, we specialised to a class of stationary black hole spacetimes, discussed previously by Harmark [207]. The metric ansatz we considered geometrically describes a fibration of the Killing directions over a base manifold and we then argued that the Harmonic Einstein equations truncate to an elliptic system on this ansatz subject to the assumption that the base space manifold is Riemannian - a condition we showed to be satisfied in $D = 4$ by the Kerr solution. The Killing horizons and axes of symmetry constitute boundaries for this elliptic problem and we determined the necessary conditions that must be imposed there to obtain a regular solution. Whilst we did not explicitly consider numerical applications of this technology here (examples may be found in [1]), related methods were used in the closing chapter on Einstein-Aether theory.

In the final chapter of this thesis, 4, we turned to a discussion of black holes in Einstein-Aether theory. As a consequence of the spontaneously broken Lorentz symmetry in this theory, there exist propagating wave modes of different speeds (that each in general differ from the metric speed of light) and it is hence somewhat unclear what is meant by a 'black hole' in such situations. Following Jacobson [150], we argued that the notion is well defined in the sense that aether black holes have multiple horizons each trapping a wavemode of different spin and that a true black hole must possess a 'universal' outer horizon that traps the fastest of these modes. With these definitions we demonstrated that one can indeed construct both spherically symmetric and stationary aether black holes. In order to numerically construct these solutions, we used a generalisation of the numerical techniques of chapter 3. In particular, since aether black holes possess multiple horizons, we were required to develop the solution interior to the metric horizon to exhibit their full structure. In these regions however, the Harmonic Einstein equations ceased to be elliptic and we hence framed the problem as a mixed elliptic-hyperbolic PDE problem, specifying in detail the new boundary conditions for the system. (In particular, unlike in the formalism of chapter 3, no data must now be imposed at the innermost points of the PDE domain). We were then able to solve the resulting PDE system by implementing the Newton method. With this setup we were able to construct the same spherically symmetric aether black holes that had previously been found in the literature by shooting techniques and moreover were able to construct the first examples of general stationary black holes in Einstein-Aether theory. We closed our discussion by initiating an analysis of the physics of such stationary solutions looking at the relative sizes of the spin-0, 1 and 2 horizons in the equatorial plane as a function of the aether parameter c_1 and comparing with the Kerr solution of the same mass. As further work it would be very interesting to develop the physics of these solutions further, in particular by studying the structure of the full horizon embeddings (as opposed to simply at the axes and plane of reflection symmetry) as well as studying in greater depth the full parameter space of stationary solutions (and in particular intoducing non-zero c_3 and c_4 parameters). It would also be of interest to consider applying our new technology to study black holes in related theories of modified gravity notably Horava-Lifshitz gravity.

A. Boundary Conditions for Horizons and Axes

The procedure of deriving the regularity conditions at an axis or horizon boundary plays a central role in both static and stationary elliptic numerical relativity and is the subject of this appendix.

The technique is best illustrated by way of an example. We shall derive the regularity conditions for a smooth $(0,2)$ tensor J, which is symmetric with respect to a vector field R and which generates $U(1)$ orbits with period 2π and fixed action at some point p. Following the prescription outlined above in the main text, the tensor is first written in 'Cartesian coordinates' (a,b) that do not manifest the $U(1)$ isometry, but crucially in which the components are C^∞ smooth everywhere, including the fixed point. We then shift to polar coordinates (r,α) adapted to the symmetry, so that $R = \partial/\partial\alpha$ and in which the components do not depend explicitly on α. In detail, we begin with,

$$J = N(a,b)da^2 + M(a,b)db^2 + K(a,b)dadb\,, \tag{A.0.1}$$

and now introduce 'polar coordinates' r,α that make explicit the $U(1)$ isometry

$$a = r\sin\alpha\,,\ b = r\cos\alpha\,, \tag{A.0.2}$$

where we note once again that $\frac{\partial}{\partial\alpha}$ is Killing and $r = 0$ at the fixed point. The metric may then be recast in the form

$$J = r^2 A(r^2)d\alpha^2 + B(r^2)dr^2 + r^3\, C(r^2)dr\, d\alpha\,, \tag{A.0.3}$$

where the metric functions $A(r^2), B(r^2), C(r^2)$ are trivially related to those in the Cartesian coordinates by the chain rule. The isometry conditions, $\frac{\partial A(r^2)}{\partial\alpha} = \frac{\partial B(r^2)}{\partial\alpha} = \frac{\partial C(r^2)}{\partial\alpha} = 0$ then translate into conditions on the original metric functions $N(a,b), M(a,b)$ and $K(a,b)$ and evaluation of these equations at the origin gives the regularity conditions,

$$N(0,0) = M(0,0)\,, \qquad K(0,0) = 0\,, \tag{A.0.4}$$

which when expressed in terms of the polar metric functions become,

$$A(0) = B(0)\,. \tag{A.0.5}$$

These functions may be written in the form

$$A(r^2(a,b)) = N(a,b)\frac{b^2}{a^2+b^2} + M(a,b)\frac{a^2}{a^2+b^2} - K(a,b)\frac{ab}{a^2+b^2}\,, \tag{A.0.6}$$

with similar equations for $B(r^2(a,b))$ and $C(r^2(a,b))$. As a consequence of the above regularity conditions, we see that these functions are smooth everywhere in a, b (including at the origin) and since arbitrary fractional powers of (a^2+b^2) are not smooth in a, b at the origin, $A(r^2), B(r^2)$ and $C(r^2)$ must contain no odd powers of r. Consequently, $A(r^2), B(r^2)$ and $C(r^2)$ are *smooth* in r^2.

To summarise then, the conditions required for smoothness of J everywhere in polar coordinates are that A, B and C are smooth functions of r^2 that satisfy the regularity condition $A(0) = B(0)$. One may consider the Ricci-DeTurck flow or Newton method operating on this simple example metric (A.0.1) in 'Cartesian' coordinates. Let us also take the reference metric to similarly have the same $U(1)$ isometry generated by $\frac{\partial}{\partial\alpha}$. Then Ricci-DeTurck flow and the Newton method will act to preserve this isometry. At least for short flow times Ricci-DeTurck flow will preserve regularity. Let us also assume that the Newton method does too. Then both algorithms will preserve the regularity conditions deduced above for the 'Polar' form of the metric (A.0.3). The important consequence of this is that we may work directly with the 'Polar' form, taking our initial data and reference metric to be regular, and then this regularity should be preserved by the Ricci-DeTurck flow and Newton method.

A.1. Regularity and smoothness at a Killing horizon

A Killing horizon implies the existence of a normal Killing field K, whose isometry group is $\mathbb{R}$, with a fixed point at the bifurcation surface, and whose orbits close on the future and past horizons. We consider a smooth $(0,2)$ tensor that is symmetric under K, in a chart adapted to the symmetry which covers the exterior of the Killing horizon. The fixed point may be regarded as a boundary of this chart, and we determine regularity conditions on the tensor components there.

We begin in smooth Cartesian coordinates with a $(0,2)$ tensor, J, written in components as

$$J \;=\; N da^2 + M db^2 + U da db + Q_i da dx^i + R_i db dx^i + T_{ij} dx^i dx^j \,, \quad \text{(A.1.7)}$$

where $i = 1, ..., D-2$. We take a Killing horizon with respect to the Killing vector K to be located at $a = b$ and $a = -b$ with bifurcation surface $a = b = 0$. Since J is smooth at the horizon these component functions are C^∞ in the neighbourhood of the horizon. The horizon Killing symmetry is not manifest in these coordinates and in analogy with the toy example, we now change to hyperbolic coordinates

$$a = r \sinh \kappa t \,, \quad b = r \cosh \kappa t \,, \quad \text{(A.1.8)}$$

so that $K = \partial / \partial t$ and $r = 0$ is the bifurcation surface, with κ a constant related to the normalization of K and giving the surface gravity. We write the metric in this polar form as

$$\begin{aligned} J \;=\; & -r^2 A dt^2 + B dr^2 + r^3 C dr dt + r F_i dr dx^i + r^2 G_i dt dx^i \\ & + T_{ij} dx^i dx^j \,, \end{aligned} \quad \text{(A.1.9)}$$

where the component functions are independent of t. Repeating the analysis outlined in the toy example one arrives at the conclusion that the functions $A, B, C, F_i, G_i, T_{ij}$ depend smoothly on r^2 and x^i, together with the regularity condition

$$A|_{r=0} \;=\; \kappa^2 B|_{r=0} \,. \quad \text{(A.1.10)}$$

Thus we see explicitly that the regularity in the chart A.1.9 depends on the normalization of K, and hence the surface gravity. If we take the tensor J to be the metric, we deduce the regularity conditions on the metric at the Killing horizon. Taking J to be the Ricci-DeTurck tensor we see the behaviour it will exhibit if it shares the symmetry and is regular.

A.2. Axis of rotation

We now consider a $(0,2)$ tensor which is symmetric under a Killing field R which generates rotation about an axis with period 2π. In a chart which manifests the symmetry the axis is fixed under the $U(1)$ action, and may be regarded as a boundary for the chart. We determine the regularity conditions for the components in this chart there. This case is very close to the toy example before.

We begin with a Cartesian line element of the form

$$J \;=\; N da^2 + M db^2 + U da db + Q_i da dx^i + R_i db dx^i + T_{ij} dx^i dx^j \,, \tag{A.2.11}$$

and the component functions depend smoothly on a, b, x^i in the neighbourhood of the axis which we take to be $a = b = 0$. We now change to polar coordinates defined by

$$a = r \sin\alpha \,, \quad b = r \cos\alpha \,, \tag{A.2.12}$$

where α has period 2π and $R = \partial/\partial\alpha$ and $r = 0$ is the axis. In these coordinates we write the tensor as

$$J \;=\; r^2 A d\alpha^2 + B dr^2 + r^3 C dr d\alpha + r F_i dr dx^i + r^2 G_i d\alpha dx^i + T_{ij} dx^i dx^j \,, \tag{A.2.13}$$

and the symmetry is manifest so the metric functions are independent of α. Repeating the analysis outlined in the toy example, one finds the metric functions $A, B, C, F_i, G_i, T_{ij}$ are *smooth* functions of r^2 and x^i, together with the regularity condition

$$A|_{r=0} \;=\; B|_{r=0} \,. \tag{A.2.14}$$

B. Connection Components and Flow Equations

In this appendix, we give the connection components of the metric 3.4.20 together with the components of the Ricci tensor and ξ vector. The Christoffel symbols are given by,

$$\begin{aligned}
\Gamma^i_{jk} &= \hat{\Gamma}^i_{jk} + \frac{1}{2}h^{im}A_{Aj}F^A_{km} + \frac{1}{2}h^{im}A_{Ak}F^A_{jm} - \frac{1}{2}h^{im}A^A_k A^C_j \partial_m G_{AC}\,, \\
\Gamma^i_{AB} &= -\frac{1}{2}h^{ij}\partial_j G_{AB}\,, \\
\Gamma^A_{Bi} &= -\frac{1}{2}A^{Aj}G_{BC}F^C_{ij} + \frac{1}{2}A^{Aj}A^C_i\partial_j G_{BC} + \frac{1}{2}G^{AC}\partial_i G_{BC}\,, \\
\Gamma^A_{ij} &= -A^A_m\hat{\Gamma}^m_{ij} + \frac{1}{2}A^{Ak}A_{Bi}F^B_{kj} + \frac{1}{2}A^{Ak}A_{Bj}F^B_{ki} + \partial_{(j}A^A_{i)} + G^{AB}A^C_{(i}\partial_{j)}G_{BC} \\
&\quad + \frac{1}{2}A^{Ak}A^B_j A^D_i \partial_k G_{DB}\,, \\
\Gamma^A_{BC} &= \frac{1}{2}A^{Ai}\partial_i G_{BC}\,, \\
\Gamma^i_{jA} &= -\frac{1}{2}h^{ik}A^B_j\partial_k G_{AB} + \frac{1}{2}h^{ik}G_{AB}F^B_{jk}\,,
\end{aligned} \tag{B.0.1}$$

where $\hat{\Gamma}^i_{jk}$ is the Christoffel connection of the 'submetric' h_{ij} and $F^A_{ij} \equiv \partial_i A^A_j - \partial_j A^A_i = \hat{\nabla}_i A^A_j - \hat{\nabla}_j A^A_i$. The covariant derivative in the latter equation, $\hat{\nabla}_i$, is defined with respect to the connection $\hat{\Gamma}^i_{jk}$ of h_{ij} (and is metric compatible with respect to h_{ij}). Using these results one finds for the decomposition of the Ricci tensor,

$$\begin{aligned}
R_{AB} = \frac{1}{2}h^{ij}\hat{\nabla}_i(\partial_j G_{AB}) - \frac{1}{4}G^{CD}h^{ip}(\partial_p G_{AB})(\partial_i G_{CD}) \\
+ \frac{1}{2}h^{ij}G^{CD}(\partial_j G_{CB})(\partial_i G_{AD}) + \frac{1}{4}h^{mi}h^{jp}G_{BE}G_{AF}F^E_{mj}F^F_{ip}\,,
\end{aligned}$$

$$R_{iA} - R_{AB}A^B_i = \frac{1}{2}h^{jk}G_{AB}\hat{\nabla}_j F^B_{ik} + \frac{1}{2}h^{jk}F^B_{ij}\partial_k G_{AB} + \frac{1}{4}h^{jm}G^{CD}G_{AB}F^B_{im}\partial_j G_{CD}\,,$$

$$
\begin{aligned}
R_{ij} + R_{AB}A_i^A A_j^B - R_{Ai}A_j^A - R_{Aj}A_i^A = \hat{R}_{ij} &- \frac{1}{2}G^{CB}\hat{\nabla}_j(\partial_i G_{CB}) \\
&+ \frac{1}{4}G^{CD}G^{BA}(\partial_j G_{DA})(\partial_i G_{CB}) \\
&+ \frac{1}{2}h^{km}G_{AB}F_{jm}^A F_{ki}^B \,, \qquad \text{(B.0.2)}
\end{aligned}
$$

where $\hat{R}_{ij}$ is the Ricci tensor computed with respect to $\hat{\Gamma}^i_{jk}$. The DeTurck vector $\xi^\mu = g^{\lambda\nu}(\Gamma^\mu_{\lambda\nu} - \bar{\Gamma}^\mu_{\lambda\nu})$ decomposes as

$$
\begin{aligned}
\xi^k &= \hat{\xi}^k - \frac{1}{2}G^{AB}h^{km}\partial_m G_{AB} + \frac{1}{2}G^{AB}\bar{h}^{km}_{(-1)}\partial_m \bar{G}_{AB} + h^{ij}\bar{h}^{km}_{(-1)}\bar{G}_{AB}(A_i^A - \bar{A}_i^A)\bar{F}^B_{jm} \\
&\quad + \frac{1}{2}h^{ij}\bar{h}^{km}_{(-1)}(A_j^A A_i^B + \bar{A}_j^A \bar{A}_i^B - 2A_j^A \bar{A}_i^B)\partial_m \bar{G}_{AB} \,, \\
\xi^C &= \frac{1}{2}G^{AB}A^{Cj}\partial_j G_{AB} - \frac{1}{2}G^{AB}\bar{A}^{Cj}\partial_j \bar{G}_{AB} + h^{ij}(\hat{\nabla}_i A_j^C - \bar{\hat{\nabla}}_i \bar{A}_j^C) \\
&\quad - \frac{1}{2}h^{ij}\bar{A}^{Ck}(A_j^A A_i^B + \bar{A}_j^A \bar{A}_i^B - 2A_j^A \bar{A}_i^B)\partial_k \bar{G}_{AB} + h^{ij}\bar{A}^{Ck}\bar{G}_{AB}(A_i^A - \bar{A}_i^A)\bar{F}^B_{kj} \\
&\quad + h^{ij}\bar{G}^{CB}(A_i^A - \bar{A}_i^A)\partial_j \bar{G}_{AB} \,, \qquad \text{(B.0.3)}
\end{aligned}
$$

where $\hat{\xi}^k = h^{ij}(\hat{\Gamma}^k_{ij} - \bar{\hat{\Gamma}}^k_{ij})$ and as usual, an overbar indicates that the quantity in question is evaluated in the reference metric.

As discussed in the main text, the flow equations for the various metric components of interest decompose as,

$$
\begin{aligned}
\frac{\partial G_{AB}}{\partial \lambda} &= -2R_{AB} + 2\nabla_{(A}\xi_{B)} \,, \\
\frac{\partial A_j^C}{\partial \lambda} &= -2G^{AC}(R_{jA} - R_{AB}A_j^B) + 2G^{AC}(\nabla_{(A}\xi_{j)} - \nabla_{(A}\xi_{B)}A_j^B) \,, \\
\frac{\partial h_{ij}}{\partial \lambda} &= -2(R_{ij} + R_{AB}A_i^A A_j^B - R_{iA}A_j^A - R_{jA}A_i^A) \\
&\quad + 2(\nabla_{(i}\xi_{j)} + \nabla_{(A}\xi_{B)}A_i^A A_j^B - \nabla_{(B}\xi_{i)}A_j^B - \nabla_{(B}\xi_{j)}A_i^B) \,. \qquad \text{(B.0.4)}
\end{aligned}
$$

This form is particularly useful as the linear combinations of the components of $\nabla_{(\mu}\xi_{\nu)}$ that arise take a relatively simple form. Explicitly one finds that,

$$
\begin{aligned}
2\nabla_{(A}\xi_{B)} = \hat{\xi}^k\partial_k G_{AB} &- \frac{1}{2}G^{CD}(\partial^k G_{CD})(\partial_k G_{AB}) + \frac{1}{2}G^{CD}\bar{h}^{km}_{(-1)}(\partial_m \bar{G}_{CD})(\partial_k G_{AB}) \\
&+ \bar{h}^{km}_{(-1)}\bar{G}_{CD}\bar{F}^D_{jm}(A^{jC} - \bar{A}^{jC})\partial_k G_{AB} \\
&+ \frac{1}{2}\bar{h}^{km}_{(-1)}(A^{iC}A_i^D + \bar{A}^{iC}\bar{A}_i^D - 2A^{iC}\bar{A}_i^D)(\partial_m \bar{G}_{CD})(\partial_k G_{AB}) \,,
\end{aligned}
$$

$$
\begin{aligned}
2(\nabla_{(i}\xi_{A)} - \nabla_{(A}\xi_{B)}A_i^B) &= G_{AC}\hat{\nabla}_i(A_k^C\hat{\xi}^k) + G_{AC}\hat{\nabla}_i(\hat{\nabla}^p A_p^C - \bar{\hat{\nabla}}^p \bar{A}_p^C) \\
&+ G_{AC}\hat{\nabla}_i\left(\left(\frac{1}{2}\bar{h}^{mp}_{(-1)}G^{DE}(A_m^C - \bar{A}_m^C) + \bar{G}^{CE}(A^{pD} - \bar{A}^{pD})\right.\right. \\
&\left.\left.+\frac{1}{2}\bar{h}^{kp}_{(-1)}(A^{mD}A_m^E + \bar{A}^{mD}\bar{A}_m^E - 2A^{mD}\bar{A}_m^E)(A_k^C - \bar{A}_k^C)\right)\partial_p\bar{G}_{DE}\right) \\
&+ G_{AC}\hat{\nabla}_i(\bar{h}^{km}_{(-1)}\bar{G}_{DE}(A^{jE} - \bar{A}^{jE})(A_k^C - \bar{A}_k^C)\bar{F}_{jm}^D) \\
&+ G_{AC}\hat{\xi}^k F_{ki}^C - \frac{1}{2}G_{AC}G^{DE}F_{ki}^C(\partial^k G_{DE}) \\
&+ \frac{1}{2}\bar{h}^{km}_{(-1)}G_{AC}G^{DE}F_{ki}^C\partial_m\bar{G}_{DE} \\
&- \bar{h}^{km}_{(-1)}G_{AC}\bar{G}_{DE}(A^{jD} - \bar{A}^{jD})F_{ik}^C\bar{F}_{jm}^E \\
&+ \frac{1}{2}\bar{h}^{km}_{(-1)}G_{AC}(A^{pD}A_p^E + \bar{A}^{pD}\bar{A}_p^E - 2A^{pD}\bar{A}_p^E)F_{ki}^C\partial_m\bar{G}_{DE}\ ,
\end{aligned}
$$

$$
\begin{aligned}
2(\nabla_{(i}\xi_{j)} + \nabla_{(A}\xi_{B)}A_i^A A_j^B - \nabla_{(B}\xi_{i)}A_j^B - \nabla_{(B}\xi_{j)}A_i^B) &= 2\hat{\nabla}_{(i}\hat{\xi}_{j)} \\
&+ G^{AB}G^{CD}(\partial_i G_{CB})(\partial_j G_{AD}) - G^{AB}\hat{\nabla}_i(\partial_j G_{AB})z \\
&+ \left(\frac{1}{2}h_{ik}\hat{\nabla}_j(G^{AB}\bar{h}^{km}_{(-1)}\partial_m\bar{G}_{AB}) + h_{ik}\hat{\nabla}_j(\bar{h}^{km}_{(-1)}\bar{G}_{AB}\bar{F}_{qm}^B(A^{qA} - \bar{A}^{qA}))\right. \\
&\left.+\frac{1}{2}h_{ik}\hat{\nabla}_j(\bar{h}^{km}_{(-1)}(A^{pA}A_p^B + \bar{A}^{pA}\bar{A}_p^B - 2A^{pA}\bar{A}_p^B)\partial_m\bar{G}_{AB}) + (i \leftrightarrow j)\right)\ ,
\end{aligned}
$$

where we note that in these latter three expressions, all 'A term' base indices have been contracted with the base metric h_{ij} as appropriate. Using these results, one arrives at the flow equations in the main body of the text, contracted in the same manner.

Bibliography

[1] A. Adam, S. Kitchen, and T. Wiseman, *A numerical approach to finding general stationary vacuum black holes*, *Class.Quant.Grav.* **29** (2012) 165002, [arXiv:1105.6347].

[2] A. Adam, B. Crampton, J. Sonner, and B. Withers, *Bosonic Fractionalisation Transitions*, *JHEP* **1301** (2013) 127, [arXiv:1208.3199].

[3] L. Lehner, *Numerical relativity: A Review*, *Class.Quant.Grav.* **18** (2001) R25–R86, [gr-qc/0106072].

[4] M. D. Duez, *Numerical relativity confronts compact neutron star binaries: a review and status report*, *Class.Quant.Grav.* **27** (2010) 114002, [arXiv:0912.3529].

[5] J. A. Font, *Numerical hydrodynamics and magnetohydrodynamics in general relativity*, *Living Rev.Rel.* **11** (2007) 7.

[6] T. Piran, *Numerical relativity from gravitational radiation to cosmology*, . PRINT-86-1277 (HEBREW), C86-07-06.

[7] S. A. Hartnoll, *Lectures on holographic methods for condensed matter physics*, *Class. Quant. Grav.* **26** (2009) 224002, [arXiv:0903.3246].

[8] S. A. Hartnoll, *Horizons, holography and condensed matter*, arXiv:1106.4324.

[9] S. Sachdev, *Condensed Matter and AdS/CFT*, *Lect.Notes Phys.* **828** (2011) 273–311, [arXiv:1002.2947].

[10] C. P. Herzog, *Lectures on Holographic Superfluidity and Superconductivity*, *J.Phys.* **A42** (2009) 343001, [arXiv:0904.1975].

[11] J. McGreevy, *Holographic duality with a view toward many-body physics*, *Adv.High Energy Phys.* **2010** (2010) 723105, [arXiv:0909.0518].

[12] N. Iizuka, T. Okuda, and J. Polchinski, *Matrix Models for the Black Hole Information Paradox*, *JHEP* **1002** (2010) 073, [arXiv:0808.0530].

[13] N. Iizuka and J. Polchinski, *A Matrix Model for Black Hole Thermalization*, *JHEP* **0810** (2008) 028, [arXiv:0801.3657].

[14] D. N. Kabat, G. Lifschytz, and D. A. Lowe, *Black hole thermodynamics from calculations in strongly coupled gauge theory*, *Int.J.Mod.Phys.* **A16** (2001) 856–865, [hep-th/0007051].

[15] D. N. Kabat, G. Lifschytz, and D. A. Lowe, *Black hole entropy from nonperturbative gauge theory*, *Phys.Rev.* **D64** (2001) 124015, [hep-th/0105171].

[16] S. Catterall and T. Wiseman, *Towards lattice simulation of the gauge theory duals to black holes and hot strings*, *JHEP* **0712** (2007) 104, [arXiv:0706.3518].

[17] G. 't Hooft, *A Planar Diagram Theory for Strong Interactions*, *Nucl.Phys.* **B72** (1974) 461.

[18] J. M. Maldacena, *The Large N limit of superconformal field theories and supergravity*, *AIP Conf.Proc.* **484** (1999) 51–63.

[19] D. M. DeTurck, *Deforming metrics in the direction of their Ricci tensors*, *J. Differ. Geom.* **18** (1983) 157–62.

[20] M. Headrick and T. Wiseman, *Ricci flow and black holes*, *Class. Quant. Grav.* **23** (2006) 6683–6708, [hep-th/0606086].

[21] M. Headrick, S. Kitchen, and T. Wiseman, *A new approach to static numerical relativity, and its application to Kaluza-Klein black holes*, *Class. Quant. Grav.* **27** (2010) 035002, [arXiv:0905.1822].

[22] T. Jacobson and D. Mattingly, *Gravity with a dynamical preferred frame*, *Phys.Rev.* **D64** (2001) 024028, [gr-qc/0007031].

[23] D. Mattingly and T. Jacobson, *Relativistic gravity with a dynamical preferred frame*, gr-qc/0112012.

[24] T. Jacobson, *Einstein-aether gravity: A Status report*, *PoS* **QG-PH** (2007) 020, [arXiv:0801.1547].

[25] A. Mueller, *Experimental Evidence of Black Holes*, *PoS* **P2GC** (2006) 017, [astro-ph/0701228].

[26] M. Cavaglia, *Black hole and brane production in TeV gravity: A review*, *Int. J. Mod. Phys.* **A18** (2003) 1843–1882, [hep-ph/0210296].

[27] G. L. Landsberg, *Black Holes at Future Colliders and Beyond*, *J.Phys.* **G32** (2006) R337–R365, [hep-ph/0607297].

[28] G. Landsberg, *Out-of-this-world physics: Black holes at future colliders. proceedings of the space telescope science institute symposium, pages 21-45*, 2007.

[29] Y. V. Kovchegov, *AdS/CFT applications to relativistic heavy ion collisions: a brief review*, *Rept.Prog.Phys.* **75** (2012) 124301, [arXiv:1112.5403].

[30] J. Casalderrey-Solana, H. Liu, D. Mateos, K. Rajagopal, and U. A. Wiedemann, *Gauge/String Duality, Hot QCD and Heavy Ion Collisions*, arXiv:1101.0618.

[31] S. S. Gubser, *The gauge-string duality and heavy ion collisions*, arXiv:1103.3636.

[32] O. DeWolfe, S. S. Gubser, C. Rosen, and D. Teaney, *Heavy ions and string theory*, arXiv:1304.7794.

[33] E. Poisson, *A Relativist's Toolkit : The Mathematics of Black Hole Mechanics*. Cambridge University Press, 2004.

[34] K. Skenderis, *Lecture notes on holographic renormalization*, *Class.Quant.Grav.* **19** (2002) 5849–5876, [hep-th/0209067].

[35] R. M. Wald, *General relativity*. University of Chicago Press, 1984.

[36] S. Hawking and G. Ellis, *The Large Scale Structure of Space-Time*. Cambridge University Press, 1973.

[37] P. O. Mazur, *Black hole uniqueness theorems*, hep-th/0101012.

[38] D. Robinson, *Four decades of black holes uniqueness theorems - The Kerr spacetime: rotating black holes in general relativity pg.115-143, eds. DL Wiltshire, M Visser and S M Scott*, 2004.

[39] R. Emparan and H. S. Reall, *Black Holes in Higher Dimensions*, *Living Rev. Rel.* **11** (2008) 6, [arXiv:0801.3471].

[40] E. by David L. Wiltshire, M. Visser, and S. M. Scott, *The Kerr Spacetime: Rotating Black Holes in General Relativity.* Cambridge University Press, 2009.

[41] D. Robinson, *Uniqueness of the Kerr black hole*, *Phys.Rev.Lett.* **34** (1975) 905–906.

[42] P. Mazur, *Proof of uniqueness of the Kerr-Newman black hole solution*, *J.Phys.* **A15** (1982) 3173–3180.

[43] N. Mavromatos, *Eluding the no hair conjecture for black holes*, gr-qc/9606008.

[44] R. Emparan and H. S. Reall, *A rotating black ring in five dimensions*, *Phys. Rev. Lett.* **88** (2002) 101101, [hep-th/0110260].

[45] R. Emparan and H. S. Reall, *Black rings*, *Class. Quant. Grav.* **23** (2006) R169, [hep-th/0608012].

[46] P. T. Chrusciel and R. M. Wald, *On the topology of stationary black holes*, *Class. Quant. Grav.* **11** (1994) L147–L152, [gr-qc/9410004].

[47] J. Stewart, *Advanced General Relativity.* Cambridge University Press, 1991.

[48] G. Birkhoff, *Relativity and modern physics, harvard university press*, 1923.

[49] W. Israel, *Event horizons in static vacuum space-times*, *Phys.Rev.* **164** (1967) 1776–1779.

[50] G. L. Bunting and A. Masood-ul Alam, *Nonexistence of multiple black holes in asymptotically euclidean static vacuum space-time*, *General relativity and gravitation* **19** (1987), no. 2 147–154.

[51] F. Tangherlini, *Schwarzschild field in n dimensions and the dimensionality of space problem*, *Nuovo Cim.* **27** (1963) 636–651.

[52] W. Israel, *Event horizons in static electrovac space-times*, *Commun.Math.Phys.* **8** (1968) 245–260.

[53] B. Carter, *Black Hole Equilibrium States: II General Theory of Stationary Black Hole States.* Black Holes (proc. 1972 Les Houches Summer School), ed. B. & C. DeWitt, 1973.

[54] S. Hollands, A. Ishibashi, and R. M. Wald, *A Higher Dimensional Stationary Rotating Black Hole Must be Axisymmetric*, *Commun. Math. Phys.* **271** (2007) 699–722, [gr-qc/0605106].

[55] S. Hollands and A. Ishibashi, *Black hole uniqueness theorems in higher dimensional spacetimes*, *Class.Quant.Grav.* **29** (2012) 163001, [arXiv:1206.1164].

[56] O. J. C. Dias, P. Figueras, R. Monteiro, H. S. Reall, and J. E. Santos, *An instability of higher-dimensional rotating black holes*, *JHEP* **05** (2010) 076, [arXiv:1001.4527].

[57] O. J. Dias, P. Figueras, R. Monteiro, J. E. Santos, and R. Emparan, *Instability and new phases of higher-dimensional rotating black holes*, *Phys.Rev.* **D80** (2009) 111701, [arXiv:0907.2248].

[58] M. Durkee and H. S. Reall, *Perturbations of near-horizon geometries and instabilities of Myers-Perry black holes*, *Phys.Rev.* **D83** (2011) 104044, [arXiv:1012.4805].

[59] J. M. Bardeen, B. Carter, and S. Hawking, *The Four laws of black hole mechanics*, *Commun.Math.Phys.* **31** (1973) 161–170.

[60] A. Ashtekar and B. Krishnan, *Isolated and dynamical horizons and their applications*, *Living Rev.Rel.* **7** (2004) 10, [gr-qc/0407042].

[61] A. Ashtekar and B. Krishnan, *Dynamical horizons and their properties*, *Phys.Rev.* **D68** (2003) 104030, [gr-qc/0308033].

[62] R. M. Wald, *The thermodynamics of black holes*, gr-qc/9912119.

[63] S. Hawking, *Particle Creation by Black Holes*, *Commun.Math.Phys.* **43** (1975) 199–220.

[64] J. D. Bekenstein, *Black holes and entropy*, *Phys.Rev.* **D7** (1973) 2333–2346.

[65] A. Strominger and C. Vafa, *Microscopic origin of the Bekenstein-Hawking entropy*, *Phys.Lett.* **B379** (1996) 99–104, [hep-th/9601029].

[66] G. Gibbons and S. Hawking, *Action Integrals and Partition Functions in Quantum Gravity*, *Phys.Rev.* **D15** (1977) 2752–2756.

[67] E. by GW Gibbons and S. Hawking, *Euclidean Quantum Gravity.* World Scientific, 1993.

[68] B. F. Whiting and J. York, James W., *Action Principle and Partition Function for the Gravitational Field in Black Hole Topologies*, *Phys.Rev.Lett.* **61** (1988) 1336.

[69] J. York, James W., *Black hole thermodynamics and the Euclidean Einstein action*, *Phys.Rev.* **D33** (1986) 2092–2099.

[70] S. Hawking and D. N. Page, *Thermodynamics of Black Holes in anti-De Sitter Space*, *Commun.Math.Phys.* **87** (1983) 577.

[71] R. Gregory and R. Laflamme, *Black strings and p-branes are unstable*, *Phys. Rev. Lett.* **70** (1993) 2837–2840, [hep-th/9301052].

[72] R. Gregory and R. Laflamme, *The Instability of charged black strings and p-branes*, *Nucl. Phys.* **B428** (1994) 399–434, [hep-th/9404071].

[73] B. Kleihaus, J. Kunz, and E. Radu, *New nonuniform black string solutions*, hep-th/0603119.

[74] T. Wiseman, *Static axisymmetric vacuum solutions and nonuniform black strings*, *Class.Quant.Grav.* **20** (2003) 1137–1176, [hep-th/0209051].

[75] T. Harmark, V. Niarchos, and N. A. Obers, *Instabilities of black strings and branes*, *Class. Quant. Grav.* **24** (2007) R1–R90, [hep-th/0701022].

[76] L. Lehner and F. Pretorius, *Black Strings, Low Viscosity Fluids, and Violation of Cosmic Censorship*, *Phys. Rev. Lett.* **105** (2010) 101102, [arXiv:1006.5960].

[77] H. Kudoh and T. Wiseman, *Connecting black holes and black strings*, *Phys.Rev.Lett.* **94** (2005) 161102, [hep-th/0409111].

[78] B. Kol, *Topology change in general relativity and the black-hole black-string transition*, *JHEP* **10** (2005) 049, [hep-th/0206220].

[79] B. Kol, *The Phase Transition between Caged Black Holes and Black Strings - A Review*, *Phys. Rept.* **422** (2006) 119–165, [hep-th/0411240].

[80] R. P. Kerr, *Gravitational field of a spinning mass as an example of algebraically special metrics*, *Phys.Rev.Lett.* **11** (1963) 237–238.

[81] J. Gariel, M. A. H. MacCallum, G. Marcilhacy, and N. O. Santos, *Kerr Geodesics, the Penrose Process and Jet Collimation by a Black Hole*, gr-qc/0702123.

[82] R. C. Myers and M. Perry, *Black Holes in Higher Dimensional Space-Times*, *Annals Phys.* **172** (1986) 304.

[83] R. C. Myers, *Myers-Perry black holes*, `arXiv:1111.1903`.

[84] H. Elvang and P. Figueras, *Black Saturn*, *JHEP* **0705** (2007) 050, [`hep-th/0701035`].

[85] R. Emparan, S. Ohashi, and T. Shiromizu, *No-dipole-hair theorem for higher-dimensional static black holes*, *Phys.Rev.* **D82** (2010) 084032, [`arXiv:1007.3847`].

[86] M. M. Caldarelli, R. Emparan, and M. J. Rodriguez, *Black Rings in (Anti)-deSitter space*, *JHEP* **0811** (2008) 011, [`arXiv:0806.1954`].

[87] R. Emparan and P. Figueras, *Multi-black rings and the phase diagram of higher-dimensional black holes*, *JHEP* **1011** (2010) 022, [`arXiv:1008.3243`].

[88] R. Emparan, T. Harmark, V. Niarchos, N. A. Obers, and M. J. Rodriguez, *The Phase Structure of Higher-Dimensional Black Rings and Black Holes*, *JHEP* **0710** (2007) 110, [`arXiv:0708.2181`].

[89] T. Harmark and N. A. Obers, *Phases of Kaluza-Klein black holes: A Brief review*, `hep-th/0503020`.

[90] E. Witten, *Anti-de Sitter space and holography*, *Adv.Theor.Math.Phys.* **2** (1998) 253–291, [`hep-th/9802150`].

[91] S. Gubser, I. R. Klebanov, and A. M. Polyakov, *Gauge theory correlators from noncritical string theory*, *Phys.Lett.* **B428** (1998) 105–114, [`hep-th/9802109`].

[92] O. Aharony, S. S. Gubser, J. M. Maldacena, H. Ooguri, and Y. Oz, *Large N field theories, string theory and gravity*, *Phys.Rept.* **323** (2000) 183–386, [`hep-th/9905111`].

[93] E. D'Hoker and D. Z. Freedman, *Supersymmetric gauge theories and the AdS / CFT correspondence*, `hep-th/0201253`.

[94] H. Nastase, *Introduction to AdS-CFT*, `arXiv:0712.0689`.

[95] G. 't Hooft, *Dimensional reduction in quantum gravity*, `gr-qc/9310026`.

[96] R. Bousso, *The Holographic principle*, *Rev.Mod.Phys.* **74** (2002) 825–874, [hep-th/0203101].

[97] S. Kachru, X. Liu, and M. Mulligan, *Gravity Duals of Lifshitz-like Fixed Points*, *Phys.Rev.* **D78** (2008) 106005, [arXiv:0808.1725].

[98] S. de Haro, S. N. Solodukhin, and K. Skenderis, *Holographic reconstruction of space-time and renormalization in the AdS / CFT correspondence*, *Commun.Math.Phys.* **217** (2001) 595–622, [hep-th/0002230].

[99] S. A. Hartnoll, C. P. Herzog, and G. T. Horowitz, *Holographic Superconductors*, *JHEP* **0812** (2008) 015, [arXiv:0810.1563].

[100] J. Wilson, *Models of differentially rotating stars*, *Astrophys. J.* **176** (1972) 195–204.

[101] S. Bonazzola and J. Schneider, *An exact study of rigidly and rapidly rotating stars in general relativity with application to the crab pulsar*, *Astrophys. J.* **191** (1974) 273–286.

[102] E. Butterworth and J. Ipser, *On the structure and stability of rapidly rotating fluid bodies in general relativity. i. the numerical method for computing structure and its application to uniformly rotating homogeneous bodies*, *Astrophys. J.* **204** (1976) 200–233.

[103] N. Stergioulas, *Models of differentially rotating stars*, *Living Rev. Relativity* **6** (2003).

[104] B. Kleihaus and J. Kunz, *Static black hole solutions with axial symmetry*, *Phys. Rev. Lett.* **79** (1997) 1595–1598, [gr-qc/9704060].

[105] B. Kleihaus and J. Kunz, *Rotating hairy black holes*, *Phys. Rev. Lett.* **86** (2001) 3704–3707, [gr-qc/0012081].

[106] Y. Morisawa and D. Ida, *A boundary value problem for the five-dimensional stationary rotating black holes*, *Phys. Rev.* **D69** (2004) 124005, [gr-qc/0401100].

[107] S. Hollands and S. Yazadjiev, *Uniqueness theorem for 5-dimensional black holes with two axial Killing fields*, *Commun. Math. Phys.* **283** (2008) 749–768, [arXiv:0707.2775].

[108] T. Harmark, *Stationary and axisymmetric solutions of higher- dimensional general relativity*, *Phys. Rev.* **D70** (2004) 124002, [hep-th/0408141].

[109] T. Wiseman, *Relativistic stars in Randall-Sundrum gravity*, *Phys. Rev.* **D65** (2002) 124007, [hep-th/0111057].

[110] S. Donaldson, *Some numerical results in complex differential geometry*, arXiv:math.DG/0.

[111] M. Headrick and A. Nassar, *Energy functionals for Calabi-Yau metrics*, arXiv:0908.2635.

[112] O. A. Reula, *Hyperbolic methods for Einstein's equations*, *Living Rev.Rel.* **1** (1998) 3.

[113] H.-O. Kreiss and J. Lorenz, *Initial-boundary value problems and the Navier-Stokes equations*, vol. 136. Access Online via Elsevier, 1989.

[114] S. Hassani, *Mathematical Physics: A modern introduction to its foundation.* Springer, India, 1999.

[115] M. E. Taylor, *Partial differential equations I: Basic theory*, vol. 1. Springer, 1996.

[116] Y. Fourès-Bruhat, *Théorème d'existence pour certains systèms d'équations aux dérivées partielles non linéaires*, *Acta Mathematica* **88** (1952) 141.

[117] H. Friedrich, *On the hyperbolicity of Einstein's and other gauge field equations*, *Commun. Math. Phys.* **100** (1985) 525–543.

[118] D. Garfinkle, *Harmonic coordinate method for simulating generic singularities*, *Phys. Rev.* **D65** (2002) 044029, [gr-qc/0110013].

[119] J. Eells and L. Lemaire, *Harmonic mappings of Riemannian manifolds*, *Amer. J . Math 86* (1964).

[120] J. P. Bourguignon, *In Global differential geometry and global analysis (Berlin, 1979), volume 838 of Lecture notes in Math. pages 42-63. Springer, Berlin 1981.*, .

[121] P. Figueras, J. Lucietti, and T. Wiseman, *Ricci solitons, Ricci flow, and strongly coupled CFT in the Schwarzschild Unruh or Boulware vacua*, arXiv:1104.4489.

[122] P. M. Topping, *Lectures on the Ricci flow.* L.M.S. Lecture note series 325 C.U.P., 2006.

[123] T. Oliynyk and E. Woolgar, *Asymptotically Flat Ricci Flows*, math/0607438.

[124] S. S. Gubser and I. Mitra, *The Evolution of unstable black holes in anti-de Sitter space*, *JHEP* **0108** (2001) 018, [hep-th/0011127].

[125] S. S. Gubser and I. Mitra, *Instability of charged black holes in Anti-de Sitter space*, hep-th/0009126.

[126] H. S. Reall, *Classical and thermodynamic stability of black branes*, *Phys.Rev.* **D64** (2001) 044005, [hep-th/0104071].

[127] J. J. Friess, S. S. Gubser, and I. Mitra, *Counter-examples to the correlated stability conjecture*, *Phys.Rev.* **D72** (2005) 104019, [hep-th/0508220].

[128] D. J. Gross, M. J. Perry, and L. G. Yaffe, *Instability of Flat Space at Finite Temperature*, *Phys. Rev.* **D25** (1982) 330–355.

[129] N. E. Mavromatos, *On CPT symmetry: Cosmological, quantum gravitational and other possible violations and their phenomenology*, *Springer Proc.Phys.* **92** (2004) 43–72, [hep-ph/0309221].

[130] G. Amelino-Camelia, *The Three perspectives on the quantum gravity problem and their implications for the fate of Lorentz symmetry*, gr-qc/0309054.

[131] T. A. Jacobson, S. Liberati, D. Mattingly, and F. Stecker, *New limits on Planck scale Lorentz violation in QED*, *Phys.Rev.Lett.* **93** (2004) 021101, [astro-ph/0309681].

[132] V. A. Kostelecky and S. Samuel, *Gravitational Phenomenology in Higher Dimensional Theories and Strings*, *Phys.Rev.* **D40** (1989) 1886–1903.

[133] D. Colladay and V. A. Kostelecky, *Lorentz violating extension of the standard model*, *Phys.Rev.* **D58** (1998) 116002, [hep-ph/9809521].

[134] D. Mattingly, *Modern tests of Lorentz invariance*, *Living Rev.Rel.* **8** (2005) 5, [gr-qc/0502097].

[135] S. Liberati and L. Maccione, *Lorentz Violation: Motivation and new constraints*, *Ann.Rev.Nucl.Part.Sci.* **59** (2009) 245–267, [arXiv:0906.0681].

[136] M. Gasperini, *Singularity prevention and broken Lorentz symmetry*, *Class.Quant.Grav.* **4** (1987) 485–494.

[137] M. Gasperini, *Repulsive gravity in the very early universe*, *Gen.Rel.Grav.* **30** (1998) 1703–1709, [gr-qc/9805060].

[138] K. J. Nordtvedt and C. M. Will, *Conservation Laws and Preferred Frames in Relativistic Gravity. II. Experimental Evidence to Rule Out Preferred-Frame Theories of Gravity*, *Astrophys.J.* **177** (1972) 775–792.

[139] C. M. Will and J. Nordtvedt, Kenneth, *Conservation Laws and Preferred Frames in Relativistic Gravity. I. Preferred-Frame Theories and an Extended PPN Formalism*, *Astrophys.J.* **177** (1972) 757.

[140] R. W. Hellings and K. Nordtvedt, *Vector-Metric Theory of Gravity*, *Phys.Rev.* **D7** (1973) 3593–3602.

[141] M. Clayton and J. Moffat, *Dynamical mechanism for varying light velocity as a solution to cosmological problems*, *Phys.Lett.* **B460** (1999) 263–270, [astro-ph/9812481].

[142] J. Moffat, *Variable speed of light cosmology: An Alternative to inflation*, hep-th/0208122.

[143] B. A. Bassett, S. Liberati, C. Molina-Paris, and M. Visser, *Geometrodynamics of variable speed of light cosmologies*, *Phys.Rev.* **D62** (2000) 103518, [astro-ph/0001441].

[144] M. Clayton, *Causality, shocks and instabilities in vector field models of Lorentz symmetry breaking*, gr-qc/0104103.

[145] N. Arkani-Hamed, H.-C. Cheng, M. A. Luty, and S. Mukohyama, *Ghost condensation and a consistent infrared modification of gravity*, *JHEP* **0405** (2004) 074, [hep-th/0312099].

[146] N. Arkani-Hamed, P. Creminelli, S. Mukohyama, and M. Zaldarriaga, *Ghost inflation*, *JCAP* **0404** (2004) 001, [hep-th/0312100].

[147] V. A. Kostelecky, *Gravity, Lorentz violation, and the standard model*, *Phys.Rev.* **D69** (2004) 105009, [hep-th/0312310].

[148] C. M. Will, *Theory and Experiment in Gravitational Physics*. Cambridge University Press, 1993.

[149] T. Jacobson and D. Mattingly, *Einstein-Aether waves*, *Phys.Rev.* **D70** (2004) 024003, [gr-qc/0402005].

[150] C. Eling and T. Jacobson, *Black Holes in Einstein-Aether Theory*, *Class.Quant.Grav.* **23** (2006) 5643–5660, [gr-qc/0604088].

[151] B. Z. Foster, *Metric redefinitions in Einstein-Aether theory*, *Phys.Rev.* **D72** (2005) 044017, [gr-qc/0502066].

[152] E. Barausse, T. Jacobson, and T. P. Sotiriou, *Black holes in Einstein-aether and Horava-Lifshitz gravity*, *Phys.Rev.* **D83** (2011) 124043, [arXiv:1104.2889].

[153] D. Blas, O. Pujolas, and S. Sibiryakov, *Comment on 'Strong coupling in extended Horava-Lifshitz gravity'*, *Phys.Lett.* **B688** (2010) 350–355, [arXiv:0912.0550].

[154] C. Germani, A. Kehagias, and K. Sfetsos, *Relativistic Quantum Gravity at a Lifshitz Point*, *JHEP* **0909** (2009) 060, [arXiv:0906.1201].

[155] T. Jacobson, *Extended Horava gravity and Einstein-aether theory*, *Phys.Rev.* **D81** (2010) 101502, [arXiv:1001.4823].

[156] P. Horava, *Quantum Gravity at a Lifshitz Point*, *Phys.Rev.* **D79** (2009) 084008, [arXiv:0901.3775].

[157] B. Withers, *Einstein-aether as a quantum effective field theory*, *Class.Quant.Grav.* **26** (2009) 225009, [arXiv:0905.2446].

[158] J. F. Barbero G. and E. J. Villasenor, *Lorentz violations and Euclidean signature metrics*, *Phys.Rev.* **D68** (2003) 087501, [gr-qc/0307066].

[159] C. R. Contaldi, T. Wiseman, and B. Withers, *TeVeS gets caught on caustics*, *Phys.Rev.* **D78** (2008) 044034, [arXiv:0802.1215].

[160] B. Z. Foster and T. Jacobson, *Post-Newtonian parameters and constraints on Einstein-aether theory*, *Phys.Rev.* **D73** (2006) 064015, [gr-qc/0509083].

[161] D. Blas, O. Pujolas, and S. Sibiryakov, *Models of non-relativistic quantum gravity: The Good, the bad and the healthy*, *JHEP* **1104** (2011) 018, [arXiv:1007.3503].

[162] C. Eling and T. Jacobson, *Static postNewtonian equivalence of GR and gravity with a dynamical preferred frame*, *Phys.Rev.* **D69** (2004) 064005, [gr-qc/0310044].

[163] C. M. Will, *The Confrontation between general relativity and experiment*, *Living Rev.Rel.* **9** (2006) 3, [gr-qc/0510072].

[164] J. W. Elliott, G. D. Moore, and H. Stoica, *Constraining the new Aether: Gravitational Cerenkov radiation*, *JHEP* **0508** (2005) 066, [hep-ph/0505211].

[165] G. D. Moore and A. E. Nelson, *Lower bound on the propagation speed of gravity from gravitational Cherenkov radiation*, *JHEP* **0109** (2001) 023, [hep-ph/0106220].

[166] J. A. Zuntz, P. Ferreira, and T. Zlosnik, *Constraining Lorentz violation with cosmology*, *Phys.Rev.Lett.* **101** (2008) 261102, [arXiv:0808.1824].

[167] B. Li, D. Fonseca Mota, and J. D. Barrow, *Detecting a Lorentz-Violating Field in Cosmology*, *Phys.Rev.* **D77** (2008) 024032, [arXiv:0709.4581].

[168] E. A. Lim, *Can we see Lorentz-violating vector fields in the CMB?*, *Phys.Rev.* **D71** (2005) 063504, [astro-ph/0407437].

[169] B. Z. Foster, *Radiation damping in Einstein-aether theory*, *Phys.Rev.* **D73** (2006) 104012, [gr-qc/0602004].

[170] B. Z. Foster, *Strong field effects on binary systems in Einstein-aether theory*, *Phys.Rev.* **D76** (2007) 084033, [arXiv:0706.0704].

[171] C. Eling and T. Jacobson, *Spherical solutions in Einstein-aether theory: Static aether and stars*, *Class.Quant.Grav.* **23** (2006) 5625–5642, [gr-qc/0603058].

[172] C. Eling, T. Jacobson, and M. Coleman Miller, *Neutron stars in Einstein-aether theory*, *Phys.Rev.* **D76** (2007) 042003, [arXiv:0705.1565].

[173] S. M. Carroll, T. R. Dulaney, M. I. Gresham, and H. Tam, *Instabilities in the Aether*, *Phys.Rev.* **D79** (2009) 065011, [arXiv:0812.1049].

[174] S. A. Hartnoll and L. Huijse, *Fractionalization of holographic Fermi surfaces*, arXiv:1111.2606.

[175] L. Huijse and S. Sachdev, *Fermi surfaces and gauge-gravity duality*, *Phys. Rev.* **D84** (2011) 026001, [arXiv:1104.5022].

[176] N. Iqbal and H. Liu, *Luttinger's Theorem, Superfluid Vortices, and Holography*, `arXiv:1112.3671`. 21 pages.

[177] S. El-Showk and K. Papadodimas, *Emergent Spacetime and Holographic CFTs*, *JHEP* **1210** (2012) 106, [`arXiv:1101.4163`].

[178] E. Witten, *Anti-de Sitter space, thermal phase transition, and confinement in gauge theories*, *Adv.Theor.Math.Phys.* **2** (1998) 505–532, [`hep-th/9803131`].

[179] T. Faulkner and N. Iqbal, *Friedel oscillations and horizon charge in 1D holographic liquids*, `arXiv:1207.4208`.

[180] V. G. M. Puletti, S. Nowling, L. Thorlacius, and T. Zingg, *Holographic metals at finite temperature*, *JHEP* **01** (2011) 117, [`arXiv:1011.6261`].

[181] E. D'Hoker and P. Kraus, *Charge Expulsion from Black Brane Horizons, and Holographic Quantum Criticality in the Plane*, `arXiv:1202.2085`. 37 pages v2: reference added and cosmetic improvements.

[182] S. A. Hartnoll and E. Shaghoulian, *Spectral weight in holographic scaling geometries*, `arXiv:1203.4236`.

[183] S. A. Hartnoll and A. Tavanfar, *Electron stars for holographic metallic criticality*, *Phys.Rev.* **D83** (2011) 046003, [`arXiv:1008.2828`].

[184] U. Gursoy and E. Kiritsis, *Exploring improved holographic theories for QCD: Part I*, *JHEP* **0802** (2008) 032, [`arXiv:0707.1324`].

[185] U. Gursoy, E. Kiritsis, and F. Nitti, *Exploring improved holographic theories for QCD: Part II*, *JHEP* **0802** (2008) 019, [`arXiv:0707.1349`].

[186] O. DeWolfe, S. S. Gubser, and C. Rosen, *A holographic critical point*, *Phys.Rev.* **D83** (2011) 086005, [`arXiv:1012.1864`].

[187] M. Taylor, *Non-relativistic holography*, `arXiv:0812.0530`.

[188] K. Goldstein, S. Kachru, S. Prakash, and S. P. Trivedi, *Holography of Charged Dilaton Black Holes*, *JHEP* **1008** (2010) 078, [`arXiv:0911.3586`].

[189] C. Charmousis, B. Gouteraux, B. Kim, E. Kiritsis, and R. Meyer, *Effective Holographic Theories for low-temperature condensed matter systems*, *JHEP* **1011** (2010) 151, [`arXiv:1005.4690`].

[190] E. Shaghoulian, *Holographic Entanglement Entropy and Fermi Surfaces*, *JHEP* **1205** (2012) 065, [arXiv:1112.2702].

[191] N. Ogawa, T. Takayanagi, and T. Ugajin, *Holographic Fermi Surfaces and Entanglement Entropy*, *JHEP* **1201** (2012) 125, [arXiv:1111.1023].

[192] L. Huijse, S. Sachdev, and B. Swingle, *Hidden Fermi surfaces in compressible states of gauge-gravity duality*, *Phys.Rev.* **B85** (2012) 035121, [arXiv:1112.0573].

[193] B. Gouteraux and E. Kiritsis, *Generalized Holographic Quantum Criticality at Finite Density*, *JHEP* **1112** (2011) 036, [arXiv:1107.2116].

[194] X. Dong, S. Harrison, S. Kachru, G. Torroba, and H. Wang, *Aspects of holography for theories with hyperscaling violation*, *JHEP* **1206** (2012) 041, [arXiv:1201.1905].

[195] S. S. Gubser, *Curvature singularities: The Good, the bad, and the naked*, *Adv.Theor.Math.Phys.* **4** (2000) 679–745, [hep-th/0002160].

[196] A. Donos and J. P. Gauntlett, *Holographic striped phases*, *JHEP* **1108** (2011) 140, [arXiv:1106.2004].

[197] A. Donos and J. P. Gauntlett, *Holographic helical superconductors*, *JHEP* **1112** (2011) 091, [arXiv:1109.3866].

[198] A. Donos and J. P. Gauntlett, *Helical superconducting black holes*, *Phys.Rev.Lett.* **108** (2012) 211601, [arXiv:1203.0533].

[199] A. Donos and J. P. Gauntlett, *Black holes dual to helical current phases*, *Phys.Rev.* **D86** (2012) 064010, [arXiv:1204.1734].

[200] A. Donos, *Striped phases from holography*, *JHEP* **1305** (2013) 059, [arXiv:1303.7211].

[201] G. T. Horowitz and M. M. Roberts, *Zero Temperature Limit of Holographic Superconductors*, *JHEP* **0911** (2009) 015, [arXiv:0908.3677].

[202] J. P. Gauntlett, J. Sonner, and T. Wiseman, *Quantum Criticality and Holographic Superconductors in M- theory*, *JHEP* **02** (2010) 060, [arXiv:0912.0512].

[203] J. P. Gauntlett, S. Kim, O. Varela, and D. Waldram, *Consistent supersymmetric Kaluza–Klein truncations with massive modes*, *JHEP* **04** (2009) 102, [arXiv:0901.0676].

[204] J. P. Gauntlett, J. Sonner, and T. Wiseman, *Holographic superconductivity in M-Theory*, *Phys. Rev. Lett.* **103** (2009) 151601, [arXiv:0907.3796].

[205] H.-C. Kim, S. Kim, K. Lee, and J. Park, *Emergent Schrodinger geometries from mass-deformed CFT*, *JHEP* **08** (2011) 111, [arXiv:1106.4309].

[206] N. Iqbal, H. Liu, and M. Mezei, *Quantum phase transitions in semi-local quantum liquids*, arXiv:1108.0425.

[207] T. Harmark, *Domain Structure of Black Hole Space-Times*, *Phys. Rev.* **D80** (2009) 024019, [arXiv:0904.4246].

[208] M. M. Caldarelli, G. Cognola, and D. Klemm, *Thermodynamics of Kerr-Newman-AdS black holes and conformal field theories*, *Class. Quant. Grav.* **17** (2000) 399–420, [hep-th/9908022].

[209] V. Moncrief and J. Isenberg, *Symmetries of Higher Dimensional Black Holes*, *Class. Quant. Grav.* **25** (2008) 195015, [arXiv:0805.1451].

[210] E. Barausse and T. P. Sotiriou, *Slowly rotating black holes in Horava-Lifshitz gravity*, *Phys.Rev.* **D87** (2013) 087504, [arXiv:1212.1334].

[211] T. Tamaki and U. Miyamoto, *Generic features of Einstein-Aether black holes*, *Phys.Rev.* **D77** (2008) 024026, [arXiv:0709.1011].

[212] E. Donets, D. Galtsov, and M. Y. Zotov, *Internal structure of Einstein Yang-Mills black holes*, *Phys.Rev.* **D56** (1997) 3459–3465, [gr-qc/9612067].

[213] R. Konoplya and A. Zhidenko, *Gravitational spectrum of black holes in the Einstein-Aether theory*, *Phys.Lett.* **B648** (2007) 236–239, [hep-th/0611226].

[214] R. Konoplya and A. Zhidenko, *Perturbations and quasi-normal modes of black holes in Einstein-Aether theory*, *Phys.Lett.* **B644** (2007) 186–191, [gr-qc/0605082].

[215] E. Kiritsis, *Spherically symmetric solutions in modified Horava-Lifshitz gravity*, *Phys.Rev.* **D81** (2010) 044009, [arXiv:0911.3164].

[216] J. Greenwald, A. Papazoglou, and A. Wang, *Black holes and stars in Horava-Lifshitz theory with projectability condition*, *Phys.Rev.* **D81** (2010) 084046, [arXiv:0912.0011].

[217] H. Lu, J. Mei, and C. Pope, *Solutions to Horava Gravity*, *Phys.Rev.Lett.* **103** (2009) 091301, [arXiv:0904.1595].

[218] A. Kehagias and K. Sfetsos, *The Black hole and FRW geometries of non-relativistic gravity*, *Phys.Lett.* **B678** (2009) 123–126, [arXiv:0905.0477].

[219] E. B. Kiritsis and G. Kofinas, *On Horava-Lifshitz 'Black Holes'*, *JHEP* **1001** (2010) 122, [arXiv:0910.5487].

[220] B. Z. Foster, *Noether charges and black hole mechanics in Einstein-aether theory*, *Phys.Rev.* **D73** (2006) 024005, [gr-qc/0509121].

[221] E. Barausse and T. P. Sotiriou, *A no-go theorem for slowly rotating black holes in Horava-Lifshitz gravity*, *Phys.Rev.Lett.* **109** (2012) 181101, [arXiv:1207.6370].

[222] P. Figueras and T. Wiseman, *Stationary holographic plasma quenches and numerical methods for non-Killing horizons*, arXiv:1212.4498.

[223] C. Eling, T. Jacobson, and D. Mattingly, *Einstein-Aether theory*, gr-qc/0410001.

[224] I. Racz and R. M. Wald, *Global extensions of space-times describing asymptotic final states of black holes*, *Class.Quant.Grav.* **13** (1996) 539–553, [gr-qc/9507055].

[225] R. Baier, P. Romatschke, D. T. Son, A. O. Starinets, and M. A. Stephanov, *Relativistic viscous hydrodynamics, conformal invariance, and holography*, *JHEP* **0804** (2008) 100, [arXiv:0712.2451].

[226] S. Bhattacharyya, V. E. Hubeny, S. Minwalla, and M. Rangamani, *Nonlinear Fluid Dynamics from Gravity*, *JHEP* **0802** (2008) 045, [arXiv:0712.2456].

[227] L. N. Trefethen, *Spectral Methods in Matlab.* SIAM, 2000.

[228] C. Eling, *Energy in the Einstein-aether theory*, *Phys.Rev.* **D73** (2006) 084026, [gr-qc/0507059].

[229] B. Fornberg, *Classroom note: Calculation of weights in finite difference formulas*, *SIAM review* **40** (1998), no. 3 685–691.

[230] S. A. Hartnoll and D. Radicevic, *Holographic order parameter for charge fractionalization*, *Phys.Rev.* **D86** (2012) 066001, [arXiv:1205.5291].